Technical Readiness and Gaps Analysis of Commercial Optical Materials and Measurement Systems for Advanced Small Modular Reactors

NC Anheier
JD Suter
A Qiao
ES Andersen
EJ Berglin

M Bliss
BD Cannon
R Devanathan
A Mendoza
DM Sheen

August 2013

DISCLAIMER

This report was prepared as an account of work sponsored by an agency of the United States Government. Neither the United States Government nor any agency thereof, nor Battelle Memorial Institute, nor any of their employees, makes **any warranty, express or implied, or assumes any legal liability or responsibility for the accuracy, completeness, or usefulness of any information, apparatus, product, or process disclosed, or represents that its use would not infringe privately owned rights**. Reference herein to any specific commercial product, process, or service by trade name, trademark, manufacturer, or otherwise does not necessarily constitute or imply its endorsement, recommendation, or favoring by the United States Government or any agency thereof, or Battelle Memorial Institute. The views and opinions of authors expressed herein do not necessarily state or reflect those of the United States Government or any agency thereof.

Technical Readiness and Gaps Analysis of Commercial Optical Materials and Measurement Systems for Advanced Small Modular Reactors

NC Anheier
JD Suter
A Qiao
ES Andersen
EJ Berglin

M Bliss
BD Cannon
R Devanathan
A Mendoza
DM Sheen

August 2013

Pacific Northwest National Laboratory
Richland, Washington 99352

Executive Summary

This report supports the U.S. Department of Energy's Office of Nuclear Energy (DOE-NE) *Nuclear Energy Research and Development Roadmap* and industry stakeholders by evaluating optically based instrumentation and control (I&C) concepts for advanced small modular reactor (AdvSMR) applications. These advanced designs will require innovative thinking in terms of engineering approaches, materials integration, and I&C concepts to realize their eventual viability and deployment. The primary goals of this report include:

1. Establish preliminary I&C needs, performance requirements, and possible gaps for AdvSMR designs based on best-available published design data.

2. Document commercial off-the-shelf (COTS) optical sensors, components, and materials in terms of their technical readiness to support essential AdvSMR in-vessel I&C systems.

3. Identify technology gaps by comparing the in-vessel monitoring requirements and environmental constraints to COTS optical sensor and materials performance specifications.

4. Outline a future research, development, and demonstration (RD&D) program plan that addresses these gaps and develops optical-based I&C systems that enhance the viability of future AdvSMR designs.

The DOE-NE roadmap outlines RD&D activities intended to overcome technical barriers that currently limit advances in nuclear energy. As part of this strategy, DOE-NE is sponsoring research on advanced reactor supportive technologies to reduce the identified barriers. Key challenges that must be overcome include the high capital costs to develop nuclear power plants, maintaining safety performance as the reactor fleet expands, minimizing nuclear waste, and maintaining strong proliferation resistance. AdvSMR designs are a major component of this strategy, because these designs offer a number of unique advantages. The modular and small size of AdvSMR designs naturally lead to reduced capital investments and, potentially, construction savings through factory fabrication. However, new economic and technical challenges accompany the many attractive features offered by AdvSMR designs. Specifically, the modest power output of AdvSMRs does not provide the economy of scale afforded by large reactors. In addition, many of the AdvSMR designs operate at much higher temperatures than light-water reactors and require instrumentation to withstand harsh, in-vessel environments arising from unconventional, chemically aggressive coolants and unique reactor system configurations.

Addressing these I&C challenges will be critically important to the AdvSMR development program to ensure the viability and future success of advanced reactor designs. Solutions will likely be found through evolution of conventional reactor technology, and the development of entirely new concepts. Early pressure/boiling water reactors used conventional I&C technologies (e.g., thermocouples, ion-chambers, strain-gauge pressure sensors) to satisfy design requirements. Because these technologies worked well in the relatively low-temperature reactor designs, the demand for alternate I&C technologies was limited. At the time, optical-based reactor monitoring concepts were generally dismissed because of a number of economic and technical limitations. Optical sensor systems were not cost-competitive or failed to offer superior performance compared to conventional reactor monitoring systems. Reliability and service performance were in question because there was only a basic understanding of the radiation damage mechanisms in optical materials. In other cases, computational systems did not exist or have sufficient power to support the processing needs of optical-based monitoring systems. This trend

continued through the next several decades (i.e., 1960–1990s), as conventional I&C systems continued to offer acceptable performance.

Conventional design rules are unlikely to hold for future advanced reactor concepts, because of the demanding design requirements. Thus, new approaches will be needed to support AdvSMR I&C requirements. Because significant technology advancements have been made in the past several decades, current optical-based sensing and interface technologies now may have an impact in this area. Key elements include advancements in optical sensing performance, precision component fabrication, laser technology, integrated optoelectronics, and advanced computer signal processing hardware and software. New optical materials and purification methods that incrementally improved material properties, leading to enhanced suitability for more challenging applications, have been developed. Significant optical materials research was conducted to gain insight into radiation damage and other performance issues. This research established the physical damage pathways and productive development areas to minimize vulnerabilities to radiation-induced damage. Most likely, further advancements in many optical materials and monitoring systems will be required prior to possible use in future AdvSMR designs. Because optical systems offer many unique advantages over traditional approaches, further study commensurate with the abilities of optical systems may be very fruitful. Key advantages provided by optical systems include:

- **Noncontact, standoff sensing and monitoring** – Both passive and active remote sensing can be performed by many different optical sensing techniques. Standoff sensing can also help to isolate sensitive components from high temperatures and radiation exposure. Laser vibrometry is an example of noncontact, standoff optical monitoring.

- **Drift-free monitoring** – Many optical sensing techniques are based on first-principle measurements and therefore are less susceptible to signal drift. Time-dependent drift is a common problem in thermocouples, which estimate temperature based on changes in junction voltage. Drift in thermocouples is distinguished by metallurgical changes in the junction electrode (e.g., oxidation, depletion, contamination, strain). In contrast, optical pyrometry measures temperature based on direct measurement of black body optical emission.

- **High bandwidth** – High-bandwidth measurements and data transfer can be made in the optical fiber. High-bandwidth sensors are well suited for high-speed measuring applications. Frequency analysis techniques can be used to extract additional signal information, such as component vibration. Signal averaging of high-bandwidth measurements can improve the signal-to-noise performance. Optically encoded data can be transmitted at significantly higher data rates (i.e., > 100 Gb/s) compared to traditional electronic methods.

- **Multi-parameter measurements** – The same sensor system can support different modes of parameter monitoring (e.g., visualization, flow, and vibration). For example, advanced image processing methods can be used to extract vibration information from camera video data.

- **Multi-mode measurements** – The same sensor system can support different modes of operation (e.g., inspection, refueling, and processing monitoring). For example, camera systems can provide remote visualization of in-vessel processes (i.e., rod control motion) and servicing operations (i.e., robotic fuel handling).

- **Distributed sensing** – Optical fiber Bragg gratings and time domain reflectometry sensors are well known distributed sensing systems. Using this configuration, a single optical fiber can monitor parameters of interest along the entire length of the fiber.

- **Integrated path length measurements** – Optical sensing techniques can provide integrated path length measurements, which can be superior to point measurements. Parameter profiles are commonly estimated using discrete sensing points, such as multiple-temperature sensors positioned to estimate primary reactor outlet temperatures. A preferred method is direct-profile measurements using a single measurement sensor. Many optical systems can directly measure parameter profiles. For example, optical absorption spectroscopy can be used to measure chemical concentration profiles of trace headspace gases.

Optical-based measurement and sensing systems for AdvSMR applications have several key benefits over traditional instrumentation and control systems used to monitor reactor process parameters, such as temperature, flowrate, pressure, and coolant chemistry. However, technical challenges exist in the areas of 1) optical access that enables in-vessel optical monitoring, 2) optical materials under extreme conditions, and 3) performance limitations of COTS optical monitoring technologies.

This report proposes a comprehensive, multi-year RD&D plan to advance the concept of in-vessel optical monitoring and the technical readiness of COTS optical materials, components, and sensing instrumentation. This plan consists of three key thrust areas where RD&D is required to advance these goals:

- Thrust Area 1: In-vessel Optical Access Engineering and RD&D

- Thrust Area 2: Optical Materials and Components RD&D

- Thrust Area 3: Optical Monitoring Technology RD&D.

These three thrust areas contain interlinked RD&D, wherein the first two thrust areas define the engineering and materials advancements that are required to enable the optical monitoring technology advancements described in the third thrust area. For each thrust, we summarize the key technical readiness gaps and issues, and propose a research plan to close the gaps. Each thrust area contains a number of tasks that must be achieved to close the key gaps and address the deployment challenges.

Acknowledgements

Acronyms and Abbreviations

AHTR	advanced high-temperature reactor
AdvSMR	advanced small modular reactors
ANL	Argonne National Laboratory
AOM	acousto-optic modulation
BBO	barium borate
BOP	balance of plant
BWR	boiling water reactor
CCD	charged-coupled device
CID	charge injection device
CMOS	complementary metal-oxide semiconductor
COTS	commercial off-the-shelf
CRDM	control rod drive mechanism
CTE	coefficients of thermal expansion
CVD	chemical vapor deposition
DBE	design basis event
DFB	distributed feedback
DFT	density functional theory
DOE-NE	U.S. Department of Energy, Office of Nuclear Energy
DTS	distributed temperature sensing
EM	electromagnetic
EMCCD	electron-multiplying charge-coupled detector
EO	electro-optic
FBG	fiber Bragg grating
FHR	fluoride salt-cooled high-temperature reactor
FLiBe	$LiF\text{-}BeF_2$
fs-IR	femtosecond pulse duration infrared
FTIR	Fourier-transform infrared
GaAs	gallium arsenide
GCR	gas-cooled reactor
Gen IV	Generation IV
GFR	gas-cooled fast reactor
GIF	Generation IV International Forum
He	helium
HPHI	high pressure high temperature
HTGR	high-temperature gas-cooled reactor
I&C	instrumentation and control

IHX	intermediate heat exchanger
IR	infrared
ISI	in-service inspection
LIBS	laser-induced breakdown spectroscopy
LIDAR	light detection and ranging
LDV	laser Doppler vibrometry
LFR	lead- (or lead-bismuth-) cooled fast reactor
LOCA	loss-of-coolant accident
LWR	light-water reactor
MARS	Microfuel Molten Salt Cooled Reactor of Low Power
MCT	mercury cadmium telluride
MD	molecular dynamics
MPI	multi-photon ionization
MSR	molten salt reactor
NBOHCs	nonbridging oxygen hole centers
Nf	fast neutron
NIR	near infrared
NRC	U.S. Nuclear Regulatory Commission
Nth	thermal neutron
ODC	oxygen deficiency defect centers
ODS	oxide-dispersion strengthened
OTDR	optical time domain reflectometer
Pb	lead
Pb-Bi	lead/bismuth eutectic
PBG	photonic bandgap
PCF	photonic crystal fiber
PCS	Plant Control System
PMMA	polymethylmethacrylate
PMT	photomultiplier tube
PRISM	Power Reactor Innovative Small Module
PWR	pressurized water reactor
QCL	quantum cascade lasers
R&D	research and development
RD&D	research, development, and demonstration
RH	relative humidity
RI	reflective index
RIA	radiation-induced absorption
RIL	radiation-induced luminescence

RIS	Reactor Interface System
RPS	Reactor Protection System
RPV	reactor pressure vessel
RTD	resistance temperature detector
SCBG	semiconductor bandgap
SCC	stress corrosion cracking
SCWR	supercritical water-cooled reactors
SERS	surface-enhanced Raman scattering
SFR	sodium-cooled fast reactor
SHM	structural health monitoring
SmAHTR	small modular advanced high temperature reactor
SPD	self-powered detectors
SRS	spontaneous Raman scattering
SSTAR	small secure transportable autonomous reactor
TDLAS	tunable diode laser absorption spectroscopy
TIA	Telecommunications Industry Association
TIP	Traveling Instrument Package
TIR	total internal reflection
TWR	traveling-wave reactor
UFPA	uncooled focal plane array
UV	ultraviolet
VHTR	very-high-temperature gas reactor
WGM	whispering gallery mode

Contents

Figures

Tables

1.0   Introduction

The development of clean, affordable, safe, and proliferation-resistant nuclear power is a key goal that is documented in the U.S. Department of Energy, Office of Nuclear Energy's (DOE-NE) *Nuclear Energy Research and Development Roadmap* (DOE 2010b). This roadmap outlines research, development, and demonstration (RD&D) activities intended to overcome the technical, economic, and other barriers that limit advances in nuclear energy. These activities will ensure that nuclear energy remains a viable component to this nation energy security.

At least six primary advanced small modular reactor (AdvSMR) designs are under consideration by research and design leaders, including gas-cooled fast reactors, very high temperature gas reactors, lead-cooled fast reactors, sodium fast reactors, molten salt reactors, and supercritical water reactors (NERAC 2002). The small modular size significantly departs from massive scale nuclear power generation systems of the past few decades. AdvSMR designs feature significantly higher coolant temperatures, compared to light-water reactor (LWR) designs, and hence will require new instrumentation and control (I&C) architectures for plant operation and safety systems (DOE 2010a, c). The future viability of AdvSMRs is critically dependent on understanding and overcoming the significant technical challenges involving in-vessel reactor sensing and monitoring under the extremes of high temperature, pressures, corrosive environments, and radiation flux.

Based on a long history of success in other applications, it is likely that optical materials and sensing technology can play an enabling role in future AdvSMR designs. To date, the nuclear power industry I&C needs have largely been met by existing technology and the demand for specialized optically based I&C systems has been modest. The new AdvSMRs design architectures are likely to change this trend. New optical-based I&C systems are likely to evolve from prior technology, and will require innovative design paths; however, significant challenges lie ahead to realize the benefit potential of optical technology for this application.

1.1   Objectives and Approach

This report supports DOE-NE's *Nuclear Energy Research and Development Roadmap* and industry stakeholders by evaluating optical-based I&C concepts for AdvSMR applications. These advanced designs will require innovative thinking in terms of engineering approaches, materials integration, and I&C concepts to realize their eventual viability and deployment. The primary goals of this report include:

1. Establish preliminary I&C needs, performance requirements, and possible gaps for AdvSMR designs based on best available published design data.

2. Document commercial off-the-shelf (COTS) optical sensors, components, and materials in terms of their technical readiness to support essential AdvSMR in-vessel I&C systems.

3. Identify technology gaps by comparing the in-vessel monitoring requirements and environmental constraints to COTS optical sensor and materials performance specifications.

4. Outline a future RD&D program plan that addresses these gaps and develops optical-based I&C systems that enhance the viability of future AdvSMR designs.

Our approach begins by describing the operational characteristics of the principal AdvSMR designs. The distinctive nature of each coolant-class reactor design implies that there will be many variations in the I&C requirements across the various AdvSMR designs. For example, coolant level sensing is only relevant to molten metal and salt-cooled AdvSMRs. Furthermore, some designs have advanced to the test reactor stage or beyond (i.e., sodium fast reactors), while others (i.e., supercritical water-cooled reactors) are only at the conceptual design stage (GIF 2011). Consequentially, the availability of design information and instrumental requirements varies greatly among AdvSMR designs.

An evaluation of published literature, Internet-based information, interlaboratory consultation, and in-house nuclear engineering expertise was used to identify proposed concepts for AdvSMR designs, along with likely operational characteristics. Publicly available government reports, such as U.S. Nuclear Regulatory Commission (NRC) documents, were used to obtain important information specific to nuclear reactor designs and I&C systems. DOE national laboratory and commercial vendor documents also provided valuable advanced reactor design and requirements information. A generalized AdvSMR instrumentation architecture that describes the major control and interface elements, their respective subsystems, and finally the process monitoring parameters relevant to the reactor I&C requirements, is presented. The process monitoring parameters are then linked to specific sensor elements, having distinct locations within the reactor. While this architecture represents a pool-type reactor design, the defined set of I&C requirements is expected to be representative of other proposed AdvSMR designs. For the purposes of this report, I&C and instrumentation, control, and human-machine interface systems are generally interchangeable terms. I&C terminology is used here, because this report focuses on specific in-vessel parameter monitoring systems and to a lesser extent human-machine factors, which are important in control room system designs.

A series of literature and Internet-based surveys were conducted to identify the various optical methods that could be used to measure key reactor parameters. Monitoring parameters such as temperature resulted in a vast number of optical sensing results. The scientific basis and method for each measurement technique is described in detail in this report. Additional surveys were conducted to identify optical materials that are used to fabricate optical components (e.g., fiber optics, probes, windows, lenses). These optical materials and their key performance specifications (e.g., maximum continuous temperature, radiation resistance, and chemical compatibility) are provided, where available, in tabular form. Optical components and technologies designed for extreme environments, such as magnetic confinement fusion research (i.e., International Tokamak Physics Activity), oil drilling, steel foundries, and aerospace industries, were surveyed to identify optical measurement techniques and materials possibly applicable to the AdvSMR application. These reviews also provided extensive insight into published experimental research literature that was focused on new optical sensing concepts under development (not commercially available), advanced optical materials under development for extreme environment applications, and optical materials damage mechanisms induced by long-term exposure to extreme environmental conditions. This report captures these salient research results and technical knowledge gaps from this large body of published research. This analysis summarizes promising avenues for future RD&D investments, which could lead to advanced commercial optical materials and sensor systems that could directly support future AdvSMR programs. We found that in some cases, the damage studies have contradictory conclusions or results that are difficult to compare. Many times the experimental conditions are not completely representative of expected in-vessel AdvSMR environments. In addition, the scope of the published scientific data is so immense, that it is quite likely that important

reported study results may have been missed. Given these limitations, we consider the conclusions drawn from these studies as a representative snapshot of the current scientific knowledge.

A COTS optical materials and sensor survey was conducted to determine the market's technical readiness to support the AdvSMR development program. We commenced the survey with several objectives in mind. First we acknowledged that many, if not all, optical-based I&C concepts will require an optical pathway into the reactor. This assumption was made, because sophisticated electro-optical systems, having for example an optical source, detectors, electronics, and other active and passive components, are unlikely to survive for a useful duration within the extreme in-vessel environment. Perhaps one exception is radiation-hardened cameras, where signals are transferred through the reactor vessel walls using an electrical feedthrough. Even in this example, these cameras are typically used only during refueling operations and inspections. These operations only occur over short periods of time, while the core is relatively cool and at low reactivity.

Optical monitoring concepts discussed in this report fall into one of several operational modes, including:

1. methods that feature standoff detection and analysis, requiring an optical port into the reactor vessel;

2. optical probes that could be inserted through a mechanical port into the reactor vessel; and

3. fiber-optic (or light pipe) systems that provide optical access into the reactor vessel to interface with discrete sensor elements. In some cases the fiber-optic systems provide both optical access and distributed sensing properties.

Successful and enduring optical system integration, therefore, will be largely dependent on thermal, mechanical, radiation-resistance properties of fiber-optic components and optical elements, such as access windows, lenses, and mirrors. Second-order factors include chemical resistance and optical properties.

Commercial vendors offering optical sensor systems and components relevant to AdvSMR I&C requirements were contacted as part of this study. This review attempts to provide a comprehensive review of COTS optical products available from national and international suppliers. While some COTS products may not be included in this survey (considering the hundreds of specialty manufacturers worldwide), the framework of this COTS survey and gaps analysis is expected to be a representative snapshot of this commercial market sector. In some cases, specific vendors and product specifications are provided in this report. These references do not necessarily constitute or imply any endorsement, recommendation, or favoring, but rather are presented as archetypal of the specific methods, technology, components, or materials.

Product specifications and applications documents were acquired from vendor websites. Vendors were also directly contacted to discuss the performance specifications and environmental limitations of their products. Many vendors offer optical components and sensing instrumentation designed for high-temperature or high-radiation resistance. In most cases, the maximum continuous temperature falls significantly short of the most stringent AdvSMR applications requirements and the radiation-resistance nomenclature is only qualitative. In this report, we include many sensing systems and components, which have specifications that may not meet the most stringent AdvSMR requirements, because they may find

use in a limited set of deployment scenarios or become more widely useful if engineering solutions are devised. For example, standoff optical systems could be used if an optical pathway could be engineered into the reactor vessel. Optical components with limited maximum temperature could possibly find applications in the cover-gas region, where the temperature is significantly lower than the outlet liquid coolant temperature.

The COTS survey data were then used to calibrate the technology gap analysis. The gaps analysis had several objectives, including:

1. evaluate the current shortcomings of optical-based COTS products by comparing the product specifications against the AdvSMR requirements;

2. suggest possible product development or enhancement opportunities to the commercial sector to support the AdvSMR program and other extreme environment markets; and

3. develop a RD&D and engineering plan to remedy the identified COTS technology gaps and deployment challenges.

This analysis strove to summarize the current technical readiness of each class of optical sensor or material, rather than drilling down to specific vendor products. Although many specific operational characteristics of AdvSMR designs were somewhat unclear or are subject to change, both the key parameters used for the COTS optical-based sensor assessment (e.g., temperature, radiation flux, pressure, chemical-resistance performance) and the technical gaps identified are not expected to change significantly as these designs evolve.

Both engineering concepts and innovative technology RD&D solutions will be required to reach the AdvSMR I&C objectives. Engineering concepts that enable optical access to the in-vessel environment are critical to this approach. Concepts include mechanical ports that allow insertion of optical probes, optical viewports for remote optical sensing, and optical pass-through ports for optical fibers components. Innovative RD&D will be required to adapt current optical measurement techniques for in-vessel deployment and develop or identify the potential for new sensing methods and advanced optical materials. Innovative RD&D of this nature could lead to significant technology advancements, such as advanced optical materials that have prolonged damage resistance to high temperature, radiation, and corrosive environments, and new optical system designs and techniques for remote inspection, system control, and process monitoring. Innovative RD&D requires a longer-term investment, consistent with the planned AdvSMRs development timetable, while promising engineering concepts may provide near-term opportunities to fast track evaluation and field trial studies.

1.2   COTS Optical Technology Ranking

Each COTS optical technology is given a ranking estimate of their technical readiness. Our ranking estimates are judgments made by the report authors based on best available technology information. Additionally, the ranking depends on where the optical technology is deployed with respect to the reactor core. Optical components inserted into an AdvSMR reactor vessel, near the core outlet, must withstand temperatures from 400°C to 750°C (depending on the AdvSMR design) and in some cases to the fuel failure temperature (i.e., >1650°C). Depending on the type of reactor, and location within the reactor vessel, radiation levels can vary significantly. Average in-vessel fluxes are typically between

6×10^{12} n/cm^2·s to 3×10^{14} n/cm^2·s for total neutrons and up to 10^6 Gy/h for gamma (Knoll 2000). However, peak core fluxes can exceed 10^{15} n/cm^2·s for fast and thermal neutrons, each, depending on the reactor type (INL 2009). Peak core gamma levels have been measured at 3×10^7 Gy/h.

Near the core only optical components, such as fibers, mirrors, retroreflectors, lenses, and optical probes are even feasible for deployment. Actual lifetimes of these components depend on many factors that are discussed in this report. The temperature and radiation conditions can vary drastically across the reactor vessel. Further from the core location, both the temperature and radiation levels can be significantly lower. Areas in the containment building or below the reactor vessel lid may be more feasible for longer-term deployment of optical components in the headspace region and mounted to standpipes or periscopes.

COTS optical sensing instruments are assembled using sensitive optoelectronic components (e.g., lasers, optical detectors, circuit boards, power supplies) that typically have a maximum working temperature around 40°C. Radiation-hardness specifications are also rarely provided from vendors. In general, it is very unlike any optical measurement instrument could be deployed as an in-vessel AdvSMR I&C system. However, the remote, noncontact sensing configuration provided by the optical measurement systems reviewed in this report allow standoff placement of the sensitive instrument at regions with lower temperature and radiation exposure conditions. It should be feasible to deploy optical sensing instrumentation in the containment building, near the biological shield for example, where the instrumentation can be isolated from temperatures above 40°C and where radiation exposure (i.e., estimated ~1–10 Gy/h gamma, $<10^{11}$ n/cm^2 s) is managed using the appropriate shielding. In addition, it should be feasible to locate fiber-coupled sensing instruments further away in the instrumentation vaults if required. Having established the AdvSMR installation expectations for the sensor instrumentation, next we examined the optical front end (i.e., optical access and in-vessel optical components) of these standoff systems.

For COTS optical components located in-vessel or in direct proximity, we considered two deployment scenarios:

1. **Near-core**: The first places the optical components near the extremes of the reactor core to facilitate optical access or sensing in this region. Nominal expected conditions include temperatures up to 750°C, gamma at 10^6 Gy/h, and neutron flux at 5×10^{13} n/cm^2 s. Peak instantaneous and off-normal events can far exceed these values and conditions can vary greatly depending on the reactor design. Almost no vendor or research study information is available to confidently judge optical component lifetime under these expected extreme near-core temperature and radiation conditions. In many cases, no technical readiness or ranking can be established for these materials and components. However, a few notable optical materials, optical components, and optical fibers have been demonstrated that exhibit very promising radiation-resistance performance. The maximum working temperature specifications for these optical materials and components are also very promising, with the exception of the coatings, sheathing, and cabling materials used on optical fibers to improve their abrasion resistance and mechanical strength. Generally, there remain knowledge gaps on the combined high-temperature and chronic radiation-exposure effects with respect to component lifetime. Further RD&D efforts will be required to resolve these gaps and affirm the actual technical readiness for such a challenging

application. Nevertheless, for many materials and components, advancements are expected to come quickly with a focused effort.

2. **Near reactor lid (headspace or containment building area)**: The second scenario places optical components near the reactor lid, in the headspace area, or mounted to a standpipe to provide optical access into the reactor vessel. In this case, the temperature and radiation conditions are much lower compared to the core area. Nominal expected conditions include temperatures that range between 100°C to 400°C, gamma at $<10^4$ Gy/h, and neutron flux at 10^{11} n/cm^2 s or lower. Many optical materials have technical specifications or have received enough relevant research study to judge their technical readiness to meet the design requirements.

Based on the requirements of each scenario listed above, the following ranking criteria have been established for both optical materials and optical components:

> **Three technology readiness tiers have been established to rank COTS optical materials and components against the in-vessel optical component requirements, either for near-core or near reactor lid deployment:**
>
> 1. **HIGH** – Mature technology, readily suitable to AdvSMR optical access design requirements with modified COTS or semi-custom vendor sensor components, pending exposure studies, some further development, and demonstration studies
>
> 2. **MEDIUM** – Evolving technology, some RD&D effort is needed to develop both custom vendor and new R&D optical components, followed by extended exposure and demonstration studies
>
> 3. **LOW** – Emerging technology, considerable RD&D is needed to evaluate COTS and develop new optical materials, followed by comprehensive exposure and demonstration studies.

Technical readiness rankings are also provided for COTS optical sensing instruments, in terms of their ability to meet the AdvSMR I&C requirements. In all ranking levels, a considerable reactor engineering design effort will be required to develop and demonstrate concepts that provide optical access into the reactor vessel. All COTS instruments are either standoff or fiber-based optical sensing systems. We assumed that the sensitive sensor control instrumentation is isolated from temperatures above 40°C and radiation exposure is managed using the appropriate shielding. Based on these requirements and assumptions, the following ranking criteria have been established for optical sensing instrumentation:

> **Three technology readiness tiers have been established to rank COTS optical sensing systems against the in-vessel AdvSMR monitoring requirements:**
>
> 1. **HIGH** – Mature technology, readily suitable to AdvSMR designs with modified COTS or semi-custom vendor sensor components, pending demonstration studies and some further development
>
> 2. **MEDIUM** – Evolving technology, some RD&D effort is needed to develop both custom vendor and new R&D sensor components, followed by extended performance evaluation
>
> 3. **LOW** – Emerging technology, considerable RD&D is needed to develop new R&D sensor components and test new materials, followed by comprehensive performance evaluation.

In Sections 3.0 through 11.0 parameter COTS optical materials and measurements systems are evaluated for technical readiness using the criteria listed above. A ranking summary of the optical materials and components is provided in Table 1.1, for all rankings **MEDIUM** or higher. While many optical materials and components fail to meet the AdvSMR application requirements, we have identified many promising optical materials and components that appear feasible for this application. The maximum working temperature specifications for these optical materials and components are also very promising, with the exception of the coatings, sheathing, and cabling materials used on optical fibers to improve their abrasion resistance and mechanical strength. Generally, there remain knowledge gaps on the combined high-temperature and chronic radiation-exposure effects with respect to component lifetime. Further RD&D efforts will be required to resolve these gaps and affirm the actual technical readiness for such a challenging application. Nevertheless, for many materials and components, advancements are expected to come quickly with a focused effort. Finally, some **LOW** rankings were included in this summary, when 1) the optical technology could have significant impact to the AdvSMR application, 2) most of the performance specifications are exceptional, and 3) only one significant challenge remained to be solved.

Table 1.1. Summary of COTS Optical Materials and Components

Materials/Components	Near Core Technical Readiness	Near Lid Technical Readiness
CVD Diamond (materials)	**MEDIUM**	**HIGH**
ALON®[a] (materials)	**MEDIUM**	**HIGH**
Spinel (materials)	**MEDIUM**	**HIGH**
Sapphire (materials)	**MEDIUM**	**HIGH**
Fused Silica (materials)	**MEDIUM**	**HIGH**
Single-Crystal Molybdenum (mirror)	**HIGH**	**HIGH**
Single-Crystal Tungsten (mirror)	**HIGH**	**HIGH**
Single-Crystal Rhodium (mirror)	**MEDIUM**	**MEDIUM**
Al, Au metallized mirror	**LOW**	**HIGH**
Silica Optical Fiber	**LOW**	**HIGH**
Sapphire Optical Light Pipe	**LOW**	**HIGH**
Hollow-core Photonic Crystal Fiber	**LOW**	**HIGH**
(a) Surmet Corporation, Burlington, Massachusetts.		

The COTS optical sensing systems technical readiness rankings summary is also provided in Table 1.2 and Table 1.3 for all rankings **MEDIUM** or higher. Table 1.2 provides the ranking summary of COTS fiber-optical sensing systems. Here it assumes that the sensitive sensor control instrumentation is isolated from temperatures above 40°C and radiation exposure is managed using the appropriate shielding. This instrumentation would be deployed near the biological shield in the containment building, for example. An optical fiber would connect the sensor instrumentation to a fiber-optic feedthrough, located on the reactor vessel lid. A second optical fiber, with distributed, embedded sensor elements or a single element at the end of the fiber, is connected to the in-vessel side of the feedthrough. Both near-core and near-lid sensing applications are considered for this in-vessel sensing mode. The maximum working temperature specifications for the coatings, sheathing, and cabling materials used on optical fibers (to improve their abrasion resistance and mechanical strength) significantly limit the deployment options. Generally, there remain knowledge gaps on the combined high-temperature and chronic radiation-exposure effects with respect to component lifetime. Further RD&D efforts will be required to resolve these gaps and affirm the actual technical readiness for such a challenging application. Nevertheless, for many materials and components, advancements are expected to come quickly with a focused effort. While many of the COTS optical-sensing systems fail to meet the AdvSMR application requirements, we have identified many promising optical materials and components that appear feasible for this application.

Table 1.2. Summary of COTS Fiber-Based Optical Sensor Technology

Optical Sensing Technology	Measurement Parameter	Near Core Technical Readiness	Near Lid Technical Readiness
Semiconductor Bandgap Sensing	Temperature	**LOW**	**MEDIUM**
Backscattering OTDR	Temperature	**LOW**	**HIGH**
Fabry-Pérot Sensing	Temperature, Pressure	**LOW**	**HIGH**
Fiber Bragg Grating Sensing	Temperature, Pressure	**LOW**	**HIGH**
Intensity-Modulated Membrane	Pressure	**LOW**	**HIGH**
OTDR = optical time domain reflectometer			

Table 1.3 provides the ranking summary of standoff, noncontact optical sensing systems. Here it assumes that the sensitive sensor control instrumentation is isolated from temperatures above 40°C and radiation exposure is managed using the appropriate shielding. This instrumentation would be deployed near the biological shield in the containment building, for example. The active or passive standoff optical configuration would use an optical access port to interrogate a region within the reactor vessel. The standoff optical-sensing systems typically can meet the maximum working temperature specifications for the AdvSMR application. Standoff sensing system will require optical components for in-vessel optical access, image or sensing beam relay from the sensor instrumentation to the viewport, and additional optical components within the reactor vessel to guide the optical beam to the intended in-vessel location. Optical access represents a significant engineering challenge that will be discussed in Section 2.4. The technical readiness rankings for these optical components are given in Table 1.1 and are not factored into the standoff optical sensing systems technical rankings list in Table 1.3.

Table 1.3. Summary of COTS Standoff Optical Sensing Technology

Optical Sensing Technology	Measurement Parameter	Technical Readiness
Absorption-Based Spectroscopy	Chemical Concentration	**MEDIUM**
Tunable Diode Laser Spectroscopy	Chemical Concentration	**MEDIUM**
Emission-Based Spectroscopy	Chemical Concentration	**MEDIUM**
Laser-Induced Breakdown Spectroscopy	Chemical Concentration	**MEDIUM**
Laser Rangefinding	Coolant Level	**MEDIUM**
Laser Doppler Vibrometry	Vibration	**MEDIUM**
Radiation-Hardened/Disposable Cameras	Imaging	**MEDIUM**
Thermographic Cameras	Temperature/Imaging	**MEDIUM**
Pyrometry	Temperature	**MEDIUM**

1.3   Organization of Report

This document is organized by major sections that generally include an introduction, science background, promising R&D, COTS summary, gaps analysis, ranking, and suggested future research path subsections. There are some departures from this structure to accommodate the information content, such as the AdvSMR design and Optical Materials sections. Because of the length of this report, each section

is intended to be stand-alone in nature. References are provided at the section end for readers interested in further details of the subject matter.

Section 2.0 describes an overview of AdvSMR designs, highlighting uniqueness, principal uses, advantages, and potential shortcomings. Also presented are the potential challenge areas for sensing and monitoring instrumentation and opportunities for optical-based techniques. A generalized AdvSMR instrumentation architecture that describes the major control and interface elements, the respective subsystems, and finally the process monitoring parameters relevant to the reactor I&C requirements is provided. These monitoring parameters are shown by location within a notional pool-type reactor vessel. Finally, we present several conceptual approaches to gain optical access into the reactor vessel. Further development of these concepts is vital to enable eventual deployment of optical-based monitoring systems.

Section 3.0 contains a summary and analysis of candidate optical materials and components that could be used in-vessel to enable monitoring and sensing applications. The requirements are established for the AdvSMR application and compared against the COTS optical technology specifications. The technical gaps are established and finally a future research path is suggested. Sections 4.0 to 11.0 examine each major AdvSMR monitoring parameter (e.g., imaging, temperature, pressure, flow). In similar fashion the COTS technology analysis is provided. Section 12.0 contains the proposed future research path and Section 13.0 is the report summary. Appendixes A–E provide additional AdvSMR design details.

1.4 References

DOE. 2010a. *Nuclear Energy Enabling Technologies Workshop Report, July 29, 2010, Rockville, Maryland*. U.S. Department of Energy (DOE), Washington, D.C. Available at http://energy.gov/sites/prod/files/Neet_Workshop_07292010.pdf.

DOE. 2010b. *Nuclear Energy Research and Development Roadmap, Report to Congress, April 2010*. U.S. Department of Energy (DOE), Washington, D.C. Available at http://nuclear.gov/pdfFiles/NuclearEnergy_Roadmap_Final.pdf.

DOE. 2010c. *Panel 2 Summary - SMR Instrumentation, Controls, and Human-Machine Interface*. U. S. Department of Energy (DOE), Office of Nuclear Energy. Washington, D.C. Accessed May 29, 2013. Available at http://www.ne.doe.gov/smrworkshop/docs/Instrumentation_PanelSum.pdf

GIF. 2011. *Annual Report 2011, Gen IV International Forum*. Gen IV International Forum (GIF), Paris, France.

INL. 2009. *FY 2009 Advanced Test Reactor National Scientific User Facility Users' Guide*. INL/EXT-08-14709, Advanced Test Reactor, Idaho National Laboratory (INL), Idaho Falls, Idaho.

Knoll GF. 2000. *Radiation Detection and Measurement, Third Edition*. John Wiley & Sons, Hoboken, New Jersey.

NERAC. 2002. *A Technology Roadmap for Generation IV Nuclear Energy Systems - Ten Nations Preparing Today for Tomorrow's Energy Needs*. GIF-002-00, U.S. DOE Nuclear Energy Research Advisory Committee (NERAC) and the Generation IV International Forum (GIF), Washington, D.C. Available at http://www.osti.gov/energycitations/servlets/purl/859029-304XRr/.

2.0 Advanced Small Modular Reactor Designs

2.1 AdvSMR Design Detail

This section will introduce the various advanced small modular reactor (AdvSMR) designs, and highlight their uniqueness, principal uses, advantages, and potential shortcomings. Also presented are the potential challenge areas for sensing and monitoring instrumentation and opportunities for optical-based techniques. Sensing and monitoring instrumentation must operate under higher coolant operating temperatures, compared to light-water reactors (LWRs), which prevents direct use of some conventional instrumentation.

Defining the most significant set of AdvSMR concepts is challenging because it is subject to the interpretation of a number of government programs and national laboratory and industry development programs. Lists of candidate concepts become quickly outdated as government funding trends and economic factors shift. To minimize the risk of becoming quickly dated, we examined the concepts under consideration by the Generation IV (Gen IV) International Forum (GIF). Next, we categorized these concepts (and others) by the level of their maturity. Designs with great maturity are likely to remain on the short list longer. Many concepts share common features (i.e., coolants), but can be distinguished by their fuel geometry.

AdvSMRs are based on advanced reactor concepts with projected deployment several decades away. The GIF identified six key advanced nuclear power generating technologies to help focus future international resources and efforts to establish the feasibility and performance of future generation reactors (expected deployment beyond 2030). Many of the Gen IV concepts target alternative missions such as the generation of process heat, heat for water desalinization, or heat for hydrogen production. In addition, coupling with advanced electricity production cycles such as He-Brayton, supercritical CO_2-Brayton, and supercritical-water-Rankine cycle is a priority of Generation IV systems (NERAC 2002). Candidate technologies proposed by the GIF include (NERAC 2002; Abram and Ion 2008):

- sodium-cooled fast reactors (SFRs)
- gas-cooled fast reactors (GFRs)
- very high-temperature reactors (VHTRs)
- lead- (or lead-bismuth-) cooled fast reactors (LFRs)
- molten salt reactors (MSRs)
- supercritical water-cooled reactors (SCWRs).

The VHTR concept is an evolutionary extension of the high-temperature gas-cooled reactor (HTGR). The VHTR extends current HTGR technology to increase the coolant outlet temperature from 850°C to 1000°C. The MSR and fluoride salt-cooled high-temperature reactor (FHR) share the same molten salt coolants. MSRs use fuel that is dissolved in the coolant, whereas FHRs use coated particle fuels similar to HTGR designs. There are other reactor concepts under consideration, but these were considered outside the scope of this report.

The level of funding, concept and deployment maturity, and economic viability are convenient metrics that can be used to categorize the current interest levels for various AdvSMR concepts. Certainly this approach is subject to debate. We used a three-class system to prioritize reactor concepts, taking in account these metrics. Tier I designs are relatively mature, with test reactors having been built and operated. These include SFR and HTGR designs. Tier II concepts are technically interesting and research investments are currently advancing the concepts. These include FHR and LFR designs. Tier III concepts have desirable characteristics, but research investments are modest. They include GFR, MSR, VHTR, and SCWR concepts. We acknowledge that there may be additional criteria to rank these concepts by, but the proposed approach represented our best understanding of current government program and industry priorities.

Table 2.1 summarizes operating parameters for the major advanced reactor concepts listed above and compares them against typical operating conditions within boiling water reactors (BWRs) and pressurized water reactors (PWRs). These parameters include core inlet/outlet temperature, vessel pressure, combined total neutron flux, power density, and thermal efficiency. Advanced reactor concepts are expected to all operate at temperatures far above those found in current LWRs. Core outlet temperatures provide a sense for highest temperatures that in-vessel sensing systems would be expected to tolerate. Vessel pressures vary from atmospheric to 25 MPa depending on the AdvSMR concept. Pressure is a critical consideration when engineering optical pathways into the reactor vessel.

The radiation environment within the reactors is important, because high neutron and gamma flux can quickly damage vessel components, as well as optical components. Even though AdvSMRs do not necessarily have larger average radiation flux compared to LWRs, in-vessel components must endure higher radiation exposure, because the smaller reactor vessel size and closer proximity to the core. AdvSMR neutronics are often reported in the literature inconsistently using both flux and fluence, and in many instances are based largely on simulations and extrapolation. Published values for neutron flux in AdvSMR concepts often differed greatly. Many estimates lacked validation because of the maturity of the AdvSMR. Flux (i.e., fluence rate) is the most useful way to characterize the neutron environment, because it can be used to estimate total dose over any period of time. It is important to also estimate the fluxes of both thermal and fast neutrons, but this information was not always available. Fast neutrons typically have a larger impact on material degradation and can penetrate most materials to a greater depth compared to thermal neutrons because of decreased cross-section (Knoll 2000).

For the purposes of this report, we extrapolated the average total neutron flux for AdvSMR concepts by scaling PWR average total neutron flux (5×10^{13} n/cm^2·s) to core power density. While not exact, this is a reasonable scaling estimation (Kolev 2011). The in-vessel gamma flux is discussed later in this section. Power density describes the amount of thermal energy generated per unit area of the reactor core. Thermal efficiency describes the ability to convert thermal to electrical energy, and generally increases as a function of reactor temperature.

Table 2.1. Summary of AdvSMR Expected Operating Conditions

Reactor Type	Core Inlet/Outlet Temp. (°C)	Vessel Pressure (Mpa)	Average Total Neutron Flux ($n/cm^2 \cdot s$)	Power Density ($MWth/m^3$)	Thermal Efficiency (%)	References
BWR/PWR	292/330	7/15.5	5×10^{13}	56/98	34	Knoll (2000); Westinghouse (2002); Nelson (2008); Ragheb (2011)
SFR	500/550	Ambient (0.1)	2×10^{14}	350	36	Zrodnikov et al. (2005); Hoffman et al. (2006); Ragheb (2011)
LFR	400/480 420/567[a]	Ambient (0.1)	4×10^{13}	69	40	Sienicki et al. (2006) Ragheb (2011)
GFR	400/780	7	5×10^{13}	100	48	Driscoll et al. (2008); Stainsby et al. (2011); Tauveron and Bentivoglio (2012); Zabiego et al. (2013)
HTGR	450/750	7	3×10^{12}	6	50	Potter and Shenoy (1996); Moses (2010)
VHTR	500/1000	7	3×10^{12}	6	50	Taiwo et al. (2005); Moses (2010)
MSR	650/700	Ambient (0.1)	8×10^{12} to 3×10^{14}	15-500	43	Adamovich et al. (2007); Memoli et al. (2009); Waris et al. (2010); Cammi et al. (2011); Devanney (2012)
FHR	650/700	Ambient (0.1)	6×10^{12} to 8×10^{12}	9.4 to 12.9	45	Forsberg et al. (2005); Alekseev (2010); Greene et al. (2010); Holcomb et al. (2012)
SCWR	500/625	25	5×10^{13}	100	44	Duffey et al. (2011); Ragheb (2011)

(a) ELSY and SSTAR, respectively – see http://www.gen-4.org/Technology/systems/lfr.htm.

Table 2.1 provides guidance for typical AdvSMR operating parameters; however, actual temperature and radiation flux values will vary significantly depending on the location and distance relative to the reactor core. Expected temperature and radiation flux variations are shown in Figure 2.1 for both liquid- and gas-coolant designs operating at full power. The design requirements for in-vessel monitoring components will clearly depend on the specific component location within the reactor. Outside the core, it is expected that the neutron flux will drop quickly. Gamma flux will be high near the core, but also can remain high in coolants with high neutron activation properties (i.e., sodium).
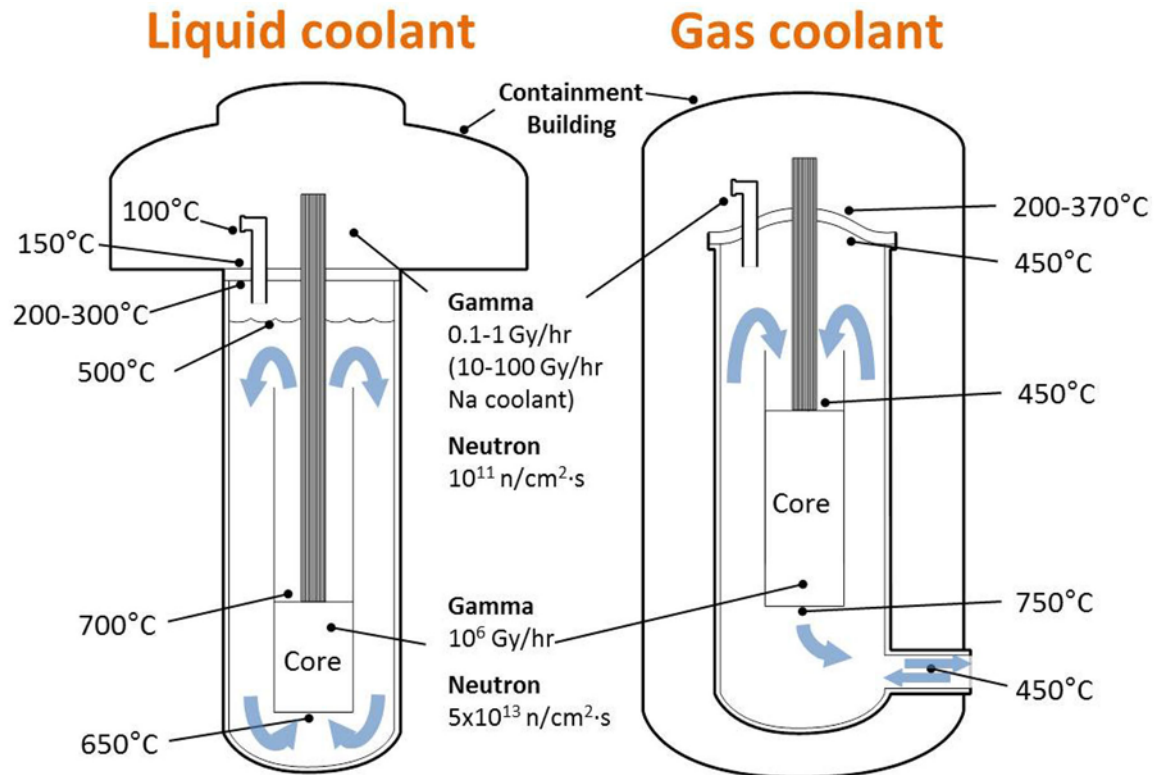
Figure 2.1. Expected Temperature and Radiation Distributions for Liquid- and Gas-Cooled Reactors

The AdvSMR concepts share many common in-vessel monitoring requirements and challenges. Monitoring challenges offer potential opportunities to introduce optical monitoring techniques to the designs if practical. In some cases, current technology provides adequate performance and further discussion of alternate optical-based solutions is unnecessary. Design-specific challenges are detailed later in each AdvSMR concept section. Not every monitoring requirement has been captured, but rather we examine key requirements and shortcomings for many of the AdvSMR concepts. Common requirements, challenges, and opportunities are described as follows.

- *Coolant Temperature*: These measurements are typically made using resistance temperature detectors (RTDs). Measurements using optical-fiber sensor or remote optical methods may be feasible to eliminate RTDs and provide mapping of spatial temperature striations. Optical fiber sensors may be feasible below the liquid coolant surfaces. Optical sensing advantages include low drift, high bandwidth, standoff sensing, and distributed sensing. Superior performance over conventional temperature sensors may be possible. Further study will be required on a case-by-case basis to determine the benefits and performance of each optical monitoring approach.

- *Coolant Flow and Pressure*: Flow monitoring is not typically measured directly, but rather is extrapolated from mass heat flow calculations and coolant pump discharge pressure. Reflective spinning rotor techniques with optical readout also may be feasible for transparent coolants. Mechanical bellows and diaphragm designs are typically used to measure pressures in-vessel. Hydraulic NaK-filled impulse lines or transducer housings physically isolate electronic strain gauges from the in-vessel measurement point. These designs are simple and effective, but have several

disadvantages. NaK leakage has occurred, which introduces undesirable impurities into the coolant. Strain gauges have well-known drift, which requires frequent recalibration and maintenance. Fiber-Bragg grating sensors can be drop-in replacements for electronic strain gauges. Advanced designs feature temperature compensation and low drift. Optical-deflecting membrane-type sensors are now available to measure pressure, although material compatibility studies would be required. Superior performance over conventional flow and pressures sensors may be possible. Further study will be required on a case-by-case basis to determine the benefits and performance of each optical monitoring approach.

- *In-vessel Viewing/Inspection:* Visual inspection and monitoring are conducted in in-vessel (gas-cooled designs) or gas headspace (for liquid-coolant designs) during refueling or to confirm process assertions (i.e., control rod motion, failure). Monitoring corrosion, creep, and metal distortion is also important. Radiation-hardened cameras are used by the nuclear power industry, but they have a limited lifetime when used at full reactor power. Technology advances and mass-production economies have reduced the cost of conventional solid-state (non-radiation-hardened) cameras to the point that it is feasible to use them as disposable sensors. Engineering designs that enable placement of cameras outside the reactor vessel would significantly increase the camera's usable lifetime. Optical component (windows, camera lenses) fouling by coolant vapor deposits will be a significant issue.

- *Annulus Viewing/Inspection:* Visual inspection and monitoring are also conducted in the inert gas area between reactor vessel and containment to monitor vessel integrity, crack formation, and corrosion processes. The camera challenges and opportunities are the same as in-vessel viewing/inspection.

- *Neutron Flux/Power*: Neutron flux is measured at several locations around the reactor core as an indirect indicator of reactor power. Neutron flux is current measured by fission counters, ion chambers, gamma thermometers, and self-powered neutron detectors. AdvSMR have very high coolant temperatures that will challenge these traditional monitoring systems. Fission chambers, in particular, are limited to a maximum working temperature of about 550°C. A number of promising optical monitoring techniques have been proposed based on optical scintillation, Cherenkov radiation monitoring (MSR or FHR only), fiber damage monitoring, radiation-induced luminescence, and other techniques. Further study will be required on a case-by-case basis to determine the benefits and performance of each optical monitoring approach.

- *Loose Parts Monitoring:* Currently, accelerometers are located at strategic positions, usually in direct contact with pipes and other coolant-flow components. Metallic loose parts that impact the pipe sidewalls produce low-frequency mechanical vibrations, which are detected by the accelerometer. Commercial off-the-shelf (COTS) accelerometers may not be feasible to use in high-temperature AdvSMR coolants. Standoff optical vibrometry techniques may be feasible through gas coolants and on components above the liquid coolant level and perhaps through transparent coolants. Further study will be required on a case-by-case basis to determine the benefits and performance of each optical monitoring approach.

- *Intermediate Heat Exchanger (IHX):* IHX inlet/outlet temperature (indirect heat transfer measurement) is measured using thermocouples or RTDs mounted in drywells near the IHX. Flow/pressure can be measured using strain-gauge pressure sensors. A variety of optical monitoring techniques may be feasible to measure temperature and pressure. The advantages of each approach will have to be evaluated against conventional methods.

- *Control Rod Drive Mechanism (CRDM):* Control rods are used to regulate the neutronic flux generated by the reactor and also scram the reactor in the event of an upset. Traditionally electromechanical reed switches are used to detect rod position, velocity, and motion failure. Because precise control of the CRDM is vital to safe and efficient reactor operation, independent monitoring systems are needed. Optical-based position sensors may be feasible, as well as direct imaging systems. The camera challenges and opportunities are the same as in-vessel viewing/inspection.

In the following sub-sections, AdvSMR reactors are briefly described and the potential challenges for sensing and monitoring instrumentation listed. Also listed are potential areas where optical sensing techniques may affect AdvSMR concepts.

2.1.1   Sodium-cooled Fast Reactors

The SFR is one of the most mature advanced reactor designs. This design is categorized as a Tier I AdvSMR, because it has strong potential for near-term deployment. It features very high core power densities, high reactor outlet temperatures, low system pressure (atmospheric), and a fast neutron spectrum. An advantage of sodium coolant is its relatively high thermal conductivity, which enables very efficient heat transfer from the core. However, internal core and reactor vessel components are exposed to a significant fast neutron flux. Sodium has well-known chemical reactivity with air and water, so maintaining SFR vessel and component integrity is critical.

The primary coolant system can either be arranged in a pool layout (a common approach, where all primary system components are housed in a single vessel), or in a compact loop layout. Several domestic SFR designs (e.g., Power Reactor Innovative Small Module [PRISM], traveling-wave reactor [TWR]) use a pool-type reactor vessel design containing the reactor core, primary heat exchanger, and electromagnetic (EM) pumps. An inert cover gas system is used to maintain sodium purity and avoid undesirable chemical reactions. In general, penetrations into the reactor vessel occur at the top of the vessel. Further information regarding modularized SFR concepts is provided in Appendix A.

SFR and LFR are the two reactor designs distinguished by their molten metal coolants. These metals are completely opaque to electromagnetic waves, which is why coolant-immersion sensors are typically electronic or acoustic in nature. Optical sensors in liquid metal reactors may find roles in gas headspace monitoring or possibly direct coolant surface measurements.

In-vessel SFR Monitoring Requirements, Challenges, and Opportunities

- *Coolant Temperature*: Measurements using optical methods may be feasible to eliminate RTDs, which typically require penetration into the primary or secondary loop and have been a source of sodium coolant leakage and resultant fires. Optical access into the reactor vessel will require a highly reliable design to prevent similar problems. Further study will be required on a case-by-case basis to determine the benefits and performance of each optical monitoring approach.

- *Coolant Flow and Pressure*: These measurements are typically made using magnetic detectors made possible by unique properties of liquid sodium. Developing optical-based sodium coolant flow monitoring methods is likely unnecessary based on the acceptable performance of conventional techniques and would be challenging because of the coolant opacity.

- *EM Pump Monitoring*: Degradation and performance is determined by monitoring vibration, temperature, voltage, and current. Vibration monitoring is used to detect impending failure. COTS

accelerometers may not be feasible to use in high temperature AdvSMR coolants. Optical vibrometry techniques may be feasible on components above the coolant level. Further study will be required on a case-by-case basis to determine the benefits and performance of each optical monitoring approach.

- *Coolant Level*: In-vessel molten sodium level can be measured using ultrasonic transducers and other conventional techniques. It is unclear whether optical-based monitoring techniques have a decided advantage over current methods. If required, noncontact laser ranging or other optical methods may be feasible. Further study will be required on a case-by-case basis to determine the benefits and performance of each optical monitoring approach.

- *In-vessel Viewing/Inspection*: Higher temperatures and radiation levels (sodium-activation and high gamma flux) in sodium-cooled AdvSMR pose a challenging problem for COTS cameras. Optical component (windows, camera lenses) fouling by sodium vapor deposits will be a significant issue.

- *Coolant and Cover Gas Chemistry Monitoring*: Coolant monitoring and purification is generally conducted using process loops external to the reactor vessel; however, in-vessel monitoring could be required for future AdvSMR concepts. Impurity analysis is conducted to monitor corrosion indicators and detect component or fuel failures. H_2O, CO_2, and O_2 can be monitored in the cover gas area using optical spectroscopy methods. Fission gases and fuel pin taggant gases are noble gases without strong optical absorption spectra at usable wavelengths. Optical emission spectroscopy may be effective at detecting noble gases either by active ionization (e.g., laser, spark gap) or possibly radiation-induced autoionization. It may be possible to measure oxygen concentration (i.e., indirect measurement of NaO_2 impurity) and other impurities directly in the molten coolant using laser-induced breakdown spectroscopy (LIBS).

- *Flow Blockage Detection*: Detecting flow blockage of the coolant through the core is currently a challenging problem. Imaging and processing methods could be developed to monitor changes in coolant surface ripples, which may provide information about changes in coolant flow properties. The camera challenges and opportunities are the same as in-vessel viewing/inspection.

2.1.2   Lead- (or Lead-Bismuth-) Cooled Fast Reactors

The LFR design is categorized as a Tier II AdvSMR, because it has a long history as Russian naval reactors and research investments are advancing the design. The LFR system features a higher reactor outlet temperature, high power density core, low system pressure, and a fast neutron spectrum. The liquid metal coolant, either lead (Pb) or lead/bismuth eutectic (Pb-Bi), can utilize natural convection for heat removal or can be pumped, depending on core power requirements. Some LFR designs, like the small, secure, transportable, autonomous reactor (SSTAR), for small grids or developing countries, use a factory-built "battery" or "cassette" design and are optimized for power generation over long periods of time (10–30 years) without refueling.

LFR designs have a number of technical issues that must be managed. Corrosion can be a major problem with molten lead coolants. The dissolved oxygen content in lead-cooled reactors must be carefully balanced to minimize structural material corrosion. A proper dissolved oxygen fraction in the molten lead establishes and maintains a protective oxide barrier on stainless steels and low-alloy steels that protects them from corrosion up to about 500°C. Without this oxide barrier, nickel and other components of steel alloys are leached out and dissolved in the lead coolant over time. This process leads to embrittlement, cracking, and corrosion of the in-vessel components.

The isotope ^{210}Po is produced by neutron activation in LFRs. ^{210}Po is a pure and intense alpha emitter with a half-life of about 140 days. This alpha source tends to get distributed throughout the reactor vessel and poses a health risk for plant personnel, especially during maintenance activities. Potential issues with lead-cooled technologies arise from the solidification of the coolant, which can render the reactor inoperable. Lead is the heaviest of all proposed advanced coolants, making it challenging to circulate by mechanical pumps. Further information regarding LFR concepts is provided in Appendix B.

SFR and LFR are reactor designs distinguished by their molten metal coolants. These metals are completely opaque to electromagnetic waves, which is why coolant-immersion sensors are typically electronic or acoustic in nature. Optical applications in liquid metal reactors are expected to play some role in gas headspace monitoring or possibly direct coolant surface measurements.

In-vessel LFR Monitoring Requirements, Challenges, and Opportunities

- *Coolant and Cover Gas Chemistry Monitoring*: Coolant monitoring and purification is generally conducted using process loops external to the reactor vessel; however, in-vessel monitoring could be required for future AdvSMR concepts. Oxygen concentration in the coolant is monitored as part of Pb or Pb-Bi coolant chemistry control. The coolant is corrosive to structural steels (e.g., stainless steels and low-allow steels). Controlling dissolved oxygen in the coolant maintains an oxide barrier (effective up to about 500°C) to these structural materials to reduce corrosion. This implies the presence of dissolved oxygen in the coolant in equilibrium with oxygen gas in the cover gas plenum above the coolant (IAEA 2007a; Smith 2010). Gas phase O_2 can be monitored in the cover gas area using optical spectroscopy methods. Detection and monitoring polonium in the lead coolant is important to managing the health risk to plant personnel (IAEA 2007a). It may be possible to measure oxygen concentration and corrosion by-products (e.g., iron, nickel, and chromium) directly in the molten coolant using LIBS. CO_2 and O_2 can be monitored in the cover gas area using optical spectroscopy methods. Fission gases and fuel pin taggant gases are noble gases without strong optical absorption spectra at usable wavelengths. Optical emission spectroscopy may be effective at detecting noble gases either by active ionization (e.g., laser, spark gap) or possibly radiation-induced autoionization.

- *EM Pump Monitoring*: Degradation and performance is determined by monitoring vibration, temperature, voltage, and current. Vibration monitoring is used to detect impending failure. COTS accelerometers may not be feasible to use in high-temperature AdvSMR coolants. Optical vibrometry techniques may be feasible on components above the coolant level. Further study will be required on a case-by-case basis to determine the benefits and performance of each optical monitoring approach.

- *Coolant Flow and Pressure*: Pressure measurements may be made using strain gauge instrumented diagram transducers. Other conventional techniques are used also. Flow can indirectly be determined using differential pressure measurements. Strain gauges have well-known and undesired drift. Optical Bragg grating sensors are commonly used as a direct replacement for electronic strain gauges. Further study will be required on a case-by-case basis to determine the benefits and performance of each optical monitoring approach.

- *Coolant Level*: In-vessel molten-lead level can be measured using ultrasonic transducers and other conventional techniques. It is unclear whether optical-based monitoring techniques have a decided advantage over current methods. If required, noncontact laser ranging or other optical methods may be feasible. Further study will be required on a case-by-case basis to determine the benefits and performance of each optical monitoring approach.

- *Flow Blockage Detection*: Detecting flow blockage of the coolant through the core is a challenging problem. Imaging and processing methods could be developed to monitor changes in coolant surface ripples, which may provide information about changes in coolant flow properties. The camera challenges and opportunities are the same as in-vessel viewing/inspection.

2.1.3   Gas-Cooled Reactors

2.1.3.1   Gas-cooled Fast Reactors

The main characteristics of GFRs include operation with a fast neutron spectra, robust refractory fuel, high operating temperature, use of helium gas coolant, and potential to couple directly with He-Brayton power conversion cycles. To enable a fast neutron spectrum, the GFR does not include graphite moderators. The relatively poor heat-transfer properties of a gas coolant place severe requirements on fuel and cladding components to survive extreme temperatures. In contrast, in thermal spectrum gas-cooled reactors, the presence of graphite blocks provides a large thermal inertia to limit heating rates in the event of an accident. The GFR concept is categorized as a Tier III AdvSMR, because significant development will be required to advance the concept. Additional information about GFR concepts may be found in Appendix C.

Helium is a noble gas that has no absorption lines in the visible or infrared spectrum. Helium's optical transparency is an ideal medium in which to perform optical spectroscopy and other remote optical measurements. Complications will likely come not from intrinsic absorptions, but from spatial refractive index variations caused by extreme thermal transients and gradients.

2.1.3.2   High-Temperature Gas-cooled Reactors and Very High-Temperature Gas Reactors

The HTGR design is categorized as a Tier I AdvSMR, because helium-cooled reactors have been under development since the 1960s. HTGR reactors have been developed and operated at a number of locations (e.g., Dragon, AVR, Peach Bottom, Fort St. Vrain, THTR-300, HTTR, HTR-10). The very high-temperature gas reactor (VHTR) is an evolution of HTGR technology. VHTRs are distinguished by the intent to operate at greater temperatures (up to 1000°C) to facilitate hydrogen production. The VHTR concept is categorized as a Tier III AdvSMR, because of the unresolved materials challenges imposed by these extreme temperatures. The main characteristics of VHTRs include the use of helium gas for coolant, use of graphite for major core and in-vessel components, low power density, high operating temperature, use of coated fuel particles, and reliance on passive mechanisms for heat removal in the event of a loss-of-coolant accident (LOCA). These design characteristics help maintain the integrity of the fuel and prevent the release of radioactive materials in the event of severe accidents. Another significant advantage of the helium gas reactor designs is that they enable direct coupling to He-Brayton energy conversion cycles.

Two major HTGR concept variants include the pebble bed and prismatic block reactors. In the pebble bed reactors, coated fuel particles are embedded in spherical graphite pebbles, which circulate through the core. Reactivity is controlled through the distribution of pebbles loaded with fuel and absorber materials. This reactor concept enables online refueling as individual pebbles can be removed from the core and fresh pebbles may be added continuously. In prismatic block reactors, the reactor must

be shut down for refueling and control rods are employed for reactivity control. Appendix C contains further information about VHTR concepts.

In-vessel Gas-cooled Reactor Monitoring Requirements, Challenges, and Opportunities

- *Coolant Gas Chemistry Monitoring:* Coolant monitoring and purification is generally conducted using process loops external to the reactor vessel; however, in-vessel monitoring could be required for future AdvSMR concepts. Impurity analysis is conducted to monitor corrosion indicators and detect component or fuel failures. H_2O, CO_2, CO, CH_4, and O_2 can be monitored using optical spectroscopy methods. Fission gases and fuel pin taggant gases are noble gases without strong optical absorption spectra at usable wavelengths. Optical emission spectroscopy may be effective at detecting noble gases either by active ionization (e.g., laser, spark gap) or possibly radiation-induced autoionization. Cesium deposit could be detected using LIBS techniques. Tritium (T), HT, and TF gases may be present in the reactor vessel headspace. Further study will be required to determine if optical detection and monitoring is feasible.

- *Coolant Flow and Pressure:* There are no established methods for directly measuring flow in gas-cooled reactors, but it can indirectly be determined using differential pressure, temperature, and pumping rate. Optical techniques, like reflective rotors, may be feasible for flow measurement in a gas-cooled reactor. Pressure measurements are generally made using strain gauge diaphragm transducers located on coolant loops. Helium-filled impulse lines can sometimes be implemented, but these may be impractical because of access problems. Gas-filled impulse lines also suffer from long response times. Strain gauges also have well-known and undesired drift, especially in varying high-temperature environments. In an HTGR, both absolute and differential pressure measurements are highly desirable. Optical Bragg grating sensors are commonly used as a direct replacement for electronic strain gauges. Further study will be required on a case-by-case basis to determine the benefits and performance of each optical monitoring approach.

- *Vibrometry*: Vibration monitoring is used to detect impending failure of in-vessel components. Vibration monitoring is particularly important in gas-cooled reactor designs, because of the high coolant flow rates. Vibration in generally monitored using accelerometers. COTS accelerometers may not be feasible to use in high-temperature gas coolants. Standoff optical vibrometry techniques may be feasible through gas coolants. Further study will be required on a case-by-case basis to determine the benefits and performance of each optical monitoring approach.

2.1.4   Molten Salt Reactors and Fluoride Salt-Cooled Reactors

The MSR is an earlier, distinct, design that differs from FHRs because it uses dissolved fuel that circulates with the coolant, thus allowing refueling without reactor shutdown. This reactor type can be designed to operate with either a thermal or fast neutron flux and has the unique characteristic that very high fuel burn-up can be achieved because fuel performance in the fluid-fueled concepts is not limited by fuel cladding strength and ductility considerations. The majority of modern research focuses on FHRs, which feature moderate- to high-power density, high reactor outlet temperatures, and low system pressure. FHR designs (e.g., advanced high-temperature reactor [AHTR], pebble bed advanced high temperature reactor [PB-AHTR], small modular advanced high-temperature reactor [SmAHTR]) use molten-salt as the coolant and a more common solid fuel approach. FHRs can be used for electricity generation, actinide burning, and hydrogen and fissile fuel production. FHR concepts employ a mixture of lithium and fluoride salts as coolant. The salt mixture can be highly corrosive if impurity levels are too

high. The FHR design is categorized as a Tier II, because it has strong current interest and current research is advancing the design. Although the MSR design has a longer development history, the MSR is categorized as a Tier III, because of the limited ongoing research. Additional information about MSR and FHR concepts may be found in Appendix D.

Optical sensing and monitoring systems may be feasible in the headspace region and through the molten salt coolant. Several molten fluoride salt compositions that are being considered for FHR coolants are listed in Table 2.2. These are all mixtures of alkali metal fluorides with zirconium tetrafluoride, (ZrF_4), or in one case BeF_2. Figure 2.2 shows the optical transparency of one of these molten fluoride eutectics. Another illustration of the transparency of such materials is the metal fluoride glass ZBLAN, which is used to make infrared transmitting optical fibers. ZBLAN contains ZrF_4, NaF, BaF_2, LaF_3, and AlF_3 and can have absorption loss below 1 dB per meter between 300 nm and 3500 nm.

Table 2.2. Molten Salt Compositions under Consideration for Salt-Cooled Reactor Concepts

Molten Salt Composition	Fuel	Reference
KF-ZrF_4		Williams et al. (2006)
^7LiF	Liquid UF_4-ThF_4	Locatelli et al. (2012)
^7LiF-BeF_2	Solid TRISO Pebble	Locatelli et al. (2012)
LiF-BeF_2-ThF_4		Bamberger et al. (1971)
LiF-NaF-BeF_2		Williams et al. (2006)
LiF-NaF-KF		Young (1967)
LiF-NaF-RbF		Williams et al. (2006)
LiF-NaF-ZrF_4		Williams et al. (2006)
LiF-ZrF_4		Williams et al. (2006)
$NaCl$ (58%)-$MgCl_2$(42%)	Solid U-TRU-Zr Pins	Todreas et al. (2008)
NaF-BeF_2		Williams et al. (2006)
NaF (10%)-KF(48%)-ZrF_4(42%)		Forsberg et al. (2005)
NaF(6.2%)-RbF(45.8%)-ZrF_4(48%)		Forsberg et al. (2005)
NaF-ZrF_4	Liquid UF_4-ThF_4	Forsberg et al. (2005)
Rb-ZrF_4		Williams et al. (2006)
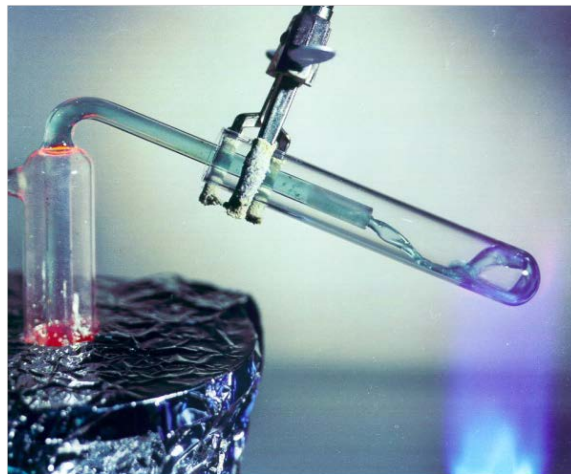
Figure 2.2. Demonstration Showing that Molten Fluoride Salts are Transparent (Forsberg 2004)

In between 1959 and 1973 Oak Ridge National Laboratory conducted extensive experiments on spectroscopy of certain solutes in molten fluoride salts (Young and White 1959, 1960a, b; Young and Smith 1964; Young 1967; Young et al. 1967; Whiting et al. 1969; Young et al. 1974). Four distinct eutectic fluoride salts are mentioned in this body of work: $LiF-BeF_2$ (known as FLiBe), $LiF-NaF-KF$ (known as FLiNaK), $LiF-BeF_2-ZrF_4$, and $LiF-BeF_2-ThF_4$. Among these, FLiBe and FLiNaK make up the majority of the research focus.

On the whole, spectroscopy of these salts was limited to the spectrum between the near-ultraviolet (UV) (around 200 nm on the low end) and the upper near-infrared (IR) (no results exist beyond 2400 nm in these studies). The molten salts of interest transmit light well beyond this range according to anecdotal evidence, but information beyond 2400 nm simply has not been disseminated to our knowledge. Within the very interesting range of 200 to 2400 nm, however, fluoride salts have been explored looking at a number of interesting solutes over a range of temperatures.

Young and White published studies of several metal ions in molten LiF and the LiF-NaF-KF eutectic mixture (Young and White 1959, 1960a, b) and showed small shifts in peak wavelengths for three lanthanide ions in solvents ranging from molten LiF at 900°C to aqueous 0.1 M perchloric acid at room temperature. These measurements were made on pendant drops with no windows and refraction in the near UV limited spectra to longer than 300 nm. Uranium has been extensively studied in both FLiBe and FLiNaK. Spectra are available for uranyl fluoride, U(III), and U(IV), each of which is very distinct. U(III) is not very stable in fluoride salts at high temperature and tend to reduce to U(IV), which has a very distinctive absorption spectrum shown in Figure 2.3 (Young 1967). Plutonium (Bamberger et al. 1971), chromium (Whiting et al. 1972), nickel (Young and White 1960b; Young and Smith 1964), and dissolved oxygen (Whiting et al. 1972) have also been characterized by spectroscopy in fluoride salts between 200 and 2400 nm.
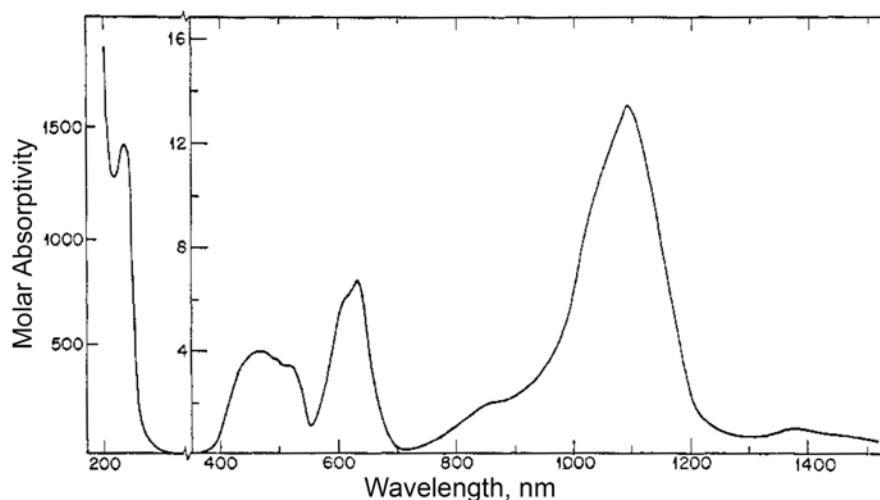
Figure 2.3.   Spectrum of U(IV) in Molten FLiBe at 550°C. Reprinted with permission from Young (1967). Copyright 1967 Americal Chemical Society.

Figure 2.4 shows spectra of the molten eutectic mixture of NaCl-KCl with various concentrations of TiCl$_3$. Minimal absorbance is present between 400 to 2000 nm. Optical transparency to the long wave infrared is likely, because most halide optical materials make excellent infrared elements. This figure also shows this molten salt is an excellent solvent in which to measure the absorption spectra of Ti^{+3} ions.
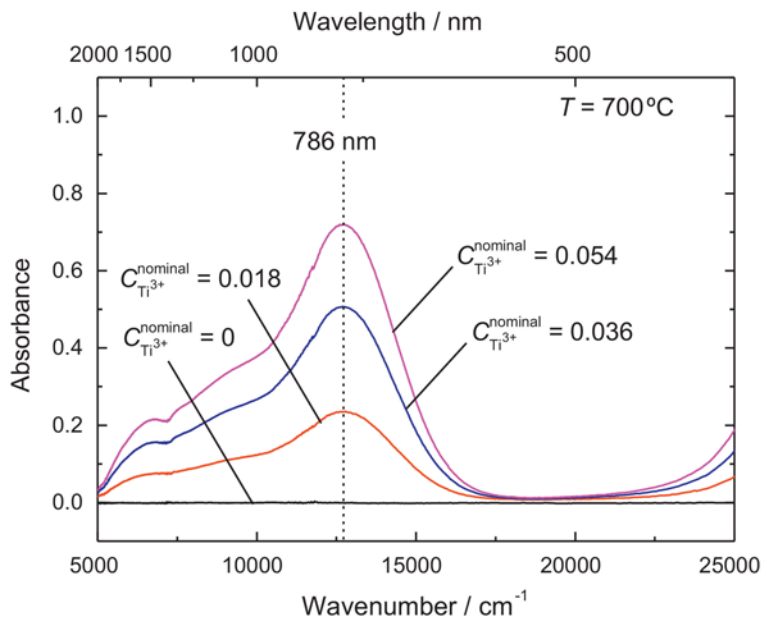
Figure 2.4.   Absorption Spectra of TiCl$_3$ in Molten NaCl-KCl Eutectic Mixture. Reprinted from Sekimoto et al. (2011), with permission from Elsevier.

The opacity of molten LiF-BeF$_2$ (FLiBe) was modeled based on the sum of the absorption cross sections of the lithium, beryllium, and fluorine components and their relative molar ratios (Zaghloul et al. 2003). This publication showed relatively low opacity (and thus high transmission) in the ultraviolet (UV) and visible range.

In addition to studies of electronic transitions of ions, there have been studies of vibrational spectra of molecular ions in molten salts using both Raman and IR absorption. An example is a study of vibrational spectra of fluoro and oxofluoro complexes in LiF-NaF-KF eutectic melts (Von Barner et al. 1991). Another example is measurement of Raman spectra of intermediates in the electrolysis of HgCl$_2$ in molten chloride salts (Voyiatzis et al. 1991).

Spectroscopy from the near UV to the IR has been conducted in molten salts including fluoride salts similar to those proposed for cooling nuclear reactors. Absorbing species, such as nickel and cobalt ions, as well as intermediates in electrolysis have been spectrally analyzed. Because molecular fluorine, F$_2$, has a visible electronic transition, it is reasonable to expect that formation of F$_2$ by radiolysis in fluoride molten salts may be detectable. Other compounds associated with corrosion or contamination could also be monitored using optical spectroscopy techniques.

The primary weaknesses of existing fluoride salt spectroscopy lie in the age of the existing data and in the limited spectral bandwidths available. It is quite possible that signatures of interest lie well above the near IR, but data in that range are not available because of the limitations of technology in the 1960s. Also, it should be mentioned that in many of the existing studies, the concentration of solutes was not identified. Even where this was specified, we did not get a good idea for the minimum limit of detection for these materials. It would be extremely useful to see systematic studies of spectroscopy on uranium or metal ions at different concentrations.

Compounds containing chlorides and fluorides can quickly (hours) begin to dissolve (Passerini 2010). However, prior to the point of mechanical failure, degraded optical window surfaces will retain good transparency at the interface with the salt because of refractive index matching (Li and Dasgupta 2000). Diamond is the optical window material of choice in molten salt applications (Toth et al. 1969).

In-vessel MSR/FHR Monitoring Requirements, Challenges, and Opportunities

- *Coolant & Cover Gas Chemistry Monitoring*: Coolant monitoring and purification is generally conducted using process loops external to the reactor vessel; however, in-vessel monitoring could be required for future AdvSMR concepts. Impurity analysis is conducted to monitor corrosion indicators and detect component or fuel failures. Regular coolant chemistry monitoring is required because of the corrosive nature of the fluoride salt coolant. Although the chemical behavior of salt changes slowly, continuous in-situ measurement techniques will likely be required. Currently COTS monitoring instrumentation is unavailable for detailed fluoride salt coolant monitoring. The standard technique for monitoring the redox condition of salt components is based on electrochemical methods. Absorption spectroscopy may be a potentially useful methodology for identifying trace chemical constituents and their valence state. It may be possible to measure bismuth and cesium concentrations, impurities, and corrosion byproducts (e.g., iron, nickel, and chromium) directly in the molten coolant using LIBS. H_2O, CO_2, and O_2 can be monitored in the cover gas area using optical spectroscopy methods. Cesium deposits could be detected using LIBS techniques. Fission gases and fuel pin taggant gases are noble gases without strong optical absorption spectra at usable wavelengths. Optical emission spectroscopy may be effective at detecting noble and tritium gases either by active ionization (e.g., laser, spark gap) or possibly radiation-induced autoionization. Tritium (T), HT, and TF may be present in the cover gas (NERAC 2002). Further study will be required to determine if optical detection and monitoring is feasible.

- *EM Pump Monitoring*: Degradation and performance is determined by monitoring vibration, temperature, voltage, and current. Vibration monitoring is used to detect impending failure. COTS accelerometers may not be feasible to use in high-temperature AdvSMR coolants. Optical vibrometry techniques may be feasible on components above the coolant level. Further study will be required on a case-by-case basis to determine the benefits and performance of each optical monitoring approach.

- *Flow Blockage Detection*: Detecting flow blockage of the coolant through the core is a challenging problem. Imaging and processing methods could be developed to monitor changes in coolant surface ripples, which may provide information about changes in coolant flow properties. Thermal infrared spatial temperature profiling in molten salt coolants also may be feasible to infer coolant flow blockage. The camera challenges and opportunities are the same as in-vessel viewing/inspection.

- *Coolant Flow and Pressure*: Thermal infrared spatial temperature profiling in molten salt coolants may be feasible to infer coolant flow. Laser Doppler velocimetry is used to measure flow in transparent liquids, but this technique requires particles to scatter laser light back to the receiver. This technique may have some potential in molten salt coolants containing dissolved fuel. Reflective spinning rotor techniques with optical readout also may be feasible for transparent coolants. Pressure measurements may be made using strain gauge instrumented diaphragm transducers connected to NaK impulse lines. Strain gauges have well-known and undesired drift. Optical Bragg grating sensors are commonly used as a direct replacement for electronic strain gauges. Further study will be required on a case-by-case basis to determine the benefits and performance of each optical monitoring approach.

- *Coolant Level*: In-vessel coolant level can be measured using ultrasonic transducers and other conventional techniques. It is unclear whether optical-based monitoring techniques have decided advantage over current methods. If required, noncontact laser ranging or other optical methods may be feasible. Further study will be required on a case-by-case basis to determine the benefits and performance of each optical monitoring approach.

- *Neutron Flux/Power*: Cherenkov radiation monitoring may be very feasible in MSR or FHR coolants. Further study will be required on a case-by-case basis to determine the benefits and performance of each optical monitoring approach.

2.1.5   Supercritical Water-Cooled Reactors

The SCWR is a water-cooled reactor that operates above the thermodynamic critical point of water. The reactor operates at much higher temperatures and pressures resulting in higher operating efficiencies (44 percent) when compared to current LWRs (32 percent). These reactors can be designed to operate with either a thermal or fast-neutron spectrum, providing flexibility in deployment and generation options. Additionally, the energy conversion technology associated with the secondary side of the reactor plant has been fully developed and commercialized by the coal fire industry over the last several decades. The SCWR eliminates several major components, such as steam dryers, recirculation pumps, and steam generators. The SCWR concept is categorized as a Tier III, because significant research, development, and demonstration (RD&D) will be required before concepts are matured. For additional information on SCWR concepts, the reader is referred to Appendix E.

Optical sensing and monitoring systems may be feasible in supercritical water coolant. Above 374°C and 22 MPa, water becomes a supercritical fluid and many of its properties change. However, the optical transparency between the UV and the near IR remains high. Interestingly enough, supercritical water has far weaker absorption for x-rays than room temperature water; a fact often exploited for x-ray absorption studies (Pfund et al. 1994). The refractive index under supercritical conditions is much lower than at ambient conditions. At 706 nm, its value varies between 1.02 and 1.23 depending on temperature and pressure (Thormahlen et al. 1985), suggesting that optimal conditions to minimize refractive gradients may be possible. There are two important regimes in supercritical water. Within 10°C–20°C of the critical point, opalescence causes extreme amounts of optical distortion, rendering virtually any free-path optical approach impossible. Significantly above the critical point, near the operating range envisioned for nuclear reactors, opalescence disappears and optical transparency becomes high.

Another important distinction between these two regimes is corrosion, which is extremely aggressive in the first case. Well beyond the critical point, however, most of the hydrogen bonds in the water are broken and most ionic compounds become virtually insoluble. The primary implication of this is that contaminants, corrosion by-products, or reaction by-products, would likely be present in the circulating coolant at concentrations in the low ppm or less. In greater concentration, these species are likely to precipitate out of solution as deposits on reactor vessel surfaces.

While corrosion of metal decreases beyond the critical point, the solubility of materials like quartz and alumina, however, continues to increase strongly with increasing pressure and temperature. Approaching 350°C, the solubility of silica in water increases exponentially (Frederickson and Cox 1954), and it can dissolve the material's surface at linear rates up to 30 nm/s (Novitskiy et al. 2011). Literature studies report that this trend continues up to at least 900°C and 900 MPa (Anderson and Burnham 1965). It is likely that only diamond optical materials could survive under the SCWR conditions.

Because SCWR reactors are at the concept feasibility stage, very little information is available about conventional SCWR monitoring technology, such as transducer design, performance requirements, and technical gaps. New in-vessel monitoring technology likely will need to be developed to withstand the high-pressure, high-temperature, and corrosive SCWR environment. A pre-conceptual design of the SCWR control system was performed (Danielyan 2003). The main characteristics affecting the design of the SCWR control system are the relatively low vessel water inventory, the nuclear/thermal-hydraulic coupling, the lack of level indication under supercritical conditions, and the absence of recirculation flow. The main variables to be controlled include the reactor power, the core outlet temperature during supercritical pressure operation (e.g., full-power operation), the reactor pressure, the reactor level during subcritical pressure operation (e.g., during start-up), and the feed water flow (Danielyan 2003). Unique aspects of the SCWR that complicate the concept include the elimination of the recirculation pumps, the low water inventory in the reactor pressure vessel (RPV), the large change in coolant density across the core, and the absence of a coolant level under supercritical conditions. Significant materials technology gaps exist for SCWR concepts. Materials and structures suffer corrosion and stress corrosion cracking. The generation of helium by transmutation of nickel can lead to swelling and embrittlement in alloy steels at high temperatures.

In-vessel SCWR Monitoring Challenges and Opportunities

- *Coolant Chemistry Monitoring*. The single most important variable that is likely to affect the practical operation of the SCWR is the chemistry of supercritical water in the presence of radiation (Baindur 2008). While the effects of water chemistry will be most critical in the SCWR reactor core, there could also be 'spillover' effects on the balance-of-plant (BOP) systems. Control of the chemical composition of the coolant water is therefore very important. Important SCWR chemistry compounds, such as H_2O, O_2, and F_2, can be monitored using optical spectroscopy methods.

- *Other*: Technology that can identify and monitor the transition point between water and supercritical water in the reactor would be invaluable from an operator standpoint. Non-pressure tube reactors will likely have flow channels similar to those employed in BWRs and monitoring the transition point in these channels would be of interest. Structural monitoring technology is needed to detect swelling and embrittlement because of nickel transmutation.

2.2 Instrumentation Controls and Human-Machine Interface Requirements for AdvSMR Designs

In this section, we present a generalized AdvSMR instrumentation architecture that describes the major control and interface elements, their respective subsystems, and finally the process monitoring parameters relevant to the reactor I&C requirements. A detailed analysis of the sodium-cooled PRISM reactor design was conducted to baseline a generalized set of reactor I&C requirements (Carlson 1994). This baseline analysis was adapted into the AdvSMR instrumentation architecture presented here. It is impossible to fully generalize all AdvSMRs in one diagram because of differences in coolant and design configurations. For instance, reactors with naturally circulating coolants will not have EM pumps. In such a case, coolant flow rates are measured directly, rather than inferred from the EM pump pressure.

Reactor instrumentation is generally grouped into three major elements that include the plant control system (PCS), the reactor protection system (RPS), and the reactor interface system (RIS). This configuration is represented in Figure 2.5, along with the many subsystems and relevant I&C sensing parameters. In some cases subsystems were further broken down into specific AdvSMR coolant designs (i.e., the Impurity Monitoring and Analysis Sensors). These systems require a highly reliable, redundant I&C architecture that independently monitors common operation and process parameters (e.g., temperature, flow rate, and pressure). The PCS is instrumented with sensors for reactor investment protection and plant performance optimization and diagnostic monitoring. The plant performance optimization and diagnostics monitoring subsystem includes the EM pump health and discharge pressure (indirect coolant flow rate monitoring) data, the IHX temperature data, reactor power (neutron flux) data, and the CRDM position and motion data. The operator monitors the process parameter data generated by these subsystems to oversee reactor operations, optimize power generation, and diagnose performance issues. The reactor investment protection sensors subsystem includes guard piping coolant leak monitoring, IHX temperature data, and passive cooling parameters, whether air or water.

The RPS is a safety system designed to limit damage and potential release of radiological material as a result of a plant accident. The RPS protects the plant based on design basis events (DBEs). DBE risk elements are identified and quantified in terms of critical transient parameter and RPS trip level. See Table 2.3 for examples of DBEs. DBE status is continuously monitored by RPS sensor instrumentation and control systems. RPS sensor instrumentation provides signals for initiating reactor trips and reactor accident monitoring. The RPS responds to a reactor trip event, issued from the reactor trip sensors subsystem, by initiating an automatic reactor module power reduction or shutdown to protect the plant, onsite personnel, and the public. Trip sensors include reactor core neutron flux, reactor core outlet temperature, cold/hot pool temperature (molten metal coolants only), coolant pressure (VHTRs and SCWRs), and coolant flow rate. Coolant flow is determined using flow sensors or indirectly in forced-flow designs by coolant pump discharge pressure. Neutron flux is used to monitor reactor thermal power. Typically each RPS subsystem consists of four identical sensor modules and interfaces that provide redundant, fault tolerant, and self-diagnostic monitoring and control during a reactor trip (SCRAM) event.

Table 2.3. Design Basis Events and Trip Parameter Condition Examples

Process Measurement Parameter	Design Basis Event	Trip Parameter
Neutron Flux	Control assembly malfunction (control rod out of position caused by misoperation or radiation-induced wrapping)	Neutron flux rate change (high or low)
	Positive reactivity feedback accidents (entrainment of cover gas in sodium coolant or water in Helium coolant)	Neutron flux rate change (high)
Liquid Coolant Level	Reactor vessel breach, loss of coolant	Primary coolant level (low)
	IHX failure	Primary coolant level (high)
Temperature	Cold coolant insertion	Primary coolant inlet temperature (low)
	Hot outlet coolant	Primary coolant outlet temperature (high)
	Spurious primary EM pump trip/failure	Primary coolant outlet temperature (high)
Coolant Pressure	Flow blockage, high vapor pressure	Primary coolant pressure (high)
Coolant Flow Rate	Primary pump electrical failure	EM pump discharge pressure (low/zero)
	Loss of force convection (flow blockage)	Coolant flow rate (low)
Cover Gas Pressure	Containment seal loss from CTE mismatch	Cover gas pressure (low)
	Control rod or blade ejection	Primary coolant pressure (high)
Coolant and Cover Gas Contaminants	Fuel leak	Contaminant level (high)
	Fuel handling accidents	Contaminant level (high)
	Tritium trapping failure	Contaminant level (high)

IHX = intermediate heat exchanger
CTE = coefficients of thermal expansion
EM = electromagnetic
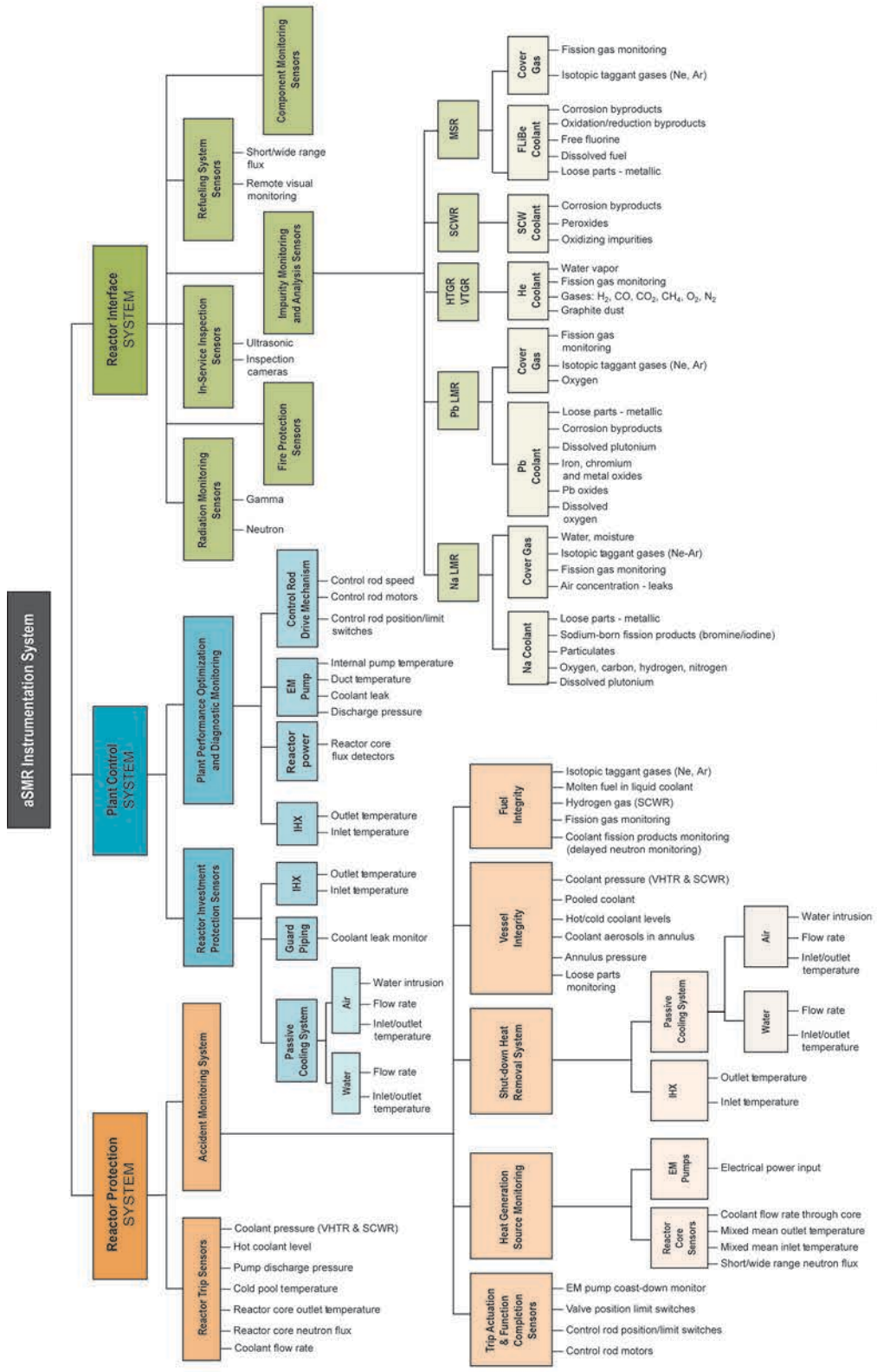
Figure 2.5. Generalized AdvSMR Control and Interface Architecture

2.19

The accident monitoring system also includes several subsystems that do not automatically trip a reactor protection response, but deliver information about the status of the reactor during accidents. These subsystems include trip actuation & function completion, heat generation source monitoring, shut-down heat removal, vessel integrity, and fuel integrity. Trip actuation & function completion monitors control rods, valves, and the EM pump during coast-down to verify successful shut down after SCRAM. The heat generation source monitoring subsystem monitors reactor core and pump sensors to determine current reactor heat loads. The mixed mean outlet and inlet temperatures and the flow rate of coolant through the core provide indirect reactor heat load information. The shut-down heat removal subsystem monitors inlet and outlet temperatures of the IHX and passive cooling systems. Vessel integrity subsystem monitors coolant leakage or material failure, including liquid or gas-phase coolant in the annulus, annulus pressure, coolant levels, and the presence of metallic loose parts. Fuel integrity subsystem monitors core integrity and fuel rod cladding breaches, which can lead to fuel circulating in the coolant and the presence of fission and isotopic taggant gases in coolant and/or headspace. Flow blockage in sodium-cooled reactors is detected by the molten fuel-cladding interaction, which activates the coolant and is monitored using delayed neutron detectors in the IHX.

The RIS is not an integral component of the safety systems described above, but rather is composed of sensor subsystems, including radiation monitoring for staff safety, fire protection, in service inspection (ISI), refueling, component monitoring, and impurity monitoring and analysis. The ISI and component monitoring sensors provide prognosis and diagnosis information for many of the reactor subsystems. The ISI and refueling systems are likely to use sophisticated radiation-hardened cameras and machine vision technologies that provide efficient human-machine interface to enable in-vessel telepresence, telerobotic control, and remote process operations.

For each of the six AdvSMR concepts identified by the Gen IV forum, coolant and headspace monitoring has significant importance to reactor operations. Coolant and headspace monitoring is typically conducted using process loops extending outside the reactor or by grab sampling and laboratory analysis. This is a reliable process, but in-vessel monitoring could be required for future AdvSMR concepts. Chemical reactions, impurities, and contaminants are driven by the specific coolant chemistries and interactions with the reactor components. Impurity-induced corrosion is a major concern in all AdvSMR concepts. Reactor coolants can have reactivity issues with contaminants that must be carefully considered. Reactor-specific contaminants and detection methods are described later on.

Detection of foreign material that circulates in the coolant is another important requirement. Loose parts monitoring is conducted using accelerometers located at different places within the vessel and the secondary coolant loops (Hashemian et al. 1998, pg. 529). The accelerometers record high-speed vibrations. These signals are reported to signal processing electronics that filter out the noise of normal operation to identify signals indicative of metal-on-metal impacts (AREVA 2007). Fission products and dissolved fuels can circulate with the coolant and will result in increased radiation signatures throughout the reactor vessel. High coolant flow rates can lead to physical erosion of metals, casings, shielding, and fuel components, producing metallic particles and debris. This is a challenge, particularly in pebble bed-type, helium-cooled reactors, where pebble erosion produces graphite particles. Accumulated particles can impact sensing instrumentation or damage moving parts (Wright 2006). Fuel rod failure because of stress, corrosion, or other processes must be quickly detected. A complete fuel rod casing breach releases fission and isotopic taggant gases. The unique isotopic ratio of taggant gases is used to identify which fuel rod(s) failed. Coolant gas or the headspace above the coolant (pool-type reactor designs) can be analyzed for these signatures (Brunson et al. 1971).

2.3 In-Vessel Parameter Monitoring

The reactor sensing parameters for all the AdvSMR concepts have many common requirements and a few distinguishing characteristics based on coolant type. The most critical sensing parameters and locations are shown in Figure 2.6. These parameters have a direct correspondence to the AdvSMR instrumentation system shown in Figure 2.5. The figure includes the concrete reactor silo, the passive cooling system, the containment vessel, and the reactor vessel. While this figure represents a pool-type reactor design, most of the sensing parameters are relevant to gas-cooled reactor designs.
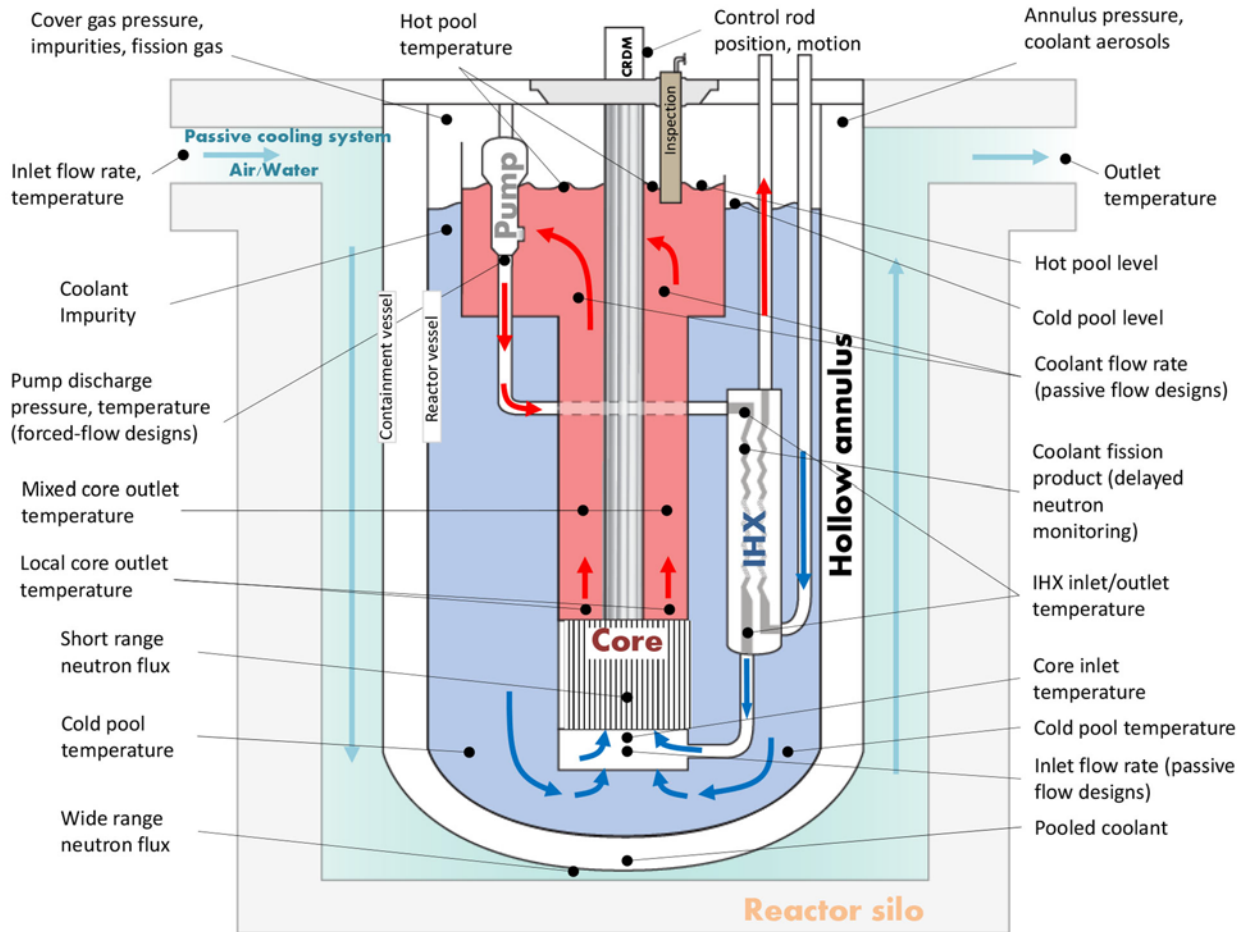
Figure 2.6. A Conceptual Pool-type Reactor, Showing Key Sensing Parameters and Locations

Table 2.4 is provided to summarize expected process parameter requirements for the advanced reactor concepts and includes BWR and PWR process ranges for comparison. These data represent an average of the information derived from an extensive review of published literature and discussions with subject matter experts. Expected measurement ranges are provided for each parameter, including core outlet temperature, vessel pressure, combined total neutron flux, flow rate, coolant level, and typical coolant impurity detection limits. These monitoring requirements form the basis to compare and examine measurement specifications of each COTS optical-based monitoring instrument described in Sections 5.0

to 9.0. The AdvSMR deployment assumptions for the optical-based monitoring instruments are discussed in Section 1.2. The measurement resolution and accuracy requirements are not included in Table 2.4, because either there were too many variables from which to derive an accurate estimate or the values are unavailable for specific AdvSMR concepts. We anticipate temperature measurement accuracy requirements at ± 1°C or ± 0.1°C, which is typical performance for thermocouples and platinum RTDs, respectively. Pressure measurements likely will require ± 100 Pa or ± 10 kPa measurement accuracy for reactor vessel pressures near atmospheric and ≥ 7 MPa, respectively. Neutron flux is generally measured in two dynamic ranges using a short-range and wide-range neutron flux monitor. The first range is zero to criticality, which is roughly 10^6 n/cm^2·s average total neutron. The wide range typically spans 10^4 n/cm^2·s to 10^{13} n/cm^2·s. Sensitivity to 1–10 n/cm^2·s is required for the short-range monitor. Flow rate measurement accuracy is estimated at ± 1 kg/sec and coolant level at ± 1 cm. For most of these parameters, we assume that the resolution requirements are generally a factor of 10 greater than the measurement accuracy. The detection limits for coolant monitoring may range between the ppm to ppb level depending on the impurity. In-vessel optical imaging and laser vibrometry are examined in Sections 4.0 and 10.0. These are diagnostic and inspection tools without clear AdvSMR performance specifications to compare against. For these optical monitoring technologies, we consider just the deployment requirements, which are discussed in the corresponding sections.

Table 2.4. Expected Parameter Monitoring Requirements for AdvSMRs

Reactor Type	Temp Range (°C)	Pressure Range (MPa)	Average Total Neutron Flux Range (n/cm^2·s)	Flow Rate (kg/s)	Coolant Level (m)	Coolant Impurity Detection Limit
BWR/PWR	40–330	0.1–15.5	Zero – 5×10^{13}	700–5000	0.5–1	ppm–ppb
SFR	40–550	0.1	Zero – 2×10^{14}	17–82	0.5–1	ppm–ppb
LFR	40–567	0.1	Zero – 4×10^{13}	2000–16000	0.5–1	ppm–ppb
GFR	40–780	0.1–7	Zero – 5×10^{13}	28–38	NA	ppm–ppb
HTGR	40–750	0.1–7	Zero – 3×10^{12}	10.2–320	NA	ppm–ppb
VHTR	40–1000	0.1–7	Zero – 3×10^{12}	192	NA	ppm–ppb
MSR	40–700	0.1	Zero – 3×10^{14}	1000–2000	0.5–1	ppm–ppb
FHR	40–700	0.1	Zero – 8×10^{12}	28,500	0.5–1	ppm–ppb
SCWR	40–625	0.1 – 25	Zero – 5×10^{13}	1800	NA	ppm–ppb

2.4 Engineering Concepts for In-vessel Optical Access

Optical access is not provided in any commercial nuclear power plant or featured in any reactor design, although successful implementation has been demonstrated in test reactors (Arkani and Gharib 2009). Optical access is a vital requirement to enable future in-vessel optical monitoring systems, because few optical monitoring systems will survive in-vessel conditions, even short-term exposure intervals, during full-power reactor operation. A sustained RD&D effort will be required to develop engineering solutions that provide optical access into the reactor vessel. This will be a challenging engineering problem to solve because of the high temperatures, extreme temperature swings and differentials, large radiation fluxes, corrosion damage and optical surface contamination issues, high pressures (e.g., SCWR, VHTR, HTGR, GFR), and vibration, all present during AdvSMR operations.

The main advantage to the optical access is that it enables the whole concept of in-vessel optical-based monitoring, which is the subject of this report. The many advantages of optical-based sensing methods can be realized by using optical viewports and optical-fiber feedthroughs. Direct and continuous visualization of the in-vessel component can be maintained using external cameras. Point and distributed sensing can be conducted using optical fiber and sensing elements. Many optical sensing techniques can be performed remotely using open optical beam path configurations. Not only are in-vessel cables eliminated by these configurations, but also sensitive optical monitoring components (e.g., electronics, lasers, detectors, cameras) can be placed outside the reactor vessel in the instrument vault or other locations where temperatures and radiation levels are much lower. Several conceptual optical access modes are envisioned, including in-vessel optical viewports, optical viewports mounted on standpipes, fiber-optic feedthroughs, and optical periscope modules, as shown in Figure 2.7.
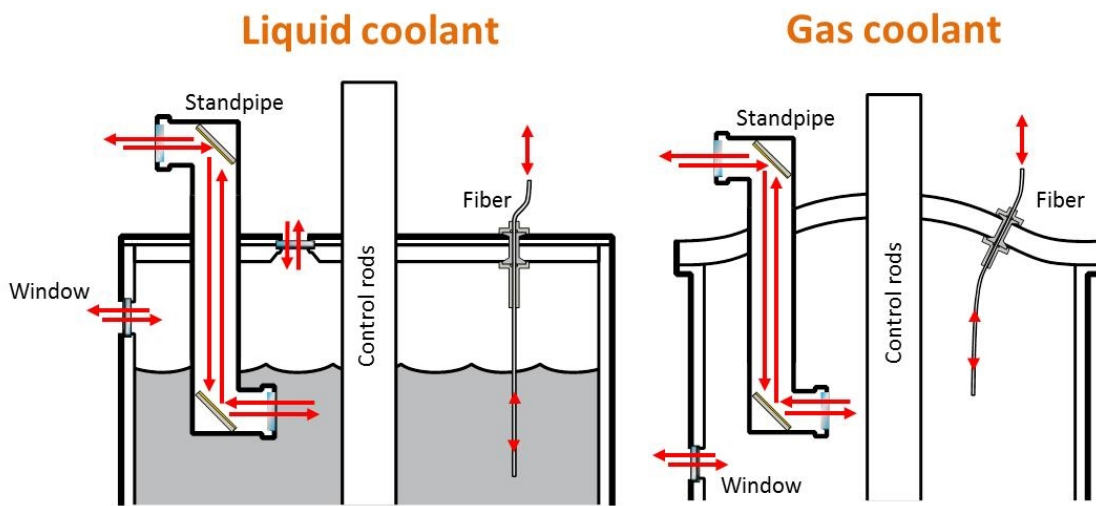
Figure 2.7.   Upper Regions of a Liquid-Cooled and Gas-Cooled Reactor, Showing Optical Access Concepts. Optical access through the containment vessel also may be required.

2.4.1   Window Access

In-vessel optical viewports will allow remote viewing and optical sensing through the reactor vessel. Optical access through the containment vessel may also be required if the balance of the sensing system cannot be located in this region. The viewport concept provides an open optical path through which moving parts may be viewed, core inlets/outlets may be monitored, and metal surfaces can be inspected for cracking or swelling. Cherenkov radiation emissions could be measured as a convenient method to monitor reactor power.

Feasible designs must accommodate large temperature excursions and high continuous operating temperature, while surviving design-basis accident scenarios. Optical materials must be selected that have radiation-resistant properties to provide long-term deployment under continuous gamma and neutron radiation exposure. High mechanical strength and chemical resistance are also important to the design, as are durable sealing concepts and materials with matched thermal expansion coefficients. Design ideas must be developed to overcome coolant condensation and debris deposits on viewport interior surfaces.

This will be a greater problem in liquid-coolant reactor designs, where coolant vapor and other contaminants could quickly coat and obscure optical components.

Feasible locations for viewports are above the liquid coolant level in pool-type reactor designs and virtually any location in He-cooled reactor designs. This configuration is likely less desirable in liquid-cooled reactor designs, because vapor from the coolant will quickly condense on the relatively cool optical window surface. In He-cooled reactor designs, the viewport could be placed at the bottom of the reactor to provide unobstructed visualization of the reactor core area. In both configurations, the optical viewport design must accommodate large dimensional changes and mechanical forces because of differential thermal expansion.

2.4.2   Standpipe Viewport Access

The optical viewport on a standpipe configuration is an extension of the optical viewport described in Section 2.4.4. This approach is perhaps the most feasible concept that could be implemented in the near-term horizon. Standpipes are routinely used in reactor vessel designs to elevate sensors, hardware, and electrical feedthroughs above regions of very high temperature and radiation. Viewport temperatures for He-cooled reactor designs are expect to be 300°C–450°C and around 100°C for liquid-cooled reactor designs, as shown in Figure 2.1. Thermal swings and differential gradients will continue to challenge mechanical designs. Using a 90° mirror can substantially reduce gamma exposure to the top viewport window, because it is out of the core's direct line-of-sight. A continuous inert purge gas in the standpipe riser tube (gas-cooled reactors) or an inert, periodically refreshed inert gas bubble (liquid-cooled reactors) could control vapor condensation. In addition, an internal shutter could protect optical components by opening only during periods of sensing or imaging. Standpipes for optical access into open test reactors have been used in the Tehran Research Reactor and demonstrated for long-term Cherenkov power monitoring (Arkani and Gharib 2009). Implementation in an AdvSMR design will represent additional engineering challenges, but this prior demonstration suggests that this concept is feasible.

2.4.3   Periscope Access

The standpipe could be designed as a periscope-type assembly (not shown in Figure 2.7), to inspect normally inaccessible areas within the reactor. Conceptually, a small periscope could be extended down through the downcomer to observe the outlet flow region. Maintaining optical alignment over such a large free path will be extremely challenging because of thermal expansion and vibration issues. Two radiation-hardened periscopes were designed and evaluated for applications in the international thermonuclear experimental reactor (Obara et al. 1998). This study designed and tested 6-m and 15-m periscopes that used radiation-hardened lenses made of alkaline barium glass, lead glass containing CeO_2, and OH-doped synthetic quartz. No optical degradation was observed to 50 MGy total dose. The design was configured with a steering mirror (i.e., rotate and tilt) and periscope winch system to adjust the inspection field. The design was heated to 250°C using external heaters attached to the body of the periscope. The thermal design and focus adjustment capabilities mitigated optical misalignment because of lateral and axial expansion of the periscope body. While the temperature and radiation-resistance design specifications are significantly below expected AdvSMR environmental conditions, the results of this design study support the feasibility of the periscope concept.

2.4.4 Fiber-Optic Access

Many COTS solutions are available for hermetically sealed fiber-optic feedthroughs for high-vacuum applications. Kurt Lesker Company offers a vacuum feedthrough that is guaranteed leak free to 1×10^{-14} MPa and rated to 200°C continuous operating temperature. A few vendors (i.e., AMETEK, SCP Inc.) offer high pressure (241 MPa) and temperature (350°C) components on a custom-design basis, generally for the oil and gas downhole applications. Generally a short fiber stub is held within the feedthrough assembly using a glass-to-metal seal. The fiber stub is terminated on both ends to allow connection to input/output optical-fiber cables. Fiber-optic access ports rank HIGH on the technical readiness for future AdvSMR applications, based on the maturity of COTS technology.

2.5 References

Abram T and S Ion. 2008. "Generation-IV Nuclear Power: A Review of the State of the Science." *Energy Policy* 36(12):4323-4330.

Adamovich L, S Banerjee, M Bolshunkhin, E Budylov, M Chaki, IV Dulera, P Fomichnko, K Furukawa, B Gabaraev and E Greenspan. 2007. *Status of Small Reactor Designs without On-Site Refueling*. IAEA-TECDOC-1536, International Atomic Energy Agency (IAEA), Vienna, Austria.

Alekseev P. 2010. "Concept of Small Power Autonomous Molten-Salt Reactor with Micro-Particle Fuel (Reactor MARS)." In *Fluoride Salt-Cooled High-Temperature Reactor Workshop*. September 20-21, 2010, Oak Ridge, Tennessee.

Anderson GM and CW Burnham. 1965. "The Solubility of Quartz in Supercritical Water." *American Journal of Science* 263:494-511.

AREVA. 2007. *Loose Parts Monitoring System (LPMS-VI)*. AREVA NP. Lynchburg, Virginia. Accessed January 21, 2013. Available at http://www.us.areva-np.com/cisweb/pdf/npc/Loose%20Parts%20Monitoring%20System%20(LPMS-VI).pdf.

Arkani M and M Gharib. 2009. "Reactor Core Power Measurement Using Cherenkov Radiation and Its Application in Tehran Research Reactor." *Annals of Nuclear Energy* 36:896-900.

Baindur S. 2008. "Materials Challenges for the Supercritical Water-Cooled Reactor (SCWR)." *Bulletin of the Canadian Nuclear Society* 29:32-38.

Bamberger CE, RG Ross, CF Baes, Jr., and JP Young. 1971. "Absence of an Effect of Oxide on the Solubility and the Absorption Spectra of PuF_3 in Molten LiF-BeF_2-ThF_4 and the Instability of Plutonium(III) Oxyfluorides." *Journal of Inorganic and Nuclear Chemistry* 33(10-N):3591-3594.

Brunson GS, RM Fryer and RV Strain. 1971. *Experimental Irradiations of Fuel Elements Having Known Cladding Defects in EBR-II*. ANL-7782, Argonne National Laboratory, Argonne, Illinois.

Cammi A, V Di Marcello, L Luzzi, V Memoli and ME Ricotti. 2011. "A Multi-Physics Modelling Approach to the Dynamics of Molten Salt Reactors." *Annals of Nuclear Energy* 38:1356-1372.

Carlson DE. 1994. *Preapplication Safety Evaluation Report for the Power Reactor Innovative Small Module (PRISM) Liquid-Metal Reactor Final Report*. NUREG-1368, U.S. Nuclear Regulatory Commission, Washington, D.C.

Danielyan D. 2003. *Supercritical-Water-Cooled Reactor System - As One of the Most Promising Type of Generation IV Nuclear Reactor Systems*. Available at http://tfy.tkk.fi/aes/AES/courses/crspages/Tfy-56.181_03/Danielyan.pdf.

Devanney J. 2012. *ThorCon Summary Description*. Version 0.60, Martingale, Inc., Sisyphus Beach, Tavernier, Florida.

Driscoll MJ, P Hejzlar and G Apostolakis. 2008. *Nuclear Energy Research Initiative (NERI) Final Report: Optimized, Competitive Supercritical-CO$_2$ Cycle GFR for Gen IV Service*. Report No. MIT-GFR-045, Massachusetts Institute of Technology, Cambridge, Massachusetts.

Duffey R, LKH Leung, D Martin, B Sur and M Yetisir. 2011. "A Supercritical Water-Cooled Small Modular Reactor." In *Proceedings of the ASME 2011 Small Modular Reactors Symposium*, pp. 243-250. September 28-30, 2011, Washington, D.C. DOI 10.1115/SMR2011-6548. ASME, New York. Paper No. SMR2011-6548.

Forsberg C. 2004. "Safety and Licensing Aspects of the Molten Salt Reactor." Presented at American Nuclear Society Annual Meeting, Pittsburgh, Pennsylvania, June 13-17, 2004.

Forsberg CW, PF Peterson and DF Williams. 2005. "Practical Aspects of Liquid-Salt-Cooled Fast-Neutron Reactors." In *American Nuclear Society - International Congress on Advances in Nuclear Power Plants 2005 (ICAPP'05)*, pp. 3197-3209. May 15-19, 2005, Seoul, Republic of Korea. American Nuclear Society, La Grange Park, Illinois.

Frederickson AF and JE Cox. 1954. "Mechanism of "Solution" of Quartz in Pure Water at Elevated Temperatures and Pressures." *American Minerologist* 39:886-900.

Greene SR, JC Gehin, DE Holcomb, JJ Carbajo, D Ilas, AT Cisneros, VK Varma, WR Corwin, DF Wilson, GL Yoder, Jr., AL Qualls, FJ Peretz, GF Flanagan, DA Clayton, EC Bradley, GL Bell, JD Hunn, PJ Pappano and MS Cetiner. 2010. *Pre-Conceptual Design of a Fluoride-Salt-Cooled Small Modular Advanced High-Temperature Reactor (SmAHTR)*. ORNL/TM-2010/199, Oak Ridge National Laboratory, Oak Ridge, Tennessee.

Hashemian HM, ET Riggsbee, DW Mitchell, M Hashemian, CD Sexton, DD Beverly and GW Morton. 1998. *Advanced Instrumentation and Maintenance Technologies for Nuclear Power Plants*. NUREG/CR-5501, U.S. Nuclear Regulatory Commission, Washington, D.C.

Hoffman EA, WS Yang and RN Hill. 2006. *Preliminary Core Design Studies for the Advanced Burner Reactor over a Wide Range of Conversion Ratios*. ANL-AFCI-177, Argonne National Laboratory, Argonne, Illinois. Available at http://www.osti.gov/energycitations/servlets/purl/973480-o1tvNg/.

Holcomb DE, D Ilas, AL Qualls, FJ Peretz, VK Varma, EC Bradley and AT Cisneros. 2012. "Current Status of the Advanced High Temperature Reactor." In *Proceedings of 2012 International Congress on Advances in National Power Plants (ICAPP '12)*. June 24-28, 2012, Chicago, Illinois. American Nuclear Society, La Grange, Illinois. Paper 12342.

IAEA. 2007a. "Lead-Bismuth Eutectics Cooled Long-Life Safe Simple Smal Portable Proliferation Resistant Reactor (LSPR)." In *Status of Small Reactor Designs Without On-Site Refueling*, pp. 715-737. IAEA, Vienna, Austria. IAEA-TECDOC-1536.

Knoll GF. 2000. *Radiation Detection and Measurement, Third Edition*. John Wiley & Sons, Hoboken, New Jersey.

Kolev NI. 2011. *Multiphase Flow Dynamics 5: Nuclear Thermal Hydraulics, Second Edition*. Springer-Verlag, Berlin Heidelberg.

Li J and PK Dasgupta. 2000. "A Simple Instrument for Ultraviolet-Visible Absorption Spectrophotometry in High Temperature Molten Salt Media." *Review of Scientific Instruments* 71:2283-2287.

Locatelli G, M Mancini and N Todeschini. 2012. "GEN IV Reactors: Where We Are, Where We Should Go." In *Proceedings of International Congress on Advances in Nuclear Power Plants (ICAPP '12)*. June 24-28, 2012, Chicago, Illinois. American Nuclear Society, La Grange, Illinois. Paper 12229.

Memoli V, A Cammi, V Di Marcello and L Luzzi. 2009. "A Preliminary Approach to the Neutronics of the Molten Salt Reactor by Means of COMSOL Multiphysics." In *COMSOL Conference 2009*. October 14-16, 2009, Milan, Italy.

Moses DL. 2010. *Very High-Temperature Reactor (VHTR) Proliferation Resistance and Physical Protection (PR&PP)*. ORNL/TM-2010/163, Oak Ridge National Laboratory, Oak Ridge, Tennessee.

Nelson L. 2008. *Boiling Water Reactor Basics*. GE Global Research, Schenectady, New York. Available at http://www.edf.com/fichiers/fckeditor/Commun/Innovation/conference/BWRsbasics_va.pdf.

NERAC. 2002. *A Technology Roadmap for Generation IV Nuclear Energy Systems - Ten Nations Preparing Today for Tomorrow's Energy Needs*. GIF-002-00, U.S. DOE Nuclear Energy Research Advisory Committee (NERAC) and the Generation IV International Forum (GIF), Washington, D.C. Available at http://www.osti.gov/energycitations/servlets/purl/859029-304XRr/.

Novitskiy AA, J Ke, VN Bagratashvili and M Poliakoff. 2011. "Applying a Fiber Optic Reflectometer to Phase Measurements in Subcritical and Supercritical Water Mixtures." *Journal of Physical Chemistry C* 115:1143-1149.

Obara K, A Ito, S Kakudate, K Oka, M Nakahira, Y Morita, K Taguchi, S Fukatsu, N Takeda, H Takahashi, E Tada, R Hager, K Shibanuma and R Haange. 1998. "Development of 15-m-long Radiation Hard Periscope for ITER In-vessel Viewing." *Fusion Engineering and Design* 42(1–4):501-509.

Passerini S. 2010. *Optical and Chemical Properties of Molten Salt Mixtures for Use in High Temperature Power Systems*. Masters Thesis, Massachusetts Institute of Technology, Cambridge, Massachusetts. Available at http://hdl.handle.net/1721.1/62706

Pfund DM, JG Darab, JL Fulton and Y Ma. 1994. "An XAFS Study of Strontium Ions and Krypton in Supercritical Water." *Journal of Physical Chemistry* 98:13102-13107.

Potter RC and A Shenoy. 1996. *Gas Turbine-Modular Helium Reactor (GT-MHR) Conceptual Design Description Report*. Report No. 910720, Rev. 1, General Atomics, San Diego, California. GA Project No. 7658.

Ragheb M. 2011. *Traveling Wave Reactor*. Available at http://www.uxc.com/smr/Library/Design%20Specific/TWR/Papers/2011%20-%20TWR.pdf.

Sekimoto H, Y Nose, T Uda, A Uehara, H Yamana and H Sugimura. 2011. "Revaluation of Equilibrium Quotient Between Titanium Ions and Metallic Titanium in NaCl-KCl Equimolar Molten Salt." *Journal of Alloys and Compounds* 509(18):5477-5482.

Sienicki JJ, A Moisseytsev, WS Yang, DC Wade, A Nikiforova, P Hanania, HJ Ryu, KP Kulesza, SJ Kim, WG Halsey, CF Smith, NW Brown, E Greenspan, M de Caro, N Li, P Hosemann, J Zhang and H Yu. 2006. *Status Report on the Small Secure Transportable Autonomous Reactor (SSTAR)/Lead-cooled Fast Reactor (LFR) and Supporting Research and Development*. ANL-GenIV-089, Argonne National Laboratory, Argonne, Illinois. Available at http://www.osti.gov/energycitations/servlets/purl/932940-RHXy5s/.

Smith CM. 2010. *Lead-Cooled Fast Reactor (LFR) Design: Safety, Neutronics, Thermal Hydraulics, Structural Mechanics, Fuel, Core, and Plant Design*. LLNL-BOOK-424323, Lawrence Livermore National Laboratory, Livermore, California.

Stainsby R, K Peers, C Mitchell, C Poette, K Mikityuk and J Somers. 2011. "Gas Cooled Fast Reactor Research in Europe." *Nuclear Engineering and Design* 241:3481-3489.

Taiwo TA, TK Kim, WS Yang, HS Khalil, WK Terry, JB Briggs and DW Nigg. 2005. *Evaluation of High Temperature Gas-Cooled Reactor Physics Experiments as VHTR Benchmark Problems*. ANL-GenIV-059, Idaho National Laboratory, Idaho Falls, Idaho. Available at https://inlportal.inl.gov/portal/server.pt/gateway/PTARGS_0_2_3310_277_2604_43/http%3B/inlpublisher%3B7087/publishedcontent/publish/communities/inl_gov/about_inl/gen_iv___technical_documents/expthtreval2005.pdf.

Tauveron N and F Bentivoglio. 2012. "Preliminary Design and Study of the Indirect Coupled Cycle: An Innovative Option for Gas Fast Reactor." *Nuclear Engineering and Design* 247:76-87.

Thormahlen I, J Straub and U Grigull. 1985. "Refractive Index of Water and Its Dependence on Wavelength, Temperature, and Density." *Journal of Physical and Chemical Reference Data* 14:933-945.

Todreas NE, P Hejzlar, CJ Fong, A Nikiforova, R Petroski, E Shwageraus and J Whitman. 2008. *Flexible Conversion Ratio Fast Reactor Systems Evaluation*. MIT-NFC-PR-101, MIT Center for Advanced Nuclear Energy Systems, Cambridge, Massachusetts.

Toth LM, JP Young and GP Smith. 1969. "Diamond-Windowed Cell for Spectrophotometry of Molten Fluoride Salts." *Analytical Chemistry* 41:683-685.

Von Barner JH, RW Berg, NH Bjerrum, E Christensen and F Rasmussen. 1991. "Vibrational-Spectra of Fluoro and Oxofluoro Complexes of Nb(V) and Ta(V)." In *International Symposium on Molten Salt Chemistry and Technology*, pp. 279-283. July 15-19, 1991, Paris, France. Materials Science Forum.

Voyiatzis GA, GC Carountjos and IV Boviatsis. 1991. "Raman-Spectra of Subvalent Mercury Species Formed During Electrolysis of $HgCl_2$ in Melts." In *International Symposium on Molten Salt Chemistry and Technology*, pp. 285-289. July 15-19, 1991, Paris, France. Materials Science Forum.

Waris A, IK Aji, Y Yulianti, MA Shafii, I Taufiq and Z Su'ud. 2010. "Comparative Study on [233]U and Plutonium Utilization in Molten Salt Reactor." *Indonesian Journal of Physics* 21:77-81.

Westinghouse. 2002. *IRIS (International Reactor Innovative and Secure) Plant Overview*. Westinghouse Electric Co. Prepared for the IAEA Advanced Light Water Reactor Report. Available at http://pbadupws.nrc.gov/docs/ML0336/ML033600086.pdf.

Whiting FL, G Mamantov and JP Young. 1969. "Spectral Evidence for the Existence of the Superoxide Ion in Molten LiF-NaF-KF." *Journal of the American Chemical Society* 91(23):6531-6532.

Whiting FL, G Mamantov and JP Young. 1972. "Spectral Studies of O_2^-, NO_2^- and CrO_4^{2-} in Molten LiF-NaF-KF and of O_2^- in Liquid Amonia." *Journal of Inorganic and Nuclear Chemistry* 34:2475-2481.

Williams DF, LM Toth and KT Clarno. 2006. *Assessment of Candidate Molten Salt Coolants for the Advanced High-Temperature Reactor (AHTR)*. ORNL/TM-2006/12, Oak Ridge National Laboratory, Oak Ridge, Tennessee.

Wright RN. 2006. *Kinetics of Gas Reactions and Environmental Degradation in NGNP Helium*. INL/EXT-06-11494, Idaho National Laboratory, Idaho Falls, Idaho.

Young JP. 1967. "Spectra of Uranium(IV) and Uranium(III) in Molten Fluoride Solvents." *Inorganic Chemistry* 6(8):1486-1488.

Young JP, CE Bamberger and RG Ross. 1974. "Spectral Studies of *f-d* and *f-f* Transitions of Pa(IV) in Molten LiF-BeF$_2$-ThF$_4$." *Journal of Inorganic and Nuclear Chemistry* 36:2630-2632.

Young JP, G Mamantov and FL Whiting. 1967. "Simultaneous Voltammetric Generation of U(II1) and Spectrophotometric Observation of
the U(II1)-U(1V) System in Molten Lithium Fluoride-Beryllium Fluoride-Zirconium Fluoride." *The Journal of Physical Chemistry* 71(2):782-783.

Young JP and GP Smith. 1964. "Coordination of Fluoride Ions About Nickel (II) Ions in the Molten LiF-NaF-KF Eutectic " *The Journal of Chemical Physics* 40(3):913-914.

Young JP and JC White. 1959. "High-Temperature Cell Assembly for Spectrophotometric Studies of Molten Fluoride Salts." *Analytical Chemistry* 31:1892-1895.

Young JP and JC White. 1960a. "Absorption Spectra of Molten Fluoride Salts. Solutions of Praseodymium, Neodymium, and Samarium Fluoride in Molten Lithium Fluoride." *Analytical Chemistry* 32:1658-1661.

Young JP and JC White. 1960b. "Absorption Spectra of Molten Fluoride Salts. Solutions of Several Metal Ions in Molten Lithium Fluoride-Sodium Fluoride-Potassium Fluoride." *Analytical Chemistry* 32:799-802.

Zabiego M, C Sauder, P David, C Gueneau, L Briottet, JJ Ingremeau, A Ravenet, C Lorrette, L Chaffron, P Guedeney, M Le Flem and JL Seran. 2013. "Overview of CEA's R&D on GFR Fuel Element Design: From Challenges to Solutions." In *International Conference on Fast Reactors and Related Fuel Cycles: Safe Technologies and Sustainable Scenarios (FR13) Conference*. March 4-7, 2013, Paris, France. International Atomic Energy Agency, Vienna, Austria.

Zaghloul MR, D-K Sze and AR Raffray. 2003. "Thermo-Physical Properties and Equilibrium Vapor-Composition of Lithium Fluoride-Beryllium Fluoride (2LiF/BeF$_2$) Molten Salt." *Fusion Science and Technology* 44:344-350.

Zrodnikov AV, GI Toshinsky, OG Komlev, UG Dragunov, VS Stepanov, NN Klimov, II Kopytov and VN Krushelnitsky. 2005. "Small Size Modular Fast Reactors in Large Scale Nuclear Power." In *18th International Conference on Structural Mechanics in Reactor Technology (SMiRT 18)*, pp. 4395-4406. August 7-12, 2005, Beijing, China. Paper SMiRT18-S01-1.

3.0   Optical Materials and Components

Optical materials are used to fabricate optical elements (e.g., windows, mirrors, and lenses) and optical fiber, which form the basic building blocks for optical sensing systems. Optical windows and optical fiber are vital elements for the in-vessel optical sensing application, because these components provide the means to gain optical access into the reactor vessel. Optical materials and fibers (e.g., glass, crystalline, and polymer) are commercially available with a wide range of optical, thermal, and mechanical performance specifications.

In general, the technical readiness of most commercial off-the-shelf (COTS) optical components and optical fibers is **LOW** for near-core deployment applications. Few optical materials have the performance specifications needed to withstand advanced small modular reactors (AdvSMR) in-vessel environmental extremes near the core, even for short durations. Near maximum AdvSMR temperatures, only sapphire, chemical vapor deposition (CVD) diamond, and transparent ceramic materials can survive. More common optical materials such as fused quartz or silica can provide continuous operation near 1000°C, which allows deployment in some AdvSMR applications, if selected based on temperature performance only. Most high-temperature materials also have high mechanical rupture strengths, which are important for high-pressure optical window applications (i.e., supercritical water-cooled reactor [SCWR] designs). Chemical compatibility and resistance data for COTS optical products are typically limited and usually not relevant to expected AdvSMR conditions. This appears to be an understudied area of research. Unfortunately, specifications for radiation resistance are almost universally absent in vendor specifications. COTS optical fibers may be feasible for applications near the reactor lid, where the temperature and radiation conditions are much lower. In this case, the technical readiness for a limited list of optical materials is **HIGH**.

Optical fiber can provide both optical access into the reactor vessel, as well as integrated point and distributed sensing for specific in-vessel locations. Silica glass solid core, hollow, and photonic bandgap optical fiber is readily available as COTS products. Light pipes can be fabricated from high-temperature sapphire. While silica and sapphire have very high temperature performance, both materials require coatings over the core or cladding layers to improve the tensile strength and chemical and abrasion resistance. All coatings drastically reduce the high-temperature performance. Many commercial coatings are polymer-based, with dismal temperature ratings (i.e., 125°C–250°C). Chemical compatibility and resistance data are typically limited and usually not relevant to expected AdvSMR conditions. Optical fibers have well-known radiation damage processes (affecting both core and coatings), including darkening, luminescence, compaction, and mechanical damage. There is a large body of research regarding these processes, but very few studies have been conducted under conditions that are similar to expected AdvSMR radiation environments (e.g., high neutron and gamma fluences). A few promising exceptions are COTS hollow-core photonic crystal fibers and pure silica fibers developed by the Russian Academy of Science, Fiber Optic Research Center (FORC). A few study results suggest that these COTS fibers could survive in-vessel radiation exposure for months to almost a decade (depending on the reactor design) with only modest loss in optical transmission. The coatings that protect the fiber will limit their maximum operating temperature. This understudied area deserves further investigation.

Some COTS window and optical components have a better outlook and perhaps have a shorter timeline to resolve the technical gaps. The temperature and mechanical specifications for a few materials are very promising, but further investments will be required to understand and optimize these materials

for extended integration into AdvSMR designs. Notable optical materials include CVD diamond, ALON®, spinel, sapphire, and fused silica. These optical materials may be feasible for viewport windows at the end of a standpipe, where the temperature and radiation conditions are much lower. In this case, the technical readiness for a limited list of optical materials is **HIGH**, given a sustained engineering effort to develop the standpipe viewport concept. These materials may also be feasible for some applications that are closer to the core, but further radiation exposure studies are required. For near-core deployment application, the technical readiness for a limited list of optical materials is **MEDIUM**. COTS fiber-optic feedthroughs that could be used or modified for use in most AdvSMR designs have been identified; therefore, their technical readiness is **HIGH**. The technical readiness for molybdenum and tungsten as optical mirror materials is **HIGH** for their established high performances in high-temperature and high-radiation environments of plasma fusion reactors. Rhodium is also demonstrated as a good mirror material in fusion reactors. However, it is ranked **MEDIUM**, because these mirror components are available only as custom-order items. Common optical materials, such as gold and silver, are ranked **HIGH** when used near the reactor-lid area, but **LOW** for near-core areas because of well-known radiation-induced damage.

Several research, development, and demonstration (RD&D) areas have been identified that could significantly improve the outlook for optical materials and components for the AdvSMR application. For example, theoretical simulation and modeling studies could provide further insight into the fundamental damage processes (i.e., thermal and radiation) of optical materials. Such efforts could be effective at streamlining subsequent experimental studies by down selecting optical materials that are most feasible.

This section contains a summary and analysis of candidate optical materials that could be used in-vessel, for monitoring and sensing of such things as temperatures, pressures, flow rates, and coolant levels. Section 3.1 establishes the requirements for optical components, specifically optical fibers and windows, for in-vessel sensing in the AdvSMR environment. Section 3.2 examines the in-vessel viability of commercially available optical materials. Section 3.3 reviews optical fibers, radiation-induced damage issues, and provides a COTS optical fiber analysis and suggested future research path. Section 3.4 reviews optical windows and provides a COTS gaps analysis and suggested future research path.

3.1   Requirements for In-Vessel Optical Components

In-vessel deployment of optical components requires careful review of material properties in order to maximize performance and lifetime within the extremely harsh environmental conditions associated with AdvSMR designs. It is typically very difficult to reach a workable solution, because most COTS optical materials and components have not been designed and developed for extreme applications. Furthermore, it is common that material properties, critical for this review, are unspecified by commercial manufacturers. Judicious selection of optical fibers, windows, and other optical elements for in-vessel AdvSMRs instrumentation and control (I&C) systems is based on a number of basic material properties, including (Barnes 1992):

- Optical properties
    - Refractive index as a function of wavelength and temperature
    - Optical transmission
    - Birefringence constant

- Thermal properties
  - Coefficient of thermal expansion
  - Thermal conductivity
  - Maximum operating temperatures
  - Surface emissivity
  - Thermal shock
- Structural properties – Mechanical strength, toughness, hardness
  - Poisson's Ratio
  - Modulus of rupture
  - Shear modulus
  - Bulk modulus
  - Knoop hardness
- Chemical properties
  - Solvent, acid, and alkali resistance
- AdvSMR operational lifetime properties
  - Radiation damage
    - Radiation resistance (i.e., gamma, fast neutron, and slow neutron) as a function of flux and exposure time
    - Material activation and transmutation
  - Corrosion – Material compatibility with reactor coolants, cover gases, and impurities
  - Mechanical failure – High vibration, large temperature gradients
  - Mechanical erosion – High velocity coolant flow rates.

3.2 Optical Materials for In-Vessel Deployment

Optical materials are a vital aspect to enabling new, optical-based, in-vessel sensing and measurement concepts, because they provide a means to gain optical access into the in-vessel environs. Optical materials are used to fabricate optical elements (e.g., windows, mirrors, and lenses) and optical fiber, which form the basic building blocks for optical sensing systems. The range of commercially available glass and crystalline materials spans an incredible parameter space. However, only a few optical materials have the potential to be considered in future AdvSMR designs because of the extreme in-vessel environmental conditions. The thermal, mechanical, chemical-compatibility, and radiation-resistance specifications must be carefully considered for each AdvSMR design application. Depending on the relative placement within the reactor vessel, the optical materials may have to survive sustained exposure to the combined effects of high temperature, mechanical forces, concentrations of reactive chemical compounds, and radiation fluxes. The actual performance requirements change significantly depending on the AdvSMR coolant design and placement location relative to the reactor vessel. In many cases, the

manufacturers do not provide all the vital optical material specifications (i.e., radiation-resistance) that are needed to evaluate a design feasibility. In other instances, the specifications have a wide range of possible values, making comparisons between materials difficult.

For the purpose of this survey, we have chosen to rank the applicability of the optical materials to AdvSMR design application based on temperature performance. Many optical materials have softening points or melting temperatures well below expected AdvSMR coolant temperature range, so the thermal specifications can serve as an effective screening parameter for optical materials. Table 3.1 lists some common optical materials, sorted by descending temperature specifications. Melting point temperature (T_m) is given for crystalline materials. The glass transition temperature (T_g) is given for amorphous materials. When T_g is unavailable, the annealing temperature, T_a, is given. The continuous working temperature, T_w, is given when available. These are physical thermodynamic properties that can be measured. Melting point is given for crystalline materials. The glass transition (T_g) or annealing temperature is given for amorphous materials. It should be noted that it is very common to find thermal specifications for the same material, from different sources, to vary by >100°C. The maximum continuous temperature should be at least 100°C–200°C lower than the thermal specifications, to maintain a reasonable design margin for a given AdvSMR application. Even for single crystals, high-temperature creep can be significant, especially under applied mechanical loads. In some cases, optical materials with lower temperature specifications could be considered if an engineering solution could be devised to reduce the maximum deployment temperature (i.e., active or passive cooling). Table 3.1 also provides a mechanical strength specification in terms of rupture modulus, which provides a sense of the fracture strength under load (i.e., a window port in a pressurized reactor vessel). Known chemical incompatibilities are shown for each AdvSMR coolant class. Radiation resistance is not included in this table, because few manufacturers provide any specifications. Radiation-resistance estimates typically only come from published research focused on a limited set of materials and exposure conditions. In-depth discussion of radiation damage mechanisms and research study results are provided in Section 3.3.

Several optical materials have working temperature specifications that exceed the highest expected AdvSMR temperature. A smaller set could even operate beyond fuel failure temperatures (>1650°C). Most optical materials have much lower maximum temperature specifications, but could potentially be used in reactors that operate with lower coolant temperatures. Active cooling with gas or liquids may be possible, but this approach creates other design and implementation challenges.

The expected stresses and potential loads must be considered when designing an optical window for a pressurized reactor vessel. Table 3.1 includes the rupture modulus specification (also known as bending or fracture strength). Because vessel optical windows are unlikely to experience shear forces, the shear modulus has been omitted (but those data are readily available).

Table 3.1. Important Properties of Some Common Glasses Ranked by Melting or Glass Transition
Temperature

Material	$T_g/T_a/T_w/T_m$ (°C)	Rupture Modulus (MPa)[a]	Transmission Range (μm)	Potential Coolant Compatibility Issues[b]	References
CVD Diamond	4027 m	200–1000	0.225–200		Diamond Materials (2008); II-VI Infrared (2010); MatWeb (2013)
Magnesium Oxide (MgO)	2800 m	105	0.3–6		Crystran (2012)
ALON ($Al_{23}O_{27}N_5$)	2150 m	379	0.22–5		Surmet (2013a)
Spinel ($MgAl_2O_4$)	2135 m	170	0.25–6.5	MS?	Surmet (2013b)
Sapphire (Al_2O_3)	2,040 m	448	0.17–5	SCW	Duffey et al. (2011); ICL (2012)
YAG ($Y_3Al_5O_{12}$)	1,940 m	350	0.25-5		Koechner (1973); Crystran (2012)
Zinc Sulfide Cleartran	1,827 m	69	0.4–12		Tosi (2013)
Zinc Selenide (ZnSe)	1,520 m	55	0.55–18		Tosi (2013)
Calcium Fluoride (CaF_2)	1,418 m	37	0.13–10		ISP (2002); Tosi (2013)
Silicon (Si)	1,412 m	124	1.2–10	Na, MS, SCW	Tosi (2013)
Barium Fluoride (BaF_2)	1,354 m	26	0.15–12.5		ISP (2002); Almaz Optics (2011); Tosi (2013)
Magnesium Fluoride (MgF_2)	1,255 m	49	0.11–7.5		Tosi (2013)
Gallium Arsenide (GaAs)	1,238 m	72	1–15		ISP (2002); Tosi (2013)
Fused Silica[c]	1,185 g	49	0.25–3.5	SCW, Na	Tosi (2013)
Cadmium Telluride (CdTe)	1,092 m	22	1–25		IPS (2002); Tosi (2013)
Vycor Glassware	1,020 a	41	0.2–2.6		SGP (2013); MatWeb (2013)
Germanium (Ge)	937 m	104	2–17		Tosi (2013)
Lithium Fluoride (LiF)	870 m	11	0.12–8.5		Tosi (2013)
Aluminosilicate	721 a	11	0.25–2.8		Prazisions (2013)
Cesium Iodide (CsI)	632 m	6	0.25–55		ISP (2002); Tosi (2013)
ZERODUR	600 w	43	0.4–2.5		Russell (2011); Prazisions (2013); Schott Lithotec (2013)
Pyrex 7740	560 g	69	0.28–2.7		Valley Design (2013)
BK7 Schott	557 g	17	0.35–2		Schott (2013b)
AFO Fabry-Pérot -35	527 g		0.40–0.85, 1.10–2.50		Kigre (2009)
Borofloat 33	525 g	25	0.28–2.75		Abrisa Technologies (2012)
ZBLAN	260 g	>600	0.32–4.0		FiberLabs (2013); Zhu and Peyghambarian (2010)
Chalcogenides	185–368 g	17–19	0.7–12.5		Schott (2013a); Schott (2013b); Vitron (2013)

(a) Rupture modulus is also commonly known as flexure or bending strength. Not specified for all materials.
(b) Known chemical incompatibility with AdvSMR coolants and chemistries. Listed categories include supercritical water = SCW, high temperature gas = He, molten sodium = Na, molten lead = Pb, molten salt = MS.
(c) Fused silica, fused quartz, and silica are commonly interchangeable terms.

The rupture modulus (M_R) is obtained by loading a beam of thickness d and width b, which is supported at two points distance L apart, directly at its midpoint up to the point of failure, P. The M_R can then be calculated from (Warren and Shimizu 1963):

$$M_R = \frac{3PL}{2db^2} \tag{3.1}$$

Based on Eq. (3.1), the M_R for a specific material can help predict the window thickness (t) that would be required to withstand a given vessel pressure (P) and an aperture radius (R) (ISP 2009):

$$t \propto \sqrt{\frac{P \cdot R^2}{M_R}} . \tag{3.2}$$

Typically, the rupture modulus of glass will be related to the tensile strength of the material; however, the results can vary considerably, in part because of the material structure and molecular orientation. Surface finish and corrosion have significant effects on the strength of brittle materials. Additional research and calculations will be needed to determine the failure modes of the optical window based not only upon the material characteristics, but also with an emphasis on how the glass will be loaded against mounting hardware and gaskets and chronic exposure to high temperature, chemical exposure, vibration, and radiation flux.

Young's modulus is a measure of the material's elasticity, or stress-strain slope, in the elastic region, which has important implications for its usability. Young's modulus is defined as the slope of the stress-strain curve between no load and the elastic yield strength. Once a material reaches its yield strength, it leaves the elastic regime, and enters into plastic deformation, which means the material shape is physically changing and typically will not recover. A representation of a classical stress-strain curve for a ductile material (e.g., carbon or stainless steels) is shown in Figure 3.1. Brittle optical materials are much more susceptible to failure as a result of strain (mechanical tension) forces, and so can tolerate little flexing or movement of the material before failure.
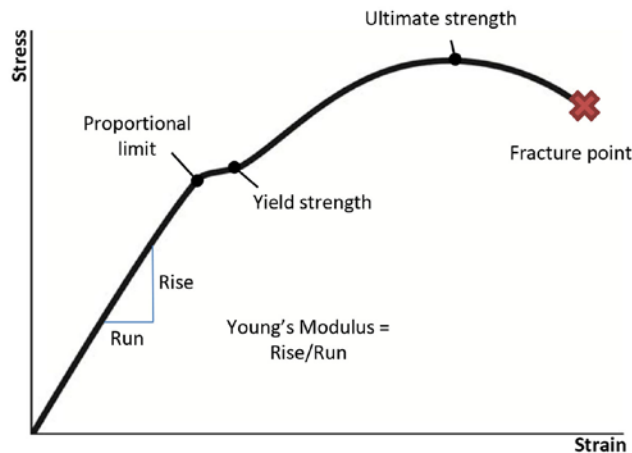
Figure 3.1. Typical Stress-Strain Curve Illustrating Young's Modulus and Fracture Point

In the AdvSMR, pressures are expected to be less than 25 MPa. The rupture moduli for many of the optical materials are well above that limit. The tabulated data also show that many high-temperature materials also have high rupture moduli. Caution must be used for any design when approaching pressurized window design. Manufacturers specify strength in terms of apparent elastic limit, flexural strength, or rupture modulus, but these three terms relate to different methods of test. Furthermore, the published data vary widely for the same material provided by different sources. Common optical materials, such as silica, quartz, and sapphire, may be ideal optical window applications in pressurized AdvSMR designs, but calculation of minimum thickness of a window to withstand a pressure gradient should be approached with conservative safety factors. Optical materials must be selected that stay within the elastic limit for the reactor fuel life cycle. This in itself may be the biggest challenge in obtaining a functional optical window for use in AdvSMR designs, particularly for the high-temperature, high-pressure reactors. Surface finish is also a critical factor in the strength of brittle materials. Defects on a tensile surface will dramatically reduce strength and shorten life of the component. Time to failure for brittle materials is typically reported using Weibull statistics. Time-to-failure estimates typically have large uncertainties, and therefore require "proof testing" to some nominal applied load.

Another important optical material specification is the coefficient of thermal expansion (CTE). Large thermal gradients are expected in AdvSMR designs, through startup to full power. Optical materials, coatings, and mechanical interfaces should be designed with well-matched CTE values; otherwise, differential expansion can quickly delaminate or fracture optical components. Thermal expansion will also affect optical material's refractive index (i.e., strain-induced birefringence). Designs with poorly compensated thermal expansion can also quickly lead to optical component failure because of excessive compression or tension forces.

3.3 Optical Fiber

3.3.1 Introduction

Optical fibers are manufactured from plastic (i.e., polymethylmethacrylate [PMMA] and polystyrene), glass (i.e., doped-silica), and specialty materials, such as chalcogenides, heavy metal fluoride glasses (i.e., ZBLAN), and sapphire (typically unclad light pipes). Optical fiber is available as single-mode, multimode, photonic bandgap (also known as photonic crystal), and hollow core designs. A typical single-mode optical fiber design is shown in Figure 3.2. A core surrounded by a slightly lower index cladding confines a single optical mode. The index difference between the core/clad controls the acceptance angle, called the numerical aperture, for which light can couple into the core from an external source. The low loss core/clad material can promote efficient optical waveguide propagation through long lengths of fiber.

Fused silica and silica-based formulations make up the majority of commercially available fiber products. Silica fiber is available for less than a dollar per meter and can provide near-infrared (IR) losses of less than 0.2 dB/km. Pure fused silica has a T_g around 1200°C and a working temperature of about 1000°C, but will be limited in practical applications by the coatings and jackets used to reinforce it. In most commercial telecommunication applications, jacketed single-mode silica fiber (e.g., Corning SMF-28, OFS TrueWave Reach) is extremely well suited for long-term, continuous use. This fiber and similar offerings from other manufacturers are optimized for long-haul telecommunication applications, where low attenuation, dispersion, and bending loss are important design features.
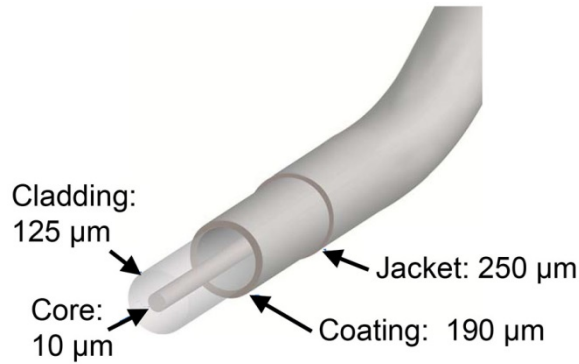
Figure 3.2.   Schematic Showing Layers and Dimensions of a "Typical" Telecom-Grade Single-Mode Fiber. Each layer must be considered for survivability.

Sapphire fiber is another candidate for AdvSMR applications because of its attractive high melting point temperature. Uncoated fiber has a very high melting point (i.e., >2000°C), thermal conductivity, and mechanical strength. Optical transmission ranges from about 0.15 to 6.5 µm. However, unlike conventional single-mode optical fibers, sapphire fibers are grown crystals in the form of rods with only large-core diameters available commercially. These sapphire waveguides are light pipe structures that are highly multimode and sensitive to bending losses and mode conversion. Few suitable high-temperature cladding materials have been developed to enable true sapphire optical fiber. A hydrogen ion doping technique has been used to decrease the sapphire refractive index forming the fiber clad; however, it also reduces the material melting temperature to 800°C (Young and White 1960a).

Transparent ceramics, such as aluminum oxynitride spinel ($Al_{23}O_{27}N_5$) or ALON and magnesium aluminate spinel ($MgAl_2O_4$), have extremely high melt points (2150°C and 2135°C, respectively) and excellent optical transparency between 0.25 to 6 microns. They can be manufactured as blanks and finished optics, including rods that possibly could function as light pipes. Protective coatings may not be required, because these materials were developed for 'transparent armor' applications. Recently single-mode spinel optical fibers were developed by an academic research group (Mangognia et al. 2013). The fiber was fabricated using a molten-core approach on a custom-built drawing tower. It is uncertain whether this fabrication approach could be scaled up to provide COTS products. Thus, they must be sleeved in a silica preform and drawn, resulting in a composite fiber that lacks many of the desirable properties of the ceramics. Significant development is needed to demonstrate functional light pipes or optical fibers made of ALON and spinel materials. The technology readiness for such fibers to be deployed for AdvSMR applications is low.

A number of mid-infrared transparent optical materials such as chalcogenide glass and heavy metal fluoride glass are available in single-mode, multimode, and hollow-core format. Multimode fibers based on AsSeTe chalcogenide glass provide transmission from 2 to 9.5 µm, but have a very low T_g at 136°C. Multimode fiber formed from As_2S_3 provides transmission from 2 to 6.0 µm, but also has a very low T_g at 180°C. All of these chalcogenide fiber products have low mechanical strength, operating temperature, and the internal loss typically limits the practical fiber lengths to 10s of meters or less. Heavy metal fluoride fibers, such as indium fluoride (InF_3) and zirconium fluoride (ZrF_4), are available as single-mode and multimode fibers. These fibers have transmission between 0.3 to 5.5 µm and 0.3 to 4.5 µm, respectively, but also have a very low T_g around 260°C. These optical fibers are not among our

recommendations of optical fibers for AdvSMR applications unless engineering solutions are developed to extend their operational temperature significantly.

In this section, the maximum continuous temperature, corrosive resistance and chemical compatibility, and radiation resistance of optical fiber are reviewed. Environmental stress is a significant factor in the useful lifetime of fiber-optic components. Extreme temperatures affect bare optical fiber, protective coatings, and cable materials, causing some materials to become very soft and fail mechanically. Hydrostatic or elevated gas pressure causes gas or liquids to permeate fiber coatings, insulation, or cable jackets. Gases, chemicals, water, and steam can also damage components. Radiation can damage all fiber-optical components, depending on the material type and dosage level. Optical-fiber materials also can be damaged by high-velocity fluid erosion or mechanical vibration.

3.3.2   Maximum Continuous Temperature

The material properties of optical fibers and cable assemblies fundamentally limit the temperature cycling and upper working temperature performance. Uncoated fibers, silica and sapphire in particular, generally cannot be handled or bent into a very tight radius without breakage. Transparent ceramic light pipes may not require protective coatings because these materials were developed for 'transparent armor' applications. But mechanical properties of these uncoated light pipes have not been widely studied at high temperatures. To increase the ruggedness, coatings, sheaths, and jacket materials are routinely used by the optical-fiber industry. The cladding can be coated with a number of materials such as acrylates, silicones, and polyimides. These coatings significantly improve the mechanical strength of optical fiber and offer increased resistance against chemical attack and abrasion. Unfortunately, these coatings significantly limit the maximum operating temperature of the optical-fiber assemblies. Most commercial single-mode and multimode optical fibers use urethane acrylate coatings that limit the maximum continuous temperature to around 85°C. Table 3.2 shows the operating temperature specifications for coating materials offered on optical fibers.

Acrylates tend to have low temperature rates, usually near 85°C to a maximum of 150°C depending on the formulation. Silicone coatings can operate to about 200°C and polyimide coatings to about 300°C. Optical fibers with coatings that require protective overcoat layers will have a maximum continuous temperature rating based on the lower of the two coating ratings. For example, carbon is usually deposited to minimize the effects of hydrogen ingression and moisture-induced static failure. Carbon coatings must be protected using an overcoat, such as polyimide. The resulting fiber assembly would then have an upper temperature limit of 300°C. Sheath and jacket materials can further reduce the upper temperature ratings of the optical fiber components. Commercial fiber-optic cables are available for military tactical and other demanding applications, but the thermal performance generally fails to meet AdvSMR requirements. These materials are typically polyester, polyvinyl chloride, and nylon compositions, with temperature ratings less than 125°C. Some Teflon-based materials have temperature ratings to 260°C. All sheathing materials for high-temperature applications, such as stainless steel, alloys, and ceramic, have temperature ratings to well above 1000°C. However, most commercial ceramic or stainless steel tubings are designed to enclose polymer-jacketed fibers for added protection. Custom processes need to be developed for bare fiber, metal, or carbon coated fibers. Under extreme temperature cycling and thermal gradients (such as in AdvSMR reactor vessels), it is likely that the fiber-optic component temperature rating will require conservative derating to maintain safety margins.

Table 3.2. Operating Temperature Specifications for Popular Fiber-Optic Coating Materials

Material	Maximum Continuous Temperature (°C)	Comments
Carbon	1000	Must be overcoated
Gold	700	Must be overcoated, potential delamination during temperature cycling
Copper Alloy	450	Must be overcoated, potential delamination during temperature cycling
Aluminum	400	Must be overcoated, potential delamination during temperature cycling
Polyimide	300	Hydrophilic
Fluoropolymer PFA	260	Low abrasion and radiation resistance
PEEK	240	Attacked by some acids
Silicone	200	High-temperature hardening and embrittlement
Fluoropolymer Tefzel	150	Limited temperature range
High-Temp Acrylate	150	Limited temperature range
Fluoroacrylate	125	Limited temperature range
Hydrocarbon Acrylate	125	Limited temperature range
Nylon	100	Limited temperature range
Urethane Acrylate	85	Limited temperature range

Coating and jacket materials must not contain elements that readily neutron-activate, such as polymer coatings that contain chlorine and stainless steel fiber cabling that contains cobalt. Fluorine-containing plastics are known to fail mechanically in high neutron environments. Some metals transmute to other elements by neutron capture, including Au to Hg and Al to Si, but this phenomenon may not significantly affect the metal stability because only a small amount of transmutations occur at very high neutron fluence; for example, 0.8 percent Si when Al is irradiated to 10^{22} n/cm^2 fast neutron (Farrell et al. 1970).

3.3.3   Chemical Compatibility and Corrosive Resistance

Little research has been conducted on optical materials solubility under expected AdvSMR conditions. High temperature and radiation exposure are known to increase chemical reaction rates and provide energy to drive reactions that would otherwise be thermodynamically improbable. Silica is known to have some solubility under high temperature and pressure water exposure. Sapphire is soluble in the most aggressive fluoride salts (e.g., PbF_2, Na_3AlF_6, BaF_2, and AlF_3) at high temperatures (>1000°C) (Elwell and Scheel 1975). Actual solubility in proposed AdvSMR molten coolants is unknown and will require further investigation.

When considering optical-fiber chemical compatibility or corrosion resistance, it is important to consider not just the fiber materials, but also the entire cable assembly. Cable assemblies may contain an air gap or gel to avoid large strains in the optical waveguide along with a strength member (wire or Kevlar) and the final outer jacket of polymer or steel. Additionally, coatings, jackets, and connectors are made from a wide variety of polymer and metal compounds. Component design optimization to enhance corrosion resistance will require a focused RD&D effort.

3.3.4   Radiation Resistance

Radiation-induced optical and mechanical effects occur in most optical materials and optical components, such as optical fibers. This section describes key aspects of radiation-induced materials damage, mainly for optical-fiber components, but the same damage mechanisms also affect other optical components (e.g., windows, lenses, and prisms). The most widely studied material is silica optical fiber. Radiation-induced darkening arises from even very low dose of gamma irradiation. Darkening or transmission loss occurs in many optical-fiber materials between the ultraviolet (UV) and visible spectral regions. Radiation-induced luminescence is found predominantly in the UV wavelengths. Radiation-induced compaction is mainly associated with high-energy neutron irradiation, resulting in refractive index change in the optical material. Non-optical effects, such as mechanical deterioration, also can occur and require consideration. Some materials, like indium and gold for example, will transmute to other elements under neutron flux. Such limitations will have to be addressed on a material-by-material basis.

The following sections summarize these damage mechanisms for each material and fiber design, as well as studies that suggest pathways to reduce their impact.

3.3.4.1   Silica

Radiation Darkening

Published literature reports that many optical materials experience the strongest darkening effects at shorter wavelengths, as shown in Figure 3.3 for a long-wave IR-transmitting glass. Radiation darkening in silica glasses, and particularly those doped with Germanium, is most strongly observed in the UV and visible range (Henschel 1994; Spencer et al. 1994). Studies using COTS optical fiber have been demonstrated in vessel temperature measurements, at near infrared wavelengths where negligible photo-darkening (Sang et al. 2008).

Radiation-darkening effects in amorphous silica fibers, have been thoroughly studied in the last 40 years since the 1970s. The general findings are that radiation darkening is result of defect precursors in the glass network, and the radiation-induced darkening effects are most impactful in the UV and visible spectra under 800 nm. Darkening effects depend on a vast number of factors, including purity of silica core, dopant, manufacturing process, jacket material, irradiation energy, dose rate, total dosage, and pre-, during, and post-irradiation treatment. Depending on the application need, radiation effects can be reduced by several techniques in parts of the spectral regions. It is difficult to compare results from decades of research performed under a variety of conditions on different optical-fiber types. Therefore, this section summarizes the results from just a few prominent international research groups that have demonstrated continuous research on this subject over the last several decades. This summary also focuses on studies conducted at high dose rate and total dosage that are similar to expected radiation levels within AdvSMR vessels.
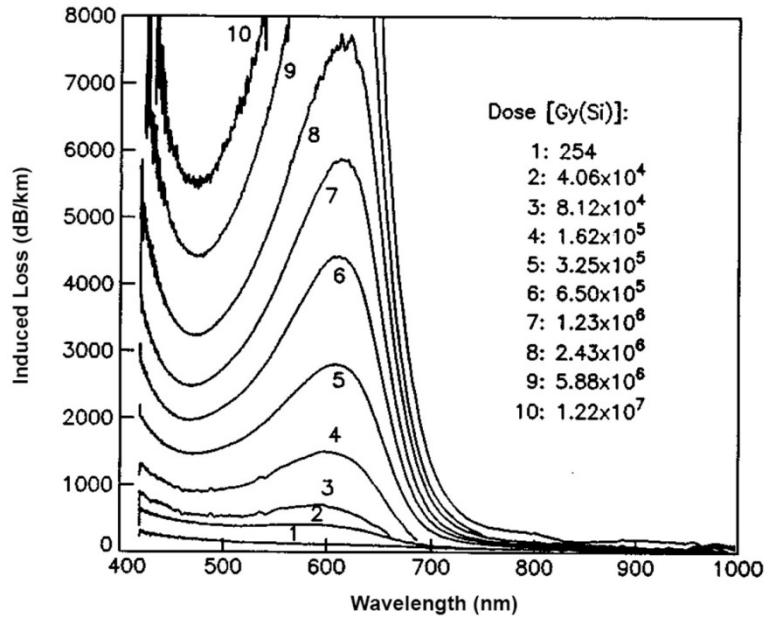
Figure 3.3.　Radiation-Induced Loss in a Pure Silica Core Optical Fiber Exposed Up to 12.2 MGy Gamma Radiation (Griscom 1996). Reprinted with permission. Copyright 1996, AIP Publishing LLC.

The research community consensus on the radiation-darkening issue is that high-purity silica core/fluorine-doped clad fibers have the greatest resistance to radiation darkening, because of dopants and impurities that introduce color center defects (EPRI 1992). However, there is no such thing as absolutely pure silica. OH and Cl are two impurities that persist even in high-purity silica at various levels depending on the manufacturer and materials processing methods. The radiation-darkening mechanism and outcomes depend on the concentration of these impurities. Insight into these dependencies can be found in studies conducted by Nagasawa et al. (1984; 1986) and Griscom (1991). Several defect centers are identified to be responsible for different radiation-induced absorption (RIA) bands. High Cl content results in radiation-induced absorption in the UV spectral region and a strong tail into the visible spectrum. High OH is associated with nonbridging oxygen hole centers (NBOHCs) that are centered in 600 nm and 630 nm, and several OH absorption bands in near infrared (NIR) and IR. Low concentration OH and Cl impurities are a result of the silica purification process and consequently result in a transient radiation-induced absorption bands at 660–760 nm that can be erased upon further irradiation. NBOHC bands peaking in the range of 600–630 nm can also be derived from precursors specific to the manufacturing process. Study suggests that the number-density profile of NBOHC has a maximum just under the core-cladding interface of silica core/fluorine-doped clad fibers. It is suggested that the origin of these excessive NBOHCs may be the conversion of paired hydroxyl groups ($\equiv$Si–OHHO–Si$\equiv$) near the surface of the core rod into peroxy linkages ($\equiv$Si–O–O–Si$\equiv$) during plasma deposition of the F-doped cladding. However, the general perception that NBOHCs result mainly from radiolysis of OH groups is not supported by literature (Nagasawa et al. 1986; Griscom 1996). Other factors including Cl impurity content and oxygen plasma treatment in the manufacturing process may also play a role.

To mitigate or reverse radiation-darkening effects, a number of concepts are under study, including hydrogen treatment, fluorine doping, cerium doping, pre-irradiation, thermal annealing, photo bleaching, and using novel fiber structures such as photonic crystal fibers. Each method is specific to application and material and not universally applicable to all fibers. Also, each method improves radiation darkening in certain spectral ranges at the expense of other spectral ranges or other fiber properties.

Hydrogen treatment of the fiber prior to irradiation has been found the most effective method to improve radiation hardness. A possible reaction of hydrogen on NBOHC sites is to reduce the number of precursors of radiation-induced defects by reversing peroxy groups to hydroxyl groups. Soaking fibers in molecular hydrogen at elevated temperature and pressure (Brichard et al. 2007a) prior to irradiation doping is found to reduce the drawing-induced absorption commonly observed in low-OH fibers, NBOHCs defects in the 600–630 nm absorption bands in all types of fibers, and transient RIA occurring around 660–760 nm in low-OH/low-Cl fibers. This was supported by earlier observation that both the NBOHC peak and the UV band tail were bleached out permanently under sustained gamma irradiation at over 10-MGy doses in acrylate jacketed fibers (Griscom 1995). This was explained as a result of photostimulated reaction of NBOHCs and Cl impurities with atomic hydrogen that is radiolytically liberated from the acrylate jacketing material. This radiation bleaching effect was not observed on the aluminum-jacketed fibers (Griscom 1996) in similar irradiation conditions. However, exposing fibers to hydrogen modifies the IR spectrum by introducing additional H_2-induced absorption bands at 1.245, 1.132, and 1.083 µm and an OH absorption band predominantly at 1.38 µm, although this problem can be solved by replacing hydrogen with deuterium (Zabezhailov et al. 2002). Hydrogen also makes fiber more sensitive to radiation in the UV region for wavelengths below 475 nm (Girard et al. 2013).

Comparing to low OH or hydrogen-treated fibers, doping the fiber core with fluorine generates lower RIA below 500 nm (Brichard et al. 2004). Fluorine tends to act in a similar way as hydrogen because of its high reactive capability. It blocks the formation of dangling bonds but without introducing optical absorption bands. However, fluorine is not as efficient as hydrogen in blocking the formation of NBOHCs and leads to high RIA in the 600-nm region. Other disadvantages of fluorine doping are reduced numerical aperture because fluorine reduces fiber core refractive index, increased fiber fragility, and higher bending loss.

Dopants such as lead and germanium are often added to the silica fiber core to increase the fiber numerical aperture. These dopants increase nonbridging oxygen ions, trapping holes upon irradiation that give rise to optical absorption bands in UV and visible spectral regions. It is well known that the addition of cerium to a lead-silicate or germanium-silicate glass decreases the intensity of the NBOHC or lead absorption bands (Barker and Richardson 1961). The Ce^{3+} in the glass competes with the hole traps such as the NBOHC or Pb^{2+} ions for the radiation-produced holes, while the Ce^{4+} competes with the electron traps for the radiation-produced electrons. Ce doping proves effective when exposed to low-dose gamma radiation. Further research is needed under high-dose gamma and neutron radiation exposure.

Pre-irradiation has shown to eliminate defects causing 660- and 760-nm bands that are intrinsic to low-OH, low-Cl silica. These bands are not impurity-related. It is speculated that the precursors may be structures involving substantial numbers of atoms and, specifically, that these structures may be local regions where Cl ions have been removed from the material. These precursors may not be eliminated during fiber fabrication, but radiation hardening can be achieved by pre-irradiation at a high dose rate and magnitude.

Radiation darkening at certain spectral regions experiences a natural recovery over time at room temperature. The gamma-irradiated UV absorption tail (< 500 nm) that originates from Cl impurity under gamma radiation subsides significantly after an 18-day recovery period at room temperature. Thermal annealing during and post-irradiation can speed recovery. Thermal annealing at $600°C$ is proven effective in removing radiation effects resulting from neutron irradiation (fluence $\sim 10^{18} \mathrm{n/cm}^2$ at energies > 0.1 MeV) (Leon et al. 2008) or gamma irradiation (11.6 MGy at 4.8 Gy/s) (Martin et al. 2011) alone on silica glass of various origin and different OH content. However, absorption bands near 630 nm resulted from consecutive high dose rate gamma (12 MGy at 5.6 Gy/s) and high energy neutron irradiation (fluence $\sim 1.9 \times 10^{16} \mathrm{n/cm}^2$ at energies > 2.8 MeV) are highly thermal stable at $600°C$ (Griscom 1996), although the same annealing conditions substantially removed the radiation induced loss at < 500 nm.

Radiation Luminescence

Radiation-induced luminescence (RIL), or radioluminescence, in the UV spectrum region is observed in all types of fibers that are transmissive in the UV. RIL produces background optical noise that can reduce the signal-to-noise ratio in optical-based sensing systems. The main contributor to the luminescence comes from the Cherenkov emission induced by the gamma radiation. There also exist other contributors arising from the defect generation or by the presence of oxygen. Radioluminescence is more pronounced in hydrogen-treated fibers because of creation of Si-ODC(II) defects and its precursor (Girard et al. 2013). Hydrogen-treated fibers also improve transmission of luminescence because of absorption reduction properties of the treatment process.

Radiation Compaction

Radiation compaction upon high-energy particle irradiation, such as neutrons, results in refractive index change in optical fibers. When the fluence of high-energy neutrons reaches a significant value, the displaced atoms will affect the microstructure of the material and, in turn, the optical properties. When subject to neutron or particle bombardment, amorphous silica, as well as its crystalline counterpart, gradually transforms into a different amorphous state, known as the metamict phase. Quartz undergoes a swelling characterized by a decrease of its density up to 14 percent. On the other hand, amorphous-irradiated silica exhibits compaction, with a density increase up to about 4 percent. The resulted refractive index change is also linked to absorption changes according to the Kramers–Kronig relationship. Infrared absorption at 1.39 µm vibration band was noted in a polymer-coated silica fiber when compacted under neutron exposure (Brichard et al. 2001).

Radiation Mechanical Damage

Studies of radiation damage in silica fiber have generated conflicting results. Many studies suggest that gamma or neutron irradiation in uncoated fiber produces very little mechanical weakening in fused silica fiber, including germanium-doped telecom-grade fiber. In fact, under gamma irradiation in excess of 1 MGy, fibers have been observed to actually increase in mechanical strength by 2 to 10 percent (Henschel et al. 1994). In one of the few side-by-side studies, gamma flux strengthened a Ge-doped single-mode fiber by 5 percent and high-energy neutrons weakened the same fiber by 3.5 percent (Henschel 1994). Very few other research groups have reported any results for mechanical effects from neutron bombardment. Small defects inside the fibers, caused by radiation, may cause some weakening under intense radiation flux; however, studies suggest that these effects are extremely minor and can be healed with time or annealed at elevated temperature (Henschel 1994). A larger concern is micro-cracking, which nucleates from surface flaws and can lead to mechanical failure in optical fiber under

tensile or bending forces. A recent study showed that after gamma radiation exposure, silica fiber is significantly surface roughened (van Uffelen et al. 2006). Exposure to certain chemical compounds has been reported to increase micro-cracking (Perry et al. 2012).

Other authors report on mechanical weakening of silica fibers from gamma and neutron bombardment. Loss in mechanical strength appears to have more to do with the coating material selection than the optical-fiber core/clad material. Several reports have demonstrated discrepancies in radiation-caused mechanical failures depending on the coating. For instance, coatings containing fluorine, like PTFE, Tefzel, or PCS 200, are prone to release silica-attacking compounds when irradiated (Norris et al. 1990; Semjonov et al. 1997). It has been conjectured that most polymer coatings are likely to release protons while exposed to radiation. Subsequent proton flux could cause "Newtonian plastic flow" in silica fiber, which would result in significant weakening. Polyimide and silicone rubber, while not suitable high-temperature coatings, have very good radiation hardness (Norris et al. 1990). Nylon does interact with silica under gamma exposure, but quickly become brittle (Yashima 1982). Fluorine-containing plastics are known to fail mechanically in high neutron environments. Fibers coated with acrylate have been studied, but the results are widely varying (Semjonov et al. 1997; van Uffelen et al. 2006). However, an acrylate-coated distributed temperature sensor was successfully demonstrated in a working test reactor for a continuous period of 22 days. This study is one of the few long-term optical sensor investigations conducted in a nuclear reactor (Cheymol et al. 2008). Materials must not contain elements that readily neutron-activate. Polymers, such as vinyl, contain chlorine, and stainless steels that contain cobalt and chromium must be avoided.

Metal coatings, such as aluminum or tin, are extremely robust to radiation, but fare poorly at elevated temperature because of metal transitions and metal-silica reactions (Semjonov et al. 1997). A thin carbon layer in between the aluminum and silica layers was shown to significantly, but not entirely, delay the aluminum-silica reaction above 400°C (Semjonov et al. 1993). Gold coatings for optical fibers are particularly well suited for extreme temperatures up to 700°C, but studies on their performance under gamma or neutron exposure were not reported. Gold is also known to transmute to mercury by neutron capture. Gold and other metal coatings may have limited potential for most AdvSMR applications. It is likely that all metal coatings will require overcoat layers to protect against abrasion, which will reduce the maximum working temperature.

Mechanical strength loss is often characterized using one of two methods: bending stress or tensile stress. The fiber under evaluation is either bent or stretched longitudinally until the fracture point. While these two methods do not measure the same precise material properties, the literature seems to show comparable degradation because of radiation exposure. Future studies would benefit from standardized exposure and evaluation methods.

3.3.4.2 Sapphire

Sapphire is a fairly gamma- and neutron-resistant material (Sporea and Sporea 2007). Only minor increases in attenuation at the UV end of its transmission spectrum are typically reported during irradiation tests. Sapphire has two predominant darkening bands in the UV-visual that are caused by gamma radiation—one at 308 nm and one at 403 nm (Fuks and Degueldre 2000). These broad peaks come from electron hole centers and largely overlap to create a general darkening in regions below 600 nm. Irradiation tests using mixed gamma and neutron sources have reported similar darkening effects. However, neutron damage is far more disruptive than gamma, causing lattice defects that quickly

create significant attenuation across the visible spectrum (Orlinski et al. 1994). It is indicated that neutron irradiation of 10^{19} n/cm^2 fluence induced a 2 percent volume expansion of sapphire (Zhang et al. 2013). The same study indicates that the elastic modulus in neutron-irradiated sapphire is lower than that in pristine specimens, which reveals that the interaction force between atoms in sapphire is decreased by neutron irradiation. However, the fracture toughness of sapphire is increased by neutron irradiation, which induces an increase of sapphire strength. The strengthening mechanism of sapphire by neutron irradiation will need further study.

Issues specific to sapphire fiber will be subject to two variables. The first is whether or not the fiber is doped with any material in order to create lower refractive index claddings. Commercially, fibers are currently sold as light pipes using air as the cladding. However, hydrogen ion implantation has been demonstrated successfully to fabricate cladding layers in sapphire fiber. The effect that this dopant will have on sapphire radiation resistance is unknown and will have to be characterized if such material is developed for reactor applications. The second variable is the coating material on the fiber. Irradiation of many types of coatings can cause the release of secondary particles (electrons or protons), which then cause damage to the underlying fiber. Selection of the coating material will have an effect on the fiber performance and will have to be taken into account.

3.3.4.3   Other Fiber Designs

Photonic crystal fiber (PCF), also called photonic bandgap (PBG) fiber, and hollow core fiber designs can offer superior radiation-resistance properties. Many PCF designs can sustain single-mode properties to about the edge of the silica transmission cutoff (about 2 µm). PCFs can be designed for multimode applications also. There are two types of PCFs—solid core and hollow core. The PCF optical waveguiding is supported by a microstructured arrangement of low refractive index elements (air holes) placed in a high index background material (pure silica). The bandgap is controlled by varying the distance between the centers of two neighboring holes and the hole diameters. The bandgap can be designed to provide continuous single-mode waveguiding over a very large wavelength range. Figure 3.4 shows the schematic cross section of a PCF structure with a hollow core.
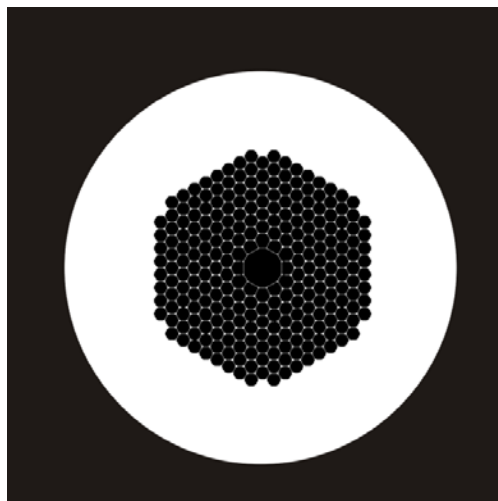
Figure 3.4. Cross Section of Photonic Crystal Fiber with a Hollow Core

Hollow-core designs are essentially metal, plastic, or glass tubes. For hollow-core design to become an effective waveguide, the inner surface of the tubing needs to be coated with a metal/dialectic coating so the refractive index of the core (air) is effectively larger than the cladding. Silica hollow-core fibers coated internally with silver/silver-iodine film layers can provide transmission from about 3 to 20µm.

The solid-core PCFs have much higher radiation-induced absorption when compared to regular silica fibers, perhaps because of the fabrication process-induced color center defects (Wang et al. 2011). Hollow-core designs including both PCFs and conventional hollow-core fiber, however, can provide extremely higher radiation-resistance. Because light is guided in air, the radiation darkening effects are significantly reduced. These hollow-core PCFs have very promising broadband waveguiding performance and their radiation-resistance is favorable for the AdvSMR application.

3.3.5   COTS Optical Fiber Analysis

This review attempts to provide a comprehensive review of optical-fiber products available from major manufacturers, as well as many of the smaller boutique manufacturers. While some COTS products may not be included in this survey (considering the hundreds of specialty manufacturers worldwide), the framework of this gaps analysis is expected to be a representative snapshot of this commercial market sector.

Generally, manufacturers provide environmental exposure specifications given only in terms of induced attenuation at specific transmission wavelengths as a function of test temperature (−60°C to +85°C), temperature-humidity cycling (−10°C to +85°C, up to 98 percent relative humidity [RH]), water immersion (23°C), heat aging (85°C), and damp heat (85°C, 85 percent RH). These are test procedures (e.g., FOTP-69, FOTP-72, FOTP-74, FOTP-4, FOTP-67, and FOTP-160, respectively) established by the Telecommunications Industry Association (TIA) for the telecom industry. Specifications regarding maximum continuous temperature, corrosive resistance, chemical compatibility, or radiation resistance are not typically given unless the fiber was developed for a specialty application.

Many commercial optical-fiber manufacturers produce specialty fiber for harsh environmental applications (e.g., aerospace, defense, down-hole drilling), where one or more of these parameters may be specified. Usually though, the manufacturers are reluctant to quantify these specifications, providing only terms like "excellent resistance" or "rad-hard" performance. Direct discussions with manufacturers suggest that quantifying these parameters is left to the consumer.

The in-vessel optical systems must contend with extremely high radiation fluxes. Average AdvSMR radiation levels are expected to be anywhere from 6×10^{12} n/cm^2·s to 3×10^{14} n/cm^2·s for neutrons and up to 10^8 R/h for gamma (Knoll 2000). Standards organizations have established a few procedures to test optical fibers and cables under gamma and neutron exposure. Relevant procedures include:

- TIA/EIA-455-49-A, FOTP-49, "Procedure for Measuring Gamma Irradiation Effects on Optical Fibers and Optical Cable"[a]

- TIA-455-64 - FOTP-64, "Procedures for Measuring Radiation-Induced Attenuation in Optical Fibers and Optical Cables"[a]

- E1614, "Guide for Procedure for Measuring Ionizing Radiation-Induced Attenuation in Silica-Based Optical Fibers and Cables for Use in Remote Fiber-Optic Spectroscopy and Broadband Systems"[b]

- E1654, "Guide for Measuring Ionizing Radiation-Induced Spectral Changes in Optical Fibers and Cables for Use in Remote Raman Fiber-Optic Spectroscopy"[b]

- MIL-PRF-49291, "Fiber, Optical, Type I, Class I, Size III, Composition A, Wavelength B, Radiation Resistant, Enhanced Performance Characteristics/Aircraft Applications (Metric)"[c]

However, few if any manufacturers test their products under these procedures or provide radiation-resistance specifications for their products, but rather leave it to the customers to conduct testing under representative test conditions. If the customer conducts testing, the results are generally not shared with manufacturers or the public for proprietary reasons.

Some vendors offer radiation-hardened fiber optics components, but generally do not provide specific performance specifications. Table 3.3 lists companies that advertise radiation-resistant fiber-optic products and specify performance to meet a radiation-resistance test standard. Gamma is given in either Rad or grey (Gy), where 1 Gy = 100 Rad. In most cases, the actual radiation-induced attenuation at a specific wavelength is not given.

Table 3.3. COTS Radiation-Resistant Fiber Optic Products

Company	Standard Certification	Product #	Test Conditions	Notes
OFS, A Furukawa Company	MIL-PRF-49291 (specific subcategory standards apply)	50/125/245, 50/125/500, 65.5/125/500	• Steady-state gamma at 50 Rad/min and 10 kRad or undisclosed total dose. • Test temperature: –28, 25, 85°C • 1.0×10^{12} neutrons/cm^2 • <50 dB/km maximum attenuation, <5 dB/km after 1,000 sec recovery time @ 1300 nm	Attenuation at specific wavelength not given

---

(a) Telecommunications Industry Association, 1320 N. Courthouse Rd., Suite 200 Arlington, Virginia 22201, (703) 907-7700.
(b) ASTM International, ASTM Subcommittee E13.09, Optical Fibers for Molecular Spectroscopy; Chairman, Tuan Bo-Dinh, (423) 574-6249.
(c) Defense Logistics Agency, Joint Fiber Optic Working Group (JFOWG).

Table 3.3. (cont'd)

Company	Standard Certification	Product #	Test Conditions	Notes
Linden Photonics, Inc.	European Space Agency - ESCC Basic Specification No. 2263010	"Radiation Resistant Patchcords"	Undisclosed	No part numbers provided
j-fiber Jena	TIA/EIA 455-64	MIL-Spec Radiation Hard Multimode Fiber MMF 62.5/125/245	Gamma (rate/total dose): • 3 Gy/min: 30 Gy • 13 Gy/min: 100 Gy • 13 Gy/min: 1000 Gy • 100 Gy/min: 10000 Gy Neutron: • 1×10^{12} n/cm^2 • 1×10^{14} n/cm^2 • at 23±2°C Vendor data: • 73 Rad/sec, 1×10^6 Rad total dose • Test temperature: 25°C • <30 dB/km @ 1550 mm	Low temperature acrylate coatings
Nufern	None specified	R1310-HTA, 1310M-HTA, and others	Not given	125°C maximum temperature
Draka, Prysmian Group	MIL-PRF-49291 (specific subcategory standards apply)	RadHard series	• 0.45 Gy/s, 10 KGy total dose • Test Temperature: 24°C • 3 dB/100m @ 1570 nm	Single-mode and multi-mode products available
Draka, Prysmian Group	MIL-PRF-49291 (specific subcategory standards apply)	Super RadHard series	• 1.25 Gy/s, 2MGy total dose • Test Temperature: 45°C • 2.2 dB/100m @ 1300 nm	Single-mode and multi-mode products available
AFL	MIL-PRF-49291 (specific subcategory standards apply)	-RH designated Tactical Tight Buffered Cable	• Steady-state gamma at 50 Rad/min and 10 kRad or undisclosed total dose • Test Temperature: –28, 25, 85°C • 1.0×10^{12} neutrons/cm^2 • <50 dB/km maximum attenuation, <5 dB/km after 1,000 sec recovery time @ 1300 nm	Attenuation at specific wavelength not given
CeramOptec	None specified	Optran Polyimide UV/WF, Ultra, UVNS series	Radiation Resistant: 10^9 Rad total dose	Attenuation at specific wavelength not given

Company	Standard Certification	Product #	Test Conditions	Notes
Sumitomo	MIL-PRF-49291 (specific subcategory standards apply)	FutureFLEX	• Steady-state gamma: 50 Rad/min and 10 kRad or undisclosed total dose • Test Temperature: –28, 25, 85°C • 1.0×10^{12} neutrons/cm^2 • <50 dB/km maximum attenuation, <5 dB/km after 1,000 sec recovery time at 1300 nm	
YOEC	TIA/EIA 455-64	RDG 50/125-20/500/900, RDG 62.5/125-27/500/900	Gamma (rate/total dose): • 3 Gy/min: 30 Gy • 13 Gy/min: 100 Gy • 13 Gy/min: 1000 Gy • 100 Gy/min: 10000 Gy Neutron: • 1×10^{12} n/cm^2 • 1×10^{14} n/cm^2 • Test Temperature: 23±2°C	Attenuation at specific wavelength not given

The TIA procedure FOTP-64, "Procedures for Measuring Radiation-Induced Attenuation in Optical Fibers and Optical Cables," specifically addresses steady-state gamma-ray and neutron exposures, and transient gamma-ray, X-ray, electron, and neutron exposures, but few if any manufacturers test their products under this procedure.

In some cases, COTS optical fiber radiation-resistance performance can be estimated from published research studies, for fiber without vendor radiation-resistance specifications. There are vast numbers of optical fiber studies under gamma irradiation, a smaller number of studies were conducted under neutron irradiation, and very few studies were conducted in fission reactors, where the radiation flux levels were similar to expected AdvSMR conditions. Gamma irradiation studies were typically conducted using ^{60}Co sources at room temperature, with gamma dose rate ranges from mGy/s to a few Gy/s. These gamma flux levels are much lower than those expected in AdvSMRs, which are on the scale of kGy/s. Typical neutron flux levels seen in neutron irradiation studies are from 10^8 n/cm^2/s to 10^9 n/cm^2/s with a total fluence from 10^{12} n/cm^2 to 10^{15} n/cm^2. These neutron radiation levels are very low compared to expected AdvSMR conditions. Depending on AdvSMR design, average neutron flux can range from 6×10^{12} n/cm$^2 \cdot$s to 3×10^{14} n/cm$^2 \cdot$s, with fluences from 10^{21} n/cm^2 to 10^{23} n/cm^2 over the lifetime of reactor. The few studies conducted in fission reactors, such as SCK•CEN in Belgium (Cheymol et al. 2011) and JMTR in Japan (Shikama et al. 1995) were performed at comparable AdvSMR radiation levels; however, these reactors operate at much lower temperatures than AdvSMRs. Depending on the type of reactor, and location within the vessel, temperatures in AdvSMRs can be anywhere from 400°C to over 1000°C. In addition, in SCWRs, vessel pressures may be as high as 25 MPa. These extremes are well beyond the testing conditions under which any published studies were performed.

3.3.5.1   Silica

Most COTS fibers research studies used high-purity silica core fiber because of the known radiation-resistant properties. Some fibers were F-doped core or were hydrogen treated for enhanced radiation resistance. A variety of fiber coatings were also used in these studies and were reported to affect radiation-induced attenuation. For example, fast neutrons produce energetic recoil protons in H-containing coating materials, which can penetrate several fiber layers, coiled on a test spool, leading to an increased dose in the fiber core (Henschel et al. 1998). Hydrogen released by the fiber coating also increased the 1.38 µm OH absorption in the fiber (Brichard et al. 2002), but reduced the NBOHC and UV-tail absorption band formation (Griscom 1995, 1996). In addition to a large selection of COTS optical fibers, the testing conditions reported varied greatly. Radiation exposure conditions were dependent the radiation generator and distance from the radiation source. As a result, the radiation fluence varied significantly between studies. Exposure temperature conditions were dependent on the radiation exposure conditions, but typically were uncontrolled or near room temperature. Finally, different wavelengths were used to characterize the radiation-induced darkening. Lacking standard testing procedures makes comparative evaluation difficult, but a subset of our survey is presented here to illustrate the significance of radiation-induced effects.

Some of the COTS optical-fiber technical readiness findings are summarized in the following tables. Table 3.4 lists a subset of COTS fibers exposed to gamma irradiation. Only studies with total dosage > 1 MGy were included in our survey. Table 3.5 lists our limited search results on COTS fibers under neutron irradiation. Table 3.6 lists our limited search results on COTS fibers under combined gamma and neutron irradiation. Some of the fibers shown in Table 3.6 were tested under similar radiation levels as expected in AdvSMRs. Manufacture part number information in the following tables are extracted from literature. The information may not be the most current as companies may have changed names, or gone out of business, merged, or was acquired by others. Companies may also have updated product numbers or discontinued certain products.

Table 3.4. COTS Optical Fibers under Gamma Irradiation

Manufacturer	Part Number	Fiber Description	Radiation Testing	Reference
Heraeus	STU 1.2	Multimode step index, 104/125/250, 0.2 NA, OH 1–20 ppm, Cl: <200 ppm, CCDR 1.2, 40 m and 70 m	• 25°C • Gamma dose rate: 1.25 Gy/s • Gamma dose: 1 MGy • 0.07 dB/m @ 829 nm • 0.004 dB/m @ 1310 nm	Henschel et al. (2002)
FORC	KS-4V	Multimode step index, 110/125/280, 0.2 NA, OH: <0.6 ppm, Cl: <20 ppm, CCDR 1.2, 40 m and 70 m	• 25°C • Gamma dose rate: 1.25 Gy/s • Gamma dose: 1 MGy • 0.18 dB/m @ 829 nm • 0.012 dB/m @ 1310 nm	Henschel et al. (2002)
Mitsubishi	STR100C-SY	Multimode step index, 100/150/300, low OH, 40 m and 70 m	• 25°C • Gamma dose rate: 1.25 Gy/s • Gamma dose: 1 MGy • 0.55 dB/m @ 829 nm • 0.76 dB/m @ 1310 nm	Henschel et al. (2002)

Table 3.4. (cont'd)

Manufacturer	Part Number	Fiber Description	Radiation Testing	Reference
Fujikura Ltd	FF	F-doped silica core, OH free; 200/250; 20 m	• 20°C • Gamma dose rate: 3.33 Gy/s • Gamma dose: 1.9 MGy • 0.8 dB/m @ 600 nm • 0 dB/m @ 1100 nm	Kakuta et al. (2002b)
Mitsubishi	MF	F-doped silica core, OH free; 200/250; 20 m	• 20°C • Gamma dose rate: 3.33 Gy/s • Gamma dose: 1.9 MGy • 0.2 dB/m @ 600 nm • 0 dB/m @ 1100 nm	Kakuta et al. (2002b)
FORC	KS-4V	Pure silica core, OH and Cl free, 200/250, 20 m	• 20°C • Gamma dose rate: 3.33 Gy/s • Gamma dose: 1.9 MGy • 1.2 dB/m @ 600 nm • 0 dB/m @ 1100 nm	Kakuta et al. (2002b)
FORC	KU-1	Original, OH: 800 ppm, 200/250, 20 m	• 20°C • Gamma dose rate: 3.33 Gy/s • Gamma dose: 1.9 MGy • 2.5 dB/m @ 600 nm • 0.4 dB/m @ 1100 nm	Kakuta et al. (2002b)
FORC	KU-H2G	Improved, hydrogen treated, OH: 800 ppm, 200/250, 20 m	• 20°C • Gamma dose rate: 3.33 Gy/s • Gamma dose: 1.9 MGy • 0.7 dB/m @ 600 nm • 0 dB/m @ 1100 nm	Kakuta et al. (2002b)
CeramOptec	UV100/140	Suprasil^{TM}-F100 pure-silica-core/F-doped-silica-clad, OH: 600–800 ppm, acrylate jacket	• 27°C • Gamma dose rate: 7 Gy/s • Gamma dose: 1.2 MGy • 1.4 dB/m @ 600 nm	Griscom (1995)
CeramOptec	WF100/140	Suprasil^{TM}-F300 pure silica core, OH: <1 ppm, acrylate jacket	• 27°C • Gamma dose rate: 7 Gy/s • Gamma dose: 1.2 MGy • 3 dB/m @ 600 nm	Griscom (1995)
Corning	LNF^{TM}62.5/ 125	Graded-index Ge-doped-silica-core/pure-silica-clad, acrylate jacket	• 27°C • Gamma dose rate: 7 Gy/s • Gamma dose: 1.2 MGy • 7 dB/m @ 660 nm	Griscom (1995)
FORC	KS-4V	Pure silica core, OH: <200 ppb, Cl: <20 ppm, aluminum jacket	• 27°C • Gamma dose rate: 5.6 Gy/s • Gamma dose: 12.2 MGy • 2.7 dB/m @ 630 nm	Griscom (1996)

Table 3.4. (cont'd)

Manufacturer	Part Number	Fiber Description	Radiation Testing	Reference
FORC		F-doped-silica core, F: ~0.54%, OH: ~4 ppm, aluminum jacket	• 27°C • Gamma dose rate: 5.6 Gy/s • Gamma dose: 12.2 MGy • 4.5 dB/m @ 630 nm	Griscom (1996)
FORC	KU	Pure silica core, OH: 800–900 ppm, aluminum jacket	• 27°C • Gamma dose rate: 5.6 Gy/s • Gamma dose: 12.2 MGy • 8 dB/m @ 650 nm	Griscom (1996)
FiberGuide Industries	Anhydroguide^{TM}	Heraus Suprasil F300 core, OH: <1ppm, Cl: 2000 ppm, aluminum jacket	• 27°C • Gamma dose rate: 5.6 Gy/s • Gamma dose: 12.2 MGy • 8 dB/m @ 650 nm	Griscom (1996)
FORC	KS-4V	Pure silica core, OH: <0.1 ppm, Cl: < 20ppm, aluminum jacket, hydrogen treated	• 50°C • Gamma dose rate: 5.6 Gy/s • Gamma dose: 5.9 MGy • 0.34 dB/m @ 630 nm • 3.7 dB/m @ 1380 nm	Brichard et al. (2007a)
FORC	KU1	Pure silica core, OH: ~1000 ppm, Cl: 100 ppm, aluminum jacket, hydrogen treated	• 50°C • Gamma dose rate: 5.6 Gy/s • Gamma dose: 5.9 MGy • 0.27 dB/m @ 630 nm • 0.08 dB/m @ 950 nm	Brichard et al. (2007a)
FORC	STU	Pure silica core, OH: 5–20 ppm, Cl: 150–250 ppm, aluminum jacket, hydrogen treated	• 50°C • Gamma dose rate: 5.6 Gy/s • Gamma dose: 5 .9 MGy • 0.32 dB/m @ 630 nm • 3.1 dB/m @ 1380 nm	Brichard et al. (2007a)
FORC	STU	Pure silica core, OH: 5–20 ppm, Cl: 150–250 ppm, aluminum jacket	• 50°C • Gamma dose rate: 5.6 Gy/s • Gamma dose: 1.6 MGy • 0.9 dB/m @ 630 nm • 0.1 dB/m @ 1380 nm	Brichard et al. (2007a)

Table 3.5. COTS Fibers under Neutron Irradiation

Manufacturer	Part Number	Fiber Description	Radiation Testing	Reference
Alcatel Kabel	E9.3/F3.5	9.3/125/250 Ge-doped single-mode	• 25°C • Fluence: 8.1×10^{12} n/cm^2 (14 MeV) • 0.002 dB/m @ 830nm	Henschel et al. (1998)
POF	CD 15865 E1	62.5/125/250 Ge-doped multimode	• 25°C • Fluence: 9.9×10^{12} n/cm^2 (14 MeV) • 0.026 dB/m @ 830nm	Henschel et al. (1998)
Siecor	SMF 1528	9.3/125/250 Ge-doped single-mode	• 25°C • Fluence: 8×10^{12} n/cm^2 (14 MeV) • 0.0025 dB/m @ 830nm	Henschel et al. (1998)
Corning	SMF-28	Ge core, silica clad, dual layer UV-cured acrylate	• 20°C • Flux: 7.0×10^8n/cm^2/s • Fluence: 2.4×10^{14}n/cm^2 (6 MeV) • 0.01 dB/m @ 1300 nm	Troska et al. (1998)
Fujikura	SM.10/125.04. UV	Ge core, silica clad, dual layer UV-cured acrylate	• 20°C • Flux: 7.4×10^8n/cm^2/s • Fluence: 2.6×10^{14}n/cm^2 (6 MeV) • 0.01 dB/m @ 1300 nm	Troska et al. (1998)
Optical Fibers	SM-03-E	Ge core, silica clad, dual layer UV-cured acrylate	• 20°C • Flux: $1.6°10^9$n/cm^2/s • Fluence: $5.6°10^{14}$n/cm^2 (6 MeV) • 0.02 dB/m @ 1300 nm	Troska et al. (1998)
Plasma	MCSM 267E	Ge/F core, silica/F clad, dual layer UV-cured acrylate	• 20°C • Flux: 7.8×10^8n/cm^2/s • Fluence: 2.7×10^{14}n/cm^2 (6 MeV) • 0.007 dB/m @ 1300 nm	Troska et al. (1998)
Siecor	SMF 1528	Ge core, silica clad, dual layer UV-cured acrylate	• 20°C • Flux: 1.5×10^9n/cm^2/s • Fluence: 5.2×10^{14}n/cm^2 (6 MeV) • 0.02 dB/m @ 1300 nm	Troska et al. (1998)
Sumitomo	PSC	Silica core, silica/F clad, acrylate coating	• 20°C • Flux: 1.7×10^9n/cm^2/s • Fluence: 5.9×10^{14}n/cm^2 (3.5 MeV) • 0.01 dB/m @ 1300 nm	Troska et al. (1998)
Nufern	S630	Silica core, silica/F clad, acrylate coating, 900 µm Hytrl buffer	• Flux: 8×10^8n/cm^2/s • Fluence: 2×10^{14}n/cm^2 (3.5 MeV) • 1.5 dB/m @ 630 nm • 0 dB/m @ 681 nm	Calderón et al. (2006)

Table 3.6. COTS Fibers under Mixed Gamma and Neutron Irradiation

Manufacturer	Part Number	Fiber Description	Radiation Testing	Reference
FORC	KS-4V	Pure silica core, OH- and Cl-free	• 135°C • N_f flux: 2.4×10^{17} n/cm²/s • N_{th} flux: 1.9×10^{18} n/cm²/s • N_f fluence: 5.1×10^{23} n/cm² • Gamma heating: 1.4 W/g (for Si) • 2 dB/m @ 800 nm • 30 dB/m @ 1380 nm	Nishitani et al. (2002)
FORC	KU-1	Original, OH: 800 ppm	• 135°C • N_f flux: 2.4×10^{17} n/cm²/s • N_{th} flux: 1.9×10^{18} n/cm²/s • N_f fluence: 5.1×10^{23} n/cm² • Gamma heating: 1.4 W/g (for Si) • 2 dB/m @ 800 nm	Nishitani et al. (2002)
FORC	KU-H2G	Improved, hydrogen treated OH: 800 ppm	• 135°C • N_f flux: 2.4×10^{17} n/cm²/s • N_{th} flux: 1.9×10^{18} n/cm²/s • N_f fluence: 5.1×10^{23} n/cm² • Gamma heating: 1.4 W/g (for Si) • 2 dB/m @ 800 nm	Nishitani et al. (2002)
Fujikura	FF	Fluorine-doped silica core, OH-free	• 135°C • N_f flux: 2.4×10^{17} n/cm²/s • N_{th} flux: 1.9×10^{18} n/cm²/s • N_f fluence: 5.1×10^{23} n/cm² • 5 dB/m @ 800 nm • 32 dB/m @ 1380 nm	Kakuta et al. (2002a)
Mitsubishi	MF	Fluorine-doped silica core, OH-free	• 135°C • N_f flux: 2.4×10^{17} n/cm²/s • N_{th} flux: 1.9×10^{18} n/cm²/s • N_f fluence: 1×10^{22} n/cm² • 32 dB/m @ 800 nm • 20 dB/m @ 1300 nm	Kakuta et al. (2002a)
FORC		SM, 10 µm/150 µm, acrylate	• N_f flux: 1.7×10^{13} n/cm²/c • N_{th} flux: 1.5×10^{14} n/cm²/s • Gamma dose rate: 2 KGy/s • N_f fluence: 1.3×10^{20} n/cm² • N_{th} fluence: 1.2×10^{21} n/cm² • Gamma dose: 16 GGy • 15 dB/m @ 1064 nm • 34 dB/m @ 1310 nm	Cheymol et al. (2009)

Table 3.6. (cont'd)

Manufacturer	Part Number	Fiber Description	Radiation Testing	Reference
Polymicro	FIP 100.110.125 STU/MM	100 µm/110 µm, polyimide	• N_f flux: 1.7×10^{13} n/cm^2/s • N_{th} flux: 1.5×10^{14} n/cm^2/s • Gamma dose rate: 2 KGy/s • N_f fluence: 1.3×10^{20} n/cm^2 • N_{th} fluence: 1.2×10^{21} n/cm^2 • Gamma dose: 16 GGy • 15 dB/m @ 1064 nm • 34 dB/m @ 1310 nm	Cheymol et al. (2009)
FORC	KS-4V+H^2	OH<0.1 ppm, Cl<20 ppm, hydrogen treated, aluminum	• 100°C • N_f flux: 2×10^{12} n/cm^2/s • Gamma dose rate: 317 Gy/s • N_f fluence: 4×10^{16} n/cm^2 • Gamma dose: 7 MGy • 13 dB/m @ 450 nm • 5 dB/m @ 67 nm	Brichard et al. (2007b)
FORC	KU-1+H^2	OH~1000 ppm, Cl 100 ppm, hydrogen treated, aluminum	• 100°C • N_f flux: 2×10^{12} n/cm^2/s • Gamma dose rate: 317 Gy/s • N_f fluence: 4×10^{16} n/cm^2 • Gamma dose: 7 MGy • 15 dB/m @ 450 nm • 25 dB/m @ 630 nm	Brichard et al. (2007b)
FORC	STU+H^2	OH 5–20 ppm, Cl 150–250 ppm, hydrogen treated, aluminum	• 100°C • N_f flux: 2×10^{12} n/cm^2/s • Gamma dose rate: 317 Gy/s • N_f fluence: 1×10^{17} n/cm^2 • Gamma dose: 20 MGy • 13 dB/m @ 450 nm • 2 dB/m @ 630 nm	Brichard et al. (2007b)
FORC	STU	OH 5–20 ppm, Cl 150–250 ppm, aluminum	• 100°C • N_f flux: 2×10^{12} n/cm^2/s • Gamma dose rate: 317 Gy/s • N_f fluence: 2×10^{16} n/cm^2 • Gamma dose: 5 MGy • 13 dB/m @ 450 nm • 25 dB/m @ 630 nm	Brichard et al. (2007b)

N_f = fast neutron
N_{th} = thermal neutron

The relatively low optical attenuation after irradiation in some of vendor specifications (Table 3.3) and published studies (Tables 3.4–3.6) suggests possible suitability for in-vessel sensing applications in AdvSMRs, if they are robust enough to survive the other extreme AdvSMR conditions. To gauge the relevance of the COTS radiation resistance standards certifications and the prior irradiation studies, we can compare the irradiation conditions to estimated AdvSMR gamma fluence and neutron flux based. A

rough average neutron flux for AdvSMR design is taken to be 10^{12} n/cm^2·s based on published data. Little information is published on AdvSMR gamma fluence. 2 kG/s gamma fluence is estimated based on irradiation conditions in the 70 MW light-water open pool OSIRIS reactor in Belgium (Cheymol et al. 2011).

Beginning with the COTS radiation-resistance procedure testing, the greatest neutron irradiation was 10^{14} n/cm^2, which corresponds to a 100 s exposure in an AdvSMR. The maximum gamma dose for procedure testing is 10 kGy and vendor specification is 10 MGy. The equivalent irradiation in an AdvSMR is 5 s and 5000 s, respectively. The maximum neutron fluences for the research investigations were 5.1×10^{23} n/cm^2 (thermal) and 10^{23} n/cm^2 (fast), which is tens to thousands of years in an AdvSMR. The maximum gamma dose was about 2 MGy, which corresponds to 1000 s exposure in an AdvSMR. Conclusive statements about the technical readiness of COTS optical fiber, in terms of gamma irradiation, is difficult because vendor specifications, testing procedures, and published research is based on irradiation that is orders of magnitude lower than expected AdvSMR conditions. Given this, we rank the gamma-resistance technical readiness uncertain. Vendor neutron irradiation hardness specifications, based on testing procedures, provided little insight into applicability of COTS optical fiber for AdvSMR deployment. On the other hand, research studies did demonstrate the feasibility of long life under intense neutron irradiation for optical fibers available from Blaze Photonics, FORC, Mitsubishi, and Polymicro.

3.3.5.2   Sapphire

Several commercial companies, including Photran, Saint-Gobain/Saphikon, Leoni, and MicroMaterials, manufacture sapphire optical fiber. Only multimode fibers are available, with diameters between 75 and 500 µm. These fibers are generally classified as "light pipes," because they do not have a cladding layer. Large-diameter fibers become increasingly more rigid, because the flexibility varies as the inverse 4th power of the diameter. COTS lengths are available only from 0.1 to 2 m, with special order to 4 m. The manufacturers recommend using a fluoropolymer overcoating to improve durability and handling, but these consequentially reduce the maximum operating temperature. Radiation-resistant studies on COTS sapphire are unavailable from manufactures. Sapphire fibers were first subjected to testing in a radiation environment in 2007 (Sporea and Sporea 2007) and this study remains the only one we found on radiation performance of sapphire fiber. Table 3.7 lists the results of this study. Although lacking of the fiber origin, it represents a snapshot of the sapphire radiation performance that can be achieved to date.

Table 3.7. Sapphire Optical Fibers under Gamma or Neutron Irradiation

Manufacturer	Part Number	Fiber Description	Radiation Testing	Reference
Photran	n/a	425-µm diameter, 25-cm length, no cladding or coating	• Gamma dose rate: 0.09 Gy/s • Gamma dose: 536.2 KGy • ~10 dB/m @ 630 nm (no change from unirradiated)	Sporea and Sporea (2007)
Photran	n/a	425-µm diameter, 25-cm length, no cladding or coating	• N_f flux: 2×10^{10} n/cm^2/s • N_f fluence: 3.15×10^{13} n/cm^2 • ~10 dB/m @ 630 nm (no change from unirradiated)	Sporea and Sporea (2007)

3.3.5.3   Other COTS Fiber Designs

Hollow-core PCF fibers are available from NKT Photonics, Crystal Fiber A/S, and other vendors. These PCF fibers have a minimum bend radius specification of < 0.5-cm (a bend radius without suffering optical transmission loss). However, PCF fibers must be protected using an overcoat layer, usually acrylate or polyimide. High temperatures and large temperature gradients could possibly damage the delicate structure of PCF designs. Silica hollow-core fibers with inner diameter from 2 to 2500 µm are available from CeramOptec and Molex Polymicro. Hollow-core (non-PCF) designs require internal metal/dielectric coatings to promote efficient waveguide transmission. The hollow-core coatings are unlikely able to survive sustained temperatures beyond the maximum operating temperatures of polyimide. Without coatings inside the hollow core, they are essentially leaky waveguides and are likely to have poor transmission performance, even for short lengths. Because of the stiffness of silica hollow core, the fibers are restricted to over 30 cm bending radius and 3 m maximum length. Additionally, capillary action could wick liquid coolants into the hollow-core and photonic crystal structures and destroy the waveguide properties of the optical fiber. These fibers could only be used above molten coolants and only immersed if a facet-sealing method was developed.

None of the manufacturers provide radiation-resistance specifications for their COTS PCF and hollow-core fiber products. There are limited published research studies on the radiation resistance of hollow-core PCF fibers, since the first reported study was published in 2005. Table 3.8 lists the literature survey results for hollow-care PCF fiber radiation studies. One study did show that one COTS PCF optical fiber (Crystal Fiber A/S, HC 1060-02/SM) suffered only modest loss about 1.9 dB/m after exposed to an excessive fast and thermal neutron fluence and 11 GGy gamma total dose (Cheymol et al. 2009). The total neutron dose is equivalent to roughly 9.2 years of extended exposure within a HTGR reactor. No published radiation-resistance study results for silica hollow-core fibers were found.

Table 3.8. PCF Fibers under Gamma or Neutron Irradiation

Manufacturer	Part Number	Fiber Description	Radiation Testing	Reference
Crystal Fiber A/S	HC19-1550-01	20 µm hallow core, 3.9 µm pitch, 1570 nm center wavelength, 50 m long	• 25°C • Gamma dose rate: 0.73 Gy/s • Gamma dose: 10 KGy • 0.6 dB/m @ 1546 nm	(Henschel et al. 2005)
Crystal Fiber A/S	HC 1060-02/SM	9.7 µm (hole)/125 µm, 1060 nm center wavelength, acrylate jacket	• N_f flux: $1.7{\times}10^{13}$ n/cm^2/s • N_{th} flux: $1.5{\times}10^{14}$ n/cm^2/s • Gamma dose rate: 2 KGy/s • N_f fluence: $9.7{\times}10^{19}$ n/cm^2 • N_{th} fluence: $8.7{\times}10^{20}$ n/cm^2 • Gamma dose: 11 GGy • 2 dB/m @ 1064 nm • 4 dB/m @ 980 nm	Cheymol et al. (2008) Cheymol et al. (2009)

3.3.6 COTS Summary, Gaps Analysis, Ranking, and Proposed Future Research

COTS Optical Fiber Summary

COTS optical-fiber analysis is a complex issue because of widely varying performance resulting from different fiber compositions, impurities, and manufacturing processes. COTS optical-fiber characterization studies use nonstandardized evaluation methods that make performance comparisons difficult. Most COTS fiber radiation-exposure studies use low, short-duration gamma or neutron fluxes, near room temperature. Only a few COTS optical-fiber products have been tested under high-thermal and fast-neutron fluxes in reactors. Several optical fibers, including several FORC silica fibers and one Crystal Fiber hollow-core PCF silica fiber, have demonstrated high radiation-resistance. Among the very limited radiation testing on sapphire fibers, one sapphire fiber from Photran shows no additional loss induced by a modest amount of radiation (gamma dose: 536.2 KGy, or N_f fluence: $3.15{\times}10^{13}$ n/cm^2). However, only in rare occasions, the testing temperatures are elevated above room temperature, and none of these fibers are tested under the AdvSMR conditions (combined high temperatures and high fluxes). Although the bare silica and sapphire fibers have higher working temperatures than the typical AdvSMR operation temperatures, bare fibers do not have the mechanical strength to survive a useful lifetime in the high-pressure, corrosion, vibration, and flow environments of AdvSMRs or mechanical handling like insertion and bending. Polyimide jackets, or metal coatings, may provide adequate protection for bare fibers for reactor containment and near-lid deployment. However, the temperature limitations of fiber coatings, sheathing, and cabling materials inhibit near-core deployment feasibility for even radiation-resistant fibers.

Gaps Analysis

The temperature and mechanical specifications for most of the optical materials used to construct optical fibers are very promising, but further RD&D will be required to enhance these materials or develop new materials for extended integration into AdvSMR designs. The most significant technology gaps that currently limit COTS optical-fiber deployment in AdvSMRs include:

- COTS optical-fiber coating, jacket, and cabling materials will not survive most in-vessel AdvSMR temperatures.

- COTS high-temperature, metallized optical-fiber coatings may not survive near-core temperatures and may transmute under intense radiation exposure.

- COTS optical-fiber materials may degrade when exposed to AdvSMR coolants and impurities.

- The vendors do not typically provide radiation-resistance specifications for COTS fiber-optic materials.

- COTS PCF and silica optical fibers and sapphire light pipes have not been tested under combined high-temperature and high-radiation conditions.

- COTS sapphire optical fibers are not available, only unclad light pipes. COTS fiber can only be grown to 1–4 meter lengths.

- COTS optical-fiber components may not have enough mechanical strength for reliable deployment in high-flow AdvSMR coolants.

- Limited theoretical studies have been conducted to develop useful predictive damage models for optical fibers' exposure to high temperature and radiation.

Technical Readiness Ranking

The technical readiness of current COTS PCF and silica fiber and sapphire light pipes, for near-lid applications, is **HIGH**. Polyimide-fiber jackets or custom metal or carbon coatings are likely to withstand expected near-lid temperatures and provide adequate protection for the optical fibers. Many radiation studies have shown that most COTS fibers with pure, F-doped or Ge-doped silica core, exhibit little loss after low gamma, neutron, or combined irradiations.

The technical readiness for near-core applications remains **LOW**. This ranking is primarily because of the poor maximum continuous operating temperature specifications for all COTS fiber components. This stems from the coatings (i.e., outer and internal), sheathing, and cabling applied to the optical fibers to improve the strength and abrasion resistance (all fibers) or transmission (hollow-core fibers).

Proposed Future Research

Successfully overcoming the technical readiness gaps listed above will enable many promising optical-fiber–based sensors to be considered for in-vessel AdvSMR monitoring applications. A number of required RD&D efforts have been identified to address the established technical readiness gaps in COTS optical fibers and materials.

Key Optical Fiber RD&D

- **Theoretical Damage Models**: Theoretical modeling studies are required to better understand fundamental damage mechanisms in fiber-optic materials and estimate component lifetime under expected AdvSMR conditions. This includes understanding noncatastrophic effects that shorten useful life, such as plastic deformation under sustained pressure at elevated temperature and slow degradation from extended radiation and chemical exposure.

- **High Temperature Fiber Optic Components**: High-temperature optical fiber coatings, sheathings, and cabling materials that protect the optical fiber from mechanical damage and chemical attack must be developed. This is especially important, because of the impressive radiation exposure study results of a COTS hollow-core PCF optical fiber (Cheymol et al. 2009). Ideal coating and jacket materials include ceramic or metals with durable properties, excellent bonding properties, and minimal transmutation issues. Materials must not contain elements that readily neutron-activate or transmute. Polymers, such as vinyl, contain chlorine, and stainless steels that contain cobalt and chromium must be avoided. Fluorine-containing plastics are known to fail mechanically in high neutron environments.

- **COTS Optical Fiber Exposure Studies**: Exposure studies are required to determine the robustness of PCF and silica optical fibers and sapphire light pipes under simulated AdvSMR conditions, such as high temperature, radiation fluence, pressure, chemical exposure, and direct coolant immersion. Studying silica optical fiber performance under combined high temperature and neutron/gamma exposure will reveal the interplay between silica optical fiber dopants, especially chemical diffusion over long time scales, and increased radiation resistance and spectral fiber darkening cutoff wavelengths. Corrosion and extreme radiation exposure studies at high temperature are especially needed. Most literature regarding radiation exposure effect in optical materials is from the 1970–1990 time frame. These studies were focused on long-term exposure effects under space or high-energy physics environments. This body of literature points to promising materials, but does not provide insight into damage issues under combined high-radiation and high-temperature exposure.

- **Sapphire Optical Fiber**: High-temperature cladding materials are required to develop useful high-temperature sapphire optical fibers. Only multimode unclad light pipes are available, with diameters between 75 and 500 µm. COTS lengths are available only from 0.1 to 2 m, with special order to 4 m. Process methods must be developed to provide long sapphire fiber lengths (>10 m).

3.4   Optical Windows

A number of optical materials have promising thermal and mechanical strength properties, including several that can tolerate sustained exposure to temperatures in excess of 2000°C. At least a dozen more materials have working temperatures above 1000°C. Most of these materials have rupture moduli that provide >2X working pressure safety margins for pressures expected in SCWR designs. A subset of COTS optical materials listed in Table 3.1 could be good candidates for optical window designs in AdvSMRs, based on working temperature, pressure, chemical compatibility, and radiation-resistance properties. This short list in the order of descending working temperature includes:

- Diamond
- ALON ($Al_{23}O_{27}N_5$)
- Spinel ($MgAl_2O_4$)
- Sapphire (Al_2O_3)
- YAG (Yttrium Aluminum Oxide, $Y_3Al_5O_{12}$)
- Silicon (Si)
- Magnesium fluoride (MgF_2)

- Gallium arsenide (GaAs)

- Fused silica

Some optical materials listed in Table 3.1 were excluded from the COTS optical window analysis because of unsuitable properties. Brittle crystalline materials, such as BaF_2, CaF_2, and LiF_2, can easily fracture as a result of tensile stress acting normal to cleaving planes. CdTe is rarely available commercially because of its toxicity during the manufacturing process. The finished optics are not particularly hazardous, but should be handled with care. Magnesium oxide exhibits several absorption peaks at ultraviolet wavelengths, around 570 nm, and 1045 nm when exposed to neutron irradiation. Radiation-induced darkening at these wavelengths increases monotonically without saturation when exposed up to fast neutron (14 MeV) fluence of 10^{19} n/cm^2 (Okada et al. 1985). Magnesium oxide therefore is considered a functional material for neutron fluence monitoring, but is not suitable as window material. ZnS, ZnSe, and Vycore Glassware are excluded because of their reactivity with moist air. Additionally, ZnS and ZnSe undergo oxidation at temperatures >300°C in the presence of oxygen, then exhibit plastic deformation at about 500°C, and finally dissociate about 700°C. The temperature-pressure engineering margin for ZnS and ZnSe windows is about 250°C under ambient atmosphere. Vycore Glassware is a getter glass that rapidly absorbs water and organic matter, which turns the optically transparent glass yellow. Around 350°C the glass turns brown.

To reserve sufficient engineering margin for most high-temperature AdvSMR optical window applications, 1000°C was selected as a working temperature cutoff. COTS optical materials with lower working temperatures may work if they are placed further away from the reactor vessels or actively cooled. But they will be evaluated on individual bases when engineering designs become available, and they are not included in this study. Ruggedized engineering solutions could also be developed to prevent oxidation and decomposition of optical windows in AdvSMR environments. However, the technical readiness of the short list COTS optical materials for AdvSMR applications is relatively good without engineering solutions.

3.4.1 COTS Optical Materials Analysis

3.4.1.1 Diamond

Diamond optical materials are an excellent choice for use in harsh environments. Diamond is transparent between 250 nm and 200 µm (Paquin 1999), making it tremendously versatile for diverse optical applications. It is mechanically strong and melts at 3550°C, which makes it a good candidate for high-pressure and high-temperature windows. In terms of radiation damage, diamond is generally considered very robust. Diamond is radiation resistant to high energy neutrons (14 MeV) to at least 5×10^{14} n/cm^2 (Girolami et al. 2011). Optical attenuation becomes apparent at the mid- to long-wave infrared beginning around 10^{17} n/cm^2 fluence, as shown in Figure 3.5. A few studies have cited "extremely" high gamma radiation tolerance up to 0.1 MGy (Bauer et al. 1995), although thorough optical studies of gamma radiation damage do not seem to be available. Carbon's cross section for 6 MeV gamma particles is relatively small. Gamma radiation produces Compton scattering, which subsequently ionizes atoms in the carbon lattice. This impact increases as the gamma energy increases. The limited data at high dose and long-term radiation exposure for diamond optical materials require further study to fully determine technical readiness for future AdvSMR designs. Chronic exposure to both radiation and high temperature could reduce mechanical strength in optical windows, leading to subsequent failure and

containment breach. For instance, lattice damage caused by high-energy gamma bombardment of diamond could degrade the mechanical properties (Campbell and Mainwood 2000). However, the few studies regarding this issue predominantly focus on optical property and micro-scale damage.
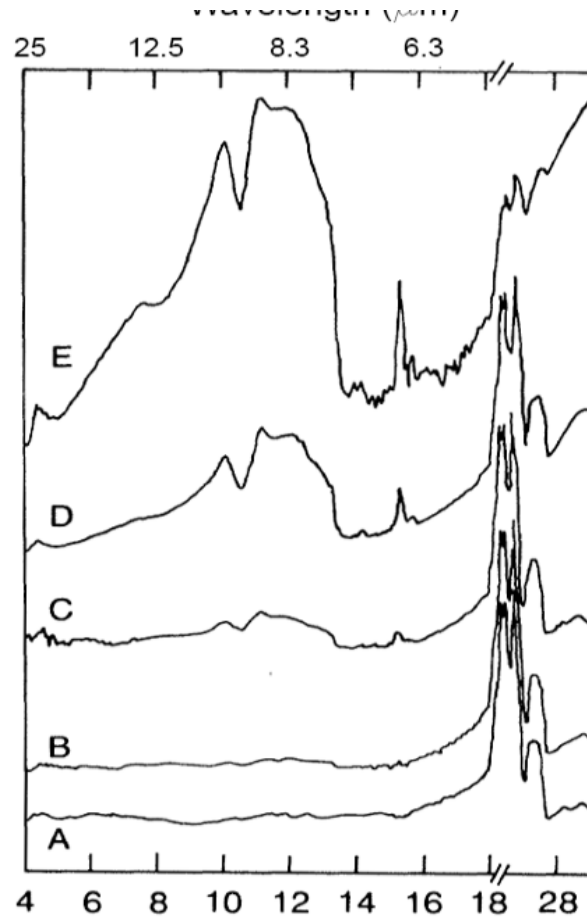
Figure 3.5.   Diamond Irradiated with Neutron Fluence of Zero (A), 3×10^{16} n/cm^2 (B), 1.2×10^{17} n/cm^2 (C), 6×10^{17} n/cm^2 (D), and 4.5×10^{18} n/cm^2 (E). Reprinted with permission from Morelli et al. (1993). Copyright 1993 by the Americal Physical Society.

Single crystal diamonds are usually produced from natural sources, high-pressure, high-temperature (HPHI) synthesis, or CVD. Single crystal diamonds are available up to 12 mm in size from manufacturers such as Element Six, Diamond DVD, Applied Diamond Inc., and ScioDiamond. Diamond substrates are primarily supplied in rectangular shapes, but are also available in square, triangle, and circle geometries. Typically, 5-mm maximum thickness is available commercially. Synthetic polycrystalline diamonds grown using CVD are COTS components available from DIDCO, Diamond Materials, and II-VI Infrared. These components are manufactured as square or round windows, lenses, prisms, and other shapes. Round CVD windows are available readily with thicknesses from 20 µm to 2 mm and diameters up to 100 mm. A diamond window with a 10-mm diameter and 2-mm thickness could sustain design pressures to 100 MPa (Eq. 3.2), which would be suitable for all AdvSMR designs. However, a

100-mm diameter window of the same thickness has a design service pressure only 1 MPa, since the strength scales inversely by the square of the diameter. In this case, this window is only suitable for ambient pressure reactors. Clearly, the rupture modulus specification is an important parameter, used to help identify suitable materials for each AdvSMR design. Diamond is likely one of the better candidates for AdvSMR applications, because of its high working temperature, mechanical strength, and radiation-resistance properties.

3.4.1.2   ALON[®]

ALON optical ceramic is an extremely durable crystalline material with excellent optical transparency from the near ultraviolet to the infrared to approximately 4.6-µm wavelength. The material combines mechanical and optical properties similar to sapphire with the advantages of an isotropic cubic crystal structure. It has an approximate composition of $Al_{23}O_{27}N_5$. This material is formed into optical components (e.g., windows, domes, plates, rods, and tubes in a wide range of sizes and thicknesses) using a proprietary powder processing technique (e.g., injection molding, isostatic pressing, and slipcasting) by Surmet Corporation.

ALON has shown promise as an excellent blast-resistant transparent armor material for aerospace and defense applications. A 1989 study suggests that ALON is radiation resistant, as well as resistant to attack from various acids, bases, and water (Corbin 1989). Neutron irradiation at 3×10^{20} n/cm^2 produced very little change in the lattice parameter (0.071 percent) (Jeanne et al. 1987). However, there has been no other radiation effects study on ALON in the past two decades. ALON is another good candidate for AdvSMR applications because of its high working temperature and mechanical strength properties. Further radiation exposures studies are needed to verify ALON's radiation-resistant properties.

3.4.1.3   Spinel

Magnesium aluminate spinel, or simply spinel, is a durable polycrystalline transparent ceramic with optical transparency from the near ultraviolet to 5.5-µm wavelength. Similar to ALON, it is an excellent transparent armor material that can be formed as windows, domes, plates, rods, and tubes in a wide range of sizes and thicknesses by conventional ceramic forming methods. Spinel is primarily manufactured by Surmet and Technology Assessment & Transfer Inc.

Radiation studies on spinel were primarily conducted during early development of the spinel material about a decade ago. Spinel was investigated for nuclear waste transportation and storage applications. This study exposed spinel to a total dose of 10 MGy (Adams et al. 2000) and demonstrated no statistically significant effects on the physical properties including geometry, density, water absorption, and porosity. Spinel has been characterized for neutron damage, and shows some displacement damage but little void formation. High-energy neutron irradiation is known to cause attenuation in spinel at the low wavelength range, primarily below 600 nm. A strong absorption in the ultraviolet and a small band around 510 nm (>100 dB/cm) were observed when a thin spinel window (0.2–0.5 mm) was exposed to a neutron fluence of 24.9×10^{26} n/cm^2 (Ibarra et al. 1996). In this study, transmission beyond 510 nm to 2 µm was unaffected by the high neutron fluence. Thermal annealing up to 762°C showed some recovery of this damage, indicating that high-temperature environments may actually improve radiation resistance. Another research study found that the optical transparency of a 1.7-mm thick spinel window only decreased by 25 percent at 370 nm when irradiated up to a total gamma dose of 3.5M Gy (He et al. 2002). Gamma energy is known to cause luminescence from spinel, generating significant luminescence peaks

around 250 nm and 525 nm (Bazilevskaya et al. 1998). Spinel is a strong candidate for AdvSMR applications because of its high working temperature and mechanical strength properties. Further radiation exposures studies are needed to verify spinel's radiation-resistant properties. Spinel is soluble in fluoride salts (e.g., BaF_2, MgF_2, PbF_2 plus oxides) at very high temperature (>1200°C) and is reported not soluble in the lower melting chloride salts (Elwell and Scheel 1975). Actual solubility in proposed molten salt reactor (MSR) and fluoride salt-cooled high-temperature reactor (FHR) coolants is unknown and will require further investigation.

3.4.1.4   Sapphire

Sapphire is grown commercially by a variety of methods. Verneuil and Czochralski (CZ) methods are usual for standard grade sapphire material. Higher-quality sapphire is manufactured by Kyropulos growth, which produces very pure material with excellent UV transmission. Large, thin sheets of sapphire can be made by ribbon growth. Sapphire is slightly birefringent and optical components are usually cut from the crystal boule without concern to specific crystallographic plane orientation. If the optical design is sensitive to birefringence, specific orientation can be specified for custom optical components. Commercial sapphire manufacturers include Saint-Gobain Crystals, GT Advanced Technology, Sapphire Materials Company, Kyocera, Crystal Systems Inc., and Gavish Inc. Some of these manufacturers produce sapphire ingots, sheets, and optical components having dimensions to 50 cm and thickness to 125 cm.

Sapphire exhibits no measureable optical absorption under gamma radiation exposure up to doses of 10^8 Gy (Islamov et al. 2007). The reactor irradiation induced a number of absorption bands at 205, 230, 257, 300, 355, and 450 nm, which increased with neutron fluence up to 10^{20} n/cm^2. Radiation-induced luminescence increased at 330 and 420 nm initially with increasing gamma and neutron exposure, but began to decrease at neutron fluence > 10^{18} n/cm^2. No significant transmission difference was found between irradiated (total fluence of 10^{22} n/cm^2) and unirradiated sapphire between 2.5 to 5.5 µm wavelength (Regan et al. 2002). Sapphire will be one of the best materials for AdvSMR applications because of its high working temperature and mechanical-strength properties. Radiation-induced darkening at mid-infrared wavelengths is negligible at large neutron fluences and gamma doses. Further radiation exposures studies may be needed to pin down sapphire's complete radiation-resistance properties. Sapphire is soluble in the most aggressive fluoride salts (e.g., PbF_2, Na_3AlF_6, BaF_2, AlF_3) at high temperatures (>1000°C) (Elwell and Scheel 1975). Actual solubility in proposed MSR and FHR molten salt coolants is unknown and will require further investigation.

3.4.1.5   YAG

YAG (yttrium aluminum oxide, $Y_3Al_5O_{12}$) is an optical crystal material that is often used as an active laser host media when doped with Nd, Tm, Er, or Cr. YAG is transparent from 0.25 to 5.0 µm and has a melting point just below sapphire. YAG is nonbirefringent and available with high optical homogeneity and surface quality. Up to 76-mm YAG boules are grown by the CZ method and windows and other optical components are available as COTS items. Undoped YAG windows are available from vendors including Laser Optex, BJP, and Newlight Photonics.

Aerospace research has studied ionizing radiation damage on Nd:YAG laser media. These studies indicate a clear and strong relationship between radiation-induced color center formation and the growth conditions of the YAG crystal (e.g., method, growth atmosphere, purity of materials). One relevant study,

conducted under pulsed irradiation (1.3×10^{12} Gy/s, total dose of 40 kGy), demonstrated that transmission loss at 1.06 µm is initially large in single crystal Nd:YAG, but undergoes a rapid recovery after irradiation. In contrast, undoped-polycrystalline YAG permanently and completely photodarkens (Vaddigiri et al. 2006). However, no studies were located that examined steady-state radiation damage on undoped YAG optical components. YAG is limited because of its known radiation-induced darkening in the NIR. Further radiation exposures studies are needed to evaluate YAG radiation damage under AdvSMR-like conditions, across the entire optical transmission window. YAG is not soluble in pure fluoride salts even at very high temperatures. It is soluble in mixtures of high-temperature oxides and fluoride salts (e.g., PbO, PbF_2, B_2O_3) at temperatures above 1100°C (Elwell and Scheel 1975). Actual solubility in proposed MSR and FHR molten salt coolants is unknown and will require further investigation.

3.4.1.6   Silicon

Silicon is a common COTS optical and electronic material. It is readily available in a variety of sizes and thicknesses from major optics and semiconductor vendors. Silicon has high melting temperature (1412°C) and bending strength (124 MPa), and optical transparency from 1.2 to 10 microns, which makes it an attractive material for infrared optical windows. Silicon is grown by the CZ method. Oxygen is an impurity that causes absorption at 9 µm. To avoid this, silicon can be prepared by a Float-Zone (FZ) process. Optical-grade silicon is generally lightly doped for best transmission above 10 µm. Very high resistivity uncompensated silicon has a further pass band region from 30 to 100 µm.

As an important semiconductor material for electronics, silicon radiation damage is primarily studied in terms of semiconductor performance. High-energy radiation produces defect complexes in silicon, which reduce minority carrier lifetime, change majority carrier density, and reduced mobility (Messenger 1992). Minority carrier lifetime is the most sensitive electronic property of silicon in the neutron environment. The degradation of minority carrier lifetime results in changes in semiconductor device properties such as current gain, storage time, saturation voltage, and sink current. Carrier removal is the next most important characteristic of displacement damage and it causes a decrease in carrier mobility and an increase in resistivity. However, there are very few silicon studies that examine radiation-induced damage of optical properties. One study cited the infrared transmission of a high-purity single-crystal silicon window remained unchanged after exposed to 20 KGy gamma irradiation (Shaw and Krogstad 1958). Another study found several absorption bands were introduced by neutron irradiation with peak absorptions at 1.8, 3.3, 3.9, 5.5, and 6.01 µm, respectively (Fan and Ramdas 1959). Few recent studies have been conducted on optical damage because of irradiation. Silicon is of limited use near-core because of its well-known radiation-induced electronic damage mechanisms and uncertain optical damage vulnerabilities. Further radiation exposures studies are needed to evaluate optical damage in silicon because of irradiation under AdvSMR-like conditions. Silicon is known to be chemically reactive with halogens, alkali metals, and high-temperature steam (Cotton and Wilkinson 1972).

3.4.1.7   Magnesium Fluoride

Magnesium fluoride is grown by the vacuum Stockbarger technique in ingots of various diameters. MgF_2 has high melting temperature (1255°C) and bending strength (49 MPa), and optical transparency from 0.1 to 7.5 microns, which makes it an attractive material for broadband optical windows. It is slightly birefringent and is usually supplied with the optic axis cut perpendicular to the window faces. MgF_2 has high resistance to thermal and mechanical shock, as well as laser damage. MgF_2 is relatively

soft and somewhat hygroscopic, so mechanical polishing is more difficult and protective coatings may be required. MgF_2 is a common optical material that is available in a variety of sizes and thicknesses from most major optical materials manufactures, including Edmund Optics and Newport. There has been very little research on MgF_2 irradiation damage, except one study that observed radiation-induced permanent absorption band near 260 nm (Brannon et al. 1985). MgF_2 is of limited use near-core because of its soft mechanical and hydroscopic properties, and uncertain vulnerabilities to optical damage by irradiation. Magnesium fluoride's major strength is transparency into the deep UV. For such applications, further radiation exposures studies are needed to evaluate optical damage in MgF_2 because of irradiation under AdvSMR-like conditions.

3.4.1.8   Gallium Arsenide

Gallium arsenide is produced by CZ or horizontal Bridgeman crystal growth techniques. Small (~25 mm) infrared transparent (1–15 microns) lenses, windows, and beam splitters are COTS items that are available from several vendors, including Crystran, Opto-Technological Laboratory, and ISP. GaAs is most useful in applications where toughness and durability are important design requirements, such as dirty, abrasive environments. The material is nonhydroscopic and chemically stable except when in contact with strong acids. The toxicity of arsenic compounds requires precautions during optical component fabrication.

GaAs is an important semiconductor material to manufacture integrated circuits, solar cells, light-emitting diodes, and laser diodes. It is commonly reported that wide, direct bandgap materials, like GaAs, have higher resistance to radiation damage than indirect bandgap materials such as silicon. GaAs is a popular electronic material for aerospace electronics. However, appreciable deterioration in the infrared transmission of GaAs was found after irradiation in a nuclear reactor (Spitsyn et al. 1977). The vast majority of radiation effect studies on GaAs are focused on doped electronic material and devices. Limited radiation effect studies on optical transmissions of single-crystal GaAs exist. GaAs will likely be a lower priority for in-vessel use because of its limited availability, high cost, small production size, and uncertain vulnerabilities to optical damage by irradiation. Gallium arsenide's major strength is its mechanical durability. For such applications, further radiation exposures studies are needed to evaluate optical damage in GaAs because of irradiation under AdvSMR-like conditions.

3.4.1.9   Fused Quartz or Fused Silica

Fused quartz or fused silica is glass consisting of high-purity silica in amorphous form. Fused quartz is manufactured by fusing (melting) naturally occurring quartz crystals of high purity at approximately 2000°C, using either an electrically heated furnace or a gas/oxygen-fueled furnace. Fused silica is produced using high-purity silica sand as the feedstock, and is normally melted using an electric furnace. Synthetic fused silica is made from a silicon-rich chemical precursor usually using a continuous flame hydrolysis process, which involves chemical gasification of silicon, oxidation of this gas to silicon dioxide, and thermal fusion of the resulting dust (although there are alternative processes). This results in ultra-high purity optical glass with transparency from 0.25 to 3.5 µm. Optical-grade fused quartz or silica has no dopants that would normally lower the glass transition temperature (~1200°C) and, therefore, has much higher working temperature than soda-lime or borosilicate glasses. Fused quartz or fused silica is tough and hard and has a very low thermal expansion. It is commonly manufactured into small and large windows, lenses, and other optical components by a large list of vendors worldwide.

Radiation effects on fused quartz or fused silica are well studied. Transmission loss in silica windows by radiation darkening is less of a problem compared to silica optical fibers, because of the smaller optical path length and color center formation (normally induced during the fiber-making process). As in silica optical fibers, most radiation darkening in fused quartz or fused silica windows occurs at UV and visible wavelengths. Near infrared and mid-infrared transparency remains high.

Fused quartz or fused silica is not suitable for super critical water or sodium coolant designs because of chemical incompatibility. Silica's potential for use in AdvSMR optical systems is strong based on its widely commercial availability, low cost, good working temperature and strength, and well understood radiation damage mechanisms. However, the relatively low maximum working temperature may limit silica's use in some AdvSMR designs. Further radiation exposures studies are needed to evaluate optical damage in silica under simultaneous high temperature and radiation flux to better understand the interplay between radiation damage and high temperature self-annealing mechanisms.

3.4.2   COTS Summary, Gaps Analysis, Ranking, and Proposed Future Research

COTS Optical Windows Summary

A number of COTS optical materials have promising thermal and mechanical strength properties, including several that can tolerate sustained exposure to temperatures well beyond fuel failure. Most of these materials have rupture moduli that provide at least two times working pressure safety margins for pressures expected in SCWR designs. Diamond, ALON, spinel, sapphire, and silica are the most promising window materials, most of which are widely available from commercial sources. Spinel and ALON are emerging optical materials for harsh environments and are only available from Suremet and Technology Assessment & Transfer Inc. Windows, lenses, domes, spheres, and a variety of forms are available for these materials.

Gaps Analysis

Knowledge gaps exist for many of the promising optical window materials in terms exposure effects and service life for in-vessel AdvSMR applications. All materials will eventually succumb to long-term high neutrons, gamma, and high-temperature exposure, but predicting expected lifetime is currently subjective. It is also suspected that chemical reactions between coolants and glasses will be accelerated by the interplay of high-temperature and radiation exposure. The most significant technology gaps that limit COTS optical materials deployment in AdvSMRs include:

- COTS optical materials may degrade when exposed to AdvSMR coolants and impurities.

- Vendors do not provide radiation-resistance specifications for COTS optical materials.

- COTS optical materials have not been tested under combined high-temperature and high-radiation conditions.

- COTS optical components may not have the abrasion resistance for reliable deployment in high-flow AdvSMR coolants.

- Limited theoretical studies have been conducted to develop useful predictive damage models for optical materials exposed to high temperature and radiation.

- Mechanical degradation under chronic extreme environmental exposure not well understood.

Technical Readiness Ranking

CVD Diamond, ALON, spinel, sapphire, and silica have **HIGH** technical readiness for near-lid AdvSMR applications; however, technical knowledge gaps with respect to radiation-induced damage still remain. Their technical readiness for near-core applications, pending further research, is considered **MEDIUM**. Silicon, magnesium fluoride, YAG, and gallium arsenide have **LOW** technical readiness primarily because of deep technical knowledge gaps with respect to radiation-induced damage. Therefore, these are second-tier materials that would likely be selected only for their specific strengths (e.g., deep UV transparency, abrasion resistance).

Proposed Future Research

The material properties of the first-tier optical materials are very promising, but further investments will be required to understand and optimize these materials for extended integration into AdvSMR designs. Further radiation exposures studies are needed to evaluate optical damage for the first tier materials under simultaneous high temperature and radiation flux to better understand the interplay between radiation damage and high-temperature self-annealing mechanisms. Computational modeling is also needed to study radiation damage mechanisms at the atom level.

Key Optical Materials (including windows) RD&D

- **Theoretical Damage Models**: Theoretical modeling studies will be required to understand fundamental damage mechanisms in optical materials and estimate component lifetime under expected AdvSMR conditions. This includes understanding noncatastrophic effects that shorten useful life, such as plastic deformation under sustained pressure at elevated temperature and slow degradation because of extended radiation and chemical exposure.

- **COTS Optical Materials Exposure Studies**: Exposure studies are required to determine the robustness of optical materials, including CVD diamond, ALON, spinel, sapphire, and silica, under simulated AdvSMR conditions, such as high temperature, radiation fluence, pressure, chemical exposure, and direct coolant immersion. High-temperature, thin-film coatings will be required to protect optical materials from corrosion and chemical attack. Corrosion and extreme radiation exposure studies at high temperature are especially needed. Past optical materials exposure studies were mostly focused on long-term, low-level radiation to simulate space environments. This body of literature points to promising materials, but does not provide insight into damage issues under combined high-radiation and high-temperature exposure.

- **Optomechanical Engineering**: Optomechanical engineering RD&D will be required to develop reliable reactor vessel penetrations. Robust metal-to-optical material sealing techniques that function under AdvSMR conditions are needed. Optomechanical sealing designs must be developed that account for thermal expansion and vibration. Glass-to-metal and ceramic-to-metals seal designs involve exotic alloys and ceramic compositions, which must have low neutron activation and transmutation properties. Long-term thermal and radiation exposure studies will be required to evaluate the performance. Optical design RD&D will be required to evaluate design tolerances, such as refractive index changes over large temperature spans, to maintain optical performance over the entire reactor power range.

3.5 Optical Mirrors

3.5.1   Introduction

Reflective, as well as refractive, optical components will be required for in-vessel optical monitoring systems. Mirrors will be needed for the standpipe viewport concept and for optical beam relay and access into the reactor vessel interior. These optical components must withstand the extreme temperature, radiation exposure, and corrosion condition of the in-vessel AdvSMR environment.

COTS mirror components are widely available from many vendors, although few are feasible for the in-vessel AdvSMR application. Custom mirror technology for military and research applications have been developed for extreme environment applications. One research example is the Tokamak fusion reactor, which generates very high neutron and gamma fields. This research program studied relay mirror performance close to the fusion plasma, where the peak fast neutron flux was 3×10^{14} n/cm^2 s, and gamma flux was 3×10^3 Gy/s (Yamamoto et al. 2000). Many metal mirror compositions, including copper, molybdenum, TZM (99 percent Mo, 0.1 percent Zr, 0.5 percent Ti), tungsten, tantalum, stainless steel, beryllium, and rhodium were found to maintain high reflectivity in the visible and infrared wavelength range, under these exposure conditions (Voitsenya et al. 1998; Yamamoto et al. 2000; Voitsenya et al. 2001; Litnovsky et al. 2007; Marot et al. 2011).

Metal mirrors will likely require coatings over the mirror surface to protect from abrasion damage. Dielectric films, such as ZrO_2, were also evaluated during the fusion studies and found to withstand high radiation dose without damage. Erosion from fast-moving particles is also a major concern in fusion reactor research. Likewise, fast-flowing AdvSMR coolants, containing particles and impurities, may have similar challenges. This problem has been explored to a limited extent in the literature. Under erosive conditions, single-crystal molybdenum metal mirrors were found to maintain good reflectivity beyond the visible wavelength range (Litnovsky et al. 2007).

Single-crystal tungsten, rhodium, and molybdenum were found to have the best performance of all materials studied and are likely the most appropriate choice for the AdvSMR application based on their high melting temperatures, 3422°C, 1964°C, and 2623°C, respectively. Chemical compatibility, corrosion, activation, and transmutation issues must also be carefully considered for any AdvSMR design.

These metal mirrors may be feasible for standpipe viewport designs, where the temperature and radiation conditions are much lower. These mirrors may also be feasible for some applications that are closer to the core, but further coolant exposure studies are required.

In addition, the maximum working temperatures of these materials are well above the highest expected AdvSMR temperature.

3.5.2   COTS Summary, Gaps Analysis, Ranking, and Proposed Future Research

COTS Optical Mirror Summary

The fusion reactor studies reviewed for this survey used custom mirrors, not COTS components. However, molybdenum and other metal mirrors can be ordered from companies such as Laser Beam Products, Spawr Industries, Laser Optics and Mechanisms, and others. Metal mirrors are generally made

to customer specfications, rather than true COTS components. Molybdenum metal mirror are used for high-power CO_2 laser applications. Tungsten metal mirrors are available from Laser Beam Products as a custom mirror product. Numerous optical coatings vendors provide hard oxide mirror coatings.

Gold, silver, and aluminum coated mirrors (i.e., glass substrates) are much more common COTS optical components, but each has incompatibilities with in-vessel deployment. Gold transmutes to mercury and silver and aluminum quickly lose reflectivity under ionizing radiation exposure.

Gaps Analysis

Commercial availability for feasible mirror options is low; therefore, the ruggedness of custom materials under harsh conditions must be independently evaluated. It is likely that most COTS and custom mirrors will be well suited for near-lid applications, but many questions remain about the ruggedness of mirrors near-core in contact with flowing coolant. Thus, as with optical window materials, lack of knowledge is the primary gap, of which the following points are considered the most pertinent:

- COTS optical metal mirrors have not been evaluated under long-term, high-temperature, and radiation exposure.

- COTS optical mirrors and coatings may degrade (e.g., chemical reaction, corrosion, and erosion) when exposed to AdvSMR coolants and impurities.

- Vendors do not typically provide radiation-resistance specifications for COTS optical materials, components, and coatings.

- COTS and semi-custom optical mirrors and coatings have not been tested under combined high-temperature and high-radiation conditions.

- Large temperature ranges and peak temperatures may induce delamination of mirror coatings and substrate layers.

Technical Ranking

Technical readiness for radiation-resistant mirrors made out of single-crystal molybdenum is **HIGH**, both for in and out-of-vessel applications. Single-crystal tungsten and rhodium mirrors have also shown great radiation-resistance properties, but have very low commercial availability, and are therefore only of **MEDIUM** technical readiness. Using well-understood sputter coating techniques, it is not challenging to deposit tungsten or rhodium coatings, so this obstacle can be considered a very minor one. Aluminum, gold, and other common COTS mirror materials are considered to have **LOW** technical readiness for near-core applications because of loss of reflectivity under radiation exposure. These same mirrors would be considered to have **MEDIUM** technical readiness for near-lid or in-containment usage though, as lifetime would likely be quite long under modest flux conditions.

Proposed Future Research

In light of the technology gaps for reactor vessel mirrors specified above, further radiation and temperature exposure studies are needed to evaluate optical damage for the first-tier materials both in air and in reactor coolants to better understand the long-term impacts. Mechanical impacts from fast-flowing coolant will have to be evaluated using erosion studies and modeling. Computational modeling may help to better understand material selection and design parameters.

Key Optical Mirrors RD&D

- Theoretical modeling studies will be required to understand fundamental damage mechanisms in optical mirrors and estimate component lifetime under expected AdvSMR conditions. This includes understanding noncatastrophic effects that shorten useful life, such as plastic deformation under sustained pressure at elevated temperature and slow loss of reflectivity and physical degradation because of extended radiation exposure, chemical reactions, and flow erosion.

- Characterizing the robustness of promising vendor-supplied and customized mirror materials to AdvSMR conditions, such as high temperature, radiation fluence, pressure, coolant flow, and chemical exposure is needed. Corrosion, erosion, and extreme radiation exposure studies at high temperature are especially needed. Mirror materials that are resistant to radiation and erosion in air at room temperature may have shorter lifetimes at high temperatures and in corrosive coolants.

- High-temperature, thin-film coatings will be required to protect optical materials from corrosion and chemical attack. This may be a solution to coolant erosion problems.

- Mirror anchoring solutions within reactor vessels will have to be explored in depth. Mirrors have been demonstrated in periscope-type apparatus for in-vessel operation, but finding clear optical paths for core inspection may require strategic positioning of mirrors inside the vessel. Anchoring holders must face challenging alignment issues, must not obstruct coolant flow, and must be fully robust to the coolant environment.

3.6 Modeling and Simulation of Degradation of Optical Properties

Theory, modeling, and simulation have an important role to play in the evaluation of optical material performance as a function to exposure to high temperature, neutron irradiation, and corrosive chemicals. Radiation-damage processes can span enormous time and distance scales, starting from the primary damage production (nm length and ns time scale) to the eventual property degradation (mm length scale and year time scale). Simulations with atomic-level detail are computationally intensive and are limited to the study of defect production by radiation. While there have been advances in extending the length scale of atomistic simulations using massively parallel computation, progress in extending the time scale of such simulations has been limited, because of the sequential nature of time integration.

At the most fundamental level, quantum chemical calculations are invaluable to relate defects in optical materials, such as silica, alumina, and ALON, to their respective absorption bands (Pacchioni and Ierano 1997). Radiation-induced defect centers, such as the well-known nonbridging oxygen hole center, result in increased optical absorption at certain wavelengths. Quantum chemical studies can shed light on dopant effects and defect properties, but are limited at present to clusters containing tens of atoms. Density functional theory (DFT) can be used to examine the formation and migration energies of defects, and the migration pathways that play a key role in the annealing of radiation damage. The system size in DFT calculations is typically of the order of 100 atoms, which limit studies to single crystal modeling.

At the next higher scale, molecular dynamics (MD) simulation is widely used to study defect production by energetic recoils, point defect accumulation, phase transformation, diffusion, and interfacial processes in irradiated materials (Devanathan et al. 2010). MD simulations can routinely handle system sizes of tens of millions of atoms. This enables the study of polycrystalline materials and interfaces between optical materials and protective coatings. These large-scale atomistic simulations can be used to fill gaps in experimental understanding of material degradation, given the difficulty in

reproducing expected reactor conditions of elevated temperature, neutron irradiation, and the corrosive effects of coolants and impurities. MD simulation, when combined with proton irradiation and characterization, offers a path to perform accelerated testing of optical materials under simulated reactor conditions. This approach provides a substantially lower cost and experimental complexity. Studies using these techniques could provide much needed insight into the defect creation processes and defect distribution following neutron irradiation at temperatures above 400°C, microstructural evolution as a function of material composition and operating conditions, and the changes in optical and mechanical properties that arise from microstructural modification. Experimentally observed changes in optical properties under neutron irradiation (Sandhu et al. 2009) can be connected to structural changes; for instance, modification of the glass network and bond angle distributions. Degradation of elastic mechanical properties and crack propagation can also be related to composition, defect accumulation, and microstructural features.

Damage annealing at elevated temperature can be simulated by extracting parameters, such as defect distributions and energies, from MD simulations and using them in subsequent kinetic Monte Carlo simulations, rate theory calculations, and phase field models. Theoretical developments that seamlessly couple methods at different scales hold the promise of improving our fundamental understanding of degradation of materials in extreme environments. Issues to be addressed by multiscale modeling include identification of key mechanisms of optical property degradation, interaction of the coolant chemistries with optical materials under neutron irradiation at high temperature, stability of the interface between protective coatings and optical materials, chemical intermixing and phase transformation at such interfaces, and diffusion of dopants in optical fibers. By combining modeling techniques with experimental exposure studies and literature data, one can estimate component lifetime under actual AdvSMR conditions and then judiciously select materials that will retain their optical and mechanical properties under prolonged exposure to in-vessel reactor conditions.

3.7 References

Abrisa Technologies. 2012. "Specialty Glass Technical Capabilities 11/12." Abrisa Technologies, Santa Paula, California. http://abrisatechnologies.com/docs/AT%20Specialty%20Glass%20Technical%20Capabilities%20Brochure.pdf.

Adams J, M Cowgill, P Moskowitz and A Rokhvarger. 2000. *Effect of Radiation on Spinel Ceramics for Permanent Containers for Nuclear Waste Transportation and Storage*. BNL-67518, Brookhaven National Laboratory, Upton, New York.

Almaz Optics. 2011. *Optical Materials*. Almaz Optics, Inc. Marlton, New Jersey. Accessed May 30, 2013. Available at http://www.almazoptics.com.

Barker RS and DA Richardson. 1961. "Effect of Gamma Radiation on Spectral Transmission of Some Commercial Glasses." *Journal of the American Ceramic Society* 44(11):552-560.

Barnes WP. 1992. "Optical Windows." *SPIE Critical Reviews* CR43:232-253.

Bauer C, I Baumann, C Colledani, J Conway, P Delpierre, F Djama, W Dulinski, A Fallou, KK Gan, RS Gilmore, E Grigoriev, G Hallewell, S Han, T Hessing, K Honschied, J Hrubec, D Husson, H Kagan, D Kania, R Kass, W Kinnison, KT Knöpfle, M Krammer, TJ Llewellyn, PF Manfredi, LS Pan, H Pernegger,

M Pernicka, R Plano, V Re, S Roe, A Rudge, M Schaeffer, S Schnetzer, S Somalwar, V Speziali, R Stone, RJ Tapper, R Tesarek, W Trischuk, R Turchetta, GB Thomson, R Wagner, P Weilhammer, C White, H Ziock and M Zoeller. 1995. "Radiation Hardness Studies of CVD Diamond Detectors." *Nuclear Instruments and Methods in Physics Research Section A: Accelerators, Spectrometers, Detectors and Associated Equipment* 367(1–3):207-211.

Bazilevskaya TA, VT Gritsyna, DV Orlinski, LV Udalova and AV Voitsenya. 1998. "The Effect of Composition, Processing Conditions, and Irradiation, on Lattice Defects in Spinel Ceramics." *Journal of Nuclear Materials* 253(1–3):133-140.

Brannon PJ, Rw Morris and JB Gerardo. 1985. "Nuclear-Radiation-Induced Absorption in Optical Materials." In *Proceedings of the SPIE, Southwest Conference on Optics, Volume 540*, pp. 451-459. March 4-8, 1985, Albuquerque, New Mexico. The International Society for Optical Engineering, Bellingham, Washington.

Brichard B, P Borgermans, AF Fernandez, K Lammens and M Decreton. 2001. "Radiation Effect in Silica Optical Fiber Exposed to Intense Mixed Neutron-Gamma Radiation Field." In *2001 Nuclear and Sapce Radiation Effects Conference (NSREC)*, pp. 2069-2073. July 16-20, 2001, Vancouver, BC, Canada. DOI 10.1109/23.983174. Institute of Electrical and Electronics Engineers Inc., Piscataway, New Jersey.

Brichard B, AF Fernandez, H Ooms, F Berghmans, M Decreton, A Tomashuk, S Klyamkin, M Zabezhailov, I Nikolin, V Bogatyrjov, E Hodgson, T Kakuta, T Shikama, T Nishitani, A Costley and G Vayakis. 2004. "Radiation-Hardening Techniques of Dedicated Optical Fibres Used in Plasma Diagnostic Systems in ITER." *Journal of Nuclear Materials* 329-333(Part B):1456-1460.

Brichard B, A Fernandez Fernandez, F Berghmans and M Decreton. 2002. "Origin of the Radiation-Induced OH Vibration Band in Polymer-Coated Optical Fibers Irradiated in a Nuclear Fission Reactor." *IEEE Transactions on Nuclear Science* 49(6):2852-2856.

Brichard B, AL Tomashuk, VA Bogatyrjov, AF Fernandez, SN Klyamkin, S Girard and F Berghmans. 2007a. "Reduction of the Radiation-Induced Absorption in Hydrogenated Pure Silica Core Fibres Irradiated in Situ with Gamma-Rays." *Journal of Non-Crystalline Solids* 353(5-7):466-472.

Brichard B, AL Tomashuk, H Ooms, VA Bogatyrjov, SN Klyamkin, AF Fernandez, F Berghmans and M Decréton. 2007b. "Radiation Assessment of Hydrogen-Loaded Aluminum-Coated Pure Silica Core Fibres for ITER Plasma Diagnostic Applications." *Fusion Engineering and Design* 82(15-24):2451-2455.

Calderón A, C Martínez-Rivero, F Matorras, T Rodrigo, M Sobrón, I Vila, AL Virto, J Alberdi, P Arce, JM Barcala, E Calvo, A Ferrando, MI Josa, JM Luque, A Molinero, J Navarrete, JC Oller, P Valdivieso, C Yuste, A Fenyvesi and J Molnár. 2006. "Effects of γ and Neutron Irradiation on the Optical Absorption of Pure Silica Core Single-Mode Optical Fibres from Nufern." *Nuclear Instruments and Methods in Physics Research, Section A: Accelerators, Spectrometers, Detectors and Associated Equipment* 565(2):599-602.

Campbell B and A Mainwood. 2000. "Radiation Damage of Diamond by Electron and Gamma Irradiation." *Physica Status Solidi A* 181:99-107.

Cheymol G, B Brichard and JF Villard. 2009. "Fibre Optics for Metrology in Nuclear Research Reactors Applications to Dimensional Measurements." In *1st International Conference on Advancements in*

Nuclear Instrumentation, Measurement Methods and their Applications, ANIMMA 2009. June 7-10, 2009, Marseille, France. IEEE Computer Society, Piscataway, New Jersey. Article 5503822.

Cheymol G, B Brichard and JF Villard. 2011. "Fiber Optics for Metrology in Nuclear Research Reactors--Applications to Dimensional Measurements." *IEEE Transactions on Nuclear Science* 58(4):1895-1902.

Cheymol G, H Long, JF Villard and B Brichard. 2008. "High Level Gamma and Neutron Irradiation of Silica Optical Fibers in CEA OSIRIS Nuclear Reactor." *IEEE Transactions on Nuclear Science* 55:2252-2258.

Corbin N. 1989. "Aluminum Oxynitride Spinel: A Review." *Journal of the European Ceramic Society* 5(3):143-154.

Cotton FA and FRS Wilkinson. 1972. *Advanced Inorganic Chemistry, A Comprehensive Text, Third Edition*. Interscience Publishers, New York.

Crystran. 2012. *CRYSTRAN - UV - Visible - IR Specialist Optics*. Crystran Ltd. Dorset, United Kingdom. Accessed June 10, 2013. Available at http://www.crystran.co.uk/.

Devanathan R, LV Brutzel, A Chartier, C Gueneau, AE Mattsson, V Tikare, T Bartel, T Besmann, M Stan and P. Van Uffelen. 2010. "Modeling and Simulation of Nuclear Fuel Materials." *Energy & Environmental Science* 3:1406-1426.

Diamond Materials. 2008. *The CVD Diamond Booklet*. Diamond Materials GmbH. Freiburg, Germany. Accessed May 29, 2013. Available at http://www.diamond-materials.com/downloads/cvd_diamond_booklet.pdf.

Duffey R, LKH Leung, D Martin, B Sur and M Yetisir. 2011. "A Supercritical Water-Cooled Small Modular Reactor." In *Proceedings of the ASME 2011 Small Modular Reactors Symposium*, pp. 243-250. September 28-30, 2011, Washington, D.C. DOI 10.1115/SMR2011-6548. ASME, New York. Paper No. SMR2011-6548.

Elwell D and HJ Scheel. 1975. *Crystal Growth from High-Temperature Solutions*. Academic Press, London. Ch. 10, pp. 558-625. ISBN 0122375508

EPRI. 1992. *Optical Fibers in Radiation Environments*. TR-100367, Electric Power Research Institute (EPRI), Palo Alto, California.

Fan HY and AK Ramdas. 1959. "Infrared Absorption and Photoconductivity in Irradiated Silicon." *Journal of Applied Physics* 30(8):1127-1134.

Farrell K, JO Stiegler and RE Gehlbach. 1970. "Transmutation-Produced Silicon Precipitates in Irradiated Aluminum." *Metallography* 3(3):275-284.

FiberLabs. 2013. *Fluoride Fiber (FF)*. Japan. FiberLabs Inc. Accessed May 30, 2013. Available at http://www.fiberlabs-inc.com/fluorideFiber.htm (last updated April 30, 2013).

Fuks L and C Degueldre. 2000. "Optical Properties of γ-irradiated Synthetic Sapphire and Yttria-Stabilized Zirconia Spectroscopic Windows." *Journal of Nuclear Materials* 280:360-364.

Girard S, J Kuhnhenn, A Gusarov, B Brichard, M Van Uffelen, Y Ouerdane, A Boukenter and C Marcandella. 2013. "Radiation Effects on Silica-Based Optical Fibers: Recent Advances and Future Challenges." *IEEE Transactions on Nuclear Science* PP(99):1-22.

Girolami M, A Galbiati and S Salvatori. 2011. "Radiation Hard Imaging Detectors Based on Diamond Electronics." In *IEEE Nuclear Science Symposium and Medical Imaging Conference (NSS/MIC)*, pp. 586-590. October 23-29, 2011, Valencia, Spain. Institute of Electrical and Electronics Engineers Inc., Piscataway, New Jersey.

Griscom DL. 1991. "Optical Properties and Structure of Defects in Silica Glass." *Nippon Seramikkusu Kyokai Gakujutsu Ronbunshi/Journal of the Ceramic Society of Japan* 99(1154):923-942.

Griscom DL. 1995. "Radiation Hardening of Pure-Silica-Core Optical Fibers by Ultra-High-Dose γ–ray Pre-irradiation." *Journal of Applied Physics* 77(10):5008-5013.

Griscom DL. 1996. "γ and Fission-Reactor Radiation Effects on the Visible-Range Transparency of Aluminum-Jacketed, All-Silica Optical Fibers." *Journal of Applied Physics* 80:2142-2155.

He J, L-b Lin, T-c Lu and P Wang. 2002. "Effects of Electron- and/or Gamma-Irradiation upon the Optical Behavior of Transparent MgAl2O4 Ceramics: Different Color Centers Induced by Electron-Beam and γ-ray." *Nuclear Instruments and Methods in Physics Research B, Beam Interactions with Materials and Atoms* 191:596-599.

Henschel H. 1994. "Radiation Hardness of Present Optical Fibres." In *Proceedings of SPIE, Optical Fibre Sensing and Systems in Nuclear Environments, Volume 2425*, pp. 21-31. September 17, 1994, Mol, Belgium. The International Society for Optical Engineering, Bellingham, Washington.

Henschel H, O Koehn, W Lennartz, S Metzger, HU Schmidt, J Rosenkranz, B Glessner and BRL Siebert. 1998. "Comparison Between Fast Neutron and Gamma Irradiation of Optical Fibres." In *Proceedings of the 1997 4th European Conference on Radiation and Its Effects on Components and Systems, RADECS'97*, pp. 430-438. September 15-19, 1997, Cannes, France. The Institute of Electrical and Electronics Engineering, Inc., Piscataway, New Jersey.

Henschel H, O Kohn and HU Schmidt. 1994. "Optical Fibres for High Radiation Dose Environments." *IEEE Transactions on Nuclear Science* 41:510-516.

Henschel H, O Kohn and U Weinand. 2002. "A New Radiation Hard Optical Fiber for High-Dose Values." *IEEE Transactions on Nuclear Science* 49(3):1432-1438.

Henschel H, J Kuhnhenn and U Weinand. 2005. "High Radiation Hardness of a Hollow Core Photonic Bandgap Fibre." In *8th European Conference on Radiation and its Effects on Components and Systems (RADECS)*, pp. LN4/1-LN4/4. September 19-23, 2005, Le Cap d'Adge, France. Institute of Electrical and Electronics Engineers, New York.

Ibarra A, R Vila and FA Garner. 1996. "Optical and Dielectric Properties of Neutron Irradiated MgAl2O4 Spinels." *Journal of Nuclear Materials* 233-237(B):1336-1339.

ICL. 2012. *Sapphire (Al$_2$O$_3$) Optical Crystals*. International Crystal Laboratories (ICL). Garfield, New Jersey. Accessed May 30, 2013. Available at http://www.internationalcrystal.net/optics_13.htm#.

II-VI Infrared. 2010. "CVD Diamond Substrates." II-VI Infrared. http://issuu.com/iivicorp/docs/ii-vi_diamond_2010-01.

Islamov AK, EM Ibragimova and I Nuritdinov. 2007. "Radiation-Optical Characteristics of Quartz Glass and Sapphire." *Journal of Nuclear Materials* 362:222-226.

ISP. 2002. "ISP Optics Infrared Catalog." ISP Optics, Irvington, New York.

ISP. 2009. *Design of Pressure Window*. ISP Optics. Irvington, New York. Accessed May 30, 2013. Available at http://ispoptics.com/designofpressurewindow.htm.

Jeanne A, JC Labbe, P Lefort and G Roult. 1987. "Behavior of Aluminum Oxynitride under Fast Neutron Irradiation." In *High Tech Ceramics: Proceedings of the World Congress on High Tech Ceramics, the 6th International Meeting on Modern Ceramics Technologies (6th CIMTEC)*, pp. 2981-2988. June 24-28, 1986, Milan, Italy. Elsevier Science Publishers, Amsterdam.

Kakuta T, T Shikama, T Nishitani, B Brichard, A Krassilinikov, A Tomashuk, S Yamamoto and S Kasai. 2002a. "Round-Robin Irradiation Test of Radiation Resistant Optical Fibers for ITER Diagnostic Application." *Journal of Nuclear Materials* 307–311, Part 2(0):1277-1281.

Kakuta T, T Shikama, T Nishitani, S Yamamoto, S Nagata, B Tsuchiya, K Toh and J Hori. 2002b. "Irradiation Tests of Radiation Resistance Optical Fibers for Fusion Diagnostic Application." In *Proceedings of SPIE: Penetrating Radiation Systems and Applications IV, Volume 4786*, pp. 196-201. July 9-11, 2002, Seattle, Washington. DOI 10.1117/12.451742. The International Society for Optical Engineering, Bellingham, Washington.

Kigre. 2009. *Leaders in Solid State Laser Components*. Kigre, Inc. Hilton Head, South Carolina. Accessed June 10, 2013. Available at http://kigre.com/.

Knoll GF. 2000. *Radiation Detection and Measurement, Third Edition*. John Wiley & Sons, Hoboken, New Jersey.

Koechner W. 1973. "Rupture Stress and Modulus of Elasticity for Nd:YAG Crystals." *Applied Physics* 2(5):279-280.

Leon M, P Martin, D Bravo, FJ Lopez, A Ibarra, A Rascon and F Mota. 2008. "Thermal Stability of Neutron Irradiation Effects on KU1 Fused Silica." *Journal of Nuclear Materials* 374(3):386-389.

Litnovsky A, AV Voitsenya, A Costley and AJH Donne. 2007. "First Mirrors for Diagnostic Systems of ITER." *Nuclear Fusion* 47:833-838.

Mangognia A, C Kucera, J Guerrier, J Furtick, T Hawkins, PD Dragic and J Ballato. 2013. "Spinel-Derived Single Mode Optical Fiber." *Optical Materials Express* 3(4):511-518.

Marot L, R Steiner, M Gantenbein, D Mathys and E Meyer. 2011. "Co-deposition of Rhodium and Tungsten Films for the First-Mirror on ITER." *Journal of Nuclear Materials* 415:S1203-S1205.

Martin P, M Leon, A Ibarra and ER Hodgson. 2011. "Thermal Stability of Gamma Irradiation Induced Defects for Different Fused Silica." *Journal of Nuclear Materials* 417(1-3):818-821.

MatWeb. 2013. *MatWeb Material Property Data*. MatWeb, LLC. Blacksburg, Virginia. Accessed May 29, 2013. Available at http://www.matweb.com/index.aspx.

Messenger GC. 1992. "A Summary Review of Displacement Damage from High Energy Radiation in Silicon Semiconductors and Semiconductor Devices." *IEEE Transactions on Nuclear Science* 39(3):468-473.

Morelli DT, TA Perry and JW Farmer. 1993. "Phonon Scattering in Lightly Neutron-Irradiated Diamond." *Physical Review B* 47:131-139.

Nagasawa K, Y Hoshi, Y Ohki and K Yahagi. 1986. "Radiation Effects on Pure-Silica Core Optical Fibers by γ-rays: Relation Between 2 eV Band and Non-bridging Oxygen Hole Centers." *Japanese Journal of Applied Physics, Part 1 (Regular Papers & Short Notes)* 25(3):464-468.

Nagasawa K, M Tanabe and K Yahagi. 1984. "Gamma-Ray-Induced Absorption Bands in Pure-Silica-Core Fibers." *Japanese Journal of Applied Physics, Part 1 (Regular Papers & Short Notes)* 23(12):1608-1613.

Nishitani T, T Shikama, T Sugie, S Kasai, E Itsishuka, H Kawamura, T Kakuta, T Yagi, S Tanaka, M Narui, M Fukao, N Yokoo, R Reichle, R Snider, T Nakayama, I Sone, M Abe and S Yamamoto. 2002. *Irradiation Effects on Plasma Diagnostic Components (II)*. JAERI Research Report 2002-07, Japan Atomic Energy Research Institute, Ibaraki-ken, Japan.

Norris JOW, SA Norman and MJ Tribble. 1990. "The Mechanical Degradation of Polymer Coated Glass Optical Fibres under Gamma Irradiation." In *Proceedings of SPIE, Fibre Optics '90, Volume 1314*, pp. 199-207. April 1, 1990, London. The International Society for Optical Engineering, Bellingham, Washington.

Okada M, T Seiyama, C Ichihara and M Nakagawa. 1985. "Optical Properties of MgO Irradiated by Fast Neutrons." *Journal of Nuclear Materials* 133-134:745-748.

Orlinski DV, IV Al'tovsky, TA Bazilevskaya, VT Gritsyna, VI In'kov, IA Ivanin, VD Koval'chuk, AV Krasil'nikov, DV Pavlov, YA Tarabrin, SI Turchin, VS Vojtsenya and IL Yudin. 1994. "Preliminary Results of Window Radiation Resistance Investigations." *Journal of Nuclear Materials* 212–215, Part B:1059-1064.

Pacchioni G and G Ierano. 1997. "On the Origin of the 5.0 and 7.6 eV Absorption Bands in Oxygen-Deficient α-Quartz and Amorphous Silica. A First Principles Quantum-Chemical Study." *Journal of Non-Crystalline Solids* 216:1-9.

Paquin RA. 1999. "Materials for Optical Systems." In *Optomechanical Engineering Handbook*, ed: A Ahmad. Ch. 3. CRC Press, Boca Raton.

Perry M, P Niewczas and M Johnston. 2012. "Effects of Neutron-Gamma Radiation on Fiber Bragg Grating Sensors: A Review." *IEEE Sensors Journal* 12:3248-3257.

Prazisions. 2013. *Prazisions Glas & Optik*. Prazisions Glas & Optik GmbH. Iserlohn, Germany. Accessed May 30, 2013. Available at http://www.pgo-online.com/index.html.

Regan TM, DC Harris, DW Blodgett, KC Baldwin, JA Miragliotta, ME Thomas, MJ Linevsky, JW Giles, TA Kennedy, M Fatemi, DR Black and KPD Lagerlöf. 2002. "Neutron Irradiation of Sapphire for

Compressive Strengthening. II. Physical Properties Changes." *Journal of Nuclear Materials* 300(1):47-56.

Russell R. 2011. *Zerodur.* University of Arizona, Tucson, Arizona. Available at http://fp.optics.arizona.edu/optomech/student%20reports/tutorials/Tutorial_Russell,%20Robert.pdf.

Sandhu AK, S Sing and OP Pandey. 2009. "Neutron Irradiation Effects on Optical and Structural Properties of Silicate Glasses." *Materials Chemistry and Physics* 115:783-788.

Sang AK, ME Froggatt, DK Gifford, ST Kreger and BD Dickerson. 2008. "One Centimeter Spatial Resolution Temperature Measurements in a Nuclear Reactor Using Rayleigh Scatter in Optical Fiber." *IEEE Sensors Journal* 8:1375-1380.

Schott. 2013a. *Infrared Chalcogenide Glasses*. Schott North America, Inc. Duryea, Pennsylvania. Accessed May 30, 2013. Available at http://www.us.schott.com/advanced_optics/english/products/optical-materials/ir-materials/infrared-chalcogenide-glasses/index.html.

Schott. 2013b. *Optical Glass Data Sheets*. Schott North America, Inc., Duryea, Pennsylvania. Available at http://edit.schott.com/advanced_optics/us/abbe_datasheets/schott_datasheet_all_us.pdf.

Schott Lithotec. 2013. *ZERODUR*. Schott Lithotec AG. Mainz, Germany. Accessed May 30, 2013. Available at http://www.sydor.com/pdfs/Schott_zerodur.pdf.

Semjonov SL, MM Bubnov, EM Dianov and AG Shchebunyaev. 1993. "Reliability of Aluminum Coated Fibers at High Temperature." In *Proceedings of SPIE, Fiber Optics Reliability and Testing: Benign and Adverse Environments, Volume 2074*, pp. 25-33. September 7, 1993, Boston, Massachusetts. The International Society for Optical Engineering, Bellingham, Washington.

Semjonov SL, MM Bubnov, NB Kurinov and AG Schebuniaev. 1997. "Stability of Mechanical Properties of Silica Based Optical Fibres under Gamma-Radiation." In *Fourth European Conference on Radiation and Its Effects on Components and Systems (RADECS 97)*, pp. 472-475. September 15-19, 1997, Cannes, France. Institute of Electrical and Electronics Engineers Inc., Piscataway, New Jersey.

SGP. 2013. *SGP Specialty Glass Products*. Speciality Glass Products (SGP). Willow Grove, Pennsylvania. Accessed May 30, 2013. Available at http://www.sgpinc.com/materials.htm.

Shaw CC and RS Krogstad. 1958. *Nuclear Radiation Effects on Infrared Materials and Components, Part I. Effects of Gamma Radiation on Infrared Transmitting Materials and Filters*. LMSD-5014, Lockheed Missiles and Space Company, Sunnyvale, California.

Shikama T, T Kakuta, M Narui, T Sagawa and H Kayano. 1995. "Optical Properties in Fibers During Irradiation in a Fission Reactor." *Journal of Nuclear Materials* 225:324-327.

Spencer JW, R Smith, SR Smith, J Humphries, GR Jones, A Fitzgerald, RE Sharp and L Pater. 1994. "Fiber Optic Sensor System Assessment in Radiation Environments." In *Proceedings of SPIE, Optical Fibre Sensing and Systems in Nuclear Environments, Volume 2425*, pp. 96-104. September 17, 1994, Mol, Belgium. The International Society for Optical Engineering, Bellingham, Washington.

Spitsyn VI, AI Ryabov, NS Stel'makh and GN Pirogova. 1977. "Influence of Radiation on the Optical Properties of High-Resistance Single Crystals of Ge, GaAs, and ZnSe." *Inorganic Materials* 13(1):19-22.

Sporea D and A Sporea. 2007. "Radiation Effects in Sapphire Optical Fibers." *Physica Status Solidi C* 4(3):1356-1359.

Surmet. 2013a. *ALON Optical Ceramic*. Surmet Corporation. Burlington, Massachusetts. Accessed May 30, 2013. Available at http://www.surmet.com/technology/alon-optical-ceramics/index.php.

Surmet. 2013b. *Spinel Optical Ceramic*. Surmet Corporation. Burlington, Massachusetts. Accessed May 30, 2013. Available at http://www.surmet.com/technology/spinel/index.php.

Tosi JL. 2013. *Common Infrared Optical Materials: A Guide to Properties and Applications*. Photonics Media, Laurin Publishing Co., Inc. Pittsfield, Massachusetts. Accessed May 30, 2013. Available at http://photonics.com/edu/Handbook.aspx?SID=29&AID=25495.

Troska J, J Batten, K Gill and F Vasey. 1998. "Radiation Effects in Commercial Off-the-Shelf Single-Mode Optical Fibres." In *Proceedings of SPIE: Photonics for Space Environments VI, Volume 3440*, pp. 112-119. July 22, 1998, San Diego, California. The International Society for Optical Engineering, Bellingham, Washington.

Vaddigiri A, KS Potter, WJ Thomes, Jr., and DC Mesiter. 2006. "Ionizing Radiation Effects in Single-Crystal and Polycrystalline YAG." *IEEE Transactions on Nuclear Science* 53(6):2882-2888.

Valley Design. 2013. *Substrates and Wafers*. Valley Design Corp. Shirley, Massachusetts. Accessed May 30, 2013. Available at www.valleydesign.com (last updated April 16, 2013).

van Uffelen M, Y El Shazly, S Kukureka, G Kuyt, E Regnier, P Matthijsse and F Berghmans. 2006. "Mechanical Reliability Studies of Optical Fibres under High-Dose Gamma Radiation." In *Proceedings of SPIE, Reliability of Optical Fiber Components, Devices, Systems, and Networks III, Volume 6193*, p. 619303. April 3, 2006, Strasbourg, France. The International Society for Optical Engineering, Bellingham, Washington.

Vitron. 2013. *IR Glasses*. VITRON Spezialwerkstoff GmbH. Jena-Maua, Germany. Accessed May 30, 2013. Available at http://www.vitron.de/english/.

Voitsenya VS, AF Bardamid, VN Bondarenko, W Jacob, VG Konovalov, S Masuzaki, O Motojima, DV Orlinskij, VL Poperenko, IV Ryzhkov, A Saraga, AF Shtan, SI Solodovchenko and MV Vinnichenko. 2001. "Some Problems Arising due to Plasma-Surface Interaction for Operation of the In-vessel Mirrors in a Fusion Reactor." *Journal of Nuclear Materials* 290-293:336-340.

Voitsenya VS, AF Bardamid, VT Gritsyna, VG Konovalov, O Motojima, DV Orlinskij, R Palladino, BJ Peterson, AN Shapoval, AF Shtan, SI Solodovchenko, KI Yakimov and K Young. 1998. "On the Choice of Materials for the First Mirrors of Plasma Diagnostics in a Fusion Reactor." *Journal of Nuclear Materials* 258-263:1919-1923.

Wang X, C Zhang, J Jin, N Song and H Xu. 2011. "Radiation-Induced Attenuation Effect in Hydroxyl-Rich Pure-Silica-Core Photonic Crystal Fiber." *Optik - International Journal for Light and Electron Optics* 122(21):1918-1921.

Warren IH and H Shimizu. 1963. "The Modulus of Rupture of Unsintered Uranium Oxide Compacts." *Journal of Nuclear Materials* 10:365-369.

Yamamoto S, T Shikama, V Belyakov, E Farnum, E Hodgson, T Nishitani, D Orlinski, S Zinkle, S Kasai, P Stott, K Young, V Zaveriaev, A Costley, L deKock, C Walker and G Janeschitz. 2000. "Impact of Irradiation Effects on Design Solutions for ITER Diagnostics." *Journal of Nuclear Materials* 283-287:60-69.

Yashima H. 1982. "Effect of Gamma-Radiation on Optical Fiber Strength." *IEEE Transactions on Nuclear Science* NS-29:1026-1028.

Young JP and JC White. 1960a. "Absorption Spectra of Molten Fluoride Salts. Solutions of Praseodymium, Neodymium, and Samarium Fluoride in Molten Lithium Fluoride." *Analytical Chemistry* 32:1658-1661.

Zabezhailov MO, AL Tomashuk, IV Nikolin and KM Golant. 2002. "Radiation-Induced Absorption in Optical Fibers in the Near-Infrared Region: the Effect of H2- and D2-loading." In *2001 6th European Conference on Radiation and Its Effects on Components and Systems*, pp. 192-194. September 10-14, 2001, Grenoble, France. Institute of Electrical and Electronics Engineers Inc., Piscataway, New Jersey.

Zhang HL, MF Zhang, ZG Hu, JC Han, HX Guo and CH Xu. 2013. "Mechanical Characteristics of Sapphire Before and After Neutron Irradiation." *Physica B: Physics of Condensed Matter* 408:34-38.

Zhu X and N Peyghambarian. 2010. "High-Power ZBLAN Glass Fiber Lasers: Review and Prospect." *Advances in OptoElectronics*. Article ID 501956. DOI:10.1155/2010/501956.

4.0   Imaging

4.1   Radiation-Hardened Cameras

In-vessel visualization could provide operators access to sophisticated sensing and machine-vision technologies that provide efficient human-machine interface for in-vessel telepresence, telerobotic control, and remote process operations. In-vessel imaging could provide multiplexed monitoring and sensing through optical viewports using commercial off-the-shelf (COTS) radiation-hardened cameras or even disposal camera components. COTS radiation-hardened cameras are a very mature technology that has been developed for inspection and maintenance applications during reactor refueling operations. Concepts that provide visualization during full reactor power could significantly enhance reactor safety and control. Cameras that produce monochrome and full color output are commonly available. Some models are designed to operate under water, but none are designed for submersion in any advanced small modular reactors (AdvSMR) molten coolants.

The technical readiness for existing COTS radiation-hardened camera systems is **MEDIUM**, because of the knowledge gaps regarding radiation-resistance specifications. Exposure studies to determine functional lifetime under defined neutron and gamma radiation exposures will be required. Some research, development, and demonstration (RD&D) effort to integrate these cameras with the standpipe viewport or periscope concept and to solve challenging deployment obstacles will be required.

Mass production and consumer market saturation of board-level complementary metal-oxide semiconductor (CMOS) cameras have brought the cost down to $10 in some cases. For example, the new Apple iPhone 5 has two miniature 8-megapixel cameras capable of capturing high-quality images and video. The low cost and high integration may herald a new approach of "throwaway" cameras for in-vessel monitoring, servicing, and inspection applications. Rather than spending many thousands of dollars for a radiation-hardened camera, single-use, disposal cameras could be used with reduced lifetime and radiation-damage concerns. The maximum working temperature specification (typically 45°C) would still limit the deployment options. It is possible these cameras could survive in-vessel long enough to collect useful information. Disposable cameras could be much more feasible for the AdvSMR application, given development of engineering solutions as discussed with the radiation-hardened cameras. Given this approach and assumption regarding useful in-vessel lifetime, the technical readiness for existing COTS miniature camera systems is **MEDIUM**.

4.1.1   Fundamentals of Operation

Video cameras are a very mature technology with a wide range of applications. The four most common types of video cameras are charged-coupled device (CCD), CMOS, charge injection device (CID), and Chalnicon. Both the CCD and CMOS types of cameras are constructed using processes directly from the semiconductor industry. Many thin layers of dielectric are separated from thin layers of insulation to form the CCD/CMOS structure. It is these boundaries that make such devices susceptible to damage from radiation exposure. In a CCD, this means that the charge transfer becomes inefficient and the device quickly stops working. In a CMOS transistor, it means that the threshold voltage of the transistor slowly shifts, until the device is either always on, or completely closed off (Rad-icon 2002). A CID camera is also a semiconductor device. However, the design of the readout structure makes this type of camera more tolerant to radiation exposure. Each pixel can be read directly without the need to

transfer the charge to neighboring pixels, as is the case for CCDs. The readout for a CCD is accomplished by transferring the charge from a pixel to the edge where it will then be detected. The transfer of charge from pixel to pixel requires that each pixel in that row be in "good health." A pixel damaged by radiation could prevent the rest of the pixels in that row from being detected properly. Because each pixel in a CID is read individually, a damaged pixel will not affect the rest of the image. The last camera type, Chalnicon, is basically a vacuum-tube-type camera. Vacuum-tube cameras have been in use since the 1930s. A Chalnicon camera is a slight variation of the more common Vidicon. It operates like all vacuum-tube-type cameras, as shown in Figure 4.1. An image is projected onto a photoconductor, which forms an electric charge proportional to the amount of light. An electron beam is swept across the photoconductor, which releases the charge. The charge is then removed from the tube as an electrical output. The most sensitive component of a tube camera to radiation is the photoconductor. Because it is a macro structure compared to CCD/CMOS, it is inherently more resistant to radiation damage.
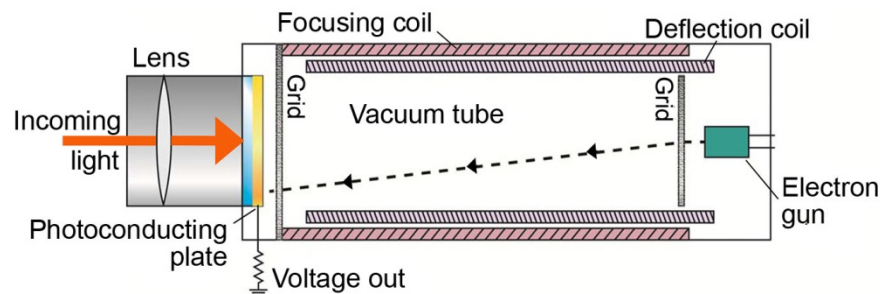
Figure 4.1. Schematic Illustration of a Chalnicon-Type Camera

4.1.2   Promising Research and Development

The video camera is a very mature technology spanning over 70 years. Until the 1980s, video cameras were predominately made using vacuum-tube devices. After semiconductor detector arrays were developed, vacuum-tube cameras were only used in very specialized niches, such as the nuclear power industry because of their inherent radiation tolerance. Both semiconductor and vacuum-tube cameras are currently in use in the nuclear power industry and have been for decades. Technology improvements have been focused primarily on increasing pixel count and developing software-based image processing algorithms. Future radiation-resistance enhancements are likely to be only incremental and mainly focused on improved radiation-shielding designs.

4.1.3   COTS Summary, Gaps Analysis, Ranking, and Proposed Future Research

COTS Radiation-Hardened Camera Summary

Radiation-hardened cameras are a very mature technology, available from many vendors. This technology represents a vital component to enable in-vessel AdvSMR visualization to meet the needs associated with monitoring process status, inspecting components, and providing operator feedback during remote refueling operations. Radiation-hardened cameras are commercially available from about a half dozen established manufacturers including Mirion, Thermo Fisher Scientific, Diakont, and Ahlberg

Electronics. The cameras come in a variety of detector technologies, including CCD, CMOS, Chalnicon, and CID. All the cameras operate in the visible spectrum; however, several models have options to function in the ultraviolet (UV) or near infrared (NIR) regions, between 300 to 1100 nm. Monochrome CCD cameras, with interlaced 730(H) × 512 (V) National Television Standards Committeee (NTSC) format, are widely available COTS items from most of the identified vendors. Several COTS cameras offer a digital video output option via a Firewire interface. One vendor (Thermo Fisher Scientific) offers a color CID format camera with the same resolution that has 3 MGy total dose operational specifications. Remote camera heads, with a 150-m umbilical, are sometimes available as an option. In this configuration, about half the electronics subsystems can be further isolated from temperature and radiation extremes.

The containment vessel headspace deployment requirements include 40°C ambient temperature, gamma at <10 Gy/h, and neutron flux at $<10^{11}$ n/cm^2 s. Molten Na coolant can become activated and thus have gamma up to 100 Gy/h. The COTS radiation-hardened camera maximum total radiation dose is generally specified between 10 KGy to 3 MGy, depending on the shielding and camera design. Cameras have been exposed to 300 Gy/h, for 45 h (13.5 KGy total dose), with only modest image degradation. Assuming a CID camera is exposed to 13.5 KGy total dose, the camera has a lifetime, before modest image degradation begins, of 1350 h and 135 h for non-sodium and sodium-cooled reactors, respectively. COTS radiation-hardened camera specifications only claim that the camera is 'tolerant' to neutron, high-energy electrons, and proton radiation, without any qualifiers. All COTS cameras have temperature specifications that meet the AdvSMR application requirements. The highest specified continuous working temperature is 70°C in water and 55°C in air. Most cameras are rated to 45°C.

Gaps Analysis

- Knowledge gaps regarding camera fundamental service-lifetime under AdvSMR deployment conditions must be determined.

- Concepts must be developed to minimize coolant vapor deposits on to optical surfaces.

- An integration and demonstration plan for COTS cameras and supporting optomechanical systems and image-processing software must be developed and executed.

- An optical image relay system will be required to interface the remote camera with the standpipe viewport or an in-vessel periscope.

- Actual performance and benefits of COTS cameras and image processing methods must be determined.

Technical Readiness Ranking

Technical readiness for radiation-resistance monitoring cameras is **MEDIUM**, because of the radiation-resistance specifications knowledge gaps. Exposure studies will be required to determine functional lifetime under defined neutron and gamma radiation exposures. Some RD&D effort will be required to integrate these cameras with the standpipe viewport or periscope concept and solve challenging optical alignment problems associated with thermal expansion and vibration.

Proposed Future Research

- A modest RD&D effort is recommended to study and establish functional service-lifetime estimates for COTS radiation-hardened cameras under the defined AdvSMR deployment conditions.

- The outcome of the exposure studies may suggest further engineering is required to improve the COTS camera performance or that a radiation-hardened enclosure must be developed.

- Further evaluation and demonstration effort will be required to provide robust interface with the standpipe viewport or periscope concepts.

COTS Disposable Camera Summary

Short-term, disposable cameras could be considered **MEDIUM** technical readiness, based on their low cost and useful deployment scenario and lifetime assumptions. Actual evaluation of lifetime performance under simulated in-vessel and annulus deployment conditions is required. Semi-custom designs could include active cooling, high-temperature solder, and shielding options. These options will increase the camera cost; therefore, a cost-to-benefit analysis will be required to determine the best path forward. These cameras are also compatible with the standpipe viewport or periscope concept.

4.2   Thermographic Imaging

Thermal imaging through transparent (i.e., molten salt and gas) coolants could possibly be conducted using thermographic camera technology. Thermal imaging could provide temperature profile information of the core and other in-vessel systems. Reactor power could be inferred by thermal profiling. It may be possible to detect coolant channeling or blockage. These measurements could substantially enhance reactor diagnostics, control, and efficiency.

Thermographic imaging cameras are multi-pixel infrared detectors, either cooled (superior thermal image quality), or uncooled (smaller and light-weight). The technical readiness for existing COTS thermographic camera systems is **MEDIUM**. Their upper working temperature (i.e., 50°C to 70°C) will meet the AdvSMR deployment requirement, but in all cases the product vendors do not provide radiation-resistance specifications. Radiation exposure effects have been studied, although typically for low earth orbit applications, where radiation is predominantly high-energy protons at levels that are significantly lower compared to AdvSMR environments that are dominated by neutrons and gammas. Thermographic cameras could be much more feasible for AdvSMR applications, given development of engineering solutions, such as infrared transparent standpipe viewports and relay imaging systems.

4.2.1   Fundamentals of Operation

Thermographic or infrared cameras are equipped with imaging detectors that are sensitive to infrared radiation typically between 1 to 14 µm, depending on the detector array used in the imager. With knowledge of an object's emissivity, a thermographic camera can remotely measure an object's temperature by processing the detected infrared radiation. Infrared imagers are available in both cooled and uncooled detector formats. Detectors are cooled, cryogenically, thermoelectrically, or by using pressurized gas. The photodetector materials used for cooled infrared detection are based on a wide range of narrow gap semiconductors, including indium antimonide, indium arsenide, mercury cadmium telluride (MCT), lead sulfide, and lead selenide. Cooling is necessary to reduce the semiconductor detector's own

thermal background and to reduce noise from thermally excited current carriers. Generally, cooled infrared cameras provide superior image quality and greater sensitivity compared to uncooled cameras.

Uncooled thermal cameras use detector arrays that are not subject to thermally excited current carrier issues. Modern uncooled detectors are all based on pyroelectric and ferroelectric materials or microbolometer technology. These highly temperature-sensitive materials are formed into pixelated two-dimensional arrays. Resistance, voltage, or current changes are produced by temperature changes resulting from exposure to infrared thermal radiation. Each pixel value is measured and processed into temperatures of the target object, which can then be used to create spatial thermal images. The diagram in Figure 4.2 depicts the structure of an uncooled detector pixel similar to the ones in a microbolometer.
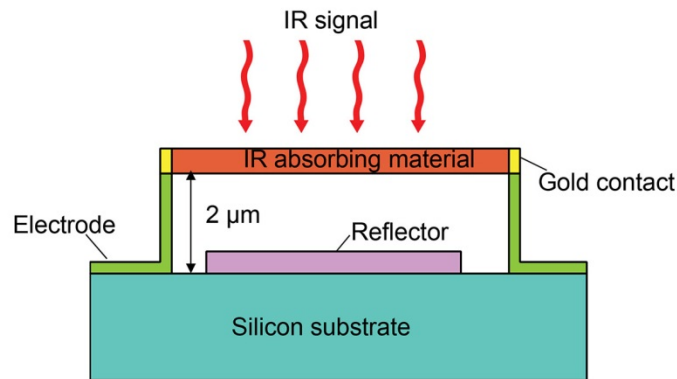
Figure 4.2. Schematic of a Pixel in an Uncooled Detector such as a Microbolometer

4.2.2   Promising Research and Development

Very little research has been conducted to improve thermal imaging camera performance for extreme environment applications. The research that has been conducted is for space applications having much lower radiation and temperature conditions. Custom-built MCT focal point arrays (Fabry-Pérot As) have been studied under gamma irradiation, displaying two types of performance disruption: transient and permanent. Under ultra-short pulses (0.2 µsec to 4 µsec) of gamma, doses totaling 1 mGy to 400 Gy MCT cameras suffered decreased performance in the form of readout noise and array offsets. Dose rates were also varied between 10^5 and 10^8 Gy/s, showing temporary radiation-induced noise in all cases. Permanent effects were only observed at the highest dose rates (Suffis et al. 2003). While permanent damage was low, even at high gamma flux, continuous transient readout noise would likely limit this camera's usefulness. To minimize these effects, heavy shielding would be required.

Microbolometer Fabry-Pérot As made from InGaAs were evaluated under simulated low earth orbit radiation environments and found radiation resistant to 60 MeV protons to a proton fluence 1.5×10^{10} 60 MeV p/cm^2 and gamma radiation from a ^{60}Co source to a total gamma dose of 1000 Gy (Hopkinson et al. 2008). This report showed good Fabry-Pérot A performance with some circuit damage because of radiation-induced current. It appears very few other studies on radiation exposure effects have been conducted.

4.2.3 COTS Summary, Gaps Analysis, Ranking, and Proposed Future Research Path

COTS Thermographic Imaging Camera Summary

COTS infrared cameras are readily available from many vendors, such as FLIR, Electrophysics, DRS Technologies, Micro-Epsilon, New Infrared Technologies, Sofradir-EC, and others. Most vendors have their own proprietary detector designs and fabrication techniques. Lead zirconate-titanate and zinc oxide are two materials with large pyroelectric properties. Lead scandium tantalite, lead titanate, and barium strontium titanate are a few important ferroelectric materials. Amorphous silicon and vanadium oxide are commonly used to fabricate microbolometers. About a dozen products were identified that provide thermal imaging of objects from a few hundred°C to 3000°C. Temperature accuracy is typically limited to a few degrees C. Current improvements of uncooled focal plane arrays (UFPA) seem to focus primarily on higher sensitivity and pixel density. Recent technology has led to the production of devices with 640×480 or 1024×768 pixels. The pixel size was typically 45 µm in older devices and has been decreased to 17 µm in current devices.

Gaps Analysis

- COTS thermographic cameras are primarily used in laboratory settings, and have not been developed for harsh industrial environments.

- Transmission through transparent coolants (particle flow in coolants and thermal index gradients) may degrade performance.

- Auto-alignment to a target surface is not provided.

- The radiation-resistance specifications for COTS thermographic cameras are not provided.

Technical Readiness Ranking

The technical readiness for COTS thermographic cameras is **MEDIUM**, because of the lack of ruggedization of commercial instrumentation and radiation-resistance specifications.

Proposed Future Research

- Enhancements and customization of COTS thermographic cameras are needed to meet the demanding AdvSMR deployment requirements.

- Optomechanical design using infrared transparent optics will be required to maintain optical alignment and performance over extreme temperature variations (e.g., start-up through steady-state operation temperatures).

- Further study will be required to evaluate measurement degradation and service life as a function of radiation exposure.

- Testbed and test reactor experiments and demonstrations will be required.

4.3   References

Hopkinson G, RH Sorensen, B Leone, R Meynart, A Mohammadzadeh and W Rabaud. 2008. "Radiation Effects in InGaAs and Microbolometer Infrared Sensor Arrays for Space Applications." *IEEE Transactions on Nuclear Science* 55:3483-3493.

Rad-icon. 2002. *AN06: Detector Lifetime and Radiation Damage*. Rad-icon Imaging Corp. Santa Clara, California. Accessed December 10, 2013. Available at http://www.couriertronics.com/docs/notes/XRay/Radicon_AN06lifetime.pdf.

Suffis S, M Caes, M Tauvy, C Planchat, B Azais, P Charre and M Vie. 2003. "Implementation and Measurement of Gamma Radiation on IR Photodetectors HgCdTe IRCMOS." In *Proceedings of SPIE, Infrared Technology and Applications XXIX, Volume 5074*, pp. 111-119. April 21, 2003, Orlando, Florida. DOI 10.1117/12.486307. The International Society for Optical Engineering (SPIE), Bellingham, Washington.

5.0   Temperature Sensors

5.1   Overview

Temperature is a basic, essential, and widely used measurement parameter for nuclear reactor control and monitoring systems. In-vessel temperature measurements provide plant operators and control systems with real-time data that can be used to monitor and optimize plant control. Temperature is measured at many locations inside the reactor, including the core and intermediate heat exchanger inlets and outlets, and the hot and cold coolant pools. These measurements provide assurances that coolant temperatures have not exceeded critical levels, as well as provide process efficiency estimates and diagnostic feedback.

Thermocouples and resistance temperature detectors (RTDs) serve as high-accuracy temperature point sensors in existing power reactors. A large number of these sensors must be used in each vessel, because there is a high degree of laminar flow stratification in the coolant that causes spatial temperature fluctuations across the core. RTDs provide only point sensing at discrete locations. Thermal distribution measurements are desirable to detect flow blockage or channeling through the core. Estimating the coolant temperature profile requires many RTDs, which increases cabling and maintenance requirements. RTDs also suffer signal drift at high temperatures, which leads to frequent calibration requirements. The ultra-high temperatures inside advanced small modular reactors (AdvSMRs) may require alternate temperature monitoring solutions.

A large number of optical temperature measurement methods have been reported in the literature. Many of these techniques are available as mature commercial off-the-shelf (COTS) sensing instruments. Some, including pyrometry, Fabry-Pérot fiber optic sensors, time-domain reflectometry, semiconductor bandgap sensors, and fiber-Bragg grating sensors, are readily available as COTS instruments that feature excellent temperature measurement performance. These instruments can be divided by their measurement configuration; namely, optical fiber-based sensors and standoff sensors. The fiber-based sensors are ranked both for near-reactor-lid and near-core deployment, where the temperature and radiation conditions are drastically different. For the standoff sensors, we assume that the sensitive sensor control instrumentation is isolated from temperatures above 40°C and radiation exposure is managed using the appropriate shielding. Some of the COTS fiber-based sensor systems have technical readiness ranked **HIGH** for near-reactor-lid applications and **LOW** for near-core applications. The primary factor for these rankings is the low temperature limits of the fiber coatings, sheathing, and cabling materials. All the COTS standoff sensor systems have technical readiness ranked **MEDIUM**. The primary gaps are related to the additional ruggedization and radiation-hardening enhancements needed for AdvSMR applications.

5.2   Pyrometry

Optical pyrometry is commonly used in steel foundries, combustion research, and industrial applications to provide noncontact temperature measurements of very hot objects. Pyrometry instruments determine temperature by analyzing the spectral distribution of thermal radiation emitted from an object's surface. The key advantage of pyrometry is that it provides standoff temperature measurement, although knowledge of the emissivity properties of the object surface is required. Pyrometry measurements can be conducted at several wavelengths to compensate for errors in emissivity estimates. Non-greybodies, such

as certain metal alloys, have wavelength-dependent emissivity, which complicates the pyrometry analysis, and affect the measurement accuracy. Pyrometry measurements at many wavelengths can generally account for non-greybody emissivity errors and minimize measurement drift.

Pyrometers systems have a small field of view, on the order of a couple of centimeters at most, making them essentially a "stand-off point sensor." Many COTS multi-wavelength pyrometry instruments that measure temperatures up to 4000°C with better than 1 percent accuracy are available. Very large temperature dynamic ranges, however, require multiple pyrometers.

Pyrometry has seen little or no use by the nuclear industry, but in-vessel temperature measurements using standoff pyrometry with a standpipe viewport should be feasible. Pyrometry measurement through molten salt, He, and supercritical water coolants may be feasible. Multi-wavelength pyrometry seems most feasible, because many in-vessel objects are likely to be non-greybodies. Pyrometry will likely have limited benefit for molten metal AdvSMRs, because only coolant surface measurements could be made. Coupled with the standpipe viewport concept, pyrometry has **MEDIUM** technical readiness.

5.2.1   Fundamentals of Operation

A pyrometer is a noncontact measurement instrument that intercepts and measures thermal radiation to determine the temperature of an object's surface. A pyrometer consists of an optical receiver that collects and focuses the energy emitted by an object onto the detector, which is sensitive to the radiation. The output of the detector is proportional to the amount of energy radiated by the target object (less the amount absorbed by the optical system), and the response of the detector to the specific radiation wavelengths. This output can be used to infer the object's temperature. Because pyrometers collect thermal radiation from a distance, the measurement provides standoff, noncontact temperature sensing. However, the emissivity, or emittance, of the object is an important variable used to process the detector output into an accurate temperature signal. The accuracy of the temperature is dependent on knowledge of the object's emittance. A blackbody absorbs all electromagnetic radiation and has a defined spectral emissivity of 1. Normally physical objects absorb and reemit electromagnetic radiation. Emittance is the amount a normal object departs from an ideal blackbody. Greybody has spectral emissivity less than 1 that is independent of wavelength. Many common objects have emittance that is a function of wavelength. These are called non-greybodies. Because emissivity of a non-greybody object such as stainless steel and metal alloy changes with wavelengths and surface conditions (as shown in Figure 5.1), multi-wavelength pyrometers are preferred over traditional single-color or two-color pyrometers, because they can provide more accurate temperature measurements of real objects with unknown or changing emissivities. Multi-wavelength pyrometers use three or more wavelengths and mathematical manipulation of the results to achieve accurate temperature measurement even when the emissivity is unknown, changing, and different at all wavelengths. Because of a small field of view, pyrometers usually only serve as a point sensor.
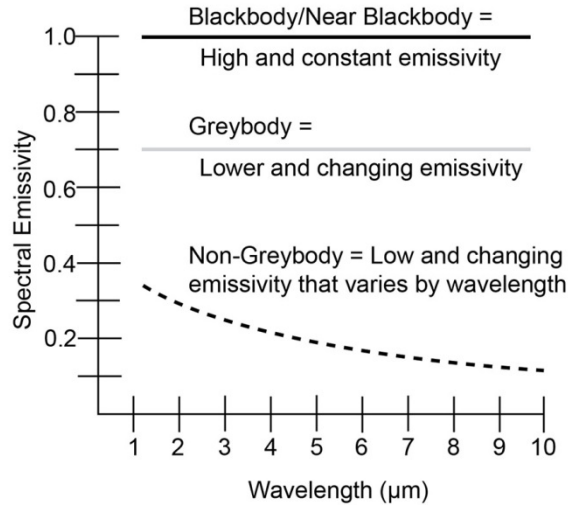
Figure 5.1. Spectral Emissivity of Blackbody, Greybody, and Non-Greybody Materials

5.2.2   Promising Research and Development

A few research institutes have been working on pyrometry technology for very high-temperature applications such as inside jet engine combustors, gas turbine engines, and industrial furnaces. For example, the National Aeronautics and Space Administration's (NASA's) Glenn Research Center has developed a temperature probe that uses multi-wavelength pyrometry to measure very high temperatures, from approximately 800°C up to 2400°C (Ng and Fralick 2001). The probe consists of a high-temperature ceramic sheath partially inserted into a high-temperature metal support section and an optical fiber inside the sheath/support assembly. A fiber-optic cable connects the probe to the pyrometer. The fiber-optic cable connects at the cool end of the probe, so a high-temperature fiber cable is not necessary.

5.2.3   COTS Summary, Gaps Analysis, Ranking, and Proposed Future Research Path

COTS Pyrometry Summary

Pyrometry instruments for measuring very high temperatures typically in industrial processes are widely available from commercial vendors. Multi-wavelength COTS pyrometers are available from Far Associates, Masibus, and others. Many COTS pyrometers are available in ruggedized packages that are compact and portable. The measurement results can usually be read out on a display integrated on the device and/or from output signals via a cable to a remote computer. Pyrometers are available with an optional optical-fiber probe to measure hard-to-access objects. Some models are designed to avoid strong water vapor and some gas absorption lines by appropriate selection of measurement wavelengths. Compensation techniques are available to eliminate reflection and scattered energy interferences from intervening media. Temperature resolution of 0.1°C and 1°C repeatability can be achieved by most models.

Since the first multi-wavelength pyrometers were envisioned at the National Institute of Standards and Technology (NIST) in the early 1990s, many commercial multi-wavelength pyrometers are now available for temperature measurements from below freezing point to as high as 4000°C (although an

individual pyrometer can only cover a portion of this range). FAR Associates offers a series of systems called Spectropyrometers, which all together can measure temperatures from 300°C to 4000°C. These systems are available with optional sapphire probes, which can sustain direct temperatures up to 1900°C. Heitronics and Williamson IR are two other companies that provide standoff dual- and multi-wavelength pyrometric instruments measure temperature to 2500°C.

Although COTS pyrometers have not been developed for the nuclear industry, the temperature measurement range and resolution performance meets the temperature monitoring requirements for AdvSMRs. COTS pyrometry instruments can be operated up to 40°C, which meets the containment vessel headspace deployment requirements. No vendor specifications are provided for radiation-resistance. Pyrometry will likely have limited benefit for molten metal AdvSMRs, because only coolant surface measurements are possible. Pyrometry measurements through molten salt, He, and supercritical water coolants may be feasible, but further RD&D will be required to determine actual performance.

Gaps Analysis

Pyrometry can be a very powerful standoff temperature measurement method for in-vessel process monitoring. Further RD&D will be required to fully characterize performance under conditions expected in the upper containment area above the reactor vessel. Key gaps that confront implementation of pyrometers include:

- Non-greybody emissivity correction may need improvement.

- Transmission media compensation is not provided for coolants vapors, particle flow in gas coolants, thermal index gradients, and window port heat and vibration.

- Pyrometer performance may be potentially limited when deployed in containment area.

- Auto-alignment to a target surface is not provided.

- The radiation-resistance specifications for COTS pyrometers are not provided.

- Pyrometry data processing methods may be required to compensate for the hot background-rich environment in order to derive useful information.

- Studies to determine feasibility of pyrometry through transparent coolant are required.

- Actual performance and benefits of COTS pyrometry must be determined.

- Service-lifetime and performance of COTS pyrometry instrumentation under AdvSMR deployment conditions must be determined.

Technical Readiness Ranking

Coupled with the standpipe viewport concept, pyrometry has **MEDIUM** technical readiness, because of the additional ruggedization and measurement compensation likely needed for AdvSMR applications.

Proposed Future Research Path

- Develop compensation for coolant vapors, particle flow in gas coolants, thermal index gradients, and window viewport heat, vibration, and coolant coatings.

- Develop compensation for non-greybody emissivity correction.

- Conduct pyrometry measurements in molten salt coolants.

- Demonstrate, optimize, and develop integration plan for COTS pyrometry for in-vessel temperature measurements.

- Determine if pyrometry through transparent coolants is feasible.

5.3 Fiber-Bragg Grating Sensors

A fiber-Bragg grating (FBG) is a periodic structure imposed upon the core of an optical fiber, causing an interference condition, or resonance as the light propagates through the fiber. The resonance condition results in a high reflection at the Bragg wavelength. All other wavelengths are unaffected and are transmitted through the grating. Multiple Bragg gratings may be written in series to create a distributed-sensing configuration. FBG sensors can be designed and fabricated to measure temperature, pressure, strain, and curvature. Sensing parameters are measured by monitoring wavelength resonance shifts because of the grating period variations as a function of temperature or mechanical strain. FBG sensors can provide distributed parameter sensing throughout a reactor vessel in both the coolant and/or gas headspace. FBG measurements are unaffected by coolant transparency. Generally the optical fibers, used to fabricate FBG sensors, do not have radiation-resistance specifications. The temperature limit imposed by the fiber coatings, sheaths, and cabling will reduce feasibility of most AdvSMR applications. However, this measurement technology is promising, because FBG sensors provide distributed sensing using only a single optical fiber. FBG sensors can provide low-cost and accurate process monitoring. FBG temperature sensors to have technical readiness ranked **HIGH**. The main drawback to FBG sensors is that the Bragg resonant condition is very sensitive to temperature, pressure, mechanical strain, and vibration. Extracting a single measurement parameter requires careful design that minimizes those sources of noise.

The gratings' recording process can affect the maximum working temperature. FBGs created by multi-photon ionization can withstand temperatures to 1000°C, which is suitable for most in-vessel conditions. Several FBG sensor research studies have been conducted in test reactors. Study results demonstrated that over short time periods, the grating structure survived radiation and high-temperature exposure. Recent research and development (R&D) efforts were successful in writing Bragg gratings in sapphire, which is a material of choice for in-vessel applications.

5.3.1 Fundamentals of Operation

Although developed initially for the telecommunications industry in the late 1990s, FBGs are increasingly being used in sensing applications. The FBG is an optical filtering device that reflects light of a specific wavelength and is present within the core of an optical-fiber waveguide. The wavelength of light that is reflected depends on the spacing of a periodic variation or modulation of the refractive index that is present within the fiber core. This grating structure acts as a band-rejection optical filter passing all wavelengths of light that are not in resonance with it and reflecting wavelengths that satisfy the Bragg condition of the core index modulation. The Nobel Laureate Sir William Lawrence Bragg established the Bragg law in 1915, describing with a simple mathematical formula how x-rays were diffracted from crystals. The Bragg condition, when applied to fiber Bragg gratings, states that the reflected wavelength of light from the grating is $\lambda_B = 2 \cdot n_{eff} \cdot \Lambda_G$ where n_{eff} is the effective refractive index seen by the light propagating down the fiber, and Λ_G is the period of the index modulation that makes up the grating. This parameter is illustrated in Figure 5.2. FBGs are relatively straightforward, inexpensive to produce,

lightweight, passive, small in size, and self-referencing with a linear response. They are ideally suited for measuring temperature and stress in harsh environments and have a capability to perform distributed sensing. FBGs can also be engineered to be sensitive to pressure, curvature, displacement, load, and ambient refractive index. Because of their telecommunication origins, FBGs can be easily integrated into large-scale optical networks and communications systems.
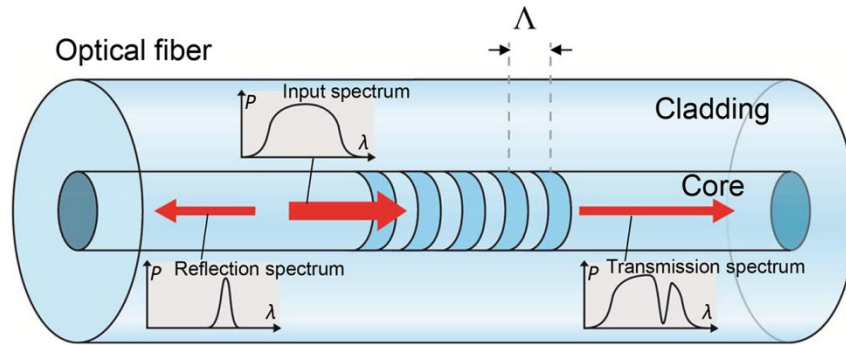
Figure 5.2.   Schematic of a Basic FBG, Showing How the Incident Light is Separated into Reflected and Transmitted Spectra

There are three basic categories of FBGs that are based on different formation mechanisms. Type I gratings are created by photoimprinting a hologram in the photosensitive glass core of the fiber. Modulation of the core index is formed by an ultraviolet (UV) single-photon absorption process that either excites oxygen deficiency defect centers (ODC) with absorption bands around 244 nm for small index change or forms defects resulting in densification of the glass matrix for larger index change. These gratings can be annealed out at temperatures above 450°C when the excited states are returned to the ground state. Both the index change and the maximum operating temperature can be improved through a hydrogen-loading process, where high-pressure hydrogen gas permeates the glass matrix and forms hydroxyl groups under UV irradiation. However, at temperatures over 700°C, the original grating is replaced by a new grating structure at a longer wavelength and the remnant index modulation and the grating reflectivity become lower. Type II gratings are created using high peak power pulsed UV laser sources by a threshold-dependent multi-photon ionization (MPI) process similar to laser-induced damage in bulk optics. High reflectivity gratings (<99 percent) can be achieved with a single laser pulse. Such gratings are stable at temperatures over 1000°C and have been used to fabricate grating arrays while the fiber is being pulled on the draw tower. However, the single-shot exposure tends to produce grating structures that can suffer from significant scattering loss. The damage-like process also has the tendency to reduce the reliability and mechanical strength of the fiber. Recently a new type of FBG was created using the ultrahigh peak power radiation generated by femtosecond pulse duration infrared (fs-IR) laser systems. The mechanism for this laser-induced index change is thought to result from a nonlinear multi-photon absorption/ionization process leading to material compaction and/or defect formation depending on the intensity of the exposure. Above the material-dependent ionization threshold intensity I_{th}, MPI-induced dielectric breakdown likely results in localized melting, material compaction, and void formation causing an index change that is permanent up to the glass transition temperature T_g of the material. The properties of the resultant index change are similar to those of Type II gratings induced by nanosecond-pulse-duration UV lasers but with much better spectral performance than their UV counterparts. Because

of the ultra-short duration of the femtosecond source, the induced dielectric breakdown is rapidly quenched upon cessation of the beam; hence, there is virtually no propagation of "damage" beyond the irradiated zone.

Ge-doped core fibers are typically used for Type I gratings in low-temperature applications because of its photosensitivity. For high temperatures less than 1000°C, gratings written in glasses such as pure silica, or radiation-hardened fluoride-doped silica, can be used for sensors in the oil, gas, and nuclear industries where losses in standard optical fiber from hydrogen ingress or ionizing radiation can significantly reduce sensor lifetime. Above 1200°C extreme temperature with Bragg gratings is relegated to sapphire optical fiber. In the case of sapphire FBGs, these robust devices are suitable for harsh combustion environments such as jet engines, coal gasification reactors, and natural gas turbines for electrical power generation.

5.3.2 Promising Research and Development

The use of silica FBGs in low-temperature nuclear research reactors has been demonstrated on several occasions according to the literature and show great potential for in-core thermometry (Fernandez et al. 2004; de Villiers et al. 2012). For operation in high-temperature environments, an important issue for any silica-based fiber-optic sensor is that of sensor packaging. At temperatures close to or above 1000°C in air, unpackaged standard silica single-mode fibers lose almost all of their mechanical strength because of oxidation. While the fibers themselves survive hundreds of hours at 1000°C when left untouched, any subsequent handling of the fiber after the test is not possible as the fiber becomes extremely brittle. Protecting the fiber from exposure to oxygen at high temperature could be achieved by using a suitable package that survives the high temperature itself. A few research institutes are working towards this goal. For example, NASA's Glenn Research Center developed a ceramic housing tube to encapsulate commercial FBGs made on polyimide-coated SMF-28 optical fiber and has demonstrated operability of the device up to 1000°C for 1000 hours. However, more development and testing efforts are still needed for fiber packaging at temperatures close to or above 1000°C.

For temperatures higher than 1200°C, silica-based optical fibers are no longer feasible. Single-crystal sapphire light pipes, which have a melting point of approximately 2040°C, are often used for high-temperature applications. A sapphire FBG has been demonstrated to exhibit no degradation in grating strength at 1745°C, with measurement repeatability of better than 1°C (Busch et al. 2009). However, unlike conventional single-mode optical fibers, sapphire fibers are made in the form of rods with only large-core diameters available commercially. This makes the sapphire waveguides highly multimode and sensitive to bending losses and mode conversion. Other drawbacks include difficulties in finding a suitable cladding material as well as the fact that sapphire becomes very brittle at high temperatures.

The effects and remedies for radiation darkening in silica fibers have been widely studied (Primak 1958; Henschel 1994; Griscom 1995; Girard et al. 2013). Using radiation-hardened fluoride-doped silica fibers and longer interrogation wavelengths in the near infrared (NIR) helps to sidestep the radiation-darkening issues occurring in commercial silica fibers in the visible wavelength spectrum. The radiation testing conditions in current radiation facilities are usually limited to temperatures lower than 100°C. Therefore, study of radiation effects on silica fibers at high temperatures is very limited. But there is some evidence suggesting that radiation-darkening effects can be annealed out at high temperatures (Martín et al. 2011). This attribute may prove itself to be beneficial in AdvSMR applications where the operation temperatures are high. Sapphire optical fiber has also been tested for radiation resistance at

room temperature, and found to be immune to various types of irradiation of high total doses (i.e., 536 kGy gamma dose) (Sporea and Sporea 2007). However, radiation testing at high temperatures still needs to be conducted to prove reliability of sapphire optical fibers in AdvSMR applications where high operation temperature and high irradiation dose conditions are both present.

5.3.3   COTS Summary, Gaps Analysis, Ranking, and Proposed Future Research Path

COTS FBG Sensor Summary

FBG sensors are available from a number of different vendors and have been demonstrated in a wide array of different applications, including industrial processing and infrastructure. Radiation hardness of FBG sensors relies on identifying and integrating fiber-optic components that are suitable for strong radiation fields. A few companies are now making temperature and strain FBG sensors using standard SMF-28 silica fibers that are readily available commercially. Vendors that either distribute or manufacture distributed feedback (DFB) sensors include JPhotonics, Timbercon, Micron Optics, Luna Innovations, FBGS International, Ascentta Inc., and many others. Products from these companies are capable of measuring temperature, pressure, vibration, and many other properties. FBG sensor packages may be purchased, which measure multiple parameters, providing backgrounds for baselining and noise subtraction. Given the large range of applications, commercial FBG sensors can be customized to achieve specific mechanical or optical properties using different glasses and different cabling approaches.

COTS FBG sensor instruments can be operated up to 40°C, which meets the containment vessel headspace deployment requirements. No vendor specifications are provided for radiation-resistance. COTS FBG sensors are available for temperatures up to 300°C, which meets the near-lid deployment requirements for many advanced reactor designs. It has been reported that FBGs created by modulating the RI with dopants will dissipate above 400°C. There are many commercial sources of femtosecond-laser-inscribed FBGs, but these are all limited by other low-temperature components. Several vendors offer so-called ruggedized FBG sensor probes, but these are designed to provide physical robustness and deliver no advantage for high-temperature environments. Some probes are even available with ceramic coatings, but are still limited to operation below 250°C because of other components in the cabling assembly. It is very possible that customized solutions using silica fiber with select coatings could be obtained from a commercial source that would meet the temperature demands of AdvSMRs.

Gratings operated at temperatures higher than this range, or written on different fiber geometries, have only been achieved by academic or research institutes. These are not available in industry because of the lack of demand for various industrial applications that would drive production. Among the commercial FBG sensors, temperature resolution of 0.05°C can be achieved. When used as strain sensors, an operation range of ±15,000 µStrain is available and a resolution of 0.4 µStrain can be achieved.

As far as this survey has been able to determine, the current commercially available FBG sensors do not use radiation-hardened components, and therefore are not suitable for nuclear applications at the current stage.

For the most part, problems stemming from radiation exposure to FBG fibers will be similar to those experienced with all optical fibers and materials, but commercial systems are either not capable or not characterized for high-radiation environments. These problems have only been explored in research facilities thus far.

Gaps Analysis

The primary technical gaps for FBG sensors involve identifying a fiber and coating material set that works within the conditions expected in AdvSMRs. Sapphire fibers may be one of the leading candidates for this, but are not available as FBG sensors currently.

Technical Readiness Ranking

Current COTS FBG sensors are capable of near-lid monitoring without modification. For this reason, we consider FBG temperature sensors to have **HIGH** technical readiness for near-lid applications. Because of the lack of current solutions or information about using these fibers in very high temperature and radiation environments though, it must be considered to have a **LOW** technical readiness for near-core applications.

Proposed Future Research

Future research will require testing existing FBG sensors in radiological environments to identify their limits, and custom building new FBG sensors out of sapphire or other candidate fiber materials. Testing FBG distributed sensors in a test reactor over long periods of time would yield some very useful information.

5.4   Semiconductor Bandgap Sensors

A semiconductor bandgap (SCBG) sensor is a fiber-optic point sensor for measuring temperature. Temperature is determined by monitoring wavelength shifts of a semiconductor bandgap, as a function of temperature. This operation principle is simple and the sensor probe is cost-effective. SCBG optical-fiber sensors are commonly used in the electrical power industry to monitor the temperature of current transformers. The optical fiber interconnect provides noise immunity and electrical isolation during transformer monitoring. A wide variety of COTS SCBG optical-fiber sensors are available for applications to 300°C. One vendor offers a Teflon-coated GaAs bandgap sensor for the nuclear power market, but specific data on radiation-resistance are not provided.

The optical-fiber materials, bandgap crystal optical coatings, and the bonding method currently limit the maximum working temperature to 300°C. As a point sensor, this platform does not offer the functionality of a distributed sensor system or a significant performance advantage over conventional thermocouples or RTDs. Fiber bandgap sensors may be feasible in the headspace area of liquid coolant reactor designs, but are unlikely to be feasible in higher temperature gas coolant reactor designs. The temperature requirements for near-core deployment are well beyond the working temperature limits of SCBG fiber-optic sensors. Semiconductor bandgap temperature sensors have **MEDIUM** technical readiness for near-lid applications and **LOW** for near-core deployment.

5.4.1   Fundamentals of Operation

A SCBG fiber-optic sensor measures temperature based on the temperature dependence of the semiconductor crystal bandgap. A semiconductor crystal is transparent to wavelengths above the bandgap and is opaque for wavelengths below the bandgap. Temperature is determined by measuring the wavelength shift of the bandgap transition region. The bandgap crystal is bonded to the end of a fiber. Broadband light is injected into the fiber, and then transits the crystal. A mirror coating on the crystal reflects the light back into the optical fiber, to an optical spectrum analyzer that measures the reflected return to determine the bandgap transition wavelength.

A SCBG fiber-optic sensor, shown in Figure 5.3, was demonstrated using a GaAs semiconductor (Roland et al. 2003). At around room temperature, GaAs is transparent above roughly 900 nm. The bandgap region cutoff slope is fairly sharp, and is extremely temperature sensitive, shifting at a rate of approximately 0.4 nm/Kelvin. This sensor configuration has a number of very promising characteristics. The bandgap of GaAs is relatively insensitive to pressure and physical strain, and measurements between −50°C and 300°C have demonstrated low long-term drift. It is unclear whether the change in index of the fiber and the crystal, as a function of temperature, will affect sensor performance.
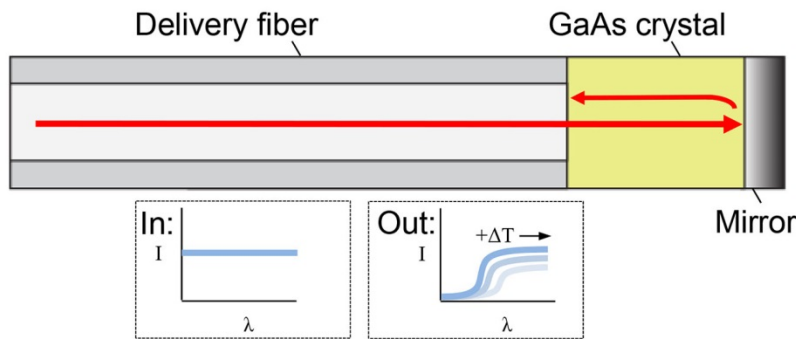
Figure 5.3. A GaAs Bandgap Fiber-Optic Temperature Sensor

The temperature-dependent bandgap (E_g) can be empirically estimated by the Varshni equation, given by

$$E_g = E_g(0) - \frac{aT^2}{T + \beta} \tag{5.1}$$

where $E_g(0)$ is the energy gap at zero Kelvin, a is an empirical constant, and β is approximately the Debye temperature at zero Kelvin. One source reports GaAs values of $E_g(0) = 1.522$ eV, $a = 5.8 \times 10^{-4}$ eV/K, and $\beta = 300$ K (Panish and Casey 1969), which are roughly consistent with other values found in the literature. There have been a few alternative models advocated by different authors, but the Varshni equation is widely used to estimate bandgap shift. Using this relationship, bandgap shift can be predicted at typical AdvSMR coolant temperatures (NERAC 2002). As Figure 5.4 shows, semiconductor materials can be selected based on the bandgap wavelength and the temperature sensitivity (slope) requirements. Other key bandgap materials properties are listed in Table 5.1. Sensor designs that use GaAs provide

better temperature resolution compared to Si, because with GaAs the bandgap cutoff slope is seven times sharper than Si (Essick and Mather 1993).

Figure 5.4 shows that the temperature-dependent bandgap shift continues beyond 1000°C; however, the material absorption begins to increase (Spitzer and Whelan 1959). In GaAs, the absorption increases by an order of magnitude between 50°C and 632°C (Johnson and Tiedje 1995). Therefore, both bandgap shift and absorption, as a function of temperature, are important SCBG sensor design parameters. Additionally, mismatched fiber-optic and bandgap crystal CTEs may lead to debonding of the sensor.
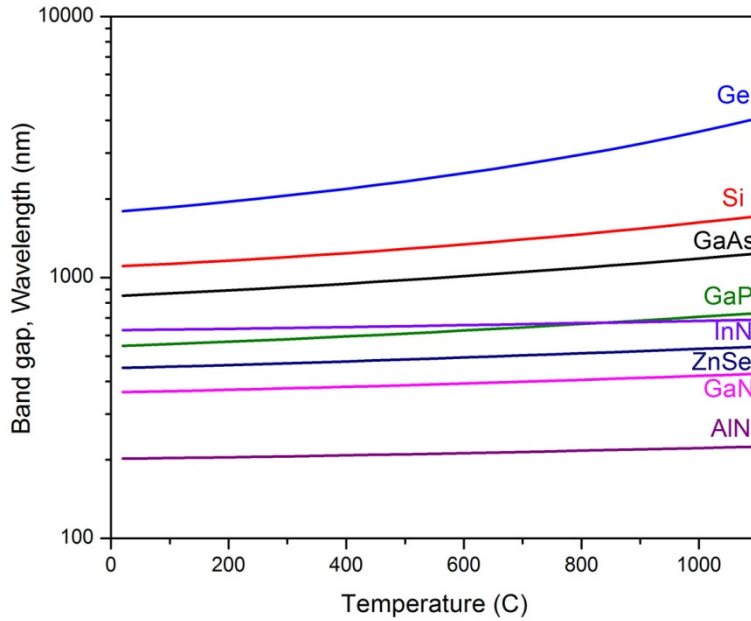
Figure 5.4.   Temperature Dependence of Bandgaps for Common Semiconductors Using Eq. (5.1) and Values from the Literature (Panish and Casey 1969; Passler 1999)

Table 5.1. Properties of Selected Bandgap Materials

Candidate	Bandgap (eV)	Melting Temp. (°C)	Density (g/cm³)	n	Transparency Window (µm)	CTE (ppm)	Solubility (other solvents)	References
Ge		938	5.3234		2–17	5.1–5.8	Dilute acid, alkali	Haynes (2011)
Si	1.12	1414 1410	2.3296	3.42	1.2–10, 50–100	2.55	Acid, strong alkali	Haynes (2011); Wakaki (2012)
GaAs	1.34	1238 1240	5.3176	3.45	1–15	5.39		Haynes (2011); Wakaki (2012)
GaP	1.42	1457 1467	4.138	3.66	0.6–11	5.3@300K, 5.6@850K		Haynes (2011); Wakaki (2012)
InP	2.27	1062	4.79	3.45		2.5-5.5		Wakaki (2012)
InN		1100	6.88					Haynes (2011)
ZnSe		>1100	5.65		0.5–20	7.1 @ 273K	Dilute acid	Haynes (2011)
GaN	3.39	>2500 2500	6.1	2–2.2	<17 µm	2.5–5.9		Haynes (2011); Wakaki (2012)
AlN		3000	3.255		<14	0.3–6.5		Haynes (2011)

5.4.2   Promising Research and Development

Overall, there is a noted lack of recent publications regarding semiconductor bandgap sensors. A few publications in recent years focused on measuring the refractive index of germanium as a function of temperature, rather than bandgap (Li and Li 2010; Liu et al. 2011). Germanium, however, becomes opaque at higher temperatures.

5.4.3   COTS Summary, Gaps Analysis, Ranking, and Proposed Future Research Path

COTS Semiconductor Bandgap Sensor Summary

A number of company supply COTS SCBG optical fiber sensors, including LumaSense Technologies, Optocon, OpSens, Neoptix, Micronor, and others. SCBG optical-fiber sensors are commonly used in the electrical power industry to monitor the temperature of current transformers. The optical fiber interconnect provides noise immunity and electrical isolation during transformer monitoring. Neoptix sells GaAs-based temperature sensors that come in a wide variety of coatings for different applications to 300°C. Optocon offers a Teflon-coated GaAs bandgap sensor for the nuclear power market, but specific data on radiation-resistance are not provided.

COTS SCBG optical spectrum analyzer instrumentation can be operated up to 75°C, which meets the containment vessel headspace deployment requirements. The SCBG fiber sensor maximum working temperature specification, ≤300°C, primarily reflects the temperature limitations of the optical-fiber materials. Fundamentally, the bandgap crystals are stable beyond 1000°C (except Ge). The mirror coatings and the fiber-to-bandgap crystal bond may further limit the maximum temperature. Fiber bandgap sensors may be feasible in the headspace area of liquid coolant reactor designs, but unlikely in higher temperature gas coolant reactor designs. The temperature requirements for near-core deployment

are well beyond the working temperature limits of SCBG fiber optic sensors. No vendor specifications are provided for radiation-resistance.

Aside from radiation-induced darkening of the optical fibers, the GaAs crystals (and other bandgap materials) may be affected by neutron and gamma exposure. Irradiation with neutrons has been observed to cause swelling of the GaAs crystal lattice, which can cause small bandgap shifts (Fleming et al. 2010). Many COTS optical fibers are available that could provide reasonably long service life (with respect to radiation damage), when deployed near the reactor lid. A smaller set of COTS optical fibers may be feasible for near-core deployment. Limited radiation-resistance data are available for bandgap crystals; therefore, judgments for near-core and near-lid service life cannot be provided.

Gaps Analysis

Technology gaps for implementation of COTS SCBG sensors are similar to those faced by other fiber-based approaches.

- The temperature limits imposed by the optical-fiber coatings, sheathing, and cabling materials are significantly below most expected in-vessel AdvSMR conditions.

- The temperature limits of bandgap crystal mirror coatings are uncertain.

- Bandgap crystal-to-fiber debonding may occur at high temperature or from mismatched CTEs.

- The impact of index changes as a function of temperature is uncertain.

- Optical fibers and materials have well-known radiation damage pathways.

- Bandgap crystals are subject to radiation damage.

- Actual performance and benefits of COTS SCBG fiber sensors must be determined.

- Service-lifetime and performance of COTS CBG fiber sensors and instrumentation under AdvSMR deployment conditions must be determined.

Technical Readiness Ranking

We consider photonic bandgap temperature sensors to have **MEDIUM** technical readiness for near-lid AdvSMR applications because they have shown some promise only for headspace temperature monitoring in pool-type reactor designs. The semiconductor crystals, optical coatings, and optical-fiber components have temperature and radiation exposure limits that currently make near-core deployment unfeasible. Based on these reasons, the technical readiness for near-core deployment is **LOW**.

Proposed Future Research

- The suggested research needed to resolve COTS optical-fiber technical gaps is discussed in Section 3.3.6.

- Bandgap crystal optical coatings and fiber bond performance must be studied under AdvSMR temperature and radiation exposure conditions.

- Study performance and benefits of COTS SCBG fiber sensors.

- Determine service-lifetime and performance of COTS SCBG fiber sensors and instrumentation under AdvSMR deployment conditions.

5.5   Backscattering Optical Time Domain Reflectometers

Backscattering optical time domain reflectometers (OTDR) provide distributed temperature sensing down a length of optical fiber. Pulsed laser light is launched into the fiber and then scatters back to an optical detector at the proximal end of the optical fiber. The amplitude and time delay of the backscattered laser light is then used to determine the temperature and measurement location. A backscattering event may be caused by a reflective index (RI) change, a physical change in the mode field diameter, or by Rayleigh or Raman scattering. Many vendors provide these distributed sensors to measure either strain or temperature. The technical readiness for COTS backscattering OTDR temperature sensors for near-lid application is **HIGH**, because of the commercial availability and the relatively high-temperature specifications. The technical readiness for in-core applications is considered **LOW**, because of the temperature limitations of fiber-optic components.

COTS backscattering OTDR products are generally rated for temperature measurements up to 300°C; however, products are offered for measurements to 1000°C. The optical fiber jacketing and coating materials limit the maximum working temperature. Spatial measurement resolution backscattering OTDR sensors are dependent on the laser pulse width used and can be on the order of millimeters. Temperature resolution is typically 1°C to 2°C. Backscattering OTDR sensors have been used for short durations to measure temperature in water-cooled test reactors.

5.5.1   Fundamentals of Operation

Backscattering OTDRs are fiber-based devices that are often implemented in distributed sensor systems, where multiple points on a single fiber can be continuously monitored. These sensors are frequently used for detecting faults or anomalies in industrial processes, where quickly locating the fault location is vital (Grattan and Sun 2000). Spatial resolution can be less than a meter in a 1-km-long fiber.

The measurement mode of OTDR requires a pulsed light source. After a pulse is launched through a sensing fiber, random scattering centers scatter laser light back to a detector, as shown in Figure 5.5. A continuous backscattering time-delay curve is collected as the pulse travels the length of the fiber. The most significantly delayed backscatter is that from the fiber's distal end. The shape of this backscatter signal versus the time delay from pulse launch is used to calculate the magnitude of temperature-related perturbations along the entire length of the fiber.
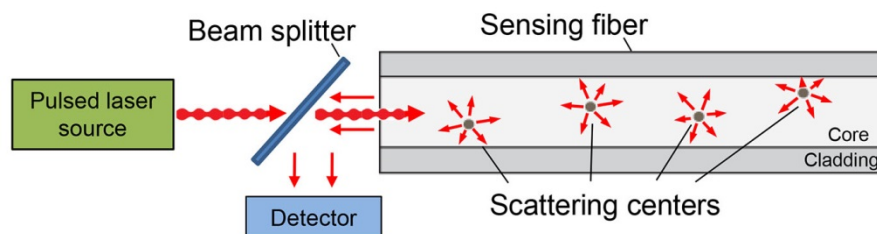
Figure 5.5. Time-Domain Scattering Reflectometer

There are two major types of backscattering OTDRs. The first is a Raleigh backscattering reflectometer, which tends to work poorly in traditional silica fibers. Rayleigh-scattering reflectometers measure in the frequency-domain rather than in the time-domain (Gifford et al. 2007). Various doped-silica and liquid-core fibers have been employed to improve the performance, but spatial resolution tends to be limited to a few meters. By far the more common type is the Raman backscattering reflectometer, which measures spontaneous Raman scattering (SRS). SRS is useful because the anti-Stokes Raman band is temperature-sensitive, and can be referenced against the comparatively insensitive Stokes Raman band (Williams et al. 2000). A third type is a Brillouin backscattering reflectometer (Rogers 1999). Brillouin scattering occurs through temporary phonon-induced RI variations, likely because of thermally excited acoustic waves. Brillouin backscattering is more intense than Raman backscattering. However, it is difficult to deconvolve the effects of temperature and physical strain on the fiber. Ongoing R&D may provide breakthroughs in the future.

5.5.2 Promising Research and Development

Recent research studies have investigated the designs that use both Raman backscattering and FBG sensors to take advantage of the strengths of both technologies (Toccafondo et al. 2012). Other research has focused on the function of Raman-based OTDRs in nuclear reactor-type environments (Jensen et al. 1998). That work has focused on environments in pressurized water reactors at temperatures $\geq 300°C$. A "thermal bleaching" phenomenon was observed in this study that demonstrated radiation-induced darkening in silica fiber could be reversed at high temperature.

5.5.3 COTS Summary, Gaps Analysis, Ranking, and Proposed Future Research Path

COTS Backscattering OTDR Summary

There are a large number of commercial suppliers of backscattering reflectometers. These instruments are mostly SRS-based distributed temperature sensing (DTS) systems. Vendors include AP Sensing, SensorTran, Brugg, Halliburton, Schlumberger, and others. Common target industries for these systems include downhole monitoring, fire detection systems, hydrological measurements, and refinery vessel monitoring. These systems can measure continuously over a fiber length in excess of 15 km. COTS Rayleigh-scattering-based DTS systems are offered by only one commercial supplier.

Commercial DTS products are often used to insert into oil and gas refinery processes where temperatures often exceed 200°C. Some COTS instruments have maxium temperature specifications up to 300°C. The optical fiber jacketing and coating materials primarily limit the maximum working temperature. High-temperature deployments have experienced optical-fiber failure because of temperature-induced stress and chemical diffusion into the fibers. In particular, in hydrogen-rich environments, H_2 diffusion into silica is a big problem, which accelerates at higher temperature and creates high optical attenuation. Barrier coatings may be feasible to minimize H_2 ingress.

COTS SRS sensor instrumentation can be operated up to 45°C, which meets the containment vessel headspace deployment requirements. The SRS optical- fiber maximum working temperature specification, $\leq 300°C$, reflects primarily the temperature limitations of the optical-fiber materials. Gold and aluminum optical-fiber coatings are offered as an option to protect the fiber from high-temperature exposure. COTS gold-coated SRS DTS sensors are specified to 700°C operation temperature. SRS DTS

sensors have been used at 1000°C for very brief periods. Fiber-based SRS DTS sensors may be feasible in the headspace area of both liquid-cooled and higher-temperature gas-cooled reactor designs. The temperature requirements for near-core deployment are well beyond the working temperature limits of optical fiber. No vendor specifications are provided for radiation-resistance.

Gaps Analysis

Technology gaps for COTS SRS temperature sensors include:

- The temperature limits imposed by the optical-fiber coatings, sheathing, and cabling materials are significantly below most expected in-vessel AdvSMR conditions.

- The impact of index changes as a function of temperature is uncertain.

- Optical fibers and materials have well-known radiation damage pathways.

- Radioluminescence in the optical fiber may produce optical background noise.

- Actual performance and benefits of COTS SRS temperature sensors must be determined.

- Service lifetime and performance of COTS SRS temperature sensors and instrumentation under AdvSMR deployment conditions must be determined.

Technical Readiness Ranking

The technical readiness for COTS SRS sensors is considered to be **HIGH** for near-lid applications. SRS sensors have been developed for high temperature, but high radiation exposure may limit service-lifetime. The upper working temperature products' specifications do not meet near-core requirements and higher radiation flux will likely further reduce service lifetime. For near-core applications, COTS SRS sensor technical readiness is **LOW**.

Proposed Future Research

- Evaluate COTS backscattering OTDR instrument, and determine and implement modification needed for AdvSMR application.

- Determine installation requirements, develop implementation plan, modify COTS instruments, and develop required installation hardware.

- Evaluate and demonstrate backscattering OTDR under laboratory conditions, simulated AdvSMR conditions, and in a test reactor, to determine performance, estimated service lifetime, and radioluminescence background. Collaborate with vendors to enhance COTS product performance.

5.6 Fabry-Pérot Sensors

Fabry-Pérot devices (interferometer or etalon) use wavelength-dependent optical interference to produce measurable fringes, the positions of which are dependent on temperature, pressure, and inherent material optical properties. Fabry-Pérot devices have been developed extensively for R&D and commercial applications, but only a few are available as COTS temperature sensors.

At least one COTS product exists that is suitable for the temperature levels within AdvSMR coolants. The upper temperature in the best case was found to be 1000°C for a sapphire Fabry-Pérot, although it used fiber connectors that were limited to 85°C. However, the radiation-resistance capabilities of these sensors are uncharacterized and the material selection for the sensors and their housing/connectors/seals will likely need to be customized to withstand the radiological and chemical environments within AdvSMRs. As a result, COTS Fabry-Pérot temperature sensors are considered **HIGH** technical readiness for near-lid applications and **LOW** for near-core deployment.

5.6.1   Fundamentals of Operation

The Fabry-Pérot device (interferometer or etalon) is a configuration defined by two parallel and highly reflective interfaces that form an optical cavity. Light passing through the pair of interfaces reflects multiple times, and therefore exhibits interference fringing. When the cavity spacing is fixed the Fabry-Pérot device is often referred to as an etalon (Pedrotti et al. 2007).

Finesse, based on the number of resolvable spectral lines, is the quantity often used to describe the performance of a Fabry-Pérot cavity. Because fringe width is a function of the coefficient of finesse, the finesse itself is also a strong function of reflectivity (Bass et al. 1995). A Fabry-Pérot interferometer with strongly reflective interfaces and a low-absorptive cavity material will have a higher finesse, which means that the fringe contrast will be higher (Pedrotti et al. 2007). High contrast is strongly desirable for applications that demand high-temperature resolution; however, this comes at the expense of overall signal strength.

The Fabry-Pérot interferometer was first discovered and described in the early 20th century. For over 20 years, Fabry-Pérot interferometers have been used in academic and commercial research to develop sensors for temperature, pressure, strain, and other parameters. In that time, fiber optics became a prominent platform for their implementation. A simplified representation of a fiber-optic interferometer is shown in Figure 5.6. Reflective structures can be fabricated into optical fibers along their length and can also be built onto a fiber tip. The integrated nature of these approaches makes it convenient to launch light into the interferometer and to collect reflected or transmitted signals.
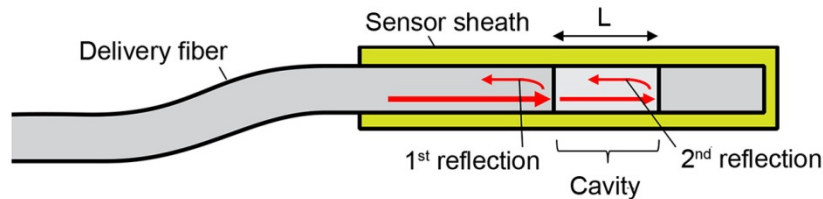
Figure 5.6. Schematic of a Fabry-Pérot Interferometer Sensor Probe

Temperature sensing is accomplished by measuring shifts in interference fringes, which themselves are caused by shifts in the relative phase ($\Delta\delta$) of interfering reflections in the fiber, modeled by:

$$\Delta\delta = \frac{4\pi\Delta(nL)}{\lambda},$$ (5.2)

where n is the refractive index (RI) of the fiber, L is the sensor cavity length, and λ is the light source wavelength. Temperature has a two-fold contribution to phase shift, as both n and L are temperature dependent (Tsai and Lin 2001). The relative magnitudes of the thermal expansion coefficient and the thermo-optic coefficient of the fiber material also strongly affect the interferometer's temperature sensitivity.

Fabry-Pérot sensors have some sensitivity to both temperature and pressure. As with most optical technologies, it is difficult, if not impossible, to completely separate out these two effects. Therefore, using Fabry-Pérot sensors in extreme environments where large changes in both temperature and pressure occur simultaneously will benefit from parallel or integrated sensor systems that can provide temperature correction (Davidson Instruments 2007).

Fabry-Pérot interferometers can be built to operate at any nominal optical wavelength, but using 1550-nm telecom wavelengths are particularly attractive because single-mode (Corning) SMF-28 used as the guiding fiber is readily available at low cost. The length of the Fabry-Pérot cavity and surface reflectivity can be tailored to the probe wavelength and to optimize the temperature resolution.

5.6.2   Promising Research and Development

Fabry-Pérot cavities can be manufactured from virtually any optical material and have been reported in the literature. This is in contrast with the relative lack of diversity in the marketplace. Fiber-based Fabry-Pérot sensors can suffer degradation by high temperature and radiation (darkening) exposure. Recent work involving sapphire fibers and waveguides has shown great promise in minimizing these issues, but to date, only sapphire light pipes are available as COTS items. Sapphire fibers can be doped with hydrogen ions to create lower-index cladding regions (Spratt et al. 2011). The fibers can then be heated up to 800°C without degrading the index contrast. For the purpose of Fabry-Pérot sensing, gratings could be inscribed into such a fiber to create reflective structures (Mihailov et al. 2010).

5.6.3   COTS Summary, Gaps Analysis, Ranking, and Proposed Future Research Path

COTS Fabry-Pérot Temperature Sensor Summary

There are a few COTS vendors that offer Fabry-Pérot temperature sensors, including Davidson Instruments and Oxsensis. These are generally designed as direct replacements for conventional thermocouple sensing probes. A typical probe (Davidson Instruments, SP1200) is designed to measure temperatures to 538°C, with accuracy of ±0.5°C full-scale range. The sensing probe is made with an uncoated fiber and Fabry-Pérot sensor mounted in a protective stainless steel housing with a male pipe thread or flange connection. The probe can be manufactured up to 12 m in length and as small as 1.27 mm in diameter. A fiber cable attaches to the fiber probe and is available in a variety of ruggedized cabling options. The maximum working temperature for the fiber cable is 288°C. The temperature probe can also be designed with multiple Fabry-Pérot sensors to provide multipoint sensing in a single probe package. The proximal end of the fiber cable is connected to a signal conditioning electronics module located an arbitrary distance from the temperature probe. Probe signals are processed into temperature output data.

Oxsensis offers a sapphire-based sensor system for measuring pressure up to 1000°C, although it is advertised as an R&D device. The mounting flange is rated to 750°C and the fiber-optic cable connector is rated only to 85°C. It is reasonable to expect that the technology could be adapted to measure pressure as well, because it is based on a Fabry-Pérot sensor.

COTS fiber-based Fabry-Pérot signal analyzer instrumentation can be operated up to 45°C, but no vendor specifications are provided for radiation-resistance. Temperatures in the headspace are between 200°C and 300°C for liquid coolant and 450°C for gas coolant AdvSMR concepts. The COTS Fabry-Pérot probe configurations appear feasible for near-lid deployment applications for both liquid- and gas-cooled reactor designs. Core outlet coolant temperatures range from 550°C to 750°C. Probe construction materials and fiber-optic cabling components have temperature limits that currently make near-core deployment unfeasible. None of the available probes have radiation-resistance specifications. It is reasonable to expect that radiation-induced photodarkening could be a major challenge for these sensors; however, hollow-core PCF and FORC optical fibers may be very feasible for the AdvSMR application.

Gaps Analysis

Technology gaps for implementation of fiber-based Fabry-Pérot sensors are similar to those faced by other fiber-based approaches.

- The temperature limits imposed by the optical-fiber coatings, sheathing, and cabling materials are significantly below most expected in-vessel AdvSMR conditions.

- The temperature limits of Fabry-Pérot cavity mirror coatings are uncertain.

- The temperature limits of the Fabry-Pérot cavity-to-fiber bond are uncertain.

- Noise from pressure and vibration in a reactor may affect Fabry-Pérot sensor performance.

- The impact of index changes as a function of temperature is uncertain.

- Coolants and chemical compounds may damage Fabry-Pérot sensors.

- Optical fibers and materials have well-known radiation-damage pathways.

- The Fabry-Pérot cavity mirrors may be subject to radiation damage.

- Actual performance and benefits of fiber Fabry-Pérot sensors must be determined.

- Service-lifetime and performance of COTS fiber Fabry-Pérot sensors and instrumentation under AdvSMR deployment conditions must be determined.

Technical Readiness Ranking

We rank the technical readiness of Fabry-Pérot temperature sensors as **HIGH** for near-lid applications, because they may be suitable for AdvSMR temperatures. Because Fabry-Pérot sensors are not characterized for the most extreme AdvSMR conditions and the question about high-temperature optical-fiber materials has not been answered, we must consider the technical readiness for near-core applications to be **LOW**.

Proposed Future Research

This technology is interesting, and further work could be warranted. It is capable of delivering more-than-adequate temperature resolution, although radiation damage to optical components over time would result in drift. Fabry-Pérot temperature sensors could be used either in gas headspaces or in reactor coolants and would require a fiber-optic access point to the reactor vessel. Coolant transparency would not be a requirement for these sensors. One of the challenges for implementation would involve decoupling temperature and pressure effects, as well as vibration, although a multiparameter Fabry-Pérot sensor package could be envisioned that would measure all of these effects at once. It is very possible that this technology could be overshadowed in utility by backscatter time domain reflectometers, which offer distributed sensing instead of point sensing (previous section).

The paths forward for Fabry-Pérot sensor implementation would include characterization of the fiber and coating material sets available with COTS systems. Radiation-induced luminescence in the fibers could be challenging in terms of reducing the signal-to-noise ratio for Fabry-Pérot sensors. It is therefore necessary to determine how extended radiation exposure affects the mechanical stability of Fabry-Pérot flexible membranes for pressure sensors. Characterizing the fundamental temperature or radiation dose limits for these Fabry-Pérot sensors is a priority in the near future to determine the extent of their feasibility for AdvSMR applications. All of these issues must be explored as first steps, and are common to many of the optical sensors considered for temperature sensing.

5.7   Birefringence-Based Sensors

Birefringence temperature sensors could be implemented in most AdvSMR concepts, regardless of coolant transparency. This sensor is available as a COTS fiber-optic point sensor, but distributed sensors could be developed with additional RD&D. Prior research suggests that birefringence is stable under radiation exposure, making drift-free temperature measurements feasible.

Birefringent optical materials have a refractive index that depends on the polarization and propagation of direct light. Light with orthogonal polarizations experience different path lengths as they propagate through birefringent material. Interferometry is typically used to track the differential path length experienced by the two polarizations. Sensors based on this configuration can measure temperature or strain. Birefringent optical components, called waveplates, can also be used to rotate the polarization angle of transmitted beam. The extent of rotation is dependent on the temperature birefringent component. However, these techniques are typically limited to change measurement and require other methods to measure absolute temperature. Spectroscopic information from the separation of resonance peaks can provide an absolute calibration.

Only a few COTS birefringent temperature sensors are available. The technical readiness of these products for all AdvSMR applications is **LOW** because deployment may be unfeasible. Further RD&D is required to understand the limitations of COTS sensors under intense radiation and high-temperature exposure.

5.7.1   Fundamentals of Operation

Birefringence-based sensors measure changes in polarization/path length as a function of changes in a target parameter, such as strain or temperature. Birefringence materials exhibit different refractive

indices depending on the transmitted light polarization or propagation direction (Pedrotti et al. 2007). Applying anisotropic strain on the optical material can induce birefringence; however, many materials are naturally birefringent. Optical fibers are also available with birefringent properties.

Path length difference, induced by a birefringent optical component, can be measured using an optical interferometer. Path length differences produce interference fringes that have strong strain and temperature dependence. Sagnac fiber loops can be assembled using a highly birefringent fiber (Sun et al. 2007) as shown in Figure 5.7. Linearly polarized light counter-propagates through the loop, which is exposed to temperature changes. When the counter-propagating light is recombined, the polarization of each propagation beam is differentially retarded as a function of temperature. Fringes or intensity oscillations can be monitored to estimate the temperature change. This method monitors temperature change, but generally does not provide absolute temperature. Absolute temperature can be determined by analyzing the spectral separation between consecutive resonances (De la Rosa et al. 1997). No COTS sensors are available that measure absolute temperature. Another sensor configuration bonds a birefringent crystal at the distal end of an optical fiber. A mirror coating is deposited on one facet of the crystal. The birefringence-induced path-length difference a between rotated and reference beam is used to estimate the temperature.
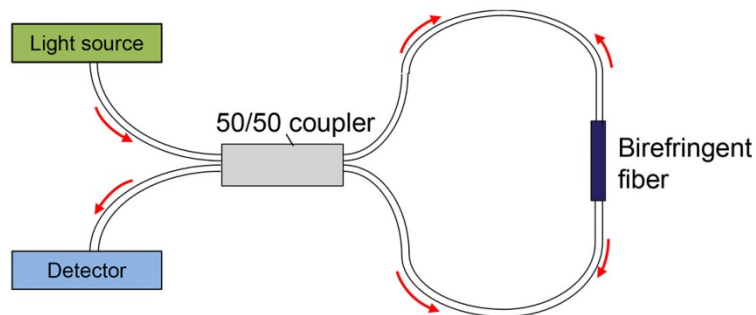
Figure 5.7. Schematic of a Sagnac Loop Interferometer

5.7.2   Promising Research and Development

Brillouin-induced birefringence has recently been demonstrated as an effective and sensitive method for creating distributed fiber-based temperature sensors (Dong et al. 2009). Polarization-maintaining fibers are commercially available, based on photonic crystal designs. Birefringence is maintained by a photonic crystal pore structure. Birefringent sensors, using radiation-resistant PCFs, may be feasible for future AdvSMR temperature monitoring (Rahman et al. 2011).

5.7.3   COTS Summary, Gaps Analysis, Ranking, and Proposed Future Research Path

COTS Birefringence Sensing Summary

Only one commercial source (OpSens) for birefringence-based temperature sensors was identified. OpSens uses the birefringent crystal sensor and offers temperature measurement to 350°C at 0.05°C

resolution and ± 0.15°C resolution. The temperature measurement dynamic range is selected based on birefringent crystal selection. The optical-fiber coatings and compounds currently limit the maximum working temperature. Barium borate (BBO) is a strongly birefringent material that has a very high melting temperature of 1060°C and is transparent from 300 nm to 2.3 µm. However, the birefringence at high temperature is not well characterized and it has a large neutron cross-section.

One research study has shown that birefringence in fibers is not significantly affected by gamma irradiation (Marrone et al. 1984). Some in-vessel temperature monitoring may be feasible, but most COTS optical birefringent components have not been studied under high-radiation exposure. A systematic investigation of birefringent materials, under realistic AdvSMR conditions, is required to determine the feasibility of this approach.

Gaps Analysis

- Existing low-temperature limitation of optical-fiber coatings, sheathings, and cabling materials must be resolved.

- Radioluminescence in the optical fiber may produce optical background noise.

- High-temperature and high-radiation exposure studies are required to evaluate birefringent PCFs.

- The impact of radiation exposure to birefringent crystals is unknown.

- The temperature limits of the birefringent crystal-to-fiber bond are uncertain.

Technical Readiness Ranking

Birefringence-based sensing is extremely interesting for temperature sensing, but only one vendor supplies COTS sensors. Significant knowledge gaps remain regarding radiation-induced damage in the birefringent materials. For these reasons, we consider its technical readiness for all AdvSMR applications to be **LOW** and do not suggest future RD&D.

5.8   Fluorescence Thermometry/Phosphor Thermometry

Fluorescence thermometry is a technique for estimating temperature based on the rate of fluorescence decay from an excited state to a lower state. When a very short pulse of light excites a fluorophore, the fluorescence intensity then falls off exponentially, the rate of which is dependent on temperature. Specifically, as temperature increases, the medium surrounding the fluorophore begins to more efficiently quench its fluorescence, and therefore the lifetime decreases. Fluorescence lifetime has been studied expansively for many years and the measurement of very short lifetimes (down to the low nanosecond range) is now a very mature technology. It does require, however, some very accurate electronic equipment and a very fast laser, which is suitable for neither high-temperature nor high-radiation environments.

This technology is unique in that it can be employed in either a free-space or fiber-based sensing configuration. In the free-space approach, a surface inside the nuclear reactor would be coated with a fluorescent film, which would be sensitive to the temperature of the surface and the coolant around it. The laser source, detector, and electronics would be in the containment area under heavy shielding. In the fiber-based approach, a fiber-optic cable would have a sensing layer at the tip that would have to be threaded into the measurement area. This latter sort of sensor is available commercially and can sustain

temperatures up to 950°C, although its radiation-resistance is unaddressed. There are no other commercial sources of these fluorescent films that we are aware of.

A great deal of information exists about this technology and its different permutations in the literature, but this body of work would require time and funding to characterize for AdvSMR conditions. Because of the relative lack of commercial sources and the number of unanswered questions regarding fluorescence thermometry in radiological environments, we consider the technical readiness of this approach to be **LOW** for all AdvSMR applications. It is also likely that the cost to set up an ultra-fast laser system to measure temperature would not be competitive with other options.

5.8.1   Fundamentals of Operation

There are two common ways of using fluorescence to measure temperature, based on the two most temperature-sensitive properties of fluorescence emitters—intensity and lifetime.

Fluorophores all have some intensity dependence on temperature, although this behavior varies in nature and magnitude from one molecule to another. Often, there is a trend of increasing fluorescence intensity with increasing temperature, which has a characteristic peak, followed by a drop off as temperature continues to rise (Haake 1961). Looking at the ratio of intensities of two fluorescent species undergoing equivalent changes in temperature will yield a characteristic trend line that can be used as a temperature metric. Alternatively, some fluorophores have a multi-peaked emission spectrum, with some peaks quenching faster than others. Examples of these types of compounds include europium-doped lanthanum sulfides (La_2O_2S:Eu, shown in Figure 5.8) and gadolinium sulfides (Gd_2O_2S:Eu), although La, Gd, and Eu all have a large neutron cross section (Alves and Wickersheim 1984). A polymer matrix with multiple fluorescent compounds can be applied to the end of a fiber to allow efficient excitation and collection of such signals.
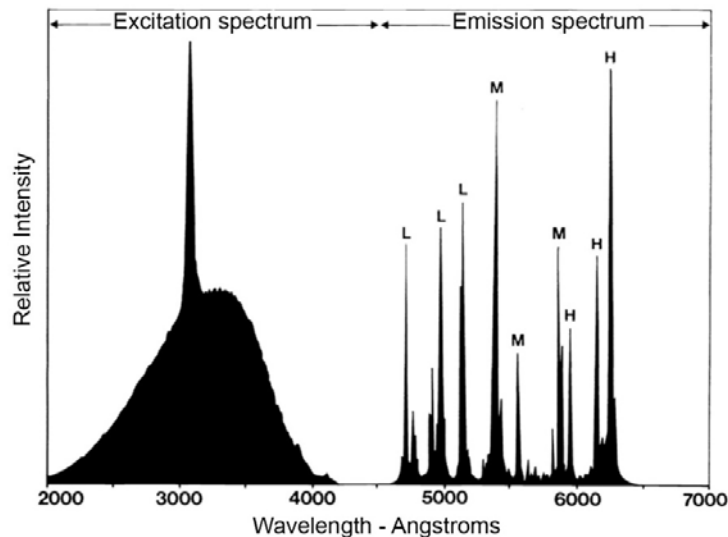
Figure 5.8.   Excitation and Emission Spectra for La_2O_2S: Eu, where "L," "M," and "H" Lines Show Strong Temperature Quenching Effects at "Low," "Medium," and "High" Temperature, Respectively (Alves and Wickersheim 1984)

The intensity ratio approach does have some limitations. The temperature dynamic range will be very different from one fluorophore to another, so selection of the correct emitter will be important. The magnitude of the dynamic ranges may be severely limiting as well and may require multiple parallel sensors with overlapping ranges to cover the entire parameter space demanded by AdvSMRs. Ultimately, all fluorophores will end up fully quenched if the temperature is high enough, and this fact may prove to be a terminal obstacle against successful implementation of fluorescent temperature sensors in high-temperature gas and molten metal reactors. More research will be required in order to fully address those doubts.

Illumination of many materials results in the production of fluorescence, which decays in intensity with a characteristic lifetime, designated by τ. In Figure 5.9, fluorescence decay curves are modeled for a single-exponential emitter using different lifetime values. The expression that relates the single-exponential decay of fluorescence intensity ($I(t)$) from its initial value (I_0) over time (t) is (Lakowicz 2006):

$$I(t) = I_0 \exp(- {t}/{\tau}) . \tag{5.3}$$

Therefore, the lifetime is defined as the time required for the fluorescence intensity to drop to its 1/e value.

For phosphors, fluorescence decay lifetime is a function of temperature, as a result of quenched phosphorescence. By placing one of these materials in thermal contact with an object, the temperature of the object can be determined by a measurement of the fluorescence lifetime. As illustrated in Figure 5.9, as the temperature increases, the fluorescence lifetime decreases.
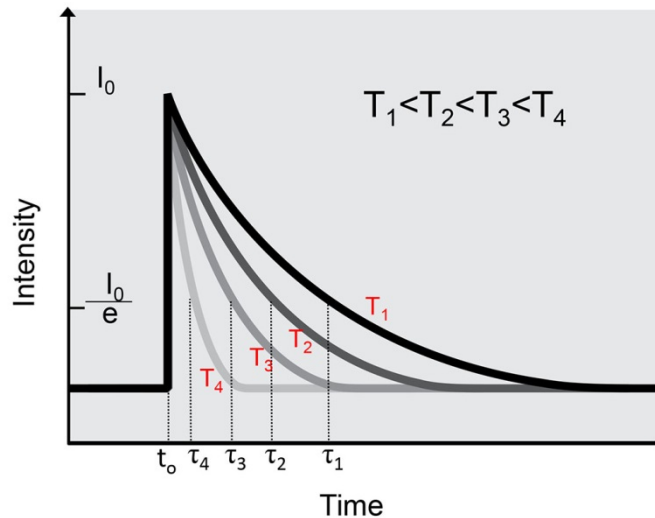
Figure 5.9. Illustration of a Single Fluorescence Decay Curve Modeled with Different Lifetimes Caused by Changing Temperature

In application, the temperature probe can be a point sensor consisting of a ceramic plate or coating the surface of the object; and using a scanning illumination over the coated surface, one can produce thermal maps of the surface. In a reactor vessel, such a configuration might appear as in Figure 5.10(a), where a window in the vessel wall permits free-space beam guiding to the coated sensing surface.

The thermal mapping is currently limited to an open path light propagation. The point source may be open path or fiber-optic based by mating a fiber optic to a phosphor plate or by doping the fiber to produce a phosphor zone within the fiber optic itself. Additionally, a quasi-distributed optical fiber temperature sensor system can be constructed by providing multiple fluorescence phosphor zones within a single optical fiber such as the configuration shown in Figure 5.10(b) (Sun et al. 1998).
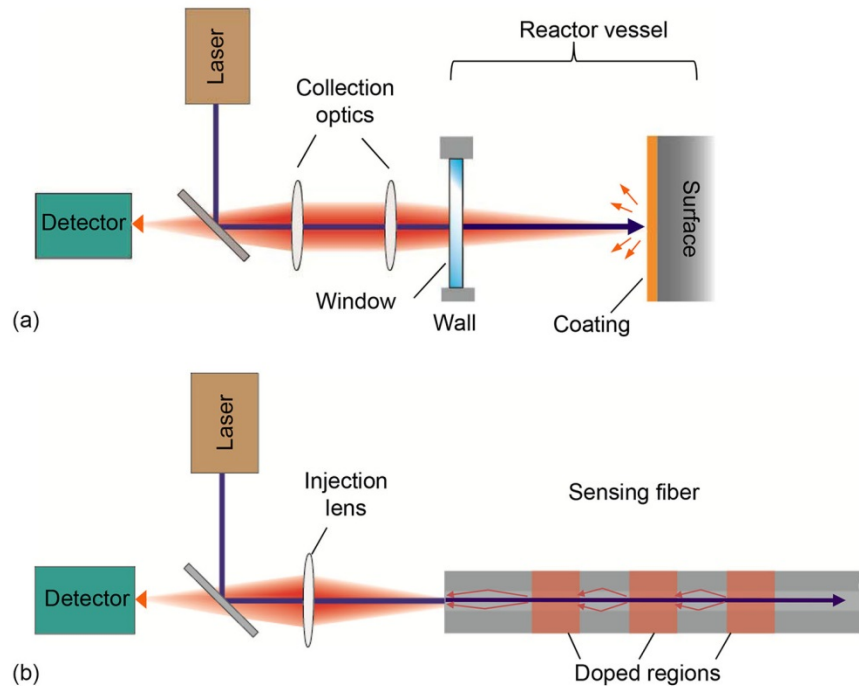
Figure 5.10.   Free-Space Point Sensor Configuration (a) and Doped-Fiber Distributed Sensing Configuration (b) for Fluorescence Lifetime Temperature Sensing

5.8.2   COTS Summary, Gaps Analysis, Ranking, and Proposed Future Research Path

COTS Fluorescence Thermometry Summary

There are not very many commercial suppliers of ready-to-go fluorescence thermometry systems. This tool exists primarily, and abundantly, in the academic realm, from which innumerable records can be found in the literature.

Coatings are offered up to 1600°C (Hollerman 2010), yttrium aluminum oxide (YAG) and Zirconia-based coatings have been developed for harsh environments such as combustion chambers. The

responsive temperature range for a single material is limited to typically a few hundreds°C; however, coating can be developed with multiple dopants to provide wider range temperature response.

MicroMaterials Inc. sells a probe system for measuring temperature between 10°C and 950°C. The probes are customized to target-specific temperature ranges using a proprietary phosphor coating and measuring the fluorescence lifetime change with temperature. The highest temperature probe is capable of withstanding 1000°C for prolonged periods of time and uses a YAG fiber coated with alumina. Beyond 1000°C the differential coefficient of thermal expansion (CTE) between the phosphor and the YAG fiber create calibration issues.

Osensa is another company that sells lifetime-based fiber-optic sensors. They use a proprietary fiber tip coating that responds to temperature with accuracies as great as 0.05°C. The company literature claims that the sensors can be customized to measure temperatures as high as 1000°C, but none of their standard off-the-shelf products are rated beyond 250°C.

Most other fiber-optic-based systems are limited to 330°C with a calibrated accuracy of 0.5°C. These temperature ceilings are typically defined by structural, rather than optical, components of the system, including fiber sheaths/jackets, O-rings, and various plastic parts.

These sensors are fiber-based, and require penetration of an optical fiber into AdvSMR vessels. Their radiation-resistance issues are the same as those described for other fiber-based optical systems.

The phosphor system produced by MicroMaterials is not characterized for performance under high radiation flux; however, the ceramic and YAG parts of the probe should be extremely rugged. The performance of the phosphor layer under gamma or neutron bombardment, however, cannot be predicted without supporting data.

Gaps Analysis

The primary technology gaps consist of lack of information about the performance limitations of fluorescence thermometry techniques. Because no high-radiation or high-temperature data exists commercially or in the literature, characterization for AdvSMR conditions would all have to be done prior to implementation. Careful selection and/or engineering of the fluorescence sensing layer would have to be done, and most likely there would be no COTS systems available for use without significant re-engineering and/or customization.

Technical Readiness Ranking

With these sensors, it is suspected that high temperature and radiological environments would create damage, drift, or quenching effects on fluorescent-sensing materials. Many unknowns remain; therefore, we consider the technical readiness of this approach to be **LOW** for all AdvSMR applications.

Proposed Future Research

Given the low technical readiness and relatively low potential benefits of this technology, no future research is suggested at this time.

5.9   References

Alves RV and KA Wickersheim. 1984. "Fluoroptic Thermometry: Temperature Sensing Using Optical Fibers." In *Proceedings of SPIE, Optical Fibers in Broadband Networks, Instrumentation, and Urban and Industrial Environments, Volume 0403*, pp. 146-152. May 16, 1983, Paris, France. The International Society for Optical Engineering, Bellingham, Washington.

Bass M, EW Van Stryland, DR Williams and WL Wolfe, Eds. 1995. *Handbook of Optics, Volume I, Fundamentals, Techniques, and Design*. McGraw-Hill, Inc., New York.

Busch M, W Ecke, I Latka, D Fischer, R Willsch and H Bartelt. 2009. "Inscription and Characterization of Bragg Gratings in Single-Crystal Sapphire Optical Fibres for High-Temperature Sensor Applications." *Measurement Science and Technology* 20:115301.

Davidson Instruments. 2007. *Model GP1200 Fiber Optic Gage Pressure Transducer.* Davidson Instruments. The Woodlands, Texas. Accessed June 12, 2013. Available at http://www.davidson-instruments.com/Product_Data_Sheets/GP1200.pdf. Product Data Sheet GP1200.

De la Rosa E, LA Zenteno, AN Starodumov and D Monzon. 1997. "All-Fiber Absolute Temperature Sensor Using an Unbalanced High-Birefringence Sagnac Loop." *Optics Letters* 22:481-483.

de Villiers GJ, J Treurnicht and RT Dobson. 2012. "In-core High Temperature Measurement Using Fiber-Bragg Gratings for Nuclear Reactors." *Applied Thermal Engineering* 38:143-150.

Dong Y, X Bao and L Chen. 2009. "Distributed Temperature Sensing Based on Birefringence Effect on Transient Brillouin Grating in a Polarization-Maintaining Photonic Crystal Fiber." *Optics Letters* 34:2590-2592.

Essick JM and RT Mather. 1993. "Characterization of a Bulk Semiconductor's Band Gap via a Near-Absorption Edge Optical Transmission Experiment." *American Journal of Physics* 61:646-649.

Fernandez AF, A Gusarov, B Brichard, M Decreton, F Berghmans, P Megret and A Delchambre. 2004. "Long-term Radiation Effects on Fibre Bragg Grating Temperature Sensors in a Low Flux Nuclear Reactor." *Measurement Science and Technology* 15:1506-1511.

Fleming RM, DV Lang, CH Seager, E Bielejec and GA Patrizi. 2010. "Continuous Distribution of Defect States and Band Gap Narrowing in Neutron Irradiated GaAs." *Journal of Applied Physics* 107:123710.

Gifford DK, ST Kreger, AK Sang, ME Froggatt, RG Duncan, MS Wolfe and BJ Soller. 2007. "Swept-Wavelength Interferometric Interrogation of Fiber Rayleigh Scatter for Distributed Sensing Applications." In *Proceedings of SPIE, Fiber Optic Sensors and Applications V, Volume 6770*, p. 67700F. September 10-12, 2007, Boston, Massachusetts. The International Society for Optical Engineering, Bellingham, Washington.

Girard S, J Kuhnhenn, A Gusarov, B Brichard, M Van Uffelen, Y Ouerdane, A Boukenter and C Marcandella. 2013. "Radiation Effects on Silica-Based Optical Fibers: Recent Advances and Future Challenges." *IEEE Transactions on Nuclear Science* PP(99):1-22.

Grattan KTV and T Sun. 2000. "Fiber Optic Sensor Technology: A Review." *Sensors and Actuators* 82:40-61.

Griscom DL. 1995. "Radiation Hardening of Pure-Silica-Core Optical Fibers by Ultra-High-Dose γ–ray Pre-irradiation." *Journal of Applied Physics* 77(10):5008-5013.

Haake CH. 1961. "The Significance of the Temperature Dependence of Fluorescence Intensity." *Journal of the Electrochemical Society* 108:78-82.

Haynes WM, Ed. 2011. *CRC Handbook of Chemistry and Physics*. CRC Press, Boca Raton, Florida.

Henschel H. 1994. "Radiation Hardness of Present Optical Fibres." In *Proceedings of SPIE, Optical Fibre Sensing and Systems in Nuclear Environments, Volume 2425*, pp. 21-31. September 17, 1994, Mol, Belgium. The International Society for Optical Engineering, Bellingham, Washington.

Hollerman A. 2010. "Measuring Temperature in Adverse Environments Using Phosphors." http://www.docstoc.com/docs/104800731/Measuring-Temperature-in-Adverse-Environments-Using-Phosphors.

Jensen FBH, E Takada, M Nakazawa, T Kakuta and S Yamamoto. 1998. "Consequences of Radiation Effects on Pure-Silica-Core Optical Fibers Used for Raman-Scattering-Based Temperature Measurements." *IEEE Transactions on Nuclear Science* 45:50-58.

Johnson SR and T Tiedje. 1995. "Temperature Dependence of the Urbach Edge in GaAs." *Journal of Applied Physics* 78:5609-5613.

Lakowicz JR. 2006. *Principles of Fluorescence Spectroscopy*. Springer, New York.

Li M and Y Li. 2010. "A Fiber Optic-film Temperature Sensor Taking Advantage of Thermal Optic Effect as well as Temperature-dependent Absorption of Semiconductor." In *Proceedings of SPIE, Advanced Sensor Systems and Applications IV, Volume 7853*, p. 78530W. October 18-20, 2010, Beijing, China. The International Society for Optical Engineering, Bellingham, Washington.

Liu P, M Li and Z Pan. 2011. "Effects of the Absorption Coefficient on the Refractive Index of Germanium in a Fiber Optic-Semiconductor Temperature Sensor." In *Proceedings of SPIE, 2011 International Conference on Optical Instruments and Technology: Optical Sensors and Applications, Volume 8199*, p. 81990Y. November 6-9, 2011, Beijing, China. The International Society for Optical Engineering, Bellingham, Washington. Paper #8199-25.

Marrone MJ, SC Rashleigh, EJ Friebele and KJ Long. 1984. "Radiation-Induced Effects in a Highly Birefringent Fibre." *Electronics Letters* 20(5):193-194.

Martín P, M León, A Ibarra and ER Hodgson. 2011. "Thermal Stability of Gamma Irradiation Induced Defects for Different Fused Silica." *Journal of Nuclear Materials* 417(1–3):818-821.

Mihailov SJ, D Grobnic and CW Smelser. 2010. "High-Temperature Multiparameter Sensor Based on Sapphire Fiber Bragg Gratings." *Optics Letters* 35:2810-2812.

NERAC. 2002. *A Technology Roadmap for Generation IV Nuclear Energy Systems - Ten Nations Preparing Today for Tomorrow's Energy Needs*. GIF-002-00, U.S. DOE Nuclear Energy Research Advisory Committee (NERAC) and the Generation IV International Forum (GIF), Washington, D.C. Available at http://www.osti.gov/energycitations/servlets/purl/859029-304XRr/.

Ng D and G Fralick. 2001. *Temperature Measurement of Beryllia Ceramic Surface in the Presence of Reflected Extraneous Radiation Using a Multiwavelength Pyrometer*. NASA/TM-2001-210891, National Aeronautics and Space Administration, Glenn Research Center, Hanover, Maryland.

Panish MB and HC Casey. 1969. "Temperature Dependence of the Energy Gap in GaAs and GaP." *Journal of Applied Physics* 40:163-167.

Passler R. 1999. "Parameter Sets Due to Fittings of the Temperature Dependencies of Fundamental Bandgaps in Semiconductors." *Physica Status Solidi (b)* 216(2):975-1007.

Pedrotti FL, LS Pedrotti and LM Pedrotti. 2007. *Introduction to Optics, Third Edition*. Pearson Prentice Hall, Upper Saddle River, New Jersey.

Primak W. 1958. "Fast-Neutron-Induced Changes in Quartz and Vitreous Silica." *Physical Review* 110(6):1240-1254.

Rahman BMA, M Uthman, N Kejalakshmy, A Agrawal and KTV Grattan. 2011. "Design of Bent Photonic Crystal Fiber Supporting a Single Polarization." *Applied Optics* 50:6505-6511.

Rogers A. 1999. "Distributed Optical-Fibre Sensing." *Measurement Science and Technology* 10:R75-R99.

Roland U, CP Renschen, D Lippik, F Stallmach and F Holzer. 2003. "A New Fiber Optical Thermometer and Its Applications for Process Control in Strong Electric, Magnetic, and Electromagnetic Fields." *Sensor Letters* 1:93-98.

Spitzer WG and JM Whelan. 1959. "Infrared Absorption and Electron Effective Mass in n-Type Gallium Arsenide." *Physical Review* 114:59-63.

Sporea D and A Sporea. 2007. "Radiation Effects in Sapphire Optical Fibers." *Physica Status Solidi C* 4(3):1356-1359.

Spratt WT, M Huang, C Jia, L Wang, VK Kamineni, AC Diebold and H Xia. 2011. "Formation of Optical Barriers with Excellent Thermal Stability in Single-Crystal Sapphire by Hydrogen Ion Implantation and Thermal Annealing." *Applied Physics Letters* 99:111909.

Sun G, DS Moon and Y Chung. 2007. "Simultaneous Temperature and Strain Measurement Using Two Types of High-Birefringence Fibers in Sagnac Loop Mirror." *IEEE Photonics Technology Letters* 19:2027-2029.

Sun T, ZY Zhang, KTV Grattan and AW Palmer. 1998. "Quasidistributed Fluorescence-Based Optical Fiber Temperature Sensor System." *Review of Scientific Instruments* 69(1):146-151.

Toccafondo I, M Taki, A Signorini, F Zaidi, T Nannipieri, S Faralli and F Di Pasquale. 2012. "Hybrid Raman/Fiber Bragg Grating Sensor for Distributed Temperature and Discrete Dynamic Strain Measurements." *Optics Letters* 37:4434-4436.

Tsai W-H and C-J Lin. 2001. "A Novel Structure for the Intrinsic Fabry-Pérot Fiber-Optic Temperature Sensor." *Journal of Lightwave Technology* 19:682-686.

Wakaki M, Ed. 2012. *Optical Materials and Applications*. Optical Science and Engineering. CRC Press, Boca Raton, Florida.

Williams G, G Brown, W Hawthorne, A Hartog and P Waite. 2000. "Distributed Temperature Sensing (DTS) to Characterize the Performance of Producing Oil Wells." In *Proceedings of SPIE, Industrial Sensing Systems, Volume 4204*, pp. 39-54. November 5, 2000, Boston, Massachusetts. The International Society for Optical Engineering, Bellingham, Washington.

6.0 Pressure Monitoring (Pressure Sensing in Vessel)

6.1 Fabry-Pérot Pressure Sensors

Fabry-Pérot devices use wavelength-dependent optical interference to produce measurable fringes, the positions of which are dependent on temperature, pressure, and inherent material optical properties. These sensor types have been described in detail for temperature sensing in Section 5.6. Fabry-Pérot devices have been developed extensively for R&D and commercial applications and are widely available as COTS pressure sensors. They are commonly configured as Fabry-Pérot cavities with one side of the cavity defined by a flexible membrane. Optical interrogation of the cavity can be conveniently accomplished with an optical fiber.

COTS Fabry-Pérot pressure sensors are available for harsh environments, but have not been characterized for the combined rigors of high temperature, high radiation, and corrosive coolants. Metal membranes that can tolerate 1000°C may embrittle from gamma radiation or corrode when in contact with certain coolants. Harsh-environment Fabry-Pérot pressure sensors may be engineered such that only deflecting membrane is exposed to the vessel environment, thereby protecting the fiber-optic leads; however, housing/connectors/seals will likely need to be customized to withstand the radiological and chemical environments within AdvSMRs.

The technical readiness for Fabry-Pérot COTS pressure sensors is **HIGH** for near-lid applications, because products exists which meet the temperature and pressure performance levels needed for measurement within AdvSMR coolants, but several questions remain unanswered. The technical readiness for near-core applications, given the harsh environment, is considered to be **LOW**.

6.1.1 Fundamentals of Operation

The fundamental operation of a Fabry-Pérot device has been fully described in the temperature sensing section (Section 5.6.1). Customizing such a Fabry-Pérot device for pressure sensing requires installing a cavity with a flexible surface defining the second interface of reflection. When the pressure increases, the membrane deflects inward, causing a shortening of the cavity length and a shift in the interference fringes between the first and second reflections. This arrangement is illustrated in Figure 6.1. As with most commercial Fabry-Pérot sensors, the light is launched through and collected using a single optical fiber. As a result, instrumentation for collecting and processing the signal can be physically remote from the site of measurement.
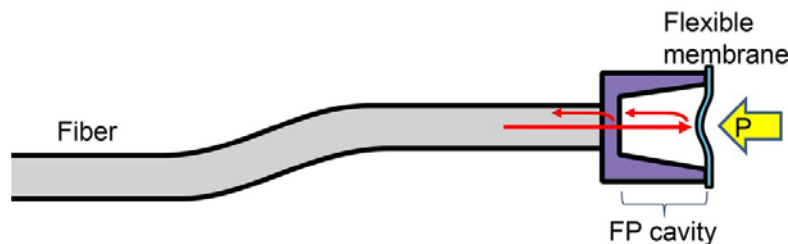
Figure 6.1. Fabry-Pérot Pressure Sensor with a Flexible Membrane

6.1.2 Promising Research and Development

Selection of the fiber material for delivery and collection of the optical signal represents an important aspect of development for any in-vessel sensing. In the case of flexible-membrane pressure sensing, the membrane material must be carefully selected as well. In the literature, a number of interesting materials have been suggested for sensing pressure ranges from kPa to GPa. These include membranes of polymer, silver (Xu et al. 2012), graphene (Ma et al. 2012), and others. The various properties of these materials, particularly CTE and melting temperature, will have to be carefully considered. Even for metals and metal alloys, function at very high temperatures (above 700 or 800°C, for instance) may be very challenging. For flexible membrane designs, it is imperative that normal operating conditions fall within the linear plastic region of the stress-strain curve. The yield point, at which stress induces irreversible deformation, is temperature-sensitive and so must be understood and characterized thoroughly.

Temperature robustness has been improved in Fabry-Pérot structures that have been fabricated from a single material. Using silica fibers in a silica ferrule with a silica membrane, CTE mismatches were decreased (Wang et al. 2012). By directly fusing the silica membrane onto the ferrule glue, deterioration at high temperature was avoided. In the same paper, the closed optical cavity was vented, allowing expanded air to escape. Without this improvement, expanding air in a trapped cavity will push the membrane outwards.

6.1.3 COTS Summary, Gaps Analysis, Ranking, and Proposed Future Research Path

COTS Fabry-Pérot Pressure Sensor Summary

For pressure sensing, Fabry-Pérot pressure sensors represent the largest category of commercially available products. Vendors include Sequoia Technologies, VIP Sensors, OpSens, Luna Innovations, and Davidson Instruments. Many of these vendors specialize in both pressure and temperature sensing. Membrane-based pressure sensing has been described for sodium-cooled reactors, using a system of bellows and NaK hydraulic fluid to keep the membrane far from coolant contact. Systems that simplify this design and eliminate the NaK volume possible would be of interest; however, they would require that the membrane in use could sustain the conditions in the vessel for long operating periods.

Davidson Instruments uses a thin metal membrane and can withstand pressures over 100 MPa and temperatures over 700°C. Sequoia Technologies' Fabry-Pérot sensors are able to work up to 69 MPa and in temperatures up to 150°C. Each of these companies offers sensor systems that cover a variety of different pressure ranges that might be suitable to different AdvSMR designs; however, the temperature exposure limits listed are typically only for the sensor head itself. The fiber-optic cable that connects the sensor to the electronics and light source is typically functional only up to around 300°C. Usage at higher temperatures would require either customization of the fiber optics or careful protection of the sensing apparatus.

Commercial Fabry-Pérot pressure sensors are not characterized under environments of high, or even moderate, radiation. As with many of the other optical methods considered in this report, the intended application space for these products is typically not one that overlaps with the environments typical of AdvSMRs. In general, the sensitivity of Fabry-Pérot sensors to radiation will depend on how the optical properties of the various components change. As a result, the delivery and collection fiber, as well as the

material from which the optical cavity is fabricated, will have to be suitable. For Fabry-Pérot pressure sensors, if the reflectivity of the first or second reflections' surface changes significantly, the fringe depth will be affected.

Because sensor manufacturers do generally not address these effects, successful implementation in-vessel will hinge on extensive initial testing. However, Davidson Instruments has estimated that their Fabry-Pérot sensors can survive total gamma doses of 2 MGy by using radiation-tolerant fibers from Polymicro. A 2-MGy dose would result in roughly a 10-dB optical loss over 100 meters, which is acceptable performance within the limitations of their instrumentation. Such estimates assume operation in room temperature, which means that these results cannot be directly extrapolated to predict performance in AdvSMRs.

We rank the technical readiness of Fabry-Pérot pressure sensors as **MEDIUM**, because they may be suitable for AdvSMR temperatures, but near-term implementation is unlikely.

Gaps Analysis

The most important technology gaps are described for any Fabry-Pérot sensors in Section 5.6.3.

Technical Readiness Ranking

We rank the technical readiness of Fabry-Pérot pressure sensors as **HIGH** for near-lid applications, because they may be suitable for AdvSMR temperatures. The effects of very high radiation on the lifetime of the Fabry-Pérot sensor cannot currently be predicted, and the question of appropriate fiber coatings is yet unanswered. For this reason, Fabry-Pérot sensors are considered to have **LOW** technical readiness for near-core application.

Proposed Future Research

As with Fabry-Pérot temperature sensors, this technology is interesting, and further work could be warranted. It is capable of delivering more-than-adequate pressure resolution and the highest pressures expected in AdvSMRs (25 MPa for SCWRs) are not high by industrial standards. Coolant transparency would not be a requirement for these sensors. These Fabry-Pérot pressure sensors could be used either in gas headspaces or in reactor coolants and would require a fiber-optic access point to the reactor vessel. If the membrane was built into the side of the vessel, then the fiber optics would either have to be built into a protective conduit or would have to exit through the side of the vessel. Sidewall vessel penetration, due to CTE mismatches and introduction of failure points, is questionable for liquid-phase coolants. One of the challenges for implementation would involve decoupling temperature and pressure effects, as well as vibration, although a multi-parameter Fabry-Pérot sensor package could be envisioned that would measure all of these effects at once. It is very possible that this technology could be overshadowed in utility by sensors that offer distributed sensing capabilities, such as FBG sensors (see Section 6.2).

The first paths forward for Fabry-Pérot pressure sensor implementation are identical to those for Fabry-Pérot temperature sensors proposed in Section 5.6.3. All of these issues would need to be explored as first steps, and are common to many of the optical sensors considered for temperature or pressure sensing. For Fabry-Pérot pressure sensors, an additional concern is the effect of radiation-induced luminescence in the fibers that could cause a lot of trouble in terms of reducing the signal-to-noise ratio. It is likely that Fabry-Pérot sensors can be pursued as multi-parameter systems for measuring both

temperature and pressure. This would give enhanced utility to this approach, but probably not enough to overcome the disadvantages of point sensing versus distributed sensing.

6.2   Fiber-Bragg Grating Sensors

Distributed pressure sensing could be enabled in most AdvSMR concepts using fiber-Bragg grating (FBG) sensors. Distributed sensing would enable high-resolution pressure measurements in multiple in-vessel locations, using just a single fiber-optic cable. This measurement mode provides greater functionality into each reactor vessel penetration. This is a tremendously useful capability that is not currently deployed in nuclear reactors.

FBG sensors have been described in detail previously in Section 5.3 for temperature sensing. Changing the pressure environment will result in radial compression or expansion of the fiber material, changing the grating spacing and the RI of the fiber. These sensors can be tailored for specific pressure sensitivities by selection of the fiber material and by sheathing them with coatings and jackets that impart an appropriate level of mechanical hardness. FBGs, however, remain simultaneously sensitive to temperature and vibration, so these effects will either have to be multiplexed and deconvolved or successfully referenced out.

There are not necessarily any unique challenges for fabricating grating structures for pressure sensing versus temperature. The sensitivity of the sensor to pressure will be dictated primarily by how much strain is induced in the fiber over a given pressure range. For AdvSMRs, it will be important that these sensors survive the rigors of the in-vessel environment for long periods of time. The technical readiness for FBG pressure sensors is ranked **HIGH** for near-lid AdvSMR applications. However, the temperature limit imposed by the fiber coatings, sheaths, and cabling of current COTS products will reduce near-core feasibility and fatigue will likely take place on an accelerated schedule if the FBG fibers are subjected to large doses of radiation. The technical readiness for current COTS FBG pressure sensors is ranked **LOW** for near-core applications.

6.2.1   Fundamentals of Operation

The fundamentals of operation and fabrication methods of FBG have been described in Section 5.3.1. Changes in pressure will lead to strain in the FBG, causing a shift in the reflection peak. FBGs have been used to measure pressure between 0 to 70 MPa (Mihailov 2012), which is a useful range for AdvSMRs. The wavelength-pressure relationship is also linear across this range, which makes calibration much easier (Shen et al. 2007). As shown in Figure 6.2, an increase in radial pressure on a fiber will cause compression. According the fiber's Poisson ratio, radial compression translates into axial strain, causing a measurable change in grating spacing.
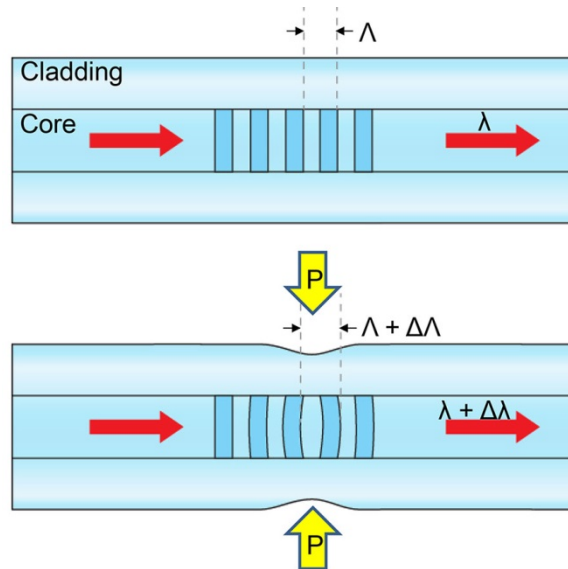
Figure 6.2. Compression Causes Changes in the Effective FBG Spacing

6.2.2 Promising Research and Development

FBG sensors can be configured to both measure high pressures and high temperatures simultaneously. In this design, thermally stable fs-IR laser-induced Type II gratings were inscribed in microstructured air-hole fiber in order to produce a sensor that could simultaneously monitor temperature and pressure in harsh environments (Jewart et al. 2010; Chen et al. 2011). These sensors were demonstrated to perform well in pressure ranges from 0.1 to 16.5 MPa and at temperatures up to 800°C. Multi-parameter measurements in a single fiber, if effective, would be a great advantage in highly integrated AdvSMR designs.

6.2.3 COTS Summary, Gaps Analysis, Ranking, and Proposed Future Research Path

COTS FBG Summary

Commercial sources for FBG sensors and support instrumentation are abundant. Timbercon and other vendors offer COTS systems specifically for pressure sensing. The Timbercon FBG sensors are offered with either silica fiber or sapphire light pipes and are specified to function up to the melting point of fibers. They also sell multi-parameter systems, which can measure both temperature and pressure simultaneously.

Gaps Analysis

The primary technical gaps for FBG pressure sensors are the same as those identified for FBG temperature sensors in Section 5.3.3.

Technical Readiness Ranking

FBG pressure sensors are commonly used for research applications. The maturity of FBG fabrication technologies and their potential for distributed sensing provides a significant advantage for AdvSMR monitoring applications. For these reasons, we consider FBG pressure sensors to have **HIGH** technical readiness for near-lid applications. The optical-fiber coatings, sheathing, and cabling materials have temperature limitations that currently make near-core deployment unfeasible. Based on these reasons, the technical readiness for near-core deployment is **LOW**.

Proposed Future Research

Future research for FBG pressure sensors are the same as those proposed for FBG temperature sensors in Section 5.3.3.

6.3   Intensity-Modulated Reflective Membrane

Intensity-modulated, reflection-based pressure sensors are simple and well-established technology that relies only on displacement of a flexible membrane to produce changes in the optical signal. This change is either an increase in light intensity when the membrane is closer to the fiber or a decrease in intensity when the membrane is farther away. This configuration is a much simpler variation of the Fabry-Pérot flexible membrane (Section 6.1), because only intensity signals are processed into pressure values. Commercial products are available that can offer both absolute and pressure-difference measurement.

COTS intensity-modulated reflective membrane systems provide pressure measurement ranges and resolutions that are well suited to the needs of AdvSMRs, but near-core deployment is likely unfeasible because of the extreme temperature and radiation conditions. For this reason, we consider the technical readiness of this approach to be **HIGH** for near-lid applications and **LOW** for near-core applications, similar to the readiness of Fabry-Pérot pressure sensors.

Intensity-modulated reflective membrane technology is promising, and further development efforts may be fruitful. The simplicity of the design and modest equipment demands leads to a cost-effective, potentially near-term AdvSMR pressure monitor. Some challenges remain that may offset the benefits of this technology. Decoupling temperature, pressure, and vibration effects could be a challenge. Distributed pressure sensors, such as FBG pressure sensors (Section 6.1.3) could likely overshadow this technology.

6.3.1   Fundamentals of Operation

Intensity-modulated reflective membrane sensors are generally configured with two side-by-side fibers. The first fiber illuminates the membrane and the second fiber collects light reflected from the membrane. Displacement of the reflective membrane changes the intensity of light collected by the second fiber.

6.3.2   Promising Research and Development

Modulation-based membrane sensors are very basic designs that have limited future R&D potential.

6.3.3 COTS Summary, Gaps Analysis, Ranking, and Proposed Future Research Path

COTS Intensity-Modulated Reflective Membrane Summary

Several companies provide absolute and pressure-change COTS sensors, including Optrand and MTI Instruments. The Operand sensor membrane is made of nickel-alloy and the entire sensor head is sheathed in a metal housing. The pressure measurement range spans from zero to 200 Mpa, with a maximum working temperature of 350°C. MTI Instruments offers a high-temperature probe, which is rated up to 482°C. The pressure and working temperature specifications suggest that these COTS sensors are feasible for near-lid AdvSMR deployment applications, but not for near-core applications. The vendors provide no radiation-resistances specifications.

Gaps Analysis

- The temperature limits imposed by the optical-fiber coatings, sheathing, and cabling materials are significantly below most expected in-vessel AdvSMR conditions.

- The temperature limits of the membrane bond and mechanical design are uncertain.

- Membrane and sensor metal components may be subject to neutron-activation or transmutation.

- Optical fibers and materials have well-known radiation damage pathways.

- Actual performance and benefits of COTS membrane fiber pressure sensors must be determined.

- Service lifetime and performance of COTS membrane fiber pressure sensors and instrumentation under AdvSMR deployment conditions must be determined.

Technical Readiness Ranking

The pressure and working temperature specifications suggest that COTS membrane pressure sensors are feasible for near-lid AdvSMR deployment applications, but not for near-core applications. Thus, we consider the technical readiness of this approach for near-lid applications to be **HIGH** and **LOW** for near-core applications.

Proposed Future Research

- The suggested research needed to resolve COTS optical-fiber technical gaps is discussed in Section 3.3.6.

- COTS membrane sensor designs must be enhanced to meet near-core deployment requirements.

- Performance and benefits of COTS membrane pressure sensors must be studied.

- Service lifetime and performance of COTS membrane pressure sensors and instrumentation under AdvSMR deployment conditions must be determined.

6.4 Birefringence-based

Birefringence-based sensing leverages the property of certain optical materials, either natural or induced, that orthogonal light polarizations experience different refractive indices. Interferometry is typically used to track the differential path length experienced by the two polarizations and sensors can

use this to measure temperature or strain. Strain that has a directional impact on a birefringent optic will induce a differential RI change on the affected polarization. Many optical materials that are not inherently birefringent, when non-uniformly compressed, will exhibit birefringence as well. This technology is typically limited to change measurement and requires complicated solutions to measure absolute parameters. However, the utility of birefringence pressure sensors for AdvSMRs will depend on their ability to work as well as current electronic membrane sensors without introducing significant complexity or cost.

Commercial suppliers of birefringent pressure sensors are very few, and the needs of AdvSMRs are not well addressed by them, so we consider the technical readiness of this approach to be **LOW** for all AdvSMR applications. Products exist that use birefringent crystals with very high melting points, such as barium borate, but other components of the system are not rated for significant temperature. Studies of radiation damage to delivery/collection fibers and birefringent crystals would need to be done to understand the limitations of off-the shelf devices.

Challenges to successful implementation include retaining polarization information through optical fibers and avoiding noise from vibration and radiation in an in-vessel environment. Another major challenge will involve access to the reactor vessel. Fiber-based sensors like these must be in contact with the measurement site and therefore must withstand some of the worst conditions inside the reactor. Hollow-core fibers or photonic crystal fibers—which can preserve polarization very well—may be used to great effect with a birefringent crystal for in-vessel sensing, but this sort of solution is not likely to be available for near-term deployment.

Birefringent sensors, as they are currently constructed, have the disadvantage (compared to backscatter techniques mentioned in the previous section) of being point sensors, which means that the payoff for developing them into functional reactor instruments may not be a significant improvement over current sensors that use flexible membranes and impulse lines. Some interesting R&D efforts have succeeded in developing distributed birefringence sensors, so they may become more practical in years to come.

6.4.1   Background

The concept of birefringence has been described in the temperature-sensing portion of this report. A birefringence-based pressure sensor is simply one that measures the difference in optical path length for light of two cross polarizations traveling through a single optical media. The path length difference changes because of induced strain, which causes an asymmetric change in index between the two polarizations.

There are a number of ways to carry this out. Birefringent fibers (microstructured, D-shaped, solid fiber fabricated with an elliptical core, and others) will support orthogonal polarizations that will have different responses to pressure depending on the axis along which force is applied. Even an isotropic single-mode telecom fiber will become linearly birefringent when subjected to radial stress.

Many different crystals can be used as birefringent pressure transducers. The benefit of crystals is that many of them are naturally birefringent, such as sapphire, quartz, barium borate, calcite, lithium niobate, and magnesium oxide. Also, crystalline optical materials often have very high melting temperatures.

The most practical way to measure birefringence is to interfere the cross-polarized light and monitor fringe shifts.

6.4.2   Promising Research and Development

The Marshall Space Flight Center has developed a pressure and temperature sensor for rocket engines that relies on two crystalline wedges made out of sapphire and magnesium oxide encased within a probe housing (NASA 2008). Stress-induced birefringence in the two crystals is measured with fiber optics.

In the literature, there is extensive demonstration of photonic crystal fibers (PCFs) being used as birefringent pressure sensors (Dabkiewicz and Jansen 1987; Zhang et al. 2011). Careful control of the optical mode profiles can be obtained using deliberately crafted hole structures in PCFs, which allows researchers to fabricate highly birefringent fibers. Compression in a specific direction will cause small deflections in the hole structure, changing the birefringence in measurable ways.

6.4.3   COTS Summary, Gaps Analysis, Ranking, and Proposed Future Research Path

COTS Birefringence Sensor Summary

Several patents describe concepts for birefringence-based pressure sensing; however, to our knowledge these are not currently available commercially. An NRC document from 1998 describes two vendors of these sensors, which upon subsequent investigation seem to no longer be in business (Hashemian et al. 1998).

Timbercon, in collaboration with Columbia Gorge Research, offers built-to-purpose side-hole fiber-based sensors that they claim are insensitive to temperature. In side-hole fibers, two holes straddle the fiber core, which cause stress to be distributed anisotropically. These sensors are promising, and are described abundantly in the literature (Clowes et al. 1998; Hu et al. 2012), but seem to be customized jobs and cannot be considered COTS systems.

Gaps Analysis

Birefringent optical sensors typically use optical fibers for delivery and signal collection. Therefore, they face a number of the same challenges that other fiber-based optical systems face. These challenges have already been described in Section 5.7.3 and are identical for temperature and pressure sensing. Technology gaps largely consist of the unknown effects of both separate or simultaneous high temperature and radiation exposure to both the fiber optics and the birefringent crystal (or fiber). Some information exists that seems to suggest that the birefringence of some fibers is not very sensitive to radiation exposure, but additional information is needed.

Technical Readiness Ranking

Birefringence-based sensing is extremely interesting for both temperature and pressure sensing, but is available only sparingly and is not well characterized for AdvSMR conditions. For this reason, we consider its technical readiness to be **LOW** for all AdvSMR applications in all locations.

Proposed Future Research

Given the low technical readiness and relatively low potential benefits of this technology, no future research is suggested at this time.

6.5   References

Chen T, R Chen, C Jewart, B Zhang, K Cook, J Canning and KP Chen. 2011. "Regenerated Gratings in Air-Hole Microstructured Fibers for High-Temperature Pressure Sensing." *Optics Letters* 36(18):3542-3544.

Clowes JR, S Syngellakis and MN Zervas. 1998. "Pressure Sensitivity of Side-Hole Optical Fiber Sensors." *IEEE Photonics Technology Letters* 10:857-859.

Dabkiewicz P and K Jansen. 1987. "Fiber-Optic Pressure Sensor Using Birefringence in Side-Hole Fiber." In *Proceedings of SPIE, Fibre Optics '87: Fifth International Conference on Fibre Optics and Opto-Electronics, Volume 0734*, pp. 202-206. April 28-30, 1987, London, United Kingdom. Society of Photo-Optical Instrumentation Engineers, Bellingham, Washington.

Hashemian HM, ET Riggsbee, DW Mitchell, M Hashemian, CD Sexton, DD Beverly and GW Morton. 1998. *Advanced Instrumentation and Maintenance Technologies for Nuclear Power Plants*. NUREG/CR-5501, U.S. Nuclear Regulatory Commission, Washington, D.C.

Hu G, D Chen and X Jiang. 2012. "Side-Hole Two-Core Microsctuctured Optical Fiber for Hydrostatic Pressure Sensing." *Applied Optics* 51:4867-4872.

Jewart CM, Q Wang, J Canning, D Grobnic, SJ Mihailov and KP Chen. 2010. "Ultrafast Femtosecond-Laser-Induced Fiber Bragg Gratings in Air-Hole Microstructured Fibers for High-Temperature Pressure Sensing." *Optics Letters* 35(9):1443-1445.

Ma J, W Jin and HL Ho. 2012. "A Fiber-Tip Fabry-Pérot Pressure Sensor with Graphene Diaphragm." In *Proceedings of SPIE, OFS2012 22nd International Conference on Optical Fiber Sensors, Volume 8421*. October 15-19, 2012, Beijing, China. Society of Photo-Optical Instrumentation Engineers, Bellingham, Washington. Paper No. 84211C.

Mihailov SJ. 2012. "Fiber Bragg Grating Sensors for Harsh Environments." *Sensors* 12(2):1898-1918.

NASA. 2008. *NASA Tech Briefs, Optical Pressure-Temperature Sensor for a Combustion Chamber*. Tech Briefs Media Group. New York. Accessed June 12, 2013. Available at http://www.techbriefs.com/component/content/article/2925 (last updated July 1, 2008). Marshall Space Flight Center, Alabama.

Shen R-S, J Zhang, Y Wang, R Teng, B-Y Wang, Y-S Zhang, W-P Yan, J Zheng and G-T Du. 2007. "Study on High-Temperature and High-Pressure Measurement by Using Metal-Coated FBG." *Microwave and Optical Technology Letters* 50:1138-1140.

Wang W, Q Yu, F Li, X Zhou and X Jiang. 2012. "Temperature-Insensitive Pressure Sensor Based on All-Fused-Silica Extrinsic Fabry-Pérot Optical Fiber Interferometer." *IEEE Sensors Journal* 12:2425-2429.

Xu F, D Ren, X Shi, C Li, W Lu, L Lu, L Lu and B Yu. 2012. "High-Sensitivity Fabry-Pérot Interferometric Pressure Sensor Based on a Nanothick Silver Diaphragm." *Optics Letters* 37:133-135.

Zhang S, X Yu, P Shum, Y Zhang, HP Ho and D Liu. 2011. "Highly Sensitive Pressure-Induced Plasmon Resonance Birefringence in a Silver-Coated Photonic Crystal Fiber." *Journal of Physics: Conference Series* 276(1):012102.

7.0   Coolant Flow Monitoring

Optical flow analyzers based on laser Doppler velocimetry are well-established instruments available in a number of different configurations to support different standoff ranges and various modes of operation. COTS models exist with moderately compact optical heads and more compact fiber-coupled optical heads. Ranges of one meter or more are easily accommodated by these systems. Modes of operation include single velocity component sensors, multidimensional (multi-component) systems, and scanning systems.

The technical readiness of existing COTS optical flow analyzer systems for AdvSMR applications is **LOW**. The commercially available systems are primarily used in laboratory settings, and have not been used extensively in harsh industrial environments. Use of optical flow analyzers in AdvSMRs will require development of ruggedized systems with extended temperature ranges and radiation resistance, line-of-sight access to the surfaces of interest, and optical windows for placement of the system outside of the vessel. The noncontact, standoff nature of these systems will enable this type of remote placement, if engineering solutions allowing such placement are developed.

Another method to detect changes in coolant flow could be accomplished by collecting images of the liquid coolant surface and processing changes in surface ripple patterns. Partial blockages of the core coolant pathways could possibly show up as spatial changes in the surface ripple pattern. This is a conceptual idea and no COTS measurement system based on this technique is available. COTS imagers and imaging processing software could be combined to vet this concept.

7.1   Introduction

Optical flow analysis measurement techniques may be feasible in some AdvSMR designs, including those with coolants that are optically transparent (e.g., SCW, He, molten salt). Liquid-metal-cooled designs would not be amenable to direct optical monitoring. Optical flow analysis techniques are mature for a number of applications and may be adaptable to future AdvSMR designs; however, they are primarily used as laboratory instruments rather than industrial sensors. Optical flow analysis using laser Doppler velocimetry is typically a very sensitive standoff measurement technique, so many of the critical components may be placed outside the vessel with suitable optical ports designed to allow monitoring of coolant flow at critical locations. Laser Doppler velocimetry may be useful for measuring the coolant flow velocity and turbulence conditions at specific points within the AdvSMR. Laser Doppler velocimetry has been suggested for determining the primary coolant mass flow within helium-cooled HTGRs by monitoring the velocity of entrained graphite dust particles within the flow (Ball et al. 2012). A potentially related flow measurement method, optically based diaphragm deflection measurement, is being considered as a potential technique for direct high-temperature measurement of differential pressures in liquid salt flowmeters (Holcomb et al. 2009).

7.2   Fundamentals of Operation – Laser Doppler Velocimetry

Laser Doppler velocimeters provide a noncontact (standoff) method for detecting and analyzing the motion of particles entrained within a flowing gas or liquid fluid. Laser Doppler velocimeters detect this motion using an optical interferometric technique in which laser light scattered from two or more beams co-incident on the moving particle is detected and analyzed for the Doppler-shifted frequency. The

scattered light from each beam is Doppler shifted because of the motion of the particle. The photodetector does not respond to the optical frequency directly, but rather mixes the two frequencies to generate a differential Doppler frequency, which is proportional to the particle velocity. Specific orientation of the two beams allows isolation of the motion along a single axis. Simultaneous multi-dimensional measurements are possible using two or three pairs of optical beams, all aligned to be co-incident at the desired measurement location.

A typical single-component laser Doppler velocimetry design is shown schematically in Figure 7.1. A continuous wave laser beam (f_0) is split into two parallel beams by a beam splitter and mirror. Argon ion and diode lasers are typically used for these systems. The upper beam in Figure 7.1 is optionally passed through an acoustic-optic modulator (AOM), also known as a Bragg cell. The AOM frequency shifts the light to a higher frequency $(f_0 + f_b)$. The two beams are maintained in a parallel alignment and passed through a lens, typically near the outer edge of the lens as shown in the figure. The lens causes the two parallel beams to coincide at the focal length of the lens and also narrows each beam. The beams overlap within the measurement volume of the system. Light scattered from each beam is collected by the primary lens and focused by it and a secondary lens onto a photodetector. For a velocity (v) in the plane of the two beams and perpendicular to the axis of the system, the upper beam is Doppler shifted to $f_1 = (f_0 + f_b)(1 + v \sin \varphi / c)$ and the lower beam is Doppler shifted to $f_2 = f_0 (1 - v \sin \varphi / c)$, where c is the speed of light and 2φ is the angle between the two beams. The photodetector responds to the difference between these two frequencies of $f_2 - f_1 = f_b + (2v / \lambda) \sin \varphi$, where λ is the wavelength at f_0.
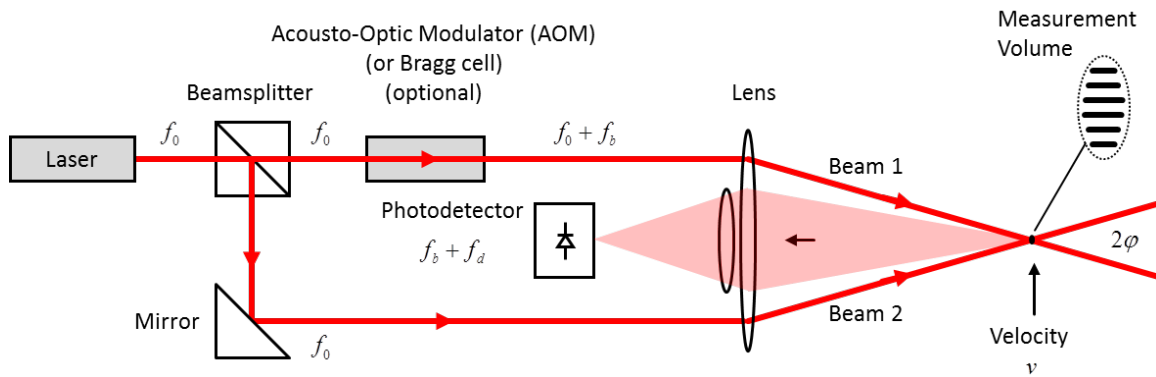
Figure 7.1. Schematic Diagram of a Heterodyne Laser Doppler Velocimeter

The laser Doppler velocimetry system shown in Figure 7.1 is a heterodyne detection system because of the introduction of the additional modulation by using an AOM operated at f_b. This additional modulation can be removed in subsequent electronic or digital signal processing to yield the desired Doppler frequency signal, $f_d = (2v/\lambda) \sin \varphi$. The heterodyne architecture has the advantage of removing the ambiguity between positive and negative velocities, and may have signal-to-noise ratio advantages because of additional filtering and amplification that may be implemented at the heterodyne intermediate frequency (f_b).

The laser Doppler velocimetry system is very similar to the laser Doppler vibrometer described in Section 10.2.1. The primary difference is that two (or more) individual laser beams illuminate the measurement zone in the velocimetry configuration rather than a single beam used in the vibrometry configuration. For vibrometry, a solid surface is typically being examined, so the measurement zone is well defined for a single beam. For moving particles in a fluid, two intersecting beams are used to define a single measurement zone. If a vibrometer configuration were used, the system would respond to all particles along the beam and the signals from these particles would interfere.

The laser Doppler velocimetry system can also be understood graphically for the special case in which no AOM is used (i.e., $f_b = 0$). When the two laser beams intersect in the measurement volume, an optical fringe pattern is set up. These optical fringes are aligned perpendicular to the velocity as shown in Figure 7.1. When a particle traverses the fringes within the measurement zone, the intensity of the light at the photodetector is modulated at the differential Doppler frequency.

The configuration shown in Figure 7.1 measures a single component of the velocity in the plane of the two beams and perpendicular to the main axis of the system. The other two components of the velocity vector can be measured using additional pairs of beams aligned in the other principal planes, with their beams coincident within the measurement volume. Two or three separate laser wavelengths are used for these measurements to eliminate interference from the component signals. Fiber-coupled laser Doppler velocimeters can be formed using an architecture similar to that shown in Figure 7.1, with the free-space optical paths to the right of the lens and photodetector replaced by optical fibers and associated fiber-coupled components.

7.2.1　Laser Doppler Velocimetry Applications

- Analyzing hot environments, such as rocket engine exhaust, flames, plasmas.

- Measuring arterial blood flow (near the surface of the body).

- Solid surface measurements for paper and steel mills.

- Fluid mechanics, flow, turbulence, and spray research.

- Combustion research, turbines, automotive (internal combustion).

7.2.2　Advantages of Laser Doppler Velocimetry

- Sensor operates in a standoff configuration, and does not interfere with the flow being measured.

- Noncontact measurement allows measurement of motion in extreme/hostile environments with high temperatures, such as combustion chambers or moving molten or hot surfaces.

- High frequency response – allows measurement of high velocities.

7.2.3　Potential Disadvantages of Laser Doppler Velocimeters

- Measurement of more than one velocity vector requires additional velocimetry lasers, adding complexity and cost.

- Range to the measurement zone is typically fixed.

- Laser beams must be carefully aligned and the velocimeter is sensitive to vibration.

- Fluid medium must contain particles, or be deliberately seeded with particles.

- Fluid medium must be optically transparent.

- Size – sensor head can be relatively large and associated electronics are required.

- Typically used in R&D settings, rather than in industrial facilities.

7.2.3.1   Related Techniques

Laser Doppler velocimetry is very similar to laser Doppler vibrometry, which is discussed in Section 10.2.1. The principal difference is that vibrometry typically uses a single laser beam incident on the vibrating or moving surface and recovers the Doppler signal using a reference beam internal to the optical head. Laser Doppler velocimetry uses the interference between two intersecting beams to recover the Doppler signal because of one component of particle velocity. Use of two beams allows isolation of a small measurement zone at a known range.

7.3   Promising Research and Development

Laser Doppler velocimetry has been suggested for monitoring the movement of graphite dust particles in HTGRs to determine the primary coolant flow rate (Ball et al. 2012). This technology may also be useful for other optically transparent coolant monitoring applications. For example, it may be possible to monitor coolant flow in liquid fuel reactor designs. A related technique referred to as Projection velocimeter may be useful for this application because it uses an optical mask to create the fringe pattern within a single laser beam (Moir 2009; Ball et al. 2012). The use of a single laser beam and a larger fringe pattern reduces the optical alignment precision that is required, and may enable use of velocimetry in harsh industrial situations in which conventional laser Doppler velocimetry has not been practical.

7.4   Summary COTS, Gaps Analysis, Ranking, and Proposed Future Research Path

COTS Flow Monitoring Summary

Laser Doppler velocimeters are well-established instruments and are available in a variety of configurations to support different standoff ranges and modes of operation. COTS models are available from TSI Inc., Measurement Science Enterprise, Inc. (MSE), and Dantec Dynamics. Laboratory-grade models tend to use larger argon ion lasers with fiber-coupled or free-space optics, while more compact fiber-coupled systems based on diode lasers are also available. Configurations that are available include one-, two-, and three-dimensional systems. Systems are also available with spatial scanning configurations. A general-purpose laser Doppler velocimetry system is available from TSI Inc. This system uses solid-state lasers and is available in a variety of configurations including one-, two-, and three-dimensional systems, and has optional fiber-optic-coupled probes. A very compact system is available from MSE. This system requires no user alignment and is optionally available with a high-temperature, high-pressure, waterproof housing.

Gap Analysis

Use of optical velocimeters in AdvSMRs will require development of ruggedized systems with extended temperature ranges and radiation-resistance, line-of-sight access to the surfaces of interest, and

optical windows for placement of the sensitive system components outside of the reactor vessel. The noncontact, standoff nature of these systems will enable this type of remote placement, if engineering solutions allowing such placement are developed. Key technical readiness gaps include:

- Laser Doppler velocimeters are not designed for high-vibration deployment.

- Laser Doppler velocimetry designs do not have methods to maintain optical alignment over extreme temperature variations (e.g., start-up will be at cooler temperatures than steady-state operation).

- Laser Doppler velocimeters operate at fixed ranges and require a change in the lens for each desired range.

- Laser Doppler velocimeters are not available as compact, robust optical designs suitable for the AdvSMR application.

- Potential performance degradation because of transmission through optical windows, coolant vapor, and thermal refractive gradients.

Technical Readiness Ranking

The technical readiness of existing COTS optical velocimetry systems for AdvSMR applications is currently **LOW**. The commercially available systems are primarily used in laboratory settings, and have not been developed for harsh industrial environments. Integration into the AdvSMR application will likely be very challenging.

Proposed Future Research Path

The suggested future research path must address the specific applicability of optical velocimeters for specific AdvSMR designs. This includes developing differential vibration and transmission media compensation, ruggedization and design advancements, variable range capability, stable target alignment techniques, and engineering solutions that provide line-of-sight to in-vessel components.

7.5 References

Ball SJ, DE Holcomb and SM Cetiner. 2012. *HTGR Measurements and Instrumentation Systems*. ORNL/TM-2012/107, Oak Ridge National Laboratory, Oak Ridge, Tennessee.

Holcomb DE, SM Cetiner, GF Flanagan, FJ Peretz and GL Yoder. 2009. *An Analysis of Testing Requirements for Fluoride Salt-Cooled High Temperature Reactor Components*. ORNL/TM-2009/297, Oak Ridge National Laboratory, Oak Ridge, Tennessee.

Moir C. 2009. "Miniature Laser Doppler Velocimetry Systems." In *Proceedings of the SPIE, Optical Sensors 2009, Volume 7356*, p. 73560I. April 20-22, 2009, Prague, Czech Republic. The International Society for Optical Engineering, Bellingham, Washington.

8.0   Coolant Level Monitoring

Laser-based time-of-flight rangefinders have a large market penetration in the consumer electronics and are used in many science and military applications. This technique is based on fundamentals of light detection and ranging (LIDAR), which has been well established for over 50 years, almost since the invention of the laser (Collis 1965). Laser rangefinder systems are not generally used for level monitoring, but they should be feasible for measuring liquid-coolant levels. The technical readiness for laser rangefinder methods is **MEDIUM**, but this technique may not provide any benefit over ultrasonic techniques.

Total internal refection (TIR) optical sensors for measuring level are COTS items, but they only change state at one level setting only. A single switch provides very little information, so vertical arrays are configured for level monitoring applications. These designs suffer from poor level resolution. Overall, the technical readiness of existing COTS optical level monitoring systems for AdvSMR applications is **LOW** for TIR optical switches. The commercially available systems are not designed for harsh industrial environments. Installation of optical switches could prove very invasive and would require multiple vessel penetrations.

8.1   Fundamentals of Operation

A laser rangefinder system consists of a laser and a detector. The laser emits pulses in the direction of an object of interest, the detector receives the scattered and reflected light, and the distance is computed from the time it takes for each pulse to return. A simplified representation of this process is illustrated in Figure 8.1. Early applications tended to focus on ground-based atmospheric research and utilized very high-powered lasers (Collis 1965; Northend et al. 1966).

Contemporary LIDAR systems are available, however, that can generate 3D maps using scanning laser systems and GPS data. Hand-held LIDAR systems can now be purchased at hardware stores for measuring relatively short distances using low-powered eye-safe NIR lasers. More powerful laser rangefinders are also commonly used for military applications, recreational hunting, and even golfing. High-speed electronics also make it possible to measure the time-of-flight by measuring the phase shift of an amplitude- or frequency-modulated continuous wave source (Amann et al. 2001). Reactor liquid-coolant levels are typically just a few meters below the vessel lid. Laser rangefinders could easily measure that distance to millimeter resolution.
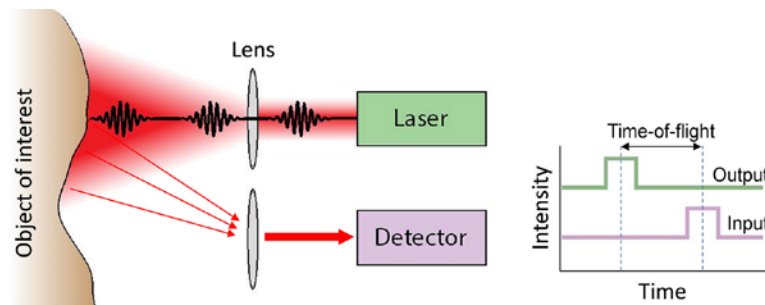
Figure 8.1. Laser Time-of-Flight Rangefinding Using a Pulsed Laser

8.2   Total Internal Reflection Optical Switches

8.2.1   Fundamentals of Operation

TIR switches are composed of an optical delivery fiber and a prism mounted to the fiber end facet, as shown in Figure 8.2. The liquid-level concept relies on spoiling the prism TIR by immersion into a high RI liquid. Normally the low index air does not change the prism TIR properties, allowing light propagation into the prism to reflect back through the prism to a photodetector. If the surrounding environment is water or another relatively high RI liquid, the critical angle defined by Snell's law is exceeded and the beam will escape from the prism into the liquid. In that case, the light intensity measured by the photodetector will be significantly decreased.
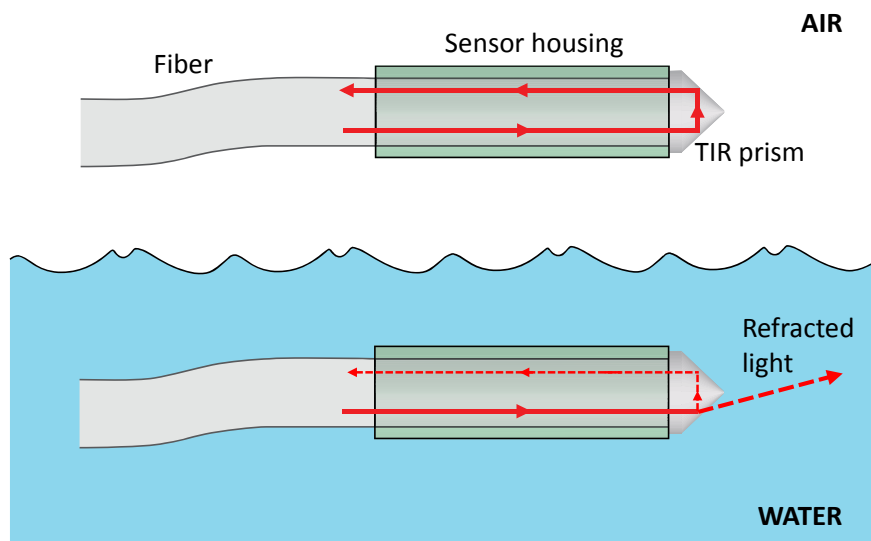
Figure 8.2. Prism-Based TIR Level Switch

8.2.2   Promising Research and Development

A fiber-based approach, designed for measuring fuel levels in aircraft, was developed based on the same principles as the prism-based switch (Zhao et al. 2013). In that study, a length of optical fiber with a thinned cladding was coiled around a support pipe and immersed in fluid. The tight radius of curvature and thin cladding allowed light propagation in the core to be influenced by the RI of the surrounding media. When surrounded by high RI fluid, the optical-guided mode transitioned into a radiative mode and the optical transmission decreased. As the sensor was immersed deeper into the fuel, the light output decreased proportionally, allowing level measurement from the top to the bottom of the fuel tank.

8.3 COTS Summary, Gaps Analysis, Ranking, and Proposed Future Research Path

8.3.1 Laser-Based Time-of-Flight Rangefinders

COTS Coolant Level Summary

COTS products for laser distance measurements fall into a few categories delineated by application. Consumer-grade rangefinders are offered by many companies, including Bosch, Parallax, Bushnell, Simmons, and Nikon. These are low-power systems that are very unfeasible for harsh environments. SICK Sensor Intelligence offers one of the widest arrays of different laser rangefinding units, both for indoor and outdoor operation. Leica manufactures a variety of rangefinding products for military applications. Accutron Instruments is one of the few vendors that target their systems for industrial applications.

The standard commercial models described above are integral units containing a laser, detector, and all of the accessory electronics. No system of this nature will be suitable for direct in-vessel measurement. The maximum operational specifications top out around 85–125°C. Even industrial models, like those made by Accutron, are suitable for temperatures below 100°C. This will be insufficient for in-vessel usage, even in the headspace. However, this may be good enough for standpipe viewing if the radiation resistance requirements can be satisfied.

Radiation-resistance information for these devices is unavailable. Given the intended applications, it is unlikely that any of them would function for very long in a high-radiation environment.

Gap Analysis

The gaps for deployment of any rangefinders involve characterization of the components under radiological conditions like those expected within reactor containment buildings. If this can be achieved, then the only difficulties in implementation will be those related to optical access.

Technical Readiness Ranking

Optical rangefinding is considered to have **MEDIUM** technical readiness, because it is a remote measurement methodology that should be readily adaptable to measuring coolant heights; however, it is not evaluated for in-containment conditions.

Proposed Future Research Path

Paths forward for developing these devices would have to involve testing under harsh environments, evaluating the technology's performance through remote optical access. The first step for optical-level sensing would logically involve laser rangefinding, as this is the most promising technique that stands to yield the most useful information. Once engineered solutions have been developed for optical access using standpipes and/or mirror relays, rangefinding will have to be tested to understand its strengths and weaknesses. It can likely be operated at the end of a standpipe, or even further off outside of containment, if necessary. In-depth analysis will have to be conducted, first off, to make sure that rangefinding represents a significant cost-benefit versus established techniques.

8.3.2   Total Internal Reflection Optical Switches

COTS TIR Optical Switches Summary

These optical switches are well represented in the marketplace, with many well-known corporations manufacturing and selling them. The list includes Kobold, Teklab, Honeywell, Dwyer Instruments, Madison, Omega, Gems Sensors & Controls, SensorTechnics, and many others. The configuration and make-up of these sensors have little variation from one vendor to another and many of them include plastic parts either in the sheath material or as gaskets or even as the TIR prism.

When specified, it seems that the TIR prism is often made from polysulfone, which has a maximum continuous service temperature of 160°C. Teklab and Gems Sensors manufacture TIR sensors with glass prisms; but because the detector is located near the end of the sensor, the maximum operating temperature is only 125°C. In fact, none of the manufacturers of these switches that we located were able to provide operation above 125°C except for Madison, which provides switches that function up to 140°C.

Gap Analysis

These switches are not manufactured for radiological or high-radiation environments and are not tested in these conditions. It is likely the prism material used in most commercial sensors is not suitable for either temperature or radiation. Also, most of these switches incorporate the LED and the photodetector in the sensor head itself. This means that these elements are under heavy exposure. Reconfiguration and different choices of materials would likely make these very robust; however, radiation hardness may not be the biggest challenge for these sensors. A significant question remains, however, regarding the reusability of these sensors after having been submerged for any period of time. Documentation from manufacturers typically specifies that these switches are suitable for "non-coating liquids" only. Buildup of coolant on the sensors would render them useless. Aside from physical replacement, there is no good solution to this problem that we are aware of.

Another significant setback is that any abrasion to the exposed optical prism will ruin its ability to reflect the light back to the sensor. Such damage is not repairable in-situ and would require replacement. Careful engineering could minimize the chances of abrasion by loose solids, but that hazard is not completely avoidable with this platform.

Technical Readiness Ranking

Optical switches are considered to have **LOW** technical readiness because there are too many unanswered questions regarding their performance under harsh conditions. There also may be fundamental limitations on their ability to function after being immersed in a liquid coolant.

Proposed Future Research Path

Given the low technical readiness and relatively low potential benefits of this technology, no future research is suggested at this time.

8.4 References

Amann M-C, T Bosch, M Lescure, R Myllyla and M Rioux. 2001. "Laser Ranging: A Critical Review of Usual Techniques for Distance Measurement." *Optical Engineering* 40(1):10-19.

Collis RTH. 1965. "Lidar Observation of Cloud." *Science* 149:978-981.

Northend CA, RC Honey and WE Evans. 1966. "Laser Radar (Lidar) for Meteorological Observations." *Review of Scientific Instruments* 37:393-400.

Zhao C, L Ye, J Ge, J Zou and X Yu. 2013. "Novel Light-Leaking Optical Fiber Liquid-Level Sensor for Aircraft Fuel Gauging." *Optical Engineering* 52:014402.

9.0   Coolant Contaminant Monitoring

Coolant and headspace gas monitoring in advanced small modular reactor (AdvSMR) designs represents a tremendous opportunity where optical sensing technology could make a major impact to critical reactor operations. Chemical monitoring systems are used to detect corrosion indicators and to maintain coolant corrosion control buffers. Noble gas taggants are monitored to detect fuel assembly damage. Fission products, produced during normal reactor operations, are carefully monitored to minimize staff radiological hazards. These monitoring systems are vital to maintain safe operations and the integrity of the reactor. Fission and noble taggant gases are typically captured on cold fingers or by carbon filtering. New AdvSMRs concepts will require better integration of sampling subsystems within the reactor vessel. In this section, we examine the feasibility of in-vessel coolant and headspace gas monitoring using powerful optical spectroscopy techniques.

Optical spectroscopies based on absorption (e.g., tunable laser and Fourier-transform infrared [FTIR]), emission (e.g., laser-induced breakdown spectroscopy [LIBS]), photo-thermal, Raman scattering, and others are well-established techniques that are used to detect and quantify trace elements or chemical compounds. There are numerous other optical-based chemical sensing approaches that have not been captured in this study, because they have limited maturity and commercial market penetration. However, these technologies are rapidly advancing, and it is likely the near-future outlook will improve for many.

The commercial sensing systems described in this section are commonly available with high sensitivity, selectivity, and fast response time for many gas, liquid, or solid chemical compositions. However, most high-resolution commercial off-the-shelf (COTS) systems are benchtop instruments used in research and under well-controlled industrial settings. Some COTS instruments feature compact, portable designs that provide standoff measurements, but systems typically target a limited user application set. However, many individual COTS components (e.g., tunable lasers, detection modules, processing electronics) are readily available to build customized and flexible sensing systems. While not a COTS instrument, it is likely that a modest research, development, and demonstration (RD&D) effort, followed by technology transfer to the commercial sector, could quickly bring these to the market to support AdvSMR coolant monitoring requirements. The technology readiness for COTS absorption and emission-spectrometer systems, for AdvSMR coolant monitoring, is **MEDIUM**. These technologies are ranked favorably because their noncontact standoff properties provide feasible AdvSMR deployment options, when combined with the standpipe viewport or fiber delivery concepts. The existing COTS systems must be ruggedized and customized to extend the current working temperature limits, shield against radiation exposure, and adapt to the specific AdvSMR deployment scenario.

Conceptually, gas-phase headspace and coolants are monitored using an open path, measurement approach. Several configurations are possible, based on optical beam paths that are introduced in-vessel, through an optical access port. Absorption spectroscopy can be used with an internal retroreflector or multi-pass absorption cell to probe target gas-phase chemical, path length integrated, concentrations. The beam is then directed back through the optical access port to an external optical detection and processing subsystem. It is possible that transparent liquid-coolant impurities could be probed directly using a subsurface retroreflector configuration. It may be feasible to directly probe molten metal surfaces using LIBS techniques. Na_2O and PbO_2 concentrations in liquid metal coolants could be monitored, for example. Other emission spectroscopy methods could be considered for monitoring noble gas and fission

gas concentrations, although this may not be feasible because of low gas concentrations, emission quenching, and high background light in the reactor vessel. While the feasibility of all these concepts must be vetted through RD&D studies, optical spectroscopy appears to be a very promising approach that could enable in-vessel coolant and cover gas monitoring.

Photo-thermal and Raman-scattering spectroscopy are promising techniques that have achieved high sensitivity performance primarily in research studies. These techniques are ranked **LOW** in technique readiness because COTS products are not available, pump-probe configuration (photo-thermal) is difficult to implement, and the signal strength (Raman-scattering) is weak. These disadvantages are likely to make deployment difficult to achieve in-vessel. Other more exotic optical techniques, not mentioned here, generally have **LOW** technical readiness, also primarily because of limited market penetration and COTS availability.

9.1   Coolant Contaminants

Coolant and headspace gas monitoring is conducted to manage corrosion processes and detect noble gas taggants and fission products. These monitoring systems are vital to maintain safe operations and the integrity of the reactor. In this subsection, we examine the major contaminant monitoring requirements by AdvSMR design. The feasibility of specific optical sensing techniques is then considered for each contaminant and coolant additive.

9.1.1   Sodium-cooled Fast Reactors

In sodium-cooled fast reactor (SFR) pool-type designs, the reactor vessel and top cover form the containment boundary and the structural support basis for the internal components. Inert argon serves as a cover gas between the reactor vessel cover and liquid-sodium layer. Molten sodium coolant has relatively low corrosive potential, leading to low in-vessel structural deterioration. Regardless, sodium-coolant chemistry must be monitored to detect corrosion indicators, ingress of outside chemical compounds, and fission and taggant noble gases. In current reactors, transfer loops circulate the coolant and cover gas to purification and monitoring systems external to the reactor vessel. Primary coolant and cover gas impurities are H_2O, and O_2 that can be introduced during startup, service and inspection, or by a subsystem or vessel breach. O_2 reacts with Na to form Na_2O, which is an undesirable impurity that tends to deposit onto surfaces and restrict and plug passageways. It also leads to mechanical erosion and reduces the overall coolant heat transfer performance. The impurities CO_2, H_2O, or He could be introduced, given simultaneous failure of the primary/immediate and immediate/secondary heat exchanger boundaries, although this is unlikely. Na has well-known exothermic reactions with CO_2 and H_2O, both liquid and vapor phase (Carlson 1994; Simon et al. 2007). CO_2 and H_2O undergo violent and energetic reactions with Na that could threaten reactor integrity. H_2 is liberated as Na reacts with H_2O. In the presence of O_2, a fire or catastrophic explosion could compromise the reactor vessel integrity and result in radioactive material release.

O_2 concentration measurements in the cover gas may be possible using absorption spectroscopy. It may be feasible to measure Na_2O directly in the Na coolant using LIBS. Most gas-phase impurities and compounds could be monitored in the cover gas using absorption (i.e., for CO_2, and H_2O) or emission (i.e., for noble and fission gases) spectroscopy techniques. Many molten metal coolants could possibly be monitored directly on the coolant surface using LIBS.

9.1.2   Lead-cooled Fast Reactors

Lead-cooled fast reactors share many of the same coolant and headspace gas monitoring requirements as sodium-cooled fast reactors. Molten lead and lead-bismuth coolants are significantly less chemically reactive than sodium. Molten Pb does not react chemically with water, but does react slowly with O_2 to form PbO_2. As a result, AdvSMR designs can use direct heat exchange with the nonreactive working fluid, thus completely eliminating the intermediate heat exchanger loop. Working fluids can be supercritical H_2O and supercritical CO_2. The dissolved O_2 content in lead-cooled fast reactors must be carefully balanced to minimize structural material corrosion. A proper dissolved O_2 fraction in the molten lead establishes and maintains a protective oxide barrier on stainless steels and low-alloy steels, which protects them from corrosion up to about 500°C (Smith 2010). Without this oxide barrier, nickel and other components of steel alloys are leached out and dissolved in the lead coolant over time. This process leads to embrittlement, cracking, and corrosion of the in-vessel components.

Dissolved O_2 in the Pb coolant may be in equilibrium with the O_2 in the cover gas; therefore, it may be feasible to infer dissolved O_2 concentration from headspace O_2 concentration measurements using absorption spectroscopy. Alternatively, it may be feasible to measure PbO_2 concentration directly in the coolant using LIBS. Most gas-phase impurities and compounds could be monitored in the cover gas using absorption (i.e., for CO_2, and H_2O). Many molten metal coolant impurities (e.g., corrosion indicators, polonium, and transmuted bismuth) could possibly be monitored directly on the coolant surface using LIBS.

9.1.3   Gas-cooled Fast Reactors and Very High-temperature Gas Reactors

Helium, used in gas-cooled fast reactors (GFRs), high-temperature gas-cooled reactors (HTGRs), and very high-temperature gas reactors (VHTRs), is intrinsically nonreactive; however, gas impurities must be carefully monitored to protect reactor components from corrosion (Wright 2006). Studies in operational helium-cooled reactors have shown that reactor chromium alloys can be protected against corrosion by maintaining surface Cr_2O_3 layers, but corrosive oxidation and carbon activity (enhancement/reduction) is dependent on the temperature, metal alloy, and gas-impurity concentrations. Most of the gas impurities, including water vapor, CO, CO_2, H_2, CH_4, and O_2, are well known indicators of the chromium corrosion process. Monitoring the relative concentrations of these gases can help manage and prevent stress corrosion cracking in normally ductile metals (Natesan et al. 2003).

Most gas-phase impurities (e.g., CO, CO_2, H_2, CH_4, and O_2) could be monitored directly in the gas coolant using absorption spectroscopy techniques. Cesium is an indicator of fuel damage and tends to deposit throughout the reactor vessel to become a dangerous gamma source. Noble, fission, and tritium-compound (i.e., HT or TF) gases will likely be difficult to detect using optical spectroscopy. In may be possible to detect cesium deposits directly on surfaces using LIBS.

9.1.4   Molten Salt Reactors

Molten salts are known for their chemical stability under high temperatures and radiation exposure. The chemistry must be monitored to maintain efficient heat transfer properties and limit corrosion processes. There are many compounds under consideration for molten salt reactor coolants, such as LiF-BeF_2, NaF-KF-ZrF_4, LiCl-KCl, and KF-KBF_4 (Forsberg et al. 2005; Sabharwall et al. 2011). A detailed list is provided in Table 2.2. Criteria for selection include chemical compatibility, thermal conductivity, and melting point. Molten salt test reactor studies in the 1970s demonstrated minimal corrosion issues

between the coolant and in-vessel components; however, it is unclear whether these results can be extrapolated to AdvSMR designs (Rosenthal et al. 1970). Metal corrosion can be controlled in LiF-BeF_2 coolants by purging the molten salt bath with H_2/HF. Sulfide reduction (from sulfur impurities in BeF_2) can generate to H_2S, which accelerates corrosion. LiF-BeF_2 coolants also present a challenge from free fluorine, released because of transmutation of the Be under radiation (McCarthy et al. 1998; Sharpe 2006). Fluorine monitoring and maintaining a redox buffer are critical to prevent aggressive fluorine attack of in-vessel structural materials. A recent research study of the LiF-NaF coolant showed strong oxidation of chromium and corrosion of tungsten in steel alloys, from dissolved oxygen and fluorine, leading to structural component weakening and corrosion (GIF 2011). Coolant contamination by oxide and ferric ions was also shown to increase this effect. Cesium and noble gases in the coolant is a fuel-damage indicator. NaK is an indication of ruptured impulse lines or transducer housings. Tritium is produced in molten salt coolants containing the ^6Li isotope. At elevated temperature, many metal compositions can become permeable to tritium gas, resulting in loss of containment.

Most gas-phase impurities and additives (e.g., O_2, H_2O, HF, H_2S, F_2, NaK, CrF_2, and other corrosion indicators) could be monitored directly in the cover gas or possibly within the coolant using absorption spectroscopy techniques. Emission spectroscopy could be used to detect H_2 gas, but noble, fission, and tritium-compound (i.e., HT or TF) gases will likely be difficult to detect using optical spectroscopy. In may be possible to detect cesium deposits directly on surfaces using LIBS.

9.1.5   Supercritical Water-cooled Reactors

Supercritical water-cooled reactor (SCWR) designs are expected to provide a higher range of operating temperatures and thermal efficiencies than light-water reactors (LWRs). Supercritical water, like sub-critical water, undergoes radiolysis to produce oxygen and hydrogen peroxide, which can lead to corrosion within the reactor vessel. H_2 can be added to the reactor coolant to suppress dissociation of water, but the effect is not well understood under supercritical conditions (Meesungnoen et al. 2010). The pH environment in SCWRs influences the corrosion potential, rate, and to some extent the mode. In pressurized water reactors, LiOH is used as an additive to raise pH, but the same approach is not well characterized for SCWRs (Carvajal-Ortiz et al. 2012). Inorganic materials, either from impurities in the coolant intake or from corrosion, are insoluble in supercritical water. As a result, inorganic impurities are deposited on reactor surfaces, potentially affecting the thermal conductivity and structural stability of the fuel cladding (Svishchev and Guzonas 2011).

The radiolysis products, O_2 and H_2O_2, possibly could be monitored directly in the coolant using absorption spectroscopy techniques. It may be possible to detect impurity deposits directly on surfaces using LIBS.

9.2   Absorption-based Optical Spectroscopy

9.2.1   Fundamentals of Operation

Optical spectroscopy is a powerful analytical method used to detect and identify chemicals in gases, liquids, or solids. Many chemical compounds have strong and sharp electronic or vibrational and rotational absorption features that can be used as a spectral "fingerprint" to identify chemical compounds with high confidence. This spectroscopy method measures the absorption of optical radiation by chemical compounds, as a function of wavelength. The optical radiation used to probe the chemical

compounds is produced by broadband light sources or laser sources. The wavelength range of broadband sources can span across UV, visible, and infrared spectral regions, depending on the application. Laser sources have a very narrow wavelength tuning range in comparison. Tuning ranges for visible lasers are typically 1 nm to 2 nm, while long-wave infrared lasers are as large as 500 nm. An absorption spectrum can be obtained using few basic steps. A background spectrum of the source is first collected. Next, the sample spectrum are collected by incrementing the source wavelength and then measuring the transmitted optical power. This are repeated until the entire desired wavelength range is scanned. The sample spectrum is divided by the background spectrum to yield the transmission spectrum, which is converted to the absorption by taking the logarithm. The absorption spectrum is compared to a library chemical spectra database to identify chemical compounds and estimate their concentrations. Lasers are selected with a tunable wavelength range that overlaps absorption bands associated with the chemical of interest. Tunable lasers commonly have a very narrow linewidth and high brightness. The linewidth establishes the resolution of the spectral absorption measurement. This is a major advantage, because a large spectrometer instrument, commonly associated with broadband source configurations, is not needed. In some cases, the detection sensitivity can scale with laser brightness. Both factors lead to a more compact measurement system.

COTS laser absorption spectroscopy systems have been successfully developed using a wide range of wavelength-tunable laser sources. Tunable diode lasers absorption spectroscopy (TDLAS) has a demonstrated detection limit at part-per-million-meter (ppm-m) in the near infrared (IR) spectral region (Frisch et al. 2005). Atmospheric measurements are usually given in ppm-m, which is total concentration of chemical species encountered by the laser beam in a 1-meter path. Recent developments in mid-IR quantum cascade laser technology has enabled a part-per-billion-meter (ppb-m) detection limit for many chemical compounds (Frisch et al. 2008). Cavity-enhanced absorption spectroscopy can improve sensitivity by increasing interaction path length, because sensitivity scales with interaction of path length. This can be achieved using a multi-pass absorption cell, such as a Herriott cell. A Herriott cell uses opposing high-reflectance mirrors to reflect the laser beam many times between the mirrors. Sample gas is introduced into the absorption cell to interact with the multi-pass laser beam. A 1-m-long, high-reflectivity Herriott cell can increase the path length and sensitivity by more than 100 times. Other techniques, such as cavity ring-down absorption spectroscopy can also achieve ppb detection limits (Awtry and Miller 2002).

Other optical absorption spectroscopy methods use a broadband optical source and an optical detector with a large wavelength response range. Unlike the preceding TDLAS example, a broadband source does not provide optical resolution, so a wavelength-resolving spectrometer is required. Spectrometers can resolve wavelengths using optical-filter wheels, diffraction gratings, dispersion prisms, and interferometer configurations. FTIR spectroscopy is a common method that uses a scanning interferometer to resolve broadband optical signals. Commercial FTIR systems are available as laboratory and open-path field instruments. The open-path FTIR spectroscopy instruments provide a standoff technique to measure gas-phase chemicals at a distance. Open-path FTIR spectroscopy has been used for remote atmospheric gas analysis and environmental monitoring for over 40 years (Griffiths et al. 2008). Open-path FTIR spectroscopy instruments can be used in both active and passive modes. In an active mode, a broadband light source passes through the sample and the absorption spectrum of the sample is measured. In a passive mode, an external blackbody source (i.e., sun) is used for the spectral absorption measurement. Open-path FTIR spectrometry can achieve low ppb detection limits for some compounds (EPA 2013). While FTIR spectroscopy is very promising, laser absorption spectroscopy may be more appropriate for

in-vessel coolant and headspace gas monitoring. Compared to laser absorption spectroscopy, FTIR spectroscopy has lower sensitivity and limited spectral resolution, unless a large laboratory instrument is used. It is difficult to collect a reference spectrum using standoff FTIR spectrometry, and the high thermal background in the reactor vessel would add noise to a normal single-beam FTIR absorption measurement. Given the appropriate RD&D, all these limitation could be resolved.

9.2.2 Absorption Spectra of Coolant and Cover Gas Impurities

A summary of key gas impurities and their corresponding optical absorption peaks are given in Table 9.1. The optical absorption spectrum for each impurity is shown in Figure 9.1. It is important to note that the optical absorption linewidths and line positions are subject to pressure, temperature, and chemical reactions. Gaseous compounds that are injected into the reactor vessel to control corrosion are also included in this assessment.

Table 9.1. Important Gas-Phase Impurities and Useful Optical Absorption Peaks

Coolant	Primary Source	Compound	Useful Optical Absorption Peaks[a]
Sodium	Primary/Secondary coolant exchanger leak	H_2O	H_2O: **5.4–7.4 µm**, **2.4–2.8 µm**
		CO_2	CO_2: **4.2–4.4 µm,** 2.70 µm, 2.08 µm, 1.93 µm
	Initial startup	O_2	O_2: 1.30 µm, **0.76 µm**, 0.68 µm
	Service, inspection ingress		
Lead	Primary/Secondary coolant exchanger leak	H_2O	H_2O: **5.4–7.4 µm**, **2.4-2.8 µm**
Lead Bismuth		CO_2	CO_2: **4.2–4.4 µm,** 2.70 µm, 2.08 µm, 1.93 µm
	Initial startup	O_2	O_2: 1.30 µm, **0.76 µm**, 0.68 µm
	Service, inspection ingress		
	Coolant dissolved oxygen equilibrium	O_2	O_2: 1.30 µm, **0.76 µm**, 0.68 µm
Helium	Chromium corrosion process	H_2O	H_2O: **5.4–7.4 µm**, **2.4–2.8 µm**
		CO_2	CO_2: **4.2–4.4 µm,** 2.70 µm, 2.08 µm, 1.93 µm
		CO	CO: **4.7–4.4 µm, 2.40 µm, 1.60 µm, 1.20 µm**
		H_2[b]	H_2: --
		CH_4	CH_4: **7.3–8.1 µm, 3.3–3.6 µm,** 1.69 µm
		O_2	O_2: 1.30 µm, **0.76 µm**, 0.68 µm
Molten Salt: LiF-BeF$_2$	Sparging gases to control corrosion	H_2[b]	H_2: --
		HF	HF: **2.4–2.7 µm,** 1.34 µm, 0.90 µm
NaF-KF-ZrF$_4$ LiCl-KCl KF-KBF$_4$	Sulfide reduction, from sulfur impurities in BeF$_2$	H_2S	H_2S: **6.5–10 µm,** 3–5 µm, **2.5–2.8 µm,** 1.80 µm, 1.45 µm
	Fluoride reaction with H_2O, producing HF and O_2	H_2O	H_2O: **5.4–7.4 µm**, **2.4–2.8 µm**
and others		O_2	O_2: 1.30 µm, **0.76 µm**, 0.68 µm
		HF	HF: **2.4–2.7 µm,** 1.34 µm, 0.90 µm
	Transmutation of Be	F_2	F_2: **0.28 µm**
Supercritical H_2O	Injected to reduce H_2O radiolysis	H_2[b]	H_2: --
	High temperature radiolysis byproducts	O_2	O_2: 1.30 µm, **0.76 µm**, 0.68 µm
		H_2O_2	H_2O_2: **7.4–8.5 µm,** 3.8–4.0 µm, **2.8–3.4 µm**

(a) Strong peaks shown in bold.

(b) Hydrogen is a homonuclear diatomic molecule and therefore has no rotational or vibrational absorption spectra. There are some higher electronic states, but transition to these would require vacuum ultraviolet wavelengths.
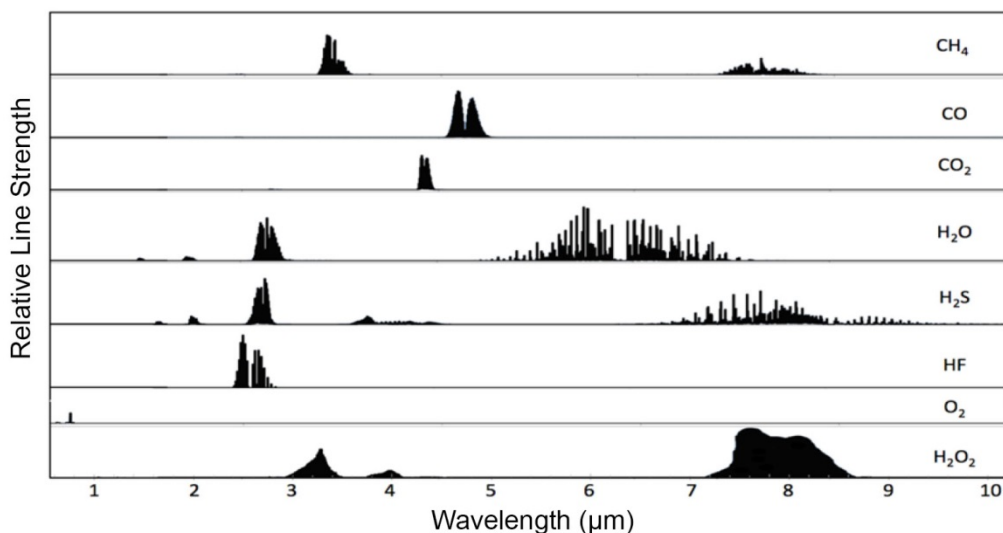
Figure 9.1.   Optical Absorption Spectra for Common Impurities, Showing Major Peaks Between 0.5 to 10 µm

9.2.3   Promising Research and Development

Fission gases and fuel pin taggant gases are not considered in the above summary, because the ground state electronic transitions of these noble gases lack strong optical absorption spectra at usable wavelengths. However, noble gases can exhibit strong electronic transitions from excited states at the visible and near-infrared wavelengths. These excited states can be efficiently populated in discharge plasma. Monitoring of xenon in the cover gas of sodium fast reactors using laser absorption spectroscopy was recently demonstrated (Jacquet and Pailloux 2013). In this study, a high-voltage direct current (DC) power supply was used to discharge a mixture of xenon and argon cover gas that was purged into a special flow cell. A detection limit of 60 ppb in molar ratio was achieved. However, this study was conducted in a flow cell with pressure in the range of 60–350 Pa, which is significantly lower than in-vessel pressures in AdvSMRs. For online measurement, pressure broadening would make it difficult to resolve absorption lines of noble gas excited electronic states. Further study will be needed to demonstrate noble gas absorption measurement in AdvSMR environments.

9.2.4   COTS Summary, Gaps Analysis, Technical Readiness Ranking, and Suggest Future Research

COTS Absorption Spectrometer and FTIR Summary

COTS chemical detection systems, based on TDLAS, are available from a few companies including Physical Science Inc., GE Measurement and Control, Ametek, Protea, and other vendors. Many of these systems can detect gases such as C_2H_2, H_2S, NH_3, CO_2, CO, O_2, and NOx at the ppm level. Most of these systems draw chemical sample vapors into an absorption cell, where a wavelength-tuned laser beam interacts with chemical vapor. Some designs circulate the sample back to the source after filtration. Typically a few parts-per-million volume (ppm_v) detection limit can be achieved in short integration times. However, all the systems are bulky benchtop type instruments except a system available from

Physical Science Inc. This instrument is designed as a hand-carried instrument that senses target vapors along the path between the instrument and a target surface up to 30 m away.

Companies such as Block Engineering, Daylight Solutions, Cascade Technology, and Physical Science Inc., provide measurement instruments that use mid-wave and long-wave infrared quantum cascade lasers (QCLs) to probe strong rotational and vibration absorption features (i.e., the molecule "fingerprint" region), common in most molecular compounds. Sensitivity at ppm_v to ppb_v is specified for many COTS QCL-based sensor systems. Most systems also require constant gas flow through the absorption cell to analyze target chemical vapors. Block Engineering provides a portable, standoff QCL spectrometer instrument for measuring vapors, liquid, and solid samples.

Many companies, including Bruker, Block Engineering, Industrial Monitoring and Control Corporation, Kassay, Cerex, OPTRA, and others, are COTS vendors for long-range, standoff FTIR spectrometers. Many of these systems are tripod-mounted units and require cryogenically cooled infrared detectors. Some systems can be configured with room-temperature detectors, at the expense of detection sensitivity. As discussed above, laser absorption spectroscopy may have configuration and performance advantages over FTIR spectroscopy for the AdvSMR application. Further study is required to fully determine comparative advantages of FTIR spectroscopy.

Some COTS laser absorption spectroscopy instruments can be operated up to 70°C, which meets the containment vessel headspace deployment requirements. Other systems have lower temperature limits and may require active cooling for contamination vessel deployment. No COTS spectroscopy instruments were identified with radiation-tolerance specifics, but this is not surprising given their intended application space. It is feasible that a ruggedized, semi-custom COTS instrument could be successfully configured with the standpipe viewport or fiber-optic access concept. Cascade Technology offers a QCL benchtop spectrometer instrument with vapor sampling up to 450°C; however, benchtop instruments that need to draw samples into their internal evaluation cells are not likely compatible with the AdvSMR integral designs. Standoff instruments are generally suitable for measuring hot vapors as long as the instruments themselves are isolated from excessive temperatures.

Gaps Analysis

- The current systems are usually bulky in size. Compact systems are available at the expense of detection sensitivity.

- Because it is absorption-based, any optical component used along the beam path, including windows and lenses, needs to be carefully selected and characterized for absorption and to avoid overlapping signature regions of chemicals under detection.

- Optical alignment, especially when a cavity-enhanced method is used, is critical and will be affected by reactor thermal cycles and vibrations.

- Pressure broadening of gas-phase absorption measurements may limit performance.

- Feasibility and detection limits uncertain for optical impurity monitoring in coolants and cover gas must be determined.

- Concepts must be developed to minimize coolant vapor deposits on optical surfaces.

- Absorption measurements will require better knowledge of the transparency of molten salts.

- Actual performance and benefits of optical-based coolant monitoring must be determined.

- Service-lifetime and performance of in-vessel components under AdvSMR deployment conditions must be determined.

Technical Readiness Ranking

The technology readiness for COTS laser absorption spectrometry systems, for AdvSMR coolant monitoring, is **MEDIUM**. Some compact standoff designs are available for other applications. Modest RD&D efforts will be needed to build customized standoff systems using existing COTS components (e.g., tunable lasers, detection modules, and processing electronics), and technology transfer efforts are needed to bring customized systems to the commercial sector. Considerable reactor engineering design effort will be required to develop and demonstrate concepts that provide optical access into the reactor vessel.

Proposed Future Research

Standoff-absorption spectrometers hold promise for in-vessel chemical detection if the gaps are addressed. Rapid developments in laser and detector miniaturization for many other applications would help to enable high-sensitivity systems in compact packages. Future research is suggested in the following areas:

- Study cover gas, coolant, and contaminant spectral signatures.

- Select the most suitable spectra for optimized instrument designs.

- Study noble gas excited-state absorption signatures in AdvSMR conditions.

- Design and develop engineering solutions to enable optical access and precision alignment.

- Evaluate feasibility of molten salt coolant impurity monitoring using optical spectroscopy.

9.3 Emission-based Optical Spectroscopy

9.3.1 Fundamentals of Operation

Many fission gases and fuel-pin taggant gases may also be detected by atomic emission. The emission spectra of noble gas ions have signature peaks in visible wavelengths that can be easily detected optically. Strong ionizing radiation is well known to ionize noble gases (Leffert et al. 1966). Fission chambers or ionization chambers rely on this phenomenon. Alternatively, ionization of noble gases can be actively induced by a high-voltage electric spark. Noble gases are frequently used in discharge tubes for many purposes from lighting, such as neon lights, to switching.

Another powerful emission-based optical technique is LIBS. LIBS uses a short-pulse-length, high-energy laser to atomize and ionize small quantities of the target material. The atomization process produces a small plasma that is localized at the focal plane of the focused laser beam. The plasma contains excited neutral and ionized atoms that were formerly chemical compounds on the sample surface. Within nanoseconds after the laser atomization pulse, atomic emission occurs from each constituent atom, as the excited atoms return to lower energy levels. The emission wavelength is directly proportional to the difference between the upper and lower electronic energy level. Using a

high-resolution spectrometer, each emission spectrum can be analyzed to identify all elements in the sample. Standoff LIBS configurations have been successfully demonstrated to greater than 100 m. Emissions can be collected using an optical telescope receiver or by using optical fiber. LIBS techniques have been demonstrated to measure oxygen concentration in solids including coal (Yin et al. 2012) and silicon (Ji et al. 2010), and gaseous fuel (Dackman et al. 2008). Detection limits at ppm and greater are commonly achieved using LIBS. Only small sample quantities are consumed during the LIBS measurement, so the technique can be considered essentially nondestructive.

For the AdvSMR application, LIBS could be used to atomize and analyze deposits on metal surfaces and possibly directly on liquid metal coolant surfaces. For example, LIBS could be a viable technique to measure Na_2O and PbO_2 concentrations in coolants by direct interrogation at the coolant surface. Noble and fission gases could possibly be detected by conducting LIBS measurements directly on carbon filters or cold finger traps.

9.3.2   Promising Research and Development

LIBS technique has been used to break down solids, liquids, and gases. In many experiments on gas-phase LIBS using nanosecond lasers, signal stability has been an issue. The recent development in gas-phase LIBS technique using femtosecond laser achieved below 1 percent standard deviation on signal stability for Krypton gas, a significant improvement compared to 5 percent in helium and 60 percent in air using longer laser purses (Heins and Guo 2012). In a separate study, a 78-ppm detection limit was achieved for helium using LIBS (Eseller et al. 2012). Both experiments were performed in atmosphere or higher pressures, which improves the promises of in-vessel gaseous contaminant detection using LIBS technique.

9.3.3   COTS Summary, Gaps Analysis, Technical Readiness Ranking, and Suggest Future Research Path

COTS Emission Spectrometer and LIBS Summary

The most common application for optical emission spectroscopy is in the metal production industry, such as steel foundries and aluminum plants. There are a vast number of other markets and applications for emission spectroscopy. Many COTS optical emission spectrometer designs use a spark gap configuration to atomize the sample. There are many benchtop, laboratory optical emission spectrometers available as COTS systems from companies such as Bruker, Thermo Scientific, OXFORD Instruments, Vericheck, and others. Several portable optical emission spectrometers are available from SPECTRO Analytical Instruments Inc., Spectro, Romquest, and others. However, most instruments are marketed for quick qualitative assessment and do not have the resolution for high-sensitivity measurements. If noble gases inside the vessel are autoionized by the reactor radiation flux, then passive, standoff monitoring is feasible using one of a large selection of COTS emission spectroscopy instruments. The spark-gap measurement configuration is unlikely feasible for in-vessel deployment.

Benchtop LIBS instruments and discrete components (i.e., COTS pulsed lasers and high-resolution spectrometers) are available from many companies, including Applied Spectra, Ocean Optics, TSI, Avantes, and others. LIBS systems may have maximum working temperature limits below 45°C and may require active cooling for contamination vessel deployment. Standoff LIBS systems have been developed largely by research institutes, such as Army Research Laboratory, NASA, the University of Central

Florida, and at least one commercial company, Applied Photonics Inc. Standoff LIBS systems are usually large, bulky, and mounted on carts. However, the Mars Curiosity Rover mission fielded an extremely compact standoff LIBS system (i.e., the ChemCam spectrometer) to analyze rocks and solid samples.

Gaps Analysis

- The current COTS systems are mostly benchtop systems or low-resolution portable systems that may not be suitable for the AdvSMR application.

- Optical alignment is critical and will be affected by reactor thermal cycles and vibrations.

- Feasibility and detection limits uncertain for optical impurity monitoring in coolants and cover gas must be determined.

- Service-lifetime and performance of in-vessel components under AdvSMR deployment conditions must be determined.

- Concepts must be developed to minimize coolant vapor deposits on optical surfaces.

- Using emission spectroscopy or other optical spectroscopy methods to detect and monitor fission gases and taggant gases is unlikely.

- It is uncertain that sufficient Na_2O and PbO_2 in coolants can be liberated by LIBS and concentrations can be measured.

Technical Readiness Ranking

The technology readiness for COTS emission-based spectrometer systems, for AdvSMR coolant monitoring, is **MEDIUM**. The existing portable spark-induced optical emission spectrometers lack the sensitivity required to detect ppm level of fission gases and taggant gases. Standoff LIBS systems are bulky and cumbersome to use. Significant RD&D will be needed to demonstrate standoff measurement using compact high-sensitivity systems in AdvSMR conditions. Considerable reactor engineering design effort will be required to develop and demonstrate concepts that provide optical access into the reactor vessel.

Proposed Future Research

- Demonstrate standoff coolant impurity monitoring using laser-induced breakdown optical spectroscopy.

- Study emission spectral signatures of chemicals to be detected in the cover gases and coolants. Select suitable spectra for optimized detection system design.

- Demonstrate and measure Na_2O and PbO_2 in coolants using LIBS.

9.4   Raman Spectroscopy

9.4.1   Fundamentals of Operation

Raman scattering is an inelastic scattering process, in which a relatively small portion of scattered light is shifted to a higher or lower wavelength (designated as the Stokes or anti-Stokes shift). This is

contrasted to the dominant Rayleigh scattering effect, in which photons are elastically scattered without experiencing a wavelength shift (Hollas 1992). A key advantage to Raman spectroscopy is that the probe laser wavelength can remain fixed, while the Stokes and anti-Stokes shift are optically resolved by a spectrometer instrument, as the case for LIBS emission analysis.

The primary challenge for this approach is the weak Raman signals. Raman scattering is roughly 1000 times weaker than Rayleigh scattering. The Raman weak signal requires significant amplification and signal processing to obtain sufficient signal-to-noise (Hendra and Vear 1970). It is also well known that Raman scattering efficiencies are greatest under ultraviolet wavelength excitation, because scattering efficiency is proportional to wavelength times 10^{-4}. Surface-enhanced Raman scattering (SERS) has been demonstrated to have significantly higher Raman signal. SERS uses textured or particle-shaped metals in contact with the Raman scatterer to amplify the Raman signal by localized surface plasmons (Kelley 2010). Raman techniques have been demonstrated to detect dilute impurities in water (Li et al. 2009).

For the AdvSMR application, Raman scattering spectroscopy could possibly be used to analyze deposits on metal surfaces and chemical compounds directly on or in liquid coolants. The weak Raman signals are likely to make this technique less feasible, compared to other optical spectroscopy methods.

9.4.2   Promising Research and Development

A research study recently used an external optical cavity configuration to enhance Raman signals. When a laser is frequency-stabilized to a resonance frequency of this external cavity, light can be efficiently coupled into the cavity and power build up can occur by several orders of magnitude. Sample gas is pumped into the optical cavity to interact with the intense laser light. A recent study demonstrated low ppm or even ppb level detection limit using cavity-enhanced Raman spectroscopy to detect H_2, N_2, and other gases (Salter et al. 2012). In this experiment, a 10-mW single-mode diode laser at 635 nm was used. The cavity-enhancement technique allowed a power build-up of three orders of magnitude. Low power consumption components will enable compact and portable instruments for standoff measurements required in AdvSMR applications.

9.4.3   COTS Summary, Gaps Analysis, Technical Readiness Ranking, and Proposed Future Research Path

Raman spectroscopy is a powerful analysis tool that is used by bioprocessing, pharmaceutical, semiconductor, and forensics industries. Benchtop Raman spectrometers are available from companies such as OPTRA, Horiba, Renishaw, and others. Portable Raman probes and analyzer modules that enable standoff detections are available from SciApe, InPhotonics, Keiser Optical System, and others.

Raman-scattering spectroscopy is ranked **LOW** in technology readiness. The Raman signals are extremely weak and the large standoff requirement of the AdvSMR application is likely to make remote Raman signal collection challenging. In addition, the high sensitivity performance reported in the literature research studies have not been realized in COTS products. The feasibility of the cavity-enhanced Raman technique is questionable, because sample gas must be drawn from the reactor vessel or sampling loop. Given the low ranking, future research for AdvSMR should be a low priority.

9.5   Other Promising Techniques

There are various techniques that could be useful for reactor coolant monitoring, given additional technology maturity. One such technique is two-laser photo-thermal spectroscopy. This technique uses a strong pulsed laser (known as the pump) to excite target chemical vapors. The laser wavelength is in resonance with a strong absorption feature of the target chemical. Excitation induces localized vapor heating that generates refractive index gradients in the vapor. A nonresonant probe laser directed through the heated vapor and chemical detection is inferred by probe-laser deviation (as measured by optical transmission loss) by the thermal gradients. A similar configuration, called photo-acoustic spectroscopy, detects the acoustic sound wave generated by the expanding heated vapor. Photo-thermal spectroscopy can be extremely sensitive, because signal strength scales with the pump laser power. Another advantage is that the pump and probe lasers wavelength can be completely different, allowing clear separation of pump and probe heating and detection channels (Bialkowski 1995).

Photo-thermal spectroscopy systems are not available as COTS monitoring systems and the pump-probe configuration may be difficult to deploy in-vessel. Many research groups have developed custom photo-thermal spectroscopy systems with impressive performance. Given more maturity, technology transfer, and commercialization, this approach may see a promising future.

9.6   References

Awtry AR and JH Miller. 2002. "Development of a CW-Laser-Based Cavity-Ringdown Sensor Aboard a Spacecraft

for Trace Air Constituents." *Applied Physics B* 75:255-260.

Bialkowski SE. 1995. *Photothermal Spectroscopy Methods for Chemical Analysis*. Wiley, New York, New York.

Carlson DE. 1994. *Preapplication Safety Evaluation Report for the Power Reactor Innovative Small Module (PRISM) Liquid-Metal Reactor Final Report*. NUREG-1368, U.S. Nuclear Regulatory Commission, Washington, D.C.

Carvajal-Ortiz RA, A Plugatyr and IM Svishchev. 2012. "On the pH Control at Supercritical Water-Cooled Reactor Operating Conditions." *Nuclear Engineering and Design* 248:340-342.

Dackman M, JW Lewis, Y-L Chen and CG Parigger. 2008. "Laser-Induced Breakdown Spectroscopy for Measurement of Fuel/Oxygen Mixing in Combustion." In *Digital Holography and Three-Dimensional Imaging*. March 17-19, 2008, St. Petersburg, Florida. DOI 10.1364/BIOMED.2008.JMA22. Optical Society of America. Paper JMA22.

EPA. 2013. *Open Path Technologies: Measurement at a Distance OP-FTIR*. 2013. Thesis, U.S. Environmental Protection Agency (EPA), Washington, D.C. Available at http://clu-in.org/programs/21m2/openpath/op-ftir/.

Eseller KE, F-Y Yueh, JP Singh and N Melikechi. 2012. "Helium Detection in Gas Mixtures by Laser-Induced Breakdown Spectroscopy." *Applied Optics* 51(7):B171-B175.

Forsberg CW, PF Peterson and DF Williams. 2005. "Practical Aspects of Liquid-Salt-Cooled Fast-Neutron Reactors." In *American Nuclear Society - International Congress on Advances in Nuclear Power Plants 2005 (ICAPP'05)*, pp. 3197-3209. May 15-19, 2005, Seoul, Republic of Korea. American Nuclear Society, La Grange Park, Illinois.

Frisch MB, RT Wainner, BD Green, MC Laderer and MG Allen. 2005. "Standoff Gas Leak Detectors Based on Tunable Diode Laser Absorption Spectroscopy." Presented at *SPIE Optics East*, October 23-26, 2005, Boston, Massachusetts. Available at http://www.psicorp.com/pdf/library/sr-1239.pdf .

Frisch MB, RT Wainner, MC Laderer, BD Green and MG Allen. 2008. "Standoff and Miniature Chemical Vapor Detectors Based on Tunable Diode Laser Absorption Spectroscopy." Paper No. 162. http://www.psicorp.com/pdf/library//SR-1343.pdf.

GIF. 2011. *Annual Report 2011, Gen IV International Forum*. Gen IV International Forum (GIF), Paris, France.

Griffiths PR, L Shao and AB Leytem. 2008. "Completely Automated Open-Path FT-IR Spectrometry." *Analytical and Bioanalytical Chemistry* 393(1):45-50.

Heins AM and C Guo. 2012. "High Stability Breakdown of Noble Gases with Femtosecond Laser Pulses." *Optics Letters* 37(4):599-601.

Hendra PJ and CJ Vear. 1970. "Laser Raman Spectroscopy: A Review." *Analyst* 95:321-342.

Hollas JM. 1992. *Modern Spectroscopy*. John Wiley & Sons, Chichester, England.

Jacquet P and A Pailloux. 2013. "Laser Absorption Spectroscopy for Xenon Monitoring in the Cover Gas of Sodium Cooled Fast Reactors." *Journal of Analytical Atomic Spectrometry* 28(8):1298-1302.

Ji Z-G, J-H Xi and Q-N Mao. 2010. "Determination of Oxygen Concentration in Heavily Doped Silicon Wafer by Laser Induced Breakdown Spectroscopy." *Journal of Inorganic Materials* 25(8):893-896.

Kelley AM. 2010. "Hyper-Raman Scattering by Molecular Vibrations." *Annual Review of Physical Chemistry* 61:41-61.

Leffert CB, DB Rees and FE Jamerson. 1966. "Noble Gas Plasma Produced by Fission Fragments." *Journal of Applied Physics* 37(1):133-142.

Li G, M Chen and T Wei. 2009. "Application of Raman Spectroscopy to Detecting Organic Contaminant in Water." In *Proceedings - 2009 IITA International Conference on Control, Automation and Systems Engineering, CASE 2009*, pp. 493-495. July 11-12, 2009, Zhangjiajie, China. DOI 10.1109/CASE.2009.149. IEEE Computer Society, Piscataway, New Jersey.

McCarthy K, M Sawan, D-K Sze, M Tillack, A Ying and S Zinkle. 1998. *Flibe Assessment Summary*. Accessed June 3, 2013. Available at http://www.fusion.ucla.edu/apex/meeting5/2sze1198.pdf.

Meesungnoen J, DA Guzonas and J-P Jay-Gerin. 2010. "Radiolysis of Supercritical Water at 400 C and Liquid-like Densities near 0.5 g/cm^3 - A Monte Carlo Calculation." *Canadian Journal of Chemistry* 88:646-653.

Natesan K, A Purohit and SW Tam. 2003. *Materials Behavior in HTGR Environments*. NUREG/CR-6824, Argonne National Laboratory, Argonne, Illinois.

Rosenthal MW, PR Kasten and RB Briggs. 1970. "Molten-Salt Reactors - History, Status, and Potential." *Nuclear Applications and Technology* 8:107-117.

Sabharwall MP, M Patterson, ES Kim and M Mckellar. 2011. "Small Modular Molten Salt Reactor (SM-MSR)." In *The ASME 2011 Small Modular Reactors Symposium (SMR2011)*, pp. 31-39. September 28-30, 2011, Washington, D.C. American Society of Mechanical Engineers, New York, New York.

Salter R, J Chu and M Hippler. 2012. "Cavity-Enhanced Raman Spectroscopy with Optical Feedback CW Diode Lasers for Gas Phase Analysis and Spectroscopy." *Analyst* 137(20):4669-4676.

Sharpe P. 2006. "Recent Progress in Flibe Chemistry Control, Corrosion, and Tritium Behavior." Presented at *HAPL Program Meetings ORNL*, March 21-22, 2006, Oak Ridge, Tennessee.

Simon N, C Latge and L Gicquel. 2007. "Investigation of Sodium-Carbon Dioxide Interactions with Calorimetric Studies." In *International Congress on Advances in Nuclear Power Plants - ICAPP 2007, The Nuclear Renaissance at Work*, pp. 2996-3003. May 13-18, 2007, Nice, France. Curran Associates, Inc., Red Hook, New York. Paper #7547.

Smith CM. 2010. *Lead-Cooled Fast Reactor (LFR) Design: Safety, Neutronics, Thermal Hydraulics, Structural Mechanics, Fuel, Core, and Plant Design*. LLNL-BOOK-424323, Lawrence Livermore National Laboratory, Livermore, California.

Svishchev IM and DA Guzonas. 2011. "Supercritical Water and Particle Nucleation: Implications for Water Chemistry Control in a GEN IV Supercritical Water Cooled Nuclear Reactor." *Journal of Supercritical Fluids* 60:121-126.

Wright RN. 2006. *Kinetics of Gas Reactions and Environmental Degradation in NGNP Helium*. INL/EXT-06-11494, Idaho National Laboratory, Idaho Falls, Idaho.

Yin WB, L Zhang, L Wang, L Dong, WG Ma and ST Jia. 2012. "Research on Accurate Measurement of Oxygen Content in Coal Using Laser-Induced Breakdown Spectroscopy in Air Environment." *Guang Pu Xue Yu Guang Pu Fen Xi* 32(1):200-203.

10.0 Optical Vibrometers

Vibration monitoring is used in many nuclear reactor applications. Loose parts monitoring systems and pumps use accelerometers to measure vibration anomalies associated with loose parts in the coolant flow or pending mechanical failure in pumps and other rotating machinery. Vibrometry measurements are important to monitor in-vessel structures to detect coolant flow-induced vibrations, which is particularly important in He-cooled reactors. Many conventional sensors to measure in-vessel vibration cannot tolerate the higher AdvSMR coolant temperatures.

Optical vibrometers are well-established instruments available in a number of different configurations to support different standoff ranges and various modes of operation. COTS models exist with moderately compact optical heads and more compact fiber-coupled optical heads. Ranges up to tens of meters or more are easily accommodated by these systems. Modes of operation include single-point sensors, differential systems, scanning systems, and multidimensional systems.

The technical readiness of existing COTS optical vibrometry systems for AdvSMR applications is **MEDIUM**. Use of optical vibrometers in AdvSMRs will require development of ruggedized systems with extended temperature ranges and radiation resistance, line-of-sight access to the surfaces of interest, and optical windows for placement of the system outside of the vessel. The noncontact, standoff nature of these systems will enable this type of remote placement, if engineering solutions allowing such placement are developed.

10.1 Introduction

Vibrational frequency analysis is a prognostic monitoring technique commonly used by the nuclear power industry to maintain efficiency and preempt mechanical failure in pumps, motors, and similar devices. Some AdvSMR concepts may require new approaches for in-vessel vibration monitoring. For example, conventional accelerometers used for EM pump prognostic monitoring will not likely survive the harsh temperature and radiation environment inside the reactor vessel.

Optical vibration measurement techniques may be feasible in some AdvSMR designs, including those with coolants that are optically transparent (e.g., SCW, He, molten salt). Liquid metal-cooled designs would not be amenable to direct optical monitoring. Optical vibrometry techniques are mature for a number of applications and may be adaptable to future AdvSMR designs; however, they are primarily used as laboratory instruments rather than industrial sensors. Optical vibrometry is typically a very sensitive standoff measurement technique, so many of the critical components may be placed outside the vessel with suitable optical ports designed to allow monitoring of critical internal components. Remote optical vibration monitoring may be particularly effective for the in-vessel EM pump and motor components used in pool-type AdvSMR designs, as well as reactor superstructure components used in all designs. A potentially related method, optically based diaphragm deflection measurement, has been suggested as a possibly advantageous technique for direct high-temperature measurement of differential pressures in liquid salt flowmeters (Holcomb et al. 2009).

This section describes optical vibrometry and related techniques, and their potential role for monitoring critical components within AdvSMRs. A brief survey of COTS systems and techniques is presented along with a discussion of the gaps in the technology for this application, promising research and development, and suggestions for future research.

10.2 Fundamentals of Operation

Laser vibrometers provide a noncontact (standoff) method for detecting and analyzing the motion of a vibrating surface. Laser vibrometers detect this motion using an interferometric technique in which laser light scattered from the surface is combined with a reference beam, derived from the source laser, onto a photodetector. The scattered light is Doppler shifted because of the velocity of the surface. The photodetector frequency response cannot directly detect the high optical laser frequency ($\sim 4.7 \times 10^{14}$ Hz), but rather mixes the two frequencies to generate a signal at the Doppler frequency, which is proportional to velocity.

A typical laser vibrometer design is shown in Figure 10.1. A continuous wave laser beam (f_0) is split into a measurement beam and a reference beam by a beam splitter. He-Ne (at 633 nm) lasers are typically used in commercial systems because of their long coherence length, stability, eye safety, and low cost. Diode lasers can also be used. The measurement beam passes through a second beam splitter and a lens and strikes a vibrating surface, assumed moving at velocity v. The surface is typically a diffuse reflector and some of the scattered measurement beam, now frequency shifted by the Doppler frequency (f_d), is collected by the lens and directed through two beam splitters onto a photodetector. The reference beam (f_0) is frequency shifted by f_b using an acousto-optic modulator (AOM), also known as a Bragg cell. The reference beam then strikes a beam-splitter, which is functioning as a beam combiner for the reference and measurement beams. The Doppler-shifted measurement beam ($f_0 + f_d$) and the reference beam ($f_0 + f_b$) are coherently combined (mixed) at the photodetector. The photodetector cannot respond to the high optical frequency (f_0) and therefore only outputs the difference frequency (f_b - f_d). This system uses a single lens for shared illumination and detection apertures, resulting in a confocal system.
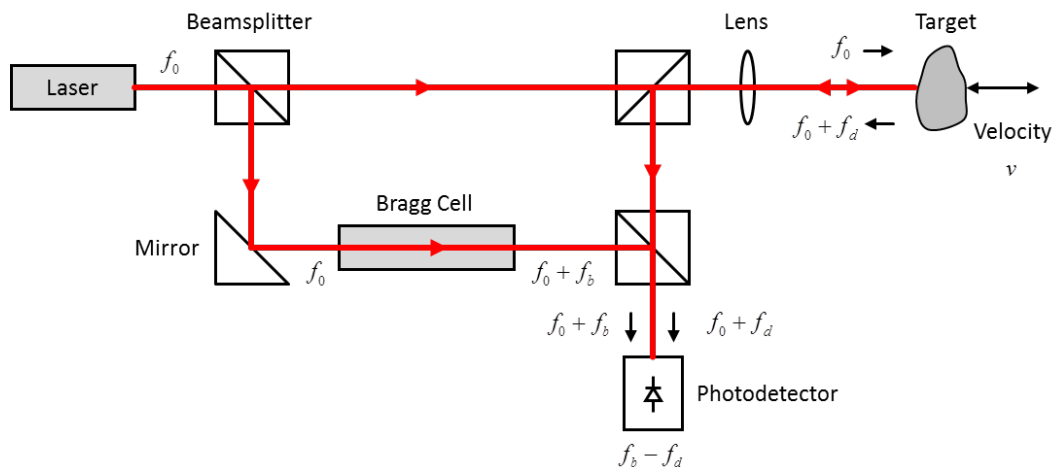
Figure 10.1. Heterodyne Laser Vibrometer

The system described in Figure 10.1 is a heterodyne laser vibrometer because of the introduction of the additional modulation of the AOM (operated at f_b). This additional modulation can be removed in subsequent electronic or digital signal processing to yield the Doppler frequency signal (f_d). The heterodyne architecture has the advantage of removing the ambiguity between positive and negative velocities, and may have signal-to-noise ratio advantages because of additional filtering and amplification that may be implemented at the heterodyne intermediate frequency (f_b in this case).

The Doppler shift can be easily understood by considering the simplest case with no reference beam modulation (f_b=0). In this case, the phase of the measurement beam will shift by 360 degrees for a $\lambda/2$ shift in target position relative to the phase of the reference beam. Therefore, a spatial translation of $\lambda/2$ will result in a full light/dark cycle of the combined beams optical intensity at the photodetector. The Doppler frequency for a target velocity v is given as $f_d = 2v/\lambda$.

These systems measure small changes in the optical phase shift of light backscattered from the surface. Signal processing of the photodetector output over time enables determination of displacement over time and the vibrational velocity frequency spectrum. Frequencies of interest are typically in the 10 Hz to 100 kHz range, with systems responding to much higher frequencies also available. Analysis of the velocity spectrum then allows modal frequencies of the target to be determined for vibrational signature analysis. Damage or wear to a component (e.g., bearing, rotor) or structure would typically cause changes in the modal frequencies and amplitudes.

10.2.1   Laser Doppler Vibrometry Applications

Laser Doppler vibrometry (LDV) is frequently used as a laboratory measurement tool for applications in which it is important to operate in a standoff configuration or where it is difficult or undesirable to attach traditional vibration sensors such as accelerometers. Applications and methods for LDV has been reviewed in the published literature (Castellini et al. 2006). Optical vibrometry is widely used for vibration analysis in the automotive industry to validate computational predictions and to facilitate reduction of noise and vibration in body panels and other structures. Optical vibrometry is also used extensively in the loudspeaker industry to measure the properties of the loudspeaker diaphragms. In both of these applications, the system can measure the velocity spectrum and determine modal frequencies for signature analysis. Scanning and 3-D laser vibrometry systems are also used for these applications to determine spatial patterns of vibrational modes and determine in-plane motion, respectively. Optical vibrometry is also used for studying structural dynamics of buildings and other large structures. Remote health monitoring of machinery is another application in which the vibrometer monitors or measures the vibrational spectra of pumps and motors to determine the health of the bearings and assess overall system balance. This can be configured in a standoff scheme. The standoff noncontact nature of laser Doppler vibrometry allows direct measurement and analysis of rotating structures, such as disk drive platters, automotive disk brakes, motors, and generators.

These applications require one or more of the advantageous properties of optical vibrometry, some of which are summarized below, along with a number of disadvantages.

Advantages of Optical Vibrometry

- System can be operated in a standoff/noncontact configuration.
    - Eliminates electrical connection to the object/surface being measured (standoff).

- Allows measurement of an inaccessible target.

- Noncontact (and no electrical connections) so it can be used to measure vibration on moving (rotating or translating) surfaces (e.g., a rotating motor shaft).

- Environment factors may prevent direct contact of a sensor (extreme heat, steam, radiation, explosive or chemical vapors, high voltage, magnetic fields, etc.).

- Suitable for applications where conventional sensors (e.g., accelerometers) cannot be used. Does not need to be attached to the surface (which could adversely affect the measurement because of the mass of an attached sensor).

- Does not require signal conditioning electronics at the source of the measurement (important for harsh environments).

- Allows collection of wideband vibration signatures to facilitate modal and vibrational analysis.

- 3-D velocities can be measured using three heads (at different angles to the surface).

- Scanning can be used to measure velocity distributions along a path or surface. Simultaneous multi-point measurements can also be made with specialized systems.

Potential Disadvantages of Optical Vibrometry

- Requires line-of-sight access to the vibrating surface.

- Cannot directly distinguish between vibration of the sensor and vibration of the interrogated surface.

- Size – sensor head can be relatively large and associated electronics are required.

- Power consumption (wall power required).

- Set up and alignment required.

- He-Ne lasers used in many systems are somewhat large, fragile (gas tube envelope), and require high voltage power supply. Solid-state or fiber or diode lasers can be used.

- Typically designed and used in R&D settings, rather than in factory or production facilities.

There are several types of optical vibrometers that can be applied to the applications described above. Most systems are LDVs, similar to that shown schematically in Figure 10.1. Free-space LDVs can be realized with several different interferometer architectures of varying complexity including heterodyne, homodyne, and self-mixing. The system shown in Figure 10.1 is a heterodyne vibrometer. The heterodyne architecture introduces an additional level of frequency modulation with the Bragg Cell (acousto-optic modulator). This additional modulation eliminates the ambiguity between positive and negative velocity, and may improve sensitivity. The homodyne architecture eliminates the AOM, which leads to a simpler, more compact and inexpensive design. A self-mixing architecture is even simpler than the homodyne architecture, and is shown schematically in Figure 10.2. This configuration takes advantage of the natural interference or optical feedback of the back-reflected Doppler-shifted optical signal within the diode laser cavity. The back reflection alters the phase and amplitude of the light within the laser cavity depending on the phase of the light reflected from the moving target, and is detected using an internal photodiode. This configuration allows for extremely simple, compact, vibrometer systems (Scalise et al. 2004). Homodyne and self-mixing vibrometers are also discussed in Grund et al. (2010).
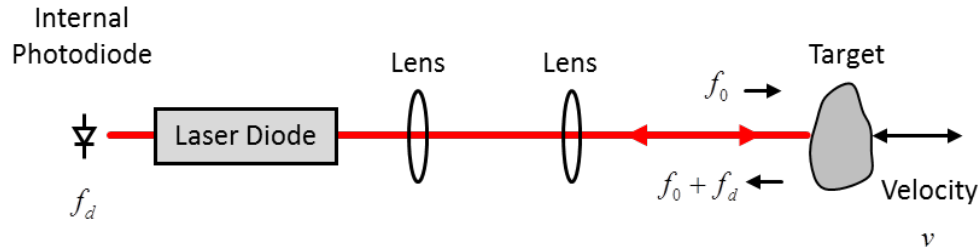
Figure 10.2. Self-Mixing Laser Vibrometer

Fiber-coupled optical vibrometers can be formed using an architecture similar to that shown in Figure 10.1 (Castellini et al. 2006). Each of the optical paths to the right of the lens can be replaced with an optical fiber; optical couplers can be used to replace the beam-splitter/combiners. The primary advantages of this type of vibrometer are the reduction in size of the optical head, and the ability to place the optical head remotely away from the remainder of the vibrometer optics. Another type of fiber-optic vibrometer uses the Sagnac effect. This type of system relies on the interference of counter-propagating waves within a fiber-optic loop to obtain the Doppler signal. An additional advantage of this architecture is that it can use an incoherent broadband optical source that may be less expensive and more stable (Davis and Bush 1999).

10.2.2   Performance Considerations with Optical Vibrometers

There are several factors that may affect the performance of LDVs. The vibrometer cannot directly differentiate between vibration of the optical measurement head and vibration of the target surface. Therefore, the vibrometer must be isolated from background vibrations. This isolation could be done mechanically, or can be separated using spectral analysis if the background is separated in frequency response from the surface of interest. This may be a significant factor for harsh industrial environments, such as AdvSMRs. Optical vibrometers may also be affected by particulates in the optical path and by index of refraction variations caused by pressure oscillations in the optical path medium. This could be a particular nuisance for measurements through gas or liquid coolants. Another consideration is the strength of the optical signal returned from the target surface. The surface may need to be conditioned to optimize the optical scattering properties. A diffusely scattering surface is usually desired, as a vibrating specular-reflecting surface may direct the optical energy away from the vibrometer receiver. A final consideration is speckle noise. Speckle is an interference pattern, encoded as a varying intensity distribution and phase across the laser beam profile. Speckle-induced phase variations can add noise during Doppler frequency recovery. This effect is most apparent in vibrometer systems with significant target lateral motion, in which the speckle pattern and beam intensity/phase distribution dramatically change as the distribution of surface roughness changes (Rothberg 2006).

10.2.3   Related Techniques

Other optical measurement techniques are related to optical vibrometry. Laser Doppler velocimetry is used to measure particle velocities in optically transparent media. Laser Doppler velocimetry operates by interfering two slightly off-axis laser beams to create an interference (optical fringe) pattern in the intersection zone of the two lasers. Detection of the scattered light intensity as a particle passes through this zone allows determination of the particle velocity. Optically generated and/or detected ultrasound (photo-acoustic imaging) uses high-power laser pulses to thermally excite ultrasonic waves within metals

or other materials. Sensitive detection is accomplished using optical interference methods similar to those used for laser vibrometry (Swenson et al. 2010). Photo-acoustic imaging or analysis may potentially be used for inspection of mechanical integrity such as cracks or component weakening (Anheier et al. 2012).

10.3 Promising Research and Development

There is current research and development that may increase the potential of optical vibrometry for future AdvSMR applications. Compact, rugged, and potentially inexpensive vibrometers are being developed that use the homodyne or self-mixing architectures described above (Grund et al. 2010; Atashkhooei et al. 2011). These vibrometers can use telecom laser diodes and can be robust and alignment-free. The self-mixing architecture may be limited to shorter range standoffs (up to 3 m) compared to the homodyne and heterodyne architectures (Grund et al. 2010). Laser Doppler vibrometry has also been developed for challenging environments, including detection of small ground vibrations from a moving platform (Jiang et al. 2011). This work was challenging because of the vibrations from the vehicle-mounted system interfering with the ground vibration signals. The authors devised a solution that used accelerometers attached to the transmitting apertures, which enabled subtracting the line-of-sight component of the signal because of vehicle motion. Using a multichannel vibrometer also allowed the use of one of the channels to provide a reference for common-mode vibration compensation.

Another technology that is receiving current attention is laser Doppler velocimetry (LDV). This technology has been suggested for monitoring the movement of graphite particles in HTGRs to determine the primary coolant flow rate (Ball et al. 2012). In particular, a related technique referred to as Projection LDV may be useful for this application, because it is uses an optical mask to create the fringe pattern within a single laser beam (Moir 2009; Ball et al. 2012). The use of a single laser beam and a larger fringe pattern reduces the optical alignment precision that is required, and may enable use of LDV in harsh industrial situations in which conventional LDV has not been practical.

10.4 COTS Summary, Gaps Analysis, Ranking, and Proposed Future Research Path

COTS Optical Vibrometer Summary

Laser Doppler vibrometers are well-established instruments available in a number of different configurations to support different standoff ranges and various modes of operation. These instruments provide large measurement frequency bandwidth, high displacement sensitivity, and wide displacement dynamic range, which will likely meet the requirements of pump monitoring, loose parts detection, and structural vibration monitoring. COTS models are available from Polytec and Metrolaser, Inc., with moderately compact optical heads and more compact fiber-coupled optical heads. Ranges up to tens of meters or more are easily accommodated by these systems. Modes of operation include single-point sensors, differential systems, scanning systems, and multidimensional systems.

The containment vessel headspace deployment requirements include 40°C ambient temperature, gamma at <10 Gy/h, and neutron flux at $<10^{11}$ n/cm^2 s. Molten Na coolant can become activated and thus have gamma up to 100 Gy/h. The maximum working temperature limits are generally 45°C, which meets the AdvSMR deployment requirement. No vibrometry measurement specifications could be identified for the AdvSMR application. Nuclear industry-grade piezoelectric accelerometers provide typical frequency response from 0.5 Hz to 10,000 Hz. Sensitivity is given in terms of pico-Coulombs per gram, where

values range from 5 to 250 pC/g. A typical LDV has vibration frequency response from 0.1 Hz to >40 kHz. The measurement range for vibration displacement is 0.1 nm to 10 mm, with a velocity range of 5 µm/s to 800 mm/s. While it is not possible to directly compare the measurement sensitivities of the two technologies, it appears feasible that the LDV is competitive with piezoelectric accelerometers. The vendors provide no radiation-resistance specifications.

Gaps Analysis

- COTS laser vibrometers are primarily used in laboratory settings, and have not been developed for harsh industrial environments.

- Auto-alignment to a target surface is not provided.

- The radiation-resistance specifications for COTS laser vibrometers are not provided.

- COTS optical monitoring instrument performance under AdvSMR deployment conditions uncertain.

- The impact of intermediate chemical vapor, thermal gradients, and vibrating transparent surfaces to COTS vibration monitoring performance unclear.

- The feasibility of measurements through transparent coolants uncertain.

- Actual performance and benefits of pyrometry monitoring must be determined.

Technical Readiness Ranking

The technical readiness for COTS optical vibrometry is **MEDIUM**. Optical vibration measurement techniques may be feasible in some AdvSMR designs, including those with coolants that are optically transparent (e.g., SCW, He, molten salt). Optical vibrometry techniques are mature for a number of applications and may be adaptable to future AdvSMR designs; however, they are primarily used as laboratory instruments rather than industrial sensors. A research effort will be required to determine the approach and effectiveness of COTS optical vibrometry measurements for in-vessel vibration monitoring.

Proposed Future Research

- Enhancements and customization of COTS laser vibrometers must be developed to meet the demanding AdvSMR deployment requirements.

- Differential vibration and transmission media compensation techniques must be developed.

- Optomechanical design must be developed to maintain optical alignment and performance over extreme temperature variations (e.g., start-up through steady-state operation temperatures).

- Demonstrate, optimize, and develop integration plan for COTS vibrometry instrument for in-vessel vibration monitoring.

- Further study is required to evaluate measurement degradation and service life as a function of radiation exposure.

10.5 References

Anheier NC, BD Cannon, AH Qiao and JD Suter. 2012. *Optical Measurement Technologies for High Temperature, Radiation Exposure, and Corrosive Environment - Significant Activities and Findings*. PNNL-21786, Pacific Northwest National Laboratory, Richland, Washington.

Atashkhooei R, U Zabit, S Royo, T Bosch and F Bony. 2011. "Adaptive Optical Head for Industrial Vibrometry Applications." In *Proceedings of the SPIE, Optical Measurement Systems for Industrial Inspection VII, Volume 8082*, p. 80821W. May 23-26, 2011, Munich, Germany. The International Society for Optical Engineering, Bellingham, Washington.

Ball SJ, DE Holcomb and SM Cetiner. 2012. *HTGR Measurements and Instrumentation Systems*. ORNL/TM-2012/107, Oak Ridge National Laboratory, Oak Ridge, Tennessee.

Castellini P, M Martarelli and EP Tomasini. 2006. "Laser Doppler Vibrometry: Development of Advanced Solutions Answering to Technology's Needs." *Mechanical Systems and Signal Processing* 20:1265-1285.

Davis P and J Bush. 1999. "Non-contact Fiber Optic Vibrometer." In *Proceedings of the SPIE, Fiber Optic Sensor Technology and Applications, Volume 3860*, pp. 390-399. September 19, 1999, Boston, Massachusetts. The International Society for Optical Engineering, Bellingham, Washington.

Grund CJ, H Guenther and J Connolly. 2010. "Compact Diode Laser Homodyne Vibrometers." In *Proceedings of the SPIE, Laser Radar Technology and Applications XV, Volume 7684*, pp. 7684-30. April 6-9, 2010, Orlando, Florida. The International Society for Optical Engineering, Bellingham, Washington. Paper #7684 0V.

Holcomb DE, SM Cetiner, GF Flanagan, FJ Peretz and GL Yoder. 2009. *An Analysis of Testing Requirements for Fluoride Salt-Cooled High Temperature Reactor Components*. ORNL/TM-2009/297, Oak Ridge National Laboratory, Oak Ridge, Tennessee.

Jiang LA, MA Albota, RW Haupt, JG Chen and RM Marino. 2011. "Laser Vibrometry from a Moving Ground Vehicle." *Applied Optics* 50(15):2263-2273.

Moir C. 2009. "Miniature Laser Doppler Velocimetry Systems." In *Proceedings of the SPIE, Optical Sensors 2009, Volume 7356*, p. 73560I. April 20-22, 2009, Prague, Czech Republic. The International Society for Optical Engineering, Bellingham, Washington.

Rothberg S. 2006. "Numerical Simulation of Speckle Noise in Laser Vibrometry." *Applied Optics* 45(19):4523-4533.

Scalise L, Y Yu, G Giuliani, G Plantier and T Bosch. 2004. "Self-Mixing Laser Diode Velocimetry: Application to Vibration and Velocity Measurement." *IEEE Transactions on Instrumentation and Measurement* 53(1):223-232.

Swenson ED, H Sohn, SE Olson and MP DeSimio. 2010. "A Comparison of 1D and 3D Laser Vibrometry Measurements of Lamb Waves." In *Proceedings of the SPIE, Health Monitoring of Structural and Biological Systems 2010, Volume 7650*, p. 765003. March 8-11, 2010, San Diego, California. The International Society for Optical Engineering, Bellingham, Washington.

11.0 Neutron Flux Monitoring

11.1 Overview

Neutron flux is measured at several locations around the reactor core as an indirect indicator of reactor power. Neutron flux is currently measured by fission counters, ion chambers, gamma thermometers, and self-powered neutron detectors. AdvSMRs have very high coolant temperatures that will challenge these traditional monitoring systems. Fission chambers, in particular, are limited to about 550°C maximum working temperature. Gamma thermometers may provide reliable service, but alternate measurement technology will likely be needed.

Reactor neutron flux monitoring and overall radiation monitoring serves three main functions:

- Basic reactor power control – steady state flux around 10^{13} n/cm^{2}sec.

- Start up control or "Approach to Criticality" – measuring flux between roughly 10^1 to 10^7 n/cm^{2}sec.

- Transient detection – sensitive transient flux detection at normal reactor flux to indicate anomalies.

The most common detectors used in current commercial nuclear power control are self-powered detectors (SPD) and fission chambers. A system of moving SPDs to characterize the reactor core is sometimes referred to as a Traveling Instrument Package (TIP). SPDs detect radiation by monitoring the induced electric current. Metal selection is key to the detector response. Some metals emit beta radiation in response to neutron capture; others are nonspecific to the type of incident radiation. SPDs are considered too slow to be used for transient detection. Both SPDs and fission chambers have long histories in nuclear power reactor applications, and full systems with software support are available commercially from large corporations that offer reactor design and construction services and much smaller independent suppliers. The Nuclear Energy Agency (Paris, France) is an international organization that supports the global nuclear power industry. They are an excellent resource on the wide variety of technologies used in various reactor systems (www.oecd-nea.org). A good summary document on reactor core monitoring is from a 1999 workshop sponsored by the NEA (OECD/Nuclear Energy Agency 2000).

Average AdvSMR in-vessel fluxes are expected to be between 6×10^{12} n/cm^2·s to 3×10^{14} n/cm^2·s for total neutrons and up to 10^6 Gy/h for gamma (Knoll 2000). However, peak core fluxes can exceed 10^{15} n/cm^2·s for fast and thermal neutrons, each, depending on the reactor type (INL 2009). Peak core gamma levels have been measured at 3×10^7 Gy/h. All the optical-based neutron flux monitoring techniques reviewed in this section are either conceptual or have been investigated only in a research study. Therefore, they have no performance specifications to compare against the expected AdvSMR neutron flux monitoring requirements. For these reasons, the technical readiness for all optical-based neutron flux monitoring techniques reviewed in this section in is **LOW**.

Several Japanese research groups conducted studies on optical concepts for neutron monitoring. A few studies evaluate design response as a function of reactor power. Only a few studies perform measurements at elevated temperatures. Several methods were conceptualized or modeled, but were never developed or demonstrated. A few exotic concepts are based on neutron capture by gas compounds. Many designs use optical fibers with either doped-active materials or use the fiber to

conduct optical signals from the active material to a detector. The technical gaps for COTS optical fiber have been discussed in other sections of this report. Because COTS systems are currently unavailable, we discuss the technical gaps in research designs only. It does appear that a few designs possibly could be adapted to high neutron flux and temperature environments, given additional research and engineering efforts. Two techniques in particular are worth further consideration, even though their technical readiness is currently low. The first technique is based on Cherenkov radiation monitoring, which scales linearly with reactor power. This has been demonstrated in a test reactor with a standpipe viewport. This approach may be useful for MSR and FHR designs. Alternatively, a passive Cherenkov gas detector concept could be pursued. This concept could work in all AdvSMR coolant designs. The Cherenkov gas detector concept could be extremely impactful by providing a high-temperature 'approach-to-criticality' power monitoring system. To advance this concept, a high-temperature gas cell design must be developed. A high radiation-resistant, hollow-core PCF could be used to couple emission from the gas chamber to an external optical detector. The second technique is based on neutron capture by CO_2 gas. This is a very simple technique, with no active in-vessel components. This approach has been demonstrated experimentally and possibly could operate at high temperature. To advance this concept, a high-temperature gas cell design must be developed, followed by testing and demonstration.

11.1.1   Self-Powered Detectors

SPDs are simple in design, consisting of a signal wire connected to a detecting metal that is protected by insulation and sealed in a metal sheath. Although small in diameter, the sensing head can be 10 cm long or greater. Figure 11.1 shows a basic SPD sensing head. Many SPDs are typically used for reactor neutron flux monitoring. They can be stationary, distributed in a network throughout the reactor, or used intermittently as they are manually moved through various sensing ports within a reactor. Several different metals can be used for the sensor element. Choice of metal impacts the length of the detector and its response time. The maximum working temperature for the SPD is dependent on the sensor and steel housing mechanical properties and typically is around 550°C (Goodings 1978). SPDs have a finite life because they eventually exhaust their supply of neutron capture atoms. Specification sheets usually list "burn rate" in terms of KW-days of service. SPDs feature output current that is very proportional to the neutron flux (Todt Sr. 1996).
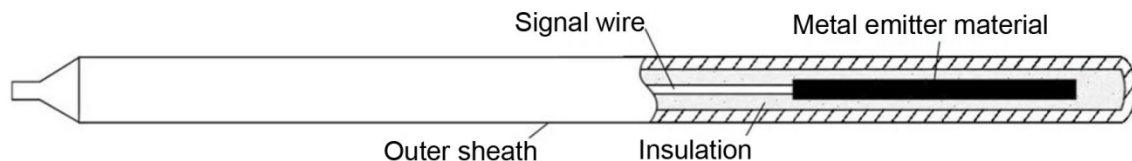
Figure 11.1. Typical Self-Powered Neutron Detector Schematic. The sensing metal is rhodium.

11.1.2   Gamma Thermometry

Gamma thermometers are designed for reactor power measurements. Unlike SPDs, gamma thermometer do not have a lifetime limit associated with depletion of sensing metal. Expected lifetimes are >10 years of continuous service. The gamma therometer housing is typically made from hollow stainless steel rod assembly. The rods can be up to 43-m long to allow deep penetration into the reactor vessel. Thermocouples are embedded inside the rod at each measurement location (up to 20) to measure

11.2

differential temperature, as shown in Figure 11.2. Chambers filled with argon gas are designed inside the rod near the measurement locations. Incident gamma flux causes heating of the rod assembly, which is transferred along the sensor axis. The argon-filled chambers interrupt the heat flow, which results in high- and low-temperature regions at each measurement location. Two thermocouples measure the temperature difference between the argon chamber and the steel rod regions, with is proportional to the gamma flux incident on the housing. Reactor power can then be inferred by the proportional relationship to gamma flux. A centrally located heater provides an in-situ method to re-calibrate the gamma thermometers.

COTS gamma thermometers can be used as distributed sensors, but each sensing location requires a distinct pair of thermocouples, making high-resolution gamma profiling impractical. The operational temperature range of gamma thermometers is >800°C. At higher temperatures, thermal conductivity begins to drop, which decreases the gamma sensitivity. Some sensitivity can be recovered by judicious selection of the rod metals and fill gases. COTS gamma thermometers provide a wide dynamic range and good sensitivity, from below 'approach-to-criticality' to maximum power.
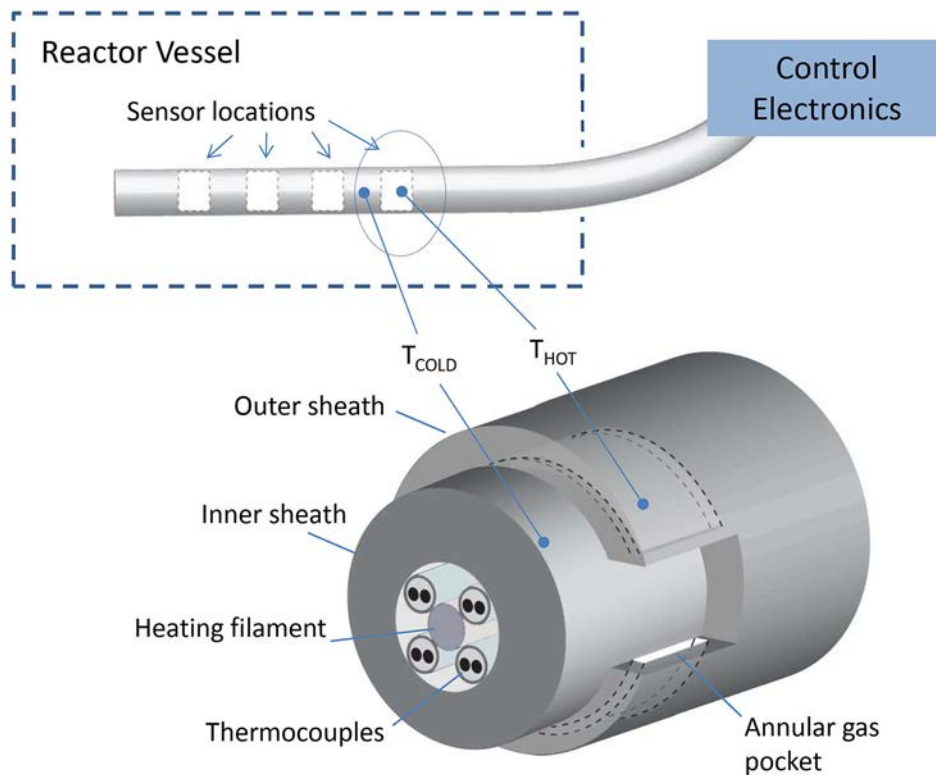
Figure 11.2. Gamma Thermometer Showing a Cross-section View and the Sensor Locations

11.1.3   Fission Chambers

Fission detectors are often used in conjunction with SPDs. Fission chambers have faster response times and are considered to be better for transient flux variation monitoring. They also have excellent neutron-discrimination capabilities. Transients in the neutron flux can indicate possible minor

mechanical failures in some reactor designs. General Electric Reuters Stokes report to have manufactured the first miniature in-core fission chamber (GE 2013). These detectors are constructed in the form of ionization chambers and include a thin layer of fissionable material (normally high-enriched U-235) coated on the anode, as shown in Figure 11.3. Fission fragments, produced by neutron-fissile atom interactions, ionize the fill gas under an applied electric field, which is detected in either pulsed or direct current mode. Care must be taken to optimize the design for fission fragments and minimize the response to alpha particles. R. W. Lamphere reviews designs and manufacturing methods for a wide variety of geometries. The housing materials and the internal gas pressure determine maximum operating temperatures for fission chambers (Lamphere 1960).
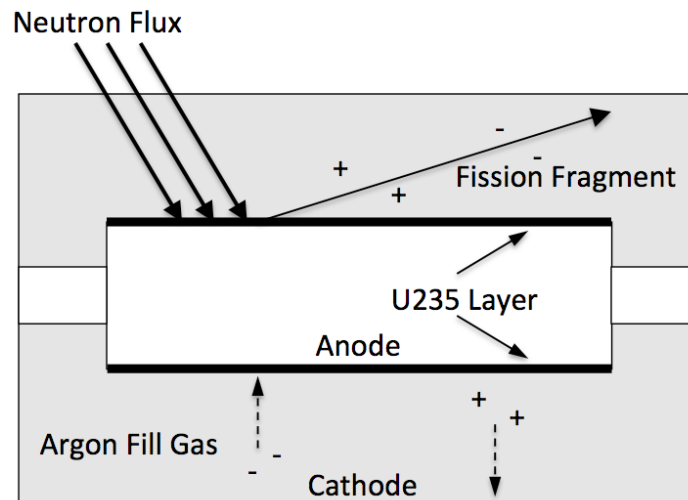
Figure 11.3. Cross Section View of a Fission Chamber

11.2 Optical-Based Systems

Optical-based neutron monitoring systems are not commercially available, so the technical readiness is **LOW**. Research in this area is somewhat scattered and can be difficult to separate from issues regarding radiation damage of materials. Reactor monitoring technology development has followed more of a systems approach than simply seeking new neutron-sensitive materials. The literature is somewhat divided between fiber-based systems and sensor materials. R&D designs use either COTS optical fibers or custom fibers and generally COTS neutron-sensitive materials, but none of these designs have matured to COTS status.

11.2.1 Neutron Flux and Power Monitoring using Radiation-induced Luminescence

There is a large body of research on RIL neutron detection materials; however, most of these materials are not compatible with the high neutron fluxes or temperatures expected in AdvSMRs. Some exceptions to high neutron fluxes have been identified. At somewhat high neutron fluxes, bulk samples of silica (SiO_2) and sapphire (Al_2O_3) are reported to luminesce (Tanabe et al. 1994). This study configured these RIL materials at the end of an optical light pipe, near the reactor core. Such a

configuration possibly could be suitable for future AdvSMR flux monitoring. The irradiations were carried out at the YAYOI reactor at the University of Tokyo. This reactor has low gamma fluence (3.0 kGy/h), neutron flux (2×10^{11} n/cm^2 s, and power (500 W) as compared to expected AdvSMR conditions. Figure 11.4 shows the optical emission of Al_2O_3 at several neutron flux levels, but the paper does not correlate this to reactor power. Figure 11.5 shows the optical emissions from single crystal SiO_2 and a high-purity silica optical fiber. The authors make a strong case that the emissions observed were not caused by Cherenkov radiation, but rather by oxygen vacancy related to radiation-induced color centers. However, they do show that the RIL intensity increases with dose, but afterward decreases because of darkening and color center formation. Such behavior may diminish the feasibility of using these materials for continuous online neutron flux monitoring.
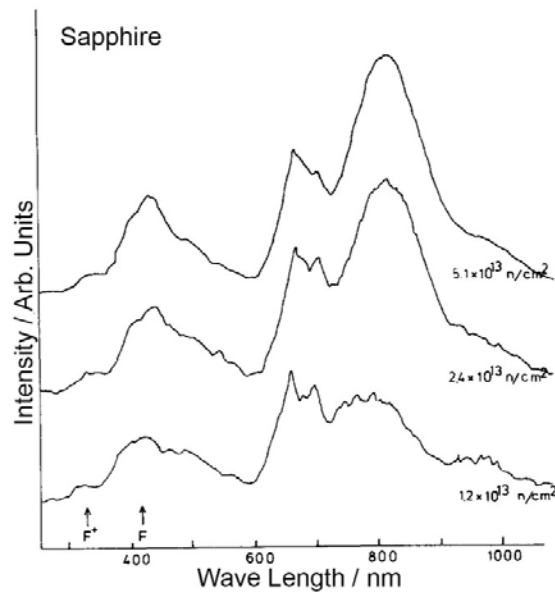
Figure 11.4.   Optical Emission of Al_2O_3 in a Nuclear Reactor Core. The emission at 600 nm is believed to be a harmonic of a shorter wavelength band Tanabe et al. (1994). Reprinted with permission from Elsevier © 1994.

11.5
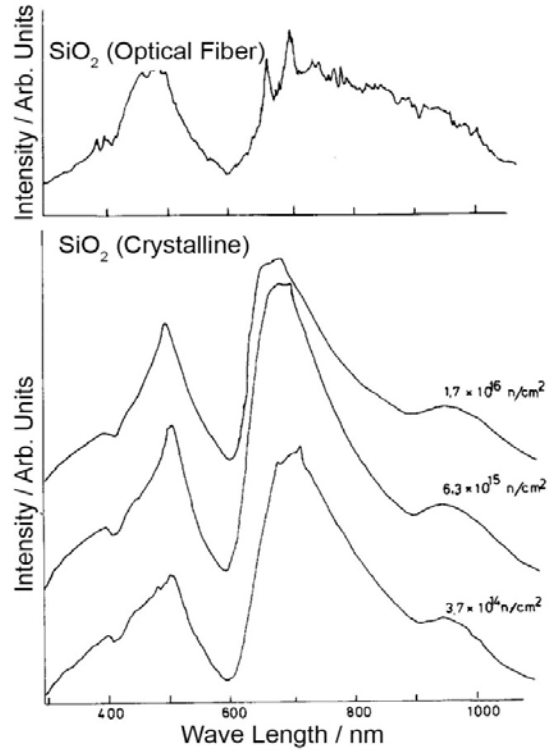
Figure 11.5. Optical Emission Comparison Between Single Crystal SiO_2 and Silica Optical Fiber under High Neutron Fluence Tanabe et al. (1994). Reprinted with permission from Elsevier © 1994.

Other Japanese research studied the problems associated with high temperature neutron sensing (Kakuta et al. 1998; Kakuta et al. 2000). Fluorine-doped silica fibers were placed in an experimental reactor along with sapphire temperature sensors. The fibers were multimode with 200-µm core diameters. The emission is described as a fluorescence process, but perhaps should be called RIL. Emission was observed between 400 to 1400 nm, with a sharp peak centered at 1270 nm. Broad gamma ray-induced Cherenkov radiation emission was observed between 700 and 1400 nm, as shown in Figure 11.6. The 1270 nm emission intensity correlated well to reactor power, as shown in Figure 11.7.
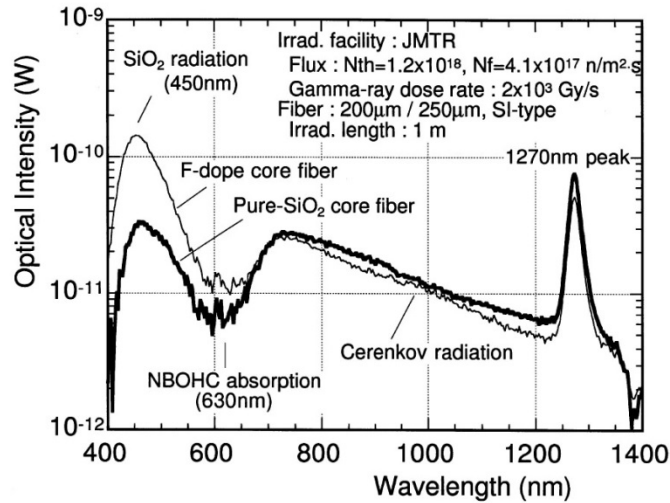
Figure 11.6.   Optical Emission from a Fluorine-Doped Waveguide in an Experimental Nuclear Reactor Kakuta et al. (1998). Reprinted with permission from Elsevier © 1998.
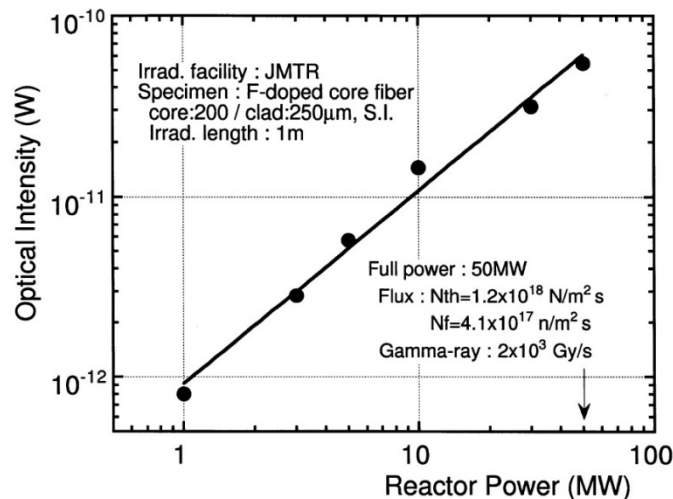
Figure 11.7.   Correlation between Reactor Power and the 1270-nm Optical Emission in a Fluorine-Doped Waveguide Kakuta et al. (1998). Reprinted with permission from Elsevier © 1998.

11.2.2   Neutron Flux Monitoring using Radiation-induced Fiber Damage

Monitoring radiation-induced damage in optical fibers has been suggested as a method to measure radiation dose (Henschel et al. 1997; Brichard et al. 2001). This topic is discussed in depth in Section 3.3.4.1. Many different cladding overcoatings were used in these studies and were reported to impact radiation-induced attenuation. Fast neutrons produce energetic recoil protons in hydrogen containing coating materials (e.g., acrylate, polymers), which can penetrate several fiber layers, coiled on a test spool, leading to an increased dose in the fiber core. Hydrogen released by the fiber coating also increased the 1.38 µm OH absorption in the fiber. It was noted that hydrogen content must be considered when modeling the response of this process. Real-time sensing of integrated dose is obtained by

comparing optical transmissions of the fiber in the radiation field to a reference fiber outside the field using a common light source. Some of the optical transmission is recovered after irradiation ceases as described in Henschel et al. (1997).

11.2.3   Neutron Flux Monitoring using Fiber-Optic Interferometry

A proposed neutron sensor design is based on a Mach-Zehnder fiber interferometer (Figure 11.8) (Weiss 2013). The interferometer design is based on COTS single-mode fiber. Neutron capture by the major glass components (e.g., Ge, Si, O) is predicted to change both the refractive index of the sample arm and the normal mode frequencies in the glass. The normal mode frequencies determine the near infrared transmission limit for the waveguide. These changes reduce the transmission characteristics of the sample fiber, and the interferometer design is predicted to track these differences with neutron dose. Figure 11.9 shows the change in the propagation constant for the sample fiber as neutron capture reactions accumulate. The model addresses the optical issues and expected response, but a detailed neutron response (i.e., Monte Carlo model) is not included in the paper. High-temperature applications will be limited by the stability of the commercial fiber. It may be possible to adapt this design to more refractory materials. A detailed MCNPX[a] model will be needed to determine if the neutron capture rate is large enough, given a reasonable integration time.

$$\varphi = \Delta(\beta L)$$
$$S_1 = I_o \cos^2(\varphi/2)$$
$$S_2 = I_o \sin^2(\varphi/2)$$
$$\frac{S_1 - S_2}{S_1 + S_2} = \cos \varphi$$
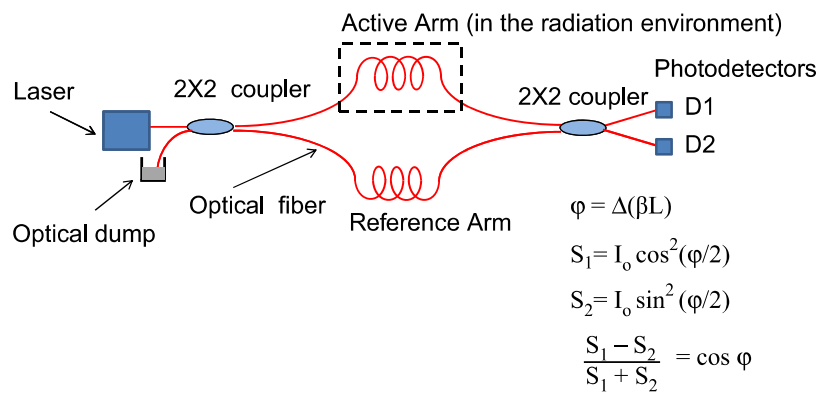
Figure 11.8.   Mach-Zender Interferometer for Neutron Sensing Proposed by J. Weiss (2013). Reprinted with permission from Elsevier © 2013.

(a) MCNPX – Monte Carlo Neutral Particle eXtend – a computer code developed at Los Alamos National Laboratory to calculate interaction of radiation with matter. X signifies a newer version of the code that includes gamma rays and more detail on nuclear reactions.
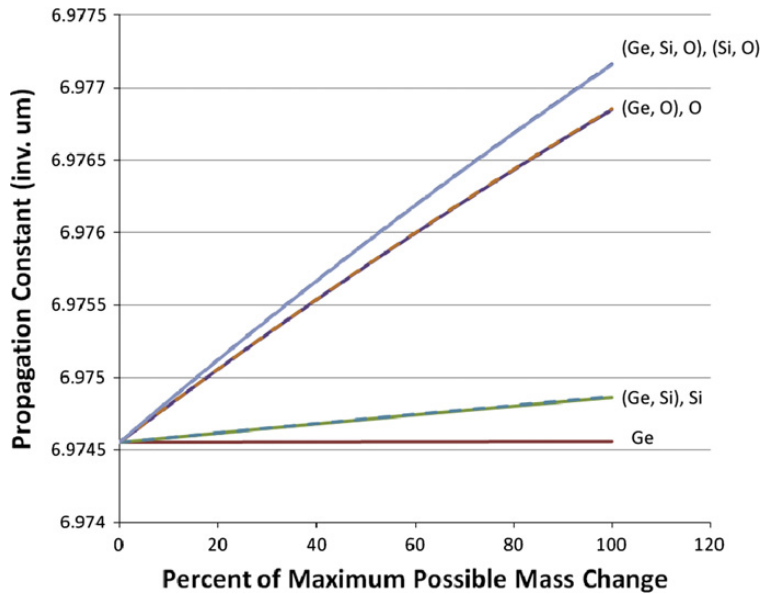
Figure 11.9. Predicted Change in Optical Propagation Constant for a Commercial Single-Mode Fiber after Successive Neutron Capture Reactions

11.2.4 Neutron Flux Monitoring using Scintillating Fiber

Custom scintillating optical fibers can be formulated to capture neutrons and then produce optical emission through a scintillation process. Lithium and boron both have isotopes that capture thermal neutrons. Designs based on boron capture are attractive because of the high natural abundance of ^{10}B along with its versatile chemistry. The lithium capture reaction is more energetic, but lithium chemistry is more challenging. In the mid-1990s, a detector was designed for nuclear reactor startup monitoring (Bliss et al. 1995). This detector used enriched and non-enriched lithium (^{6}Li has a high thermal neutron capture cross section) loaded scintillating glass. Neutron-γ discrimination was provided by the difference between the enriched and non-enriched fiber scintillation signals. The non-enriched fibers respond only to gamma rays. Single fibers were used for the high flux measurements and 200 and 3500 fiber ribbons were used at lower flux (reactor power). This detector was tested only at ambient temperatures at a TRIGA reactor and compared to a compensated ion chamber. Figure 11.10 shows the composite fiber detector response to increasing TRIGA reactor power. The detector was in a dry tube below the core. Figure 11.11 shows the response of the fiber detector compared to a compensated ion chamber in the same location at the same reactor power. These fibers are coated with a silicone rubber cladding that has a maximum working temperature of only 200°C.
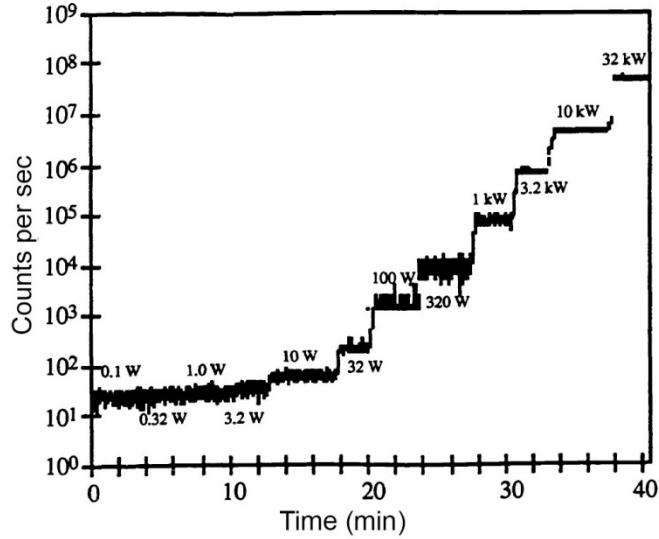
Figure 11.10. Composite Detector Response for an Enriched Lithium Fiber-Optic Monitor to Neutron Flux at Different TRIGA Reactor Powers (Bliss et al. 1995)
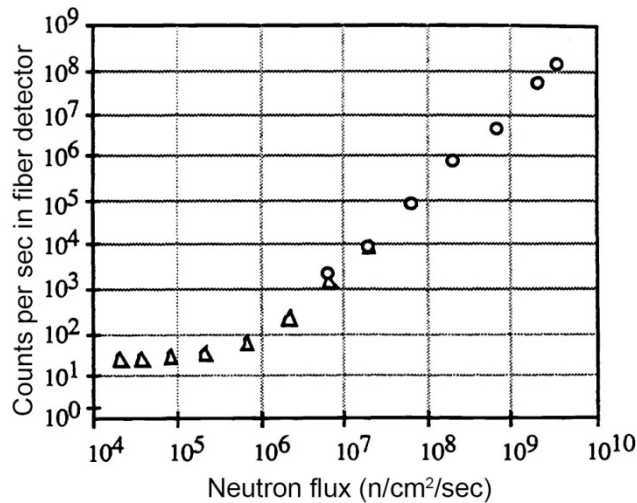
Figure 11.11. Comparison of the Enriched Lithium Fiber Detector (composite response) to a Compensated Ion Chamber in a Comparable Location at the Same Reactor Powers (Bliss et al. 1995)

11.2.5   Neutron Flux Monitoring using Fiber-coupled Scintillators

A recent study from Japan focuses on commercially available phosphors and scintillators for response to 14 MeV neutrons (Toh et al. 2007). The research goal was to develop a flux monitor for neutron flux up to 10^9 n/cm^{2}s in a gamma field of up to a few Gy/s. Irradiations were performed using a high flux neutron generator at the deuterium-tritium facility at the Tokai Research Establishment of the Japan Atomic Energy Agency. The data was collected at ambient temperatures. COTS radiation-resistant fibers were used to collect and transmit the optical emission to an optical detector external to the reactor vessel.

11.10

The materials tested were ZnS:Ag, ZnS:Cu, $SrAl_2O_4$:Eu^{2+}, $SrAl_2O_4$:Dy^{3+}, $Sr_4Al_{14}O_{25}$:Eu^{2+}, and $Sr_4Al_{14}O_{25}$:Dy^{3+}. Although not specifically stated, all the phosphors were powders with the optical fiber embedded in a small aluminum tube. The optical emissions were integrated for 50 s under constant neutron flux and energy. Figure 11.12 shows the optical emissions from the four phosphors. ZnS exhibited the shortest afterglow after irradiation ceased. The $Sr_4Al_{14}O_{25}$:Dy^{3+} exhibited the longest afterglow, extending up to 10 minutes. These results are consistent with the UV-stimulated afterglow measurements conducted on these materials. The ZnS:Ag phosphor degraded under neutron exposure after 10's of hours. The other samples were reasonably stable for the entire 80-hour exposure duration.

A similar approach was used later by another Japanese research group (Yamane et al. 1999). [6]Li or [232]Th was mixed with ZnS(Ag) scintillator powder and then attached to the tip of a fiber, as shown in Figure 11.13. The lithium captured thermal neutrons and the thorium captured fast neutrons. The fibers were inserted near the reactor core bottom and then moved up axially at a constant speed, while collecting scintillation data. A discriminator setting was used to filter out low light background events and the reactor was held at constant power during the measurements. The data was processed and analyzed to generate a normalized neutron flux profile, which varied as a function of axially distance along the core.

PNNL produced a similar fiber detector using [6]Li enriched glass fiber optics spliced to COTS fiber optics. The purpose of the device was to characterize MOX fuel rods (Bliss et al. 2007). This device underwent limited testing at a TRIGA reactor. No high-temperature testing was performed.

There is little information on actinide-loaded scintillators. These, in theory, would perform like fission chambers capturing high-energy neutrons and producing heavy energetic particles resulting in detection signals. One effort to produce Th- and U-loaded scintillating silicate glasses did not result in neutron capture signals above the intrinsic radiation signals produced by the actinides (Bliss and Stave 2012). A uranium-loaded crystalline scintillator was grown and tested in the late 1970s (Catalano and Czirr 1977). It was based on the ternary system MF_2:UF_4:CeF_3. A single crystal 20-mm diameter by 0.6-mm thick produced a pulse height spectrum as shown in Figure 11.14. The spectra exhibited a very large alpha peak and a small peak attributed to fission fragments. The authors attribute the alpha peak to 1% [234]U. The emission lifetime of the scintillation was 20 ns. The crystal was nonhydroscopic and mechanical strong. The research team produced several crystals in this system via flux-aided growth (PbF_2 flux) at processing temperatures between 800–1000°C (Catalano and Wrenn 1975). High-temperature scintillators like this show promise as possible high-temperature fast neutron detectors, especially if they can be combined with radiation-hardened optical fiber.
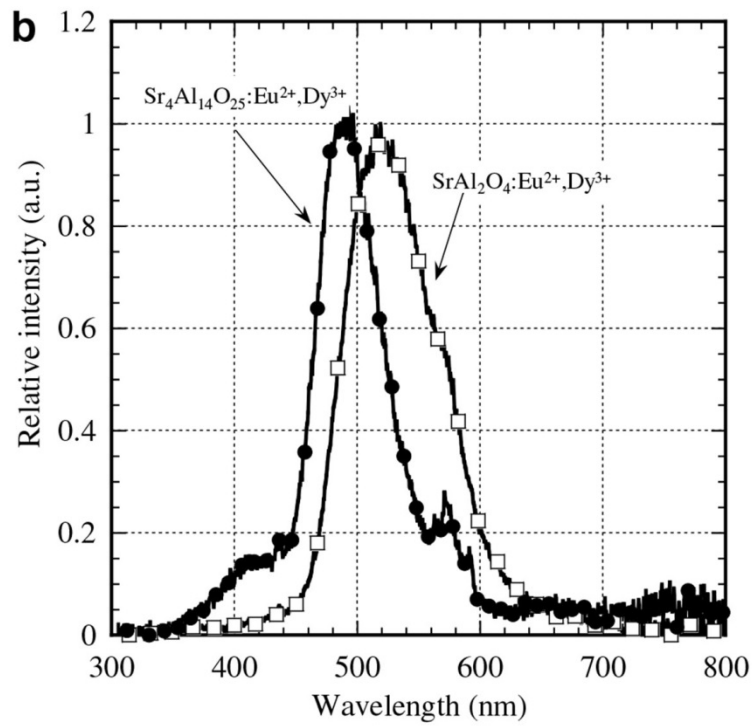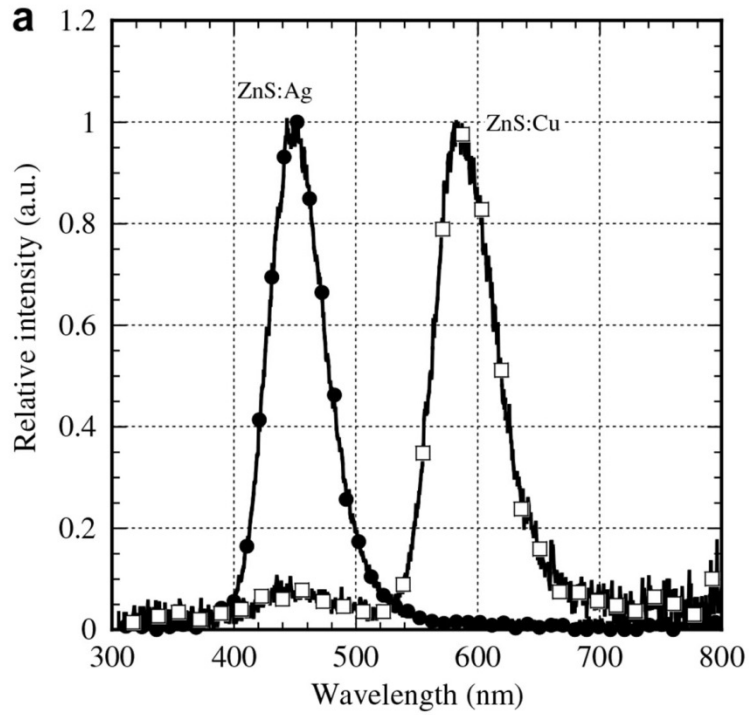
Figure 11.12. Fast Neutron Response of Several Commercial Phosphors Coupled to a Commercial Waveguide (Toh et al. 2007). Reprinted with permission from Elsevier © 2007.

11.12
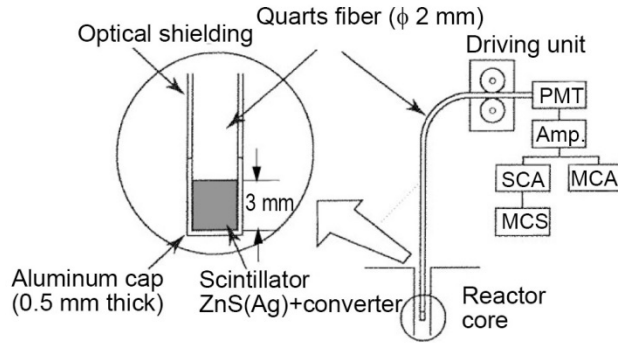
Figure 11.13. Optical Fiber Tip Sensor Coated with ^{6}Li or ^{232}Th with ZnS(Ag) Scintillator for Nuclear Reactor Profiling (Yamane et al. 1999). Reprinted with permission from Elsevier © 1999.
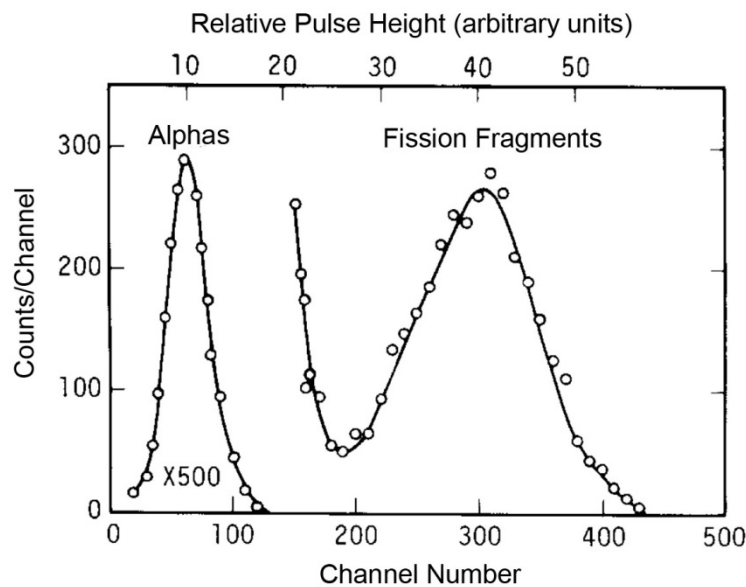
Figure 11.14. Pulse Height Spectrum from U Containing Single Crystal Scintillator (Catalano and Czirr 1977). Reprinted with permission from Elsevier © 1977.

11.3 Alternate Optical-based Neutron Detection Schemes

11.3.1   Neutron Flux Monitoring using Nuclear Pumped Lasers

There is some work on the response of Ne lasers to very high neutron flux. The phenomenon was shown experimentally but the theory is quite complex and not all authors agree (Derzhiev et al. 1989). Figure 11.15 shows a theorized energy cascade diagram of a nuclear-pumped laser from a Russian research group (Derzhiev et al. 1989). The neon transition of interest is 3p'$[1/2]_0$-3s'$[1/2]_0^1$. The transition requires neutron flux and collisions with other gas atoms at high pressures. In some experiments ^{3}He is used in the gas mix, along with argon and H_2. The transition of interest has a characteristic emission line at 585.3 nm. The intensity of the emission does appear to track with reactor power, but it does not initiate until the neutron flux is very high 10^9–10^{12} n/cm^{2}s (Nakazawa et al. 1994).

Figure 11.16 shows the variation of the neon 585.3 nm emission with reactor power and mixing gas. This data was collected at constant temperature via optical-fiber interface. Figure 11.17 shows the full visible light emission from a neon gas-mixed laser cell as a function of reactor power. The authors attribute the broad short wavelength emission band to Cherenkov radiation (Sakasai et al. 1996).
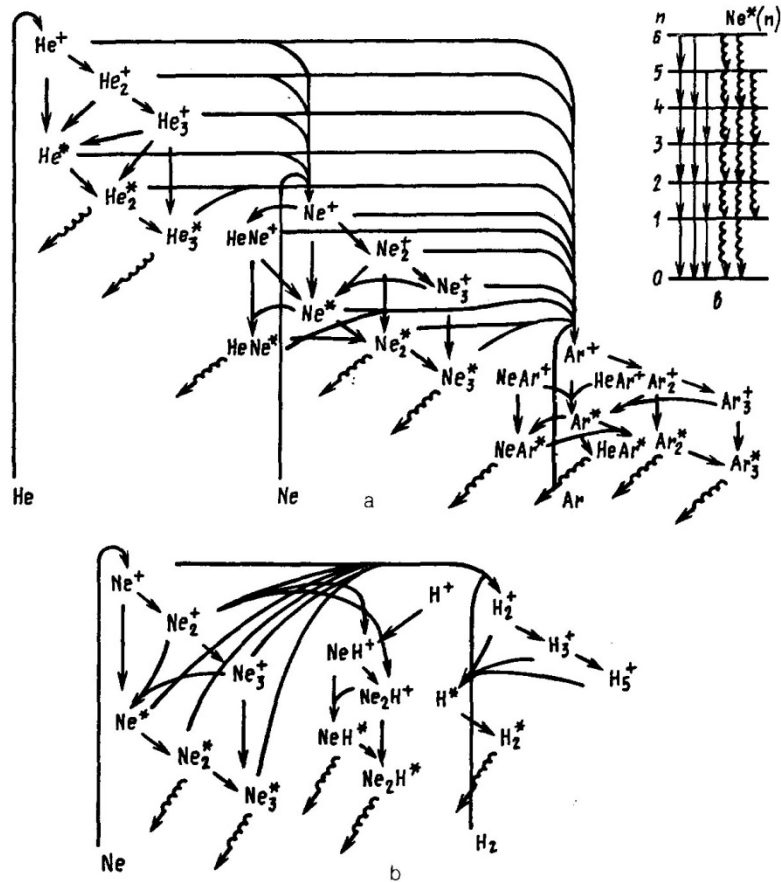
Figure 11.15. Proposed Energy Transfer Diagram for Ne-He-Ar Laser Neutron Laser (Derzhiev et al. 1989). Reprinted with permission. © 1989 AIP Publishing LLC.
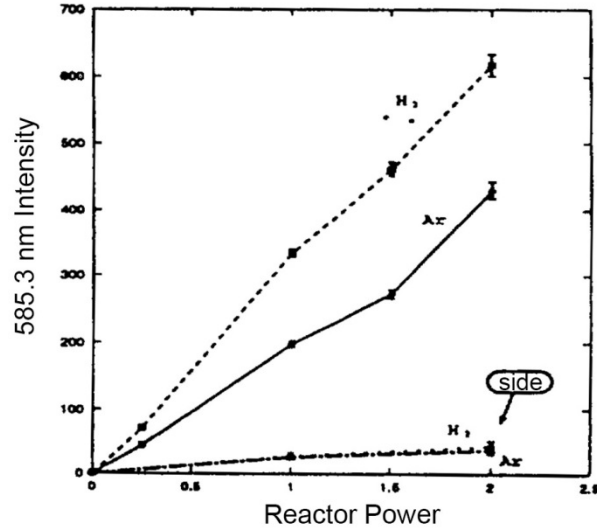
Figure 11.16. Neon 585.3 nm Emission Intensity as a Function of Nuclear Reactor Power and Mixing Gas. © 1994 IEEE. Reprinted, with permission, from Nakazawa et al. (1994).
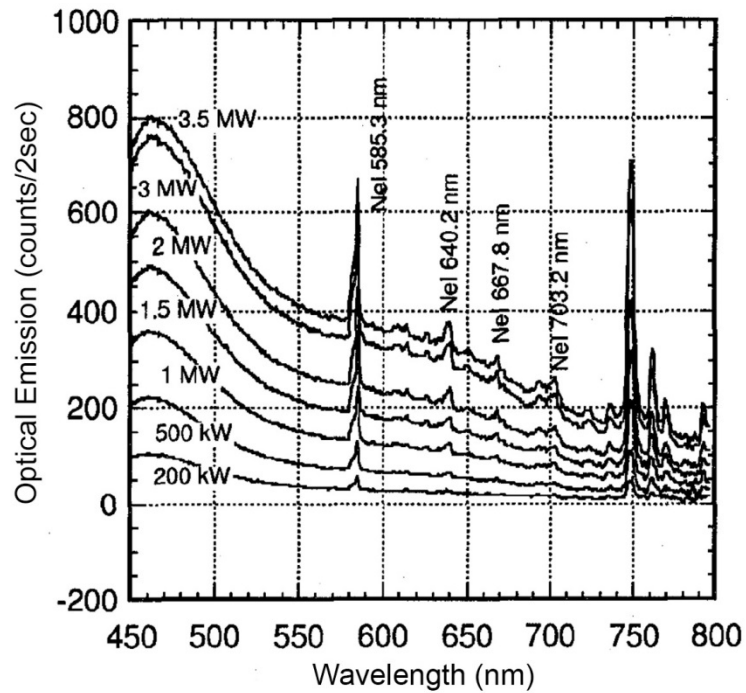
Figure 11.17. Full Emission Spectra from a Neon Mixed Gas Laser Cell as a Function of Reactor Power (Sakasai et al. 1996). © 1996. Reprinted, with permission. The broad short wavelength peak is attributed to Cherenkov radiation.

11.3.2   Neutron Flux Monitoring using Neutron Capture by CO_2 Gas

The Sudbury Neutrino Observatory applied a novel method of neutron flux monitoring that could be used in high-temperature regions (Dragowsky et al. 2002). Carbon dioxide gas serves as the detection medium (gaseous fluorocarbons can also be used for neutron capture). Fast neutrons (14 MeV) from a deuterium-tritium generator were captured by ^{16}O (or ^{19}F), then ^{16}N is produced by the n,p reaction. The ^{16}N gas has a half-life around 7 s, so some gas can be transferred from the neutron exposure area (shown in Figure 11.18) to a lower background detector region, where the characteristic decay products are measured. The decay of ^{16}N to ^{16}O emits beta particles and high-energy gamma rays. The detection cell, shown in Figure 11.19, is designed primarily to detect the betas and provide an indication of the gammas without any energy resolution. The isotopes of the CO_2 gas are very stable; therefore, signals detected are mainly attributed to ^{16}N decay. This system required extensive modeling to predict the ^{16}N generation rate, optimal gas flow, piping, and detection efficiencies. This modeling provided the optimum gas pressure and flow rate to maximize sensitivity. The design was constructed and the performance was found to be consistent with the design model. The high chamber gas pressure (6.5 atm) facilitates monitoring very high neutron flux conditions. The neutron irradiation chamber design, shown in Figure 11.18, suggests that it could be feasible to develop a design for very high temperature operation. The external detector could be placed outside the reactor chamber if the gas transfer line is short and the CO_2 gas flow high.
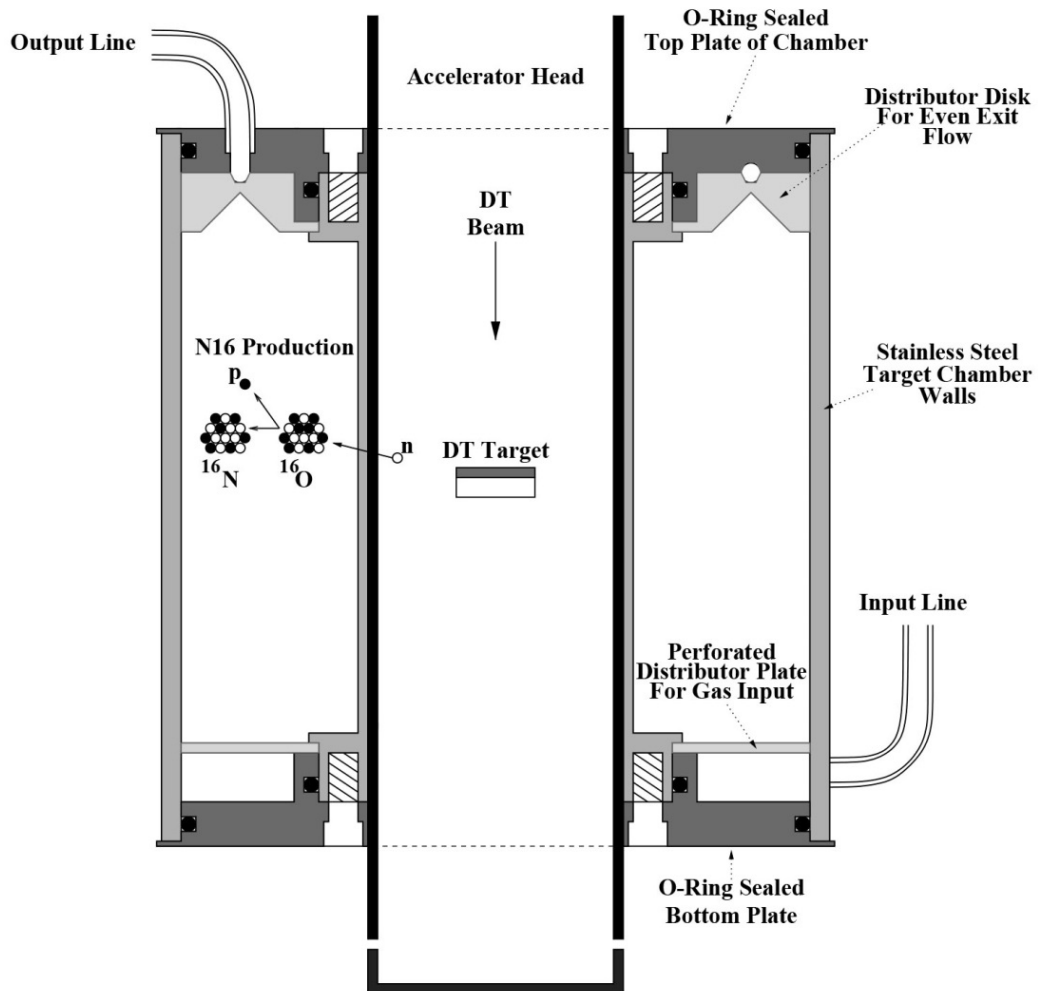
Figure 11.18. Neutron Irradiation Chamber for CO_2 Gas to Produce ^{16}N Gas (Dragowsky et al. 2002). The output line transfers ^{16}N gas to an external beta detector. Reprinted with permission from Elsevier © 2002.
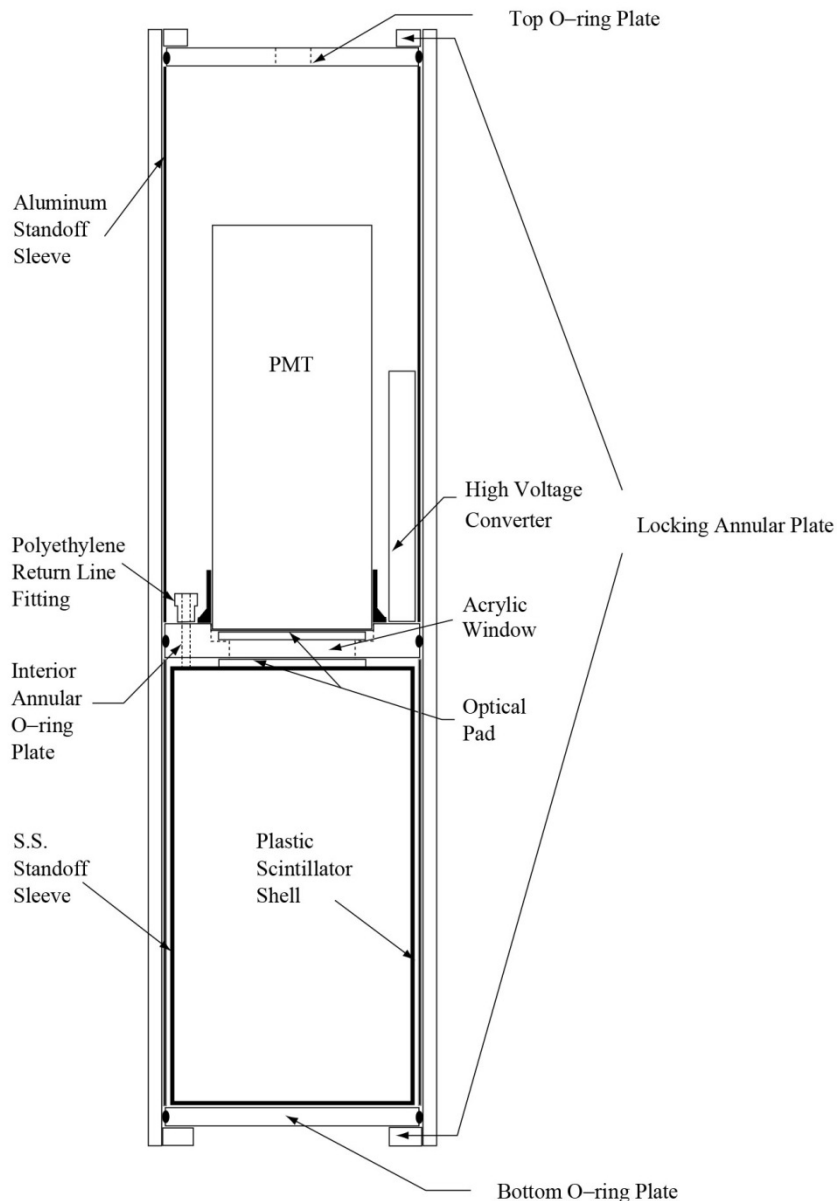
Figure 11.19. Gas Cell to Detect the Beta Decay of ^{16}N to ^{16}O (Dragowsky et al. 2002). Reprinted with permission from Elsevier © 2002.

11.3.3 Neutron Flux Monitoring using the Electro-optic Effect

Two recent papers indicate that the electro-optic (EO) effect can be sensitive to neutron flux. The two experiments published so far used a neutron port at a TRIGA reactor. The impact of gamma rays on this property was not measured. In the first paper CdZnTe and LiNbO$_3$ crystals were compared in the same experiment (Nelson et al. 2010). Figure 11.20 shows the experimental configuration. Polarized Nd:YAG laser light (1064 nm) enters the EO crystal, which is held under a constant applied voltage. A second polarizer analyzes any polarization rotation of the laser light after it passes through the EO crystal. Changing the EO crystal applied voltage can electronically control rotation. Rotation results in loss in

transmitted laser power, as measured by the photodiode detector. The authors expected neutron capture on ^{6}Li and ^{113}Cd to create small charge clouds that would counteract the applied voltage and change the optical rotation angle. Only the CdZnTe exhibited a response to neutrons. The authors attributed this to the longer charge carrier lifetime in CdZnTe. CdZnTe is a wide bandgap semiconductor while LiNbO$_3$ is an insulating material. Figure 11.21 shows the change laser transmission power at two applied voltages as a function of reactor power for CdZnTe.
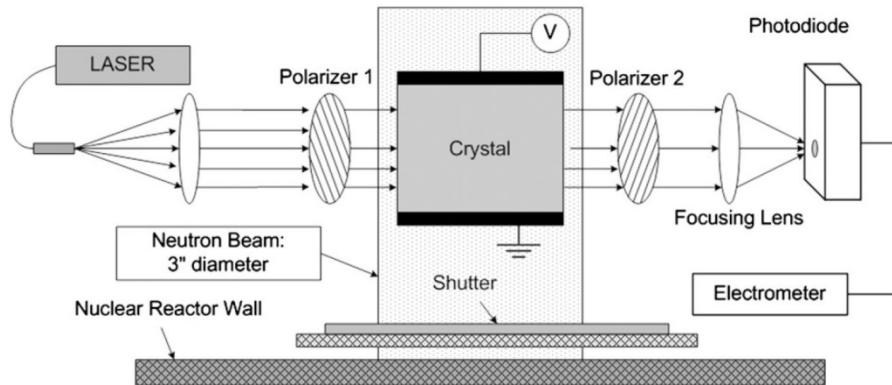
Figure 11.20. Electro-Optic Effect Experimental Setup (Nelson et al. 2010). Reprinted with permission from Elsevier © 2010.
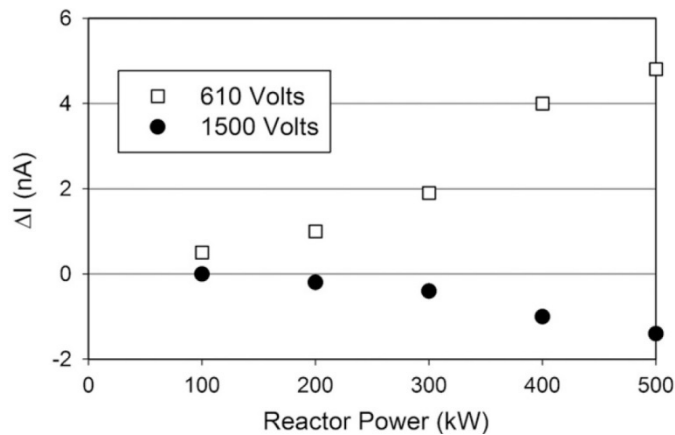
Figure 11.21. Variation in Transmitted Light Intensity with Reactor Power at Two Applied Voltages on CdZnTe Crystal (Nelson et al. 2010). Reprinted with permission from Elsevier © 2010.

A second later paper studied CdZnTe EO response to power transients in a TRIGA reactor (Nelson et al. 2012). Transient detection is important for monitoring reactor health. Transients are generally associated with a mechanical failure, such as control rods in the wrong position or location. This second paper does a more thorough characterization of the optical rotation behavior of the CdZnTe and the optimal electrode pattern from the first paper. The detector configuration, voltage, and polarizers were optimized for sensitivity and tested against reactor transients that produced a large pulse of neutrons. As

in the first paper, the experiment was performed in a pure neutron beam with most of the gamma rays filtered out. The temporal response is shown in Figure 11.22.
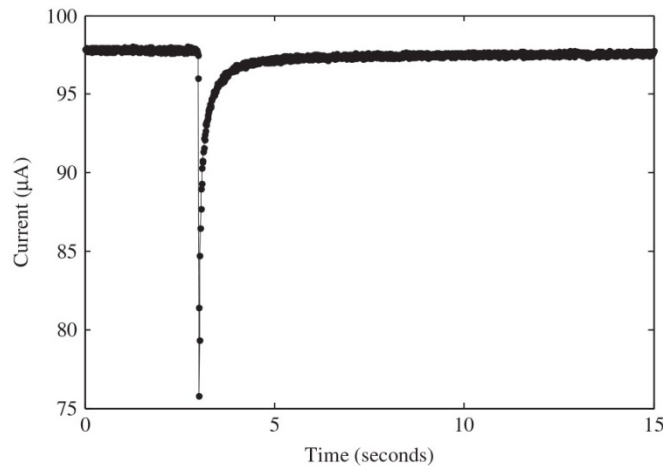
Figure 11.22. Real-Time Response of CdZnTe to a Reactor Power Transient Power (Nelson et al. 2012). Reprinted with permission from Elsevier © 2012.

11.4 Alternate Reactor Power-Monitoring Technique – Cherenkov Radiation Monitoring

Cherenkov (alternatively, "Čerenkov") radiation emission is a unique phenomenon caused by charged particles traveling through a medium faster than the phase velocity of light in that medium. When high-energy beta particles are released from fission product decay, a blue or purple glow is commonly observed in pool-type reactors with transparent coolant (i.e., water). Studies have shown that the intensity of this emission scales linearly with core power over most of the operating power range. While the Cherenkov concept looks very promising, background optical emissions (scintillation and Cherenkov) produced by residual coolant fission decay will limit the low-power monitoring performance. Coolant purification techniques may minimize some of the background noise.

Cherenkov radiation was first observed in the early 20th century and was definitively explained in the 1930s experimentally by Pavel Cherenkov, and theoretically by Igor Tamm and Ilya Frank (Al-Masri 1996). Early studies of this relatively weak electromagnetic emission were hampered by the primitive state of photodetectors. However, in the era of nuclear power, the study of Cherenkov radiation assumed renewed importance, and over the last 70 years a large body of information has resulted from many research studies.

Cherenkov radiation is made possible by the fact that light travels more slowly through media having refraction index (RI) greater than air, yet high-energy beta particles may exceed the speed of light in a high-RI medium, while still traveling slower than the fundamental speed of light in a vacuum. The particle energy at which the speed of light is exceeded in the media is known as the Cherenkov threshold, which is dependent primarily on the RI of the medium (Collins and Reiling 1938). As an example, the

11.20

Cherenkov threshold for water (RI=1.33) is 265 keV, while the threshold for air (RI=1.00029) is 21 MeV (Jelley 1955).

The spectrum of Cherenkov radiation is strongest in the deep UV and the photon distribution ($dW/d\lambda$, in photons per spectral unit) steeply drops off as (Jelley 1955),

$$\frac{dW}{d\lambda} \propto \frac{1}{\lambda^3} \tag{11.1}$$

The result of Eq. (11.1) is a spectrum that looks much like Figure 11.23. The tail of the Cherenkov spectrum is intense in the deep ultraviolet, but quickly diminishes as the wavelength increases into the visible. Normally the water coolant does not transmit the deep ultraviolet spectrum, so the glow appears visually as a pale violet to blue color in water-cooled reactor pools. Cherenkov reactor power monitoring should be very effective in MSR and FHR designs, because the molten salt coolant has very good transparency down to about 120 nm. Cherenkov light exhibits the brightest intensity in high-RI media, so helium (RI=1.000035) and supercritical water (RI≈1.1) coolants will produce weaker Cherenkov signals compared to molten salt coolants (RI=1.3-1.5). However, it has been demonstrated that increased He pressure increases the RI, which produces higher intensity Cherenkov radiation (Porges et al. 1970).
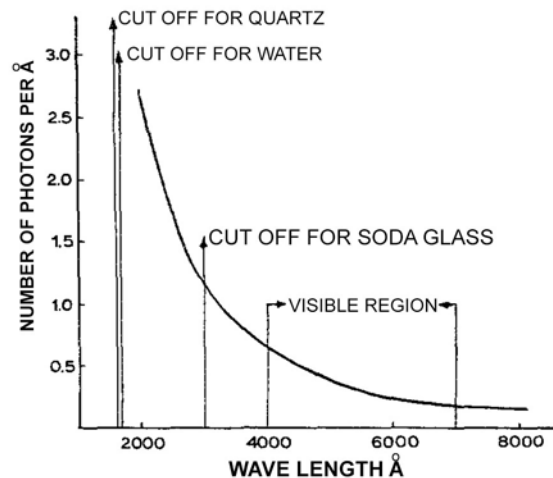
Figure 11.23. Spectrum of Cherenkov Light from a 10 MeV Electron in Water (Rippon 1963). Reprinted with permission from Elsevier © 1963.

Cherenkov radiation monitoring is feasible in both high index liquid and gas media. Coolants, such as He, SCW, and molten Na, and Pb coolants produce little or no Cherenkov radiation because of low index or opaque coolants. These reactor designs could be equipped with a high-index gas or transparent liquid-filled cell that is connected to an external optical detector using an optical fiber or free-path configuration. A gaseous Cherenkov detector has been suggested to detect high-energy gamma rays (Atkinson and Perez-Mendez 1959; Frankel et al. 1966; Lehto 1967). This in-vessel detector concept is a simple, passive chamber filled with CO_2 gas under pressure. High-energy gamma rays eject electrons from the chamber sidewalls, which in turn produce Cherenkov radiation inside the chamber. A remote optical detector then monitors this emission. The Cherenkov radiation threshold is a function of chamber

11.21

pressure. Below this threshold, no Cherenkov radiation is produced. This is a significant advantage over Cherenkov radiation monitoring directly from transparent coolants, because control of the cutoff threshold is now provided. This control is key, because gamma ray distributions above 4 to 5 MeV convey the same information as neutron distributions, and thus too the instantaneous reactor power level. Additionally, this threshold reduces background Cherenkov radiation interference produced from nonreactor sources (i.e., fission and coolant activation), which convey no information about instantaneous reactor power level. The Cherenkov gas detector concept could be extremely impactful by providing a high-temperature 'approach-to-criticality' power monitoring system. To advance this concept, a high-temperature gas cell design must be developed. A high radiation-resistant, hollow-core PCF could be used to couple emission from the gas chamber to an external optical detector.

Currently Cherenkov radiation monitoring is not used in commercial nuclear reactors for core power monitoring, likely because of the acceptable performance provide by SPD and ion chamber technology. This concept has been well described in the literature and has been successfully deployed in test reactors on multiple occasions (Rippon 1963; Arkani and Gharib 2009). Typically, either a photomultiplier tube (PMT) or a photodiode array is sealed inside a shielded tube with a collimator at the end (the collimator eliminates much of the background radiation from activated coolant). This unit can either be aimed directly into the coolant (Rippon 1963) or placed at the end of a standpipe (Arkani and Gharib 2009). The latter configuration is illustrated in Figure 11.24, and represents the most feasible approach for AdvSMR power monitoring. As described in Section 2.4.1, a standpipe configuration has several important advantages. The sensitive detectors and optic components are further separated from intense radiation and temperature exposure. The right-angle mirror directs Cherenkov light into a detector, but allows direct gamma rays to pass through, thereby further isolating the sensor components. Finally, the lower end of the standpipe can be immersed in the liquid coolant to avoid distortion and signal loss from surface ripples.
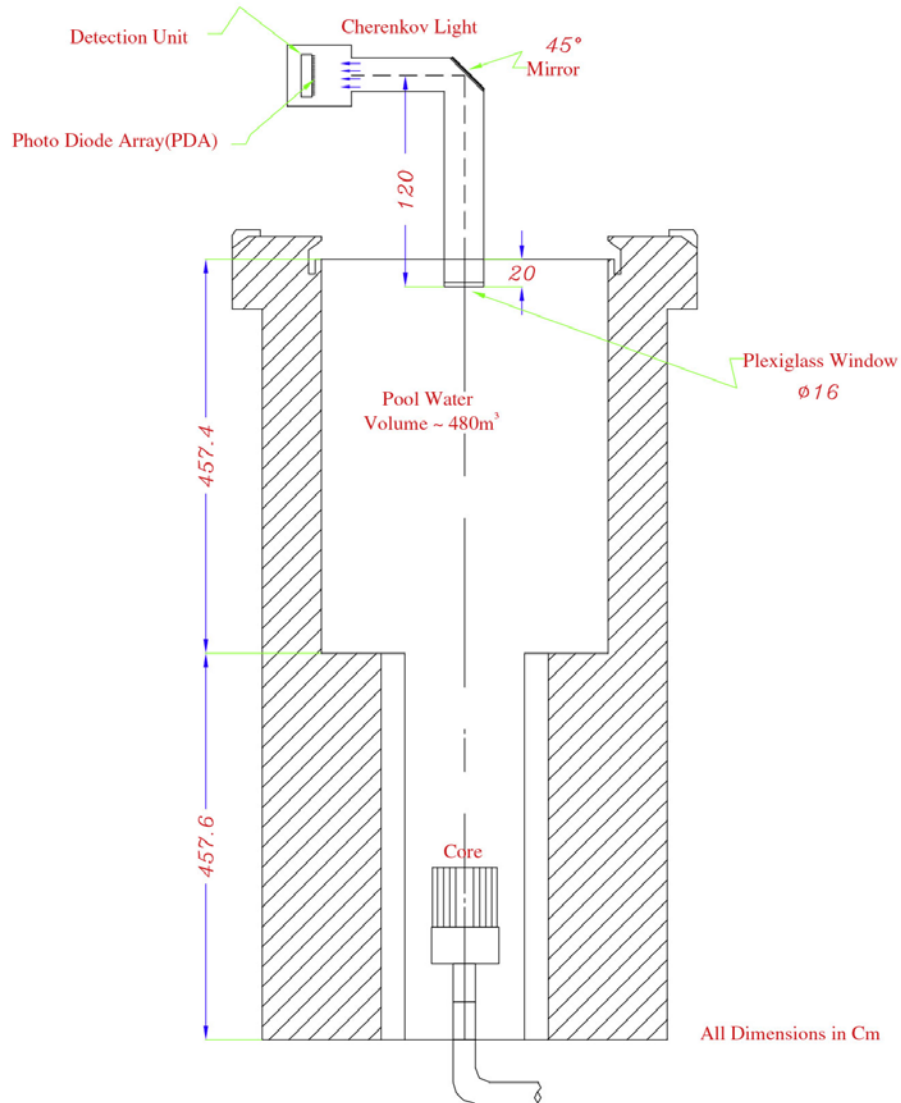
Figure 11.24. Experimental Setup for Cherenkov Radiation Monitoring in a Pool-Type Test Reactor Using a Standpipe Configuration (Arkani and Gharib 2009). Reprinted with permission from Elsevier © 2009.

11.5 COTS Summary, Gaps Analysis, Ranking, and Proposed Future Research Path

COTS Neutron Flux Monitoring Summary

Many optical-based, neutron flux monitoring concepts were identified. The technical readiness for all concepts is **LOW**, because no COTS systems were identified in this survey. Conventional gamma thermometry may satisfy AdvSMR power monitoring requirements, because this technology may provide high-temperature, high-sensitivity, and large dynamic range performance. Nevertheless, secondary power monitoring systems may be required or desirable to provide redundancy, measurement confirmation, and cross-calibration capabilities.

A few promising concepts have been developed to various maturity levels by several research groups, but for lower coolant temperatures (i.e., <550°C) it will be difficult to find an optical sensing system that is superior to commercial SPDs and ion chambers. These COTS devices have demonstrated performance in LWRs. The research information available generally focuses on studies conducted in experimental reactors. Most of this work comes from Japanese research groups. A few studies evaluate design response as a function of reactor power. Only a few studies perform measurements at elevated temperatures. Several methods were conceptualized or modeled, but were never developed or demonstrated. A few exotic concepts are based on neutron capture by gas compounds. Many designs use optical fibers with either doped-active materials or use the fiber to conduct optical signals from the active material to a detector. The technical gaps for COTS optical fiber have been discussed in other sections of this report. It is possible that some of these designs could be effective if mounted outside the reactor vessel.

11.5.1 Neutron Flux and Power Monitoring using Radiation-induced Luminescence

COTS RIL Neutron/Power Monitoring Summary

Many stable RIL materials are commercially available that produce luminescence signals under high neutron flux. Some RIL materials are compatible with high temperature. Designs can be configured as doped-optical fiber or bulk RIL material with fiber optic interconnection. COTS optical-fiber delivery components are also readily available for integration with the RIL materials.

Gaps Analysis

- Fiber optic systems have both limited high operation temperature and suffer from radiation-induced degradation. Extensive discussion of the issues is detailed in other sections of this report.

- Darkening and other radiation degradation reduce transmission of RIL signals, although the 1270-nm emission line may be beyond the wavelength range affected by radiation-induced darkening.

- Darkening and color centers can self-anneal after post irradiation, making calibration difficult.

- The absolute magnitude of the optical emission is typically not given, which makes assessment of the design or concept feasibility difficult.

- Long-term durability and stability of RIL materials placed with AdvSMRs is uncertain.

Technical Readiness Ranking

Technical readiness for the RIL-based monitoring concept is **LOW**, because of lack of complete COTS monitoring instruments and the optical fiber radiation-resistance specifications knowledge gaps. While the ranking is **LOW**, all the components needed to develop RIL monitoring systems are readily available as COTS components.

Proposed Future Research

- The research conducted by the Japanese research groups has demonstrated promising results. Further study of RIL materials, especially materials that tolerate very high temperature and have minimal damage under constant radiation exposure, is recommended.

- Further measurements of promising RIL materials are recommended at NIR wavelength range, where possible Cerenkov emission and darkening effects will be low.

- Further development of radiation-hardened optical fiber is very desirable, as discussed in more detail in other sections of the report. Radiation-hardened optical fiber is a critical enabling technology for this application.

- Study of the long-term durability and stability of these materials under AdvSMR-like conditions is needed.

11.5.2 Neutron Flux and Power Monitoring using Radiation-induced Fiber Damage

COTS Radiation-induced Fiber Damage Neutron/Power Monitoring Summary

Monitoring radiation-induced damage in optical fibers has been suggested as a method to measure radiation dose by several research groups. Many damage mechanism occur simultaneously in the core, cladding, coating, and cabling materials. Real-time sensing of integrated dose is obtained by comparing optical transmissions of the fiber in the radiation field to a reference fiber outside the field using a common light source. Some of the optical transmission is recovered after irradiation.

Gaps Analysis

- Optical fibers are damaged by radiation exposure through many processes, depending on fiber composition and construction. Not all damage pathways are well understood.

- Transmission loss because of radiation exposure continually erodes the signal-to-noise of the sensor. Darkening and color centers can self-anneal after post irradiation, making calibration difficult. Because of these issues, correlation to reactor power may be difficult.

- Optical fiber, in general, is not compatible with high temperatures, which limits deployment options.

Technical Readiness Ranking

The technical readiness for designs based on the fiber damage neutron/power monitoring concept is **LOW**, because of lack of complete COTS monitoring instruments and the optical fiber radiation-resistance specifications knowledge gaps. While the ranking is **LOW**, all the components needed to develop this monitoring system concept are readily available as COTS components.

Proposed Future Research

- Continued research on radiation-induced damage in optical fibers seems prudent, but development of sensors based on this concept has limited applicability to AdvSMRs.

11.5.3 Neutron Flux Monitoring using Fiber-Optic Interferometry

This concept has only been studied from the modeling standpoint. Given the Mach-Zehnder interferometer, the design has all the limitations of fiber optics, as discuss previously. This concept has **LOW** technical readiness, because of the lack of maturity and COTS instruments. Further work on this concept not recommended.

11.5.4 Neutron Flux and Power Monitoring using Scintillating Fiber and Fiber-coupled Scintillators

COTS Scintillating Fiber Neutron/Power Monitoring Summary

Many stable scintillator materials are commercially available that produce emission signals under high neutron flux. Readout electronics and detectors are also commercially available. Some scintillator materials are compatible with high temperature. Glass scintillators are temperature-limited to below 600–800°C depending on the specific composition. Crystalline scintillators are limited by their melting point. Neutron-γ discrimination is possible using two different scintillator materials. Designs can be configured as doped-optical fiber or bulk scintillator material with fiber-optic interconnection. Designs that use scintillator material at the tip of an optical fiber are extremely simple to manufacture.

Gaps Analysis

- Fiber-optic systems have both limited high-operation temperature and suffer from radiation-induced degradation. Extensive discussion of the issues is detailed in other sections of this report.

- The test reactors that these materials were tested in have much lower neutron flux and temperature compared to AdvSMR designs. The performance at high flux and temperature is uncertain.

- Long-term durability and stability of scintillator and phosphor materials placed with AdvSMRs is uncertain.

Technical Readiness Ranking

The technical readiness for designs based on the scintillating neutron/power monitoring concept is **LOW**, because of lack of complete COTS monitoring instruments and the optical fiber radiation-resistance specifications knowledge gaps. While the ranking is **LOW**, all the components needed to develop this monitoring system concept are readily available as COTS components.

Proposed Future Research

- The research conducted by several Japanese research groups has demonstrated promising results. Further study of scintillator and phosphor materials, especially materials that tolerate very high temperature and have minimal damage under constant radiation exposure, is recommended.

- Further measurements of promising materials are recommended at NIR wavelength range, where possible Cerenkov emission and darkening effects will be low.

- Further development of radiation-hardened optical fiber is very desirable, as discussed in more detail in other sections of the report. Radiation-hardened optical fiber is a critical enabling technology for this application.

- Study of the long-term durability and stability of these materials under AdvSMR-like conditions is needed.

Neutron Flux Monitoring using Nuclear Pumped Lasers

This concept has only been studied experimentally, but the theory is quite complex and not all authors agree on the science details. The concept is limited to somewhat high neutron flux, so start up monitoring

is not possible. The resonator mirrors are typically fabricated from fused silica, so they could suffer from darkening and other damage while under long-term exposure to radiation. The reflective multi-stack dielectric films would likely delaminate from the mirror substrates when exposed to extreme temperature cycling. It is uncertain whether the other resonator component could tolerate the extremes of in-vessel deployment. This approach has **LOW** technical readiness, because of the lack of maturity and COTS instruments. Further work on this concept not recommended.

11.5.5 Neutron Flux Monitoring using Neutron Capture by CO_2 Gas

COTS CO_2 Gas Neutron/Power Monitoring Summary

This approach is another novel concept based on neutron capture by gas compounds. The high chamber gas pressure (6.5 atm) facilitates monitoring very high neutron flux conditions. The neutron irradiation chamber design is simple and suggests that it could be feasible to develop a design for very high-temperature operation. The detector is conventional scintillator design with a COTS photomultiplier. The detector could be placed outside the reactor chamber if the gas transfer line is short and the CO_2 gas flow is high.

Gaps Analysis

- It is uncertain whether a durable neutron irradiation chamber could be designed for high-temperature deployment. The O-ring seals may be degraded by radiation exposure.

- CO_2 gas is very reactive with Na coolant and leaks into other AdvSMR coolants would be undesirable.

- The performance at low neutron flux is unclear.

Technical Readiness Ranking

The technical readiness for designs based on the CO_2 gas neutron/power monitoring concept is **LOW**, because of lack of complete COTS monitoring instruments. While the ranking is **LOW**, all the components needed to develop this monitoring system concept are readily available as COTS components.

Proposed Future Research

- A study to evaluate the implications of a CO_2 leak with all the AdvSMR designs is recommended.

- This concept is intriguing by its simple design. The sensor appears to be effective at high neutron flux. Further modeling is suggested to better understand the dynamic range and sensitivity.

- An engineering effort is recommended to evaluate and test high-temperature irradiation chamber designs.

11.5.6 Neutron Flux Monitoring using the Electro-optic Effect

Steady-state and transient neutron flux measurement were made in a TRIGA reactor using an EO sensor. The sensor is based on a standard EO laser amplitude modulators. It is unclear whether the EO assembly was COTS or not. The sensor did respond to low reactor power (i.e., 100's kW), but the response at higher reactor power is uncertain. Fast transient monitoring was demonstrated to be feasible.

The EO sensor design uses delicate optical components that would not survive the harsh AdvSMR in-vessel environment, nor does it seem feasible to change the design to improve the ruggedness and durability. In addition, high voltage is required to operate the EO sensor. Further study of EO sensors for neutron flux monitoring is not recommended.

11.5.7 Reactor Power Monitoring Using Cherenkov Radiation

COTS Cherenkov Radiation Neutron/Power Monitoring Summary

The Cherenkov power monitoring concept provides remote, standoff core power monitoring. The concept is compatible with the proposed standpipe viewport concept. Cherenkov radiation emission scales linearly with core power over most of the operating power range and is independent of fuel burn-up and core configuration. The concept is extremely simple to implement and uses very cost-effective components. The Cherenkov spectrum is independent of medium, temperature, pressure, and other effects. Power monitoring can be conducted regardless of the core outlet temperature and could be particularly useful for MSR and FHT AdvSMR designs, by directly monitoring the molten salt coolant Cherenkov radiation. Cherenkov radiation monitoring is feasible in both high index liquid and gas media. Coolants, such as He, SCW, molten Na, and molten Pb coolants produce little or no Cherenkov radiation because of low index or opaque coolants. These reactor designs could be equipped with a high-index gas or transparent liquid-filled cell that is connected to an external optical detector using an optical fiber or free-path configuration. An in-vessel detector concept is a simple, passive chamber filled with CO_2 gas under pressure. High-energy gamma rays eject electrons from the chamber sidewalls, which in turn produce Cherenkov radiation inside the chamber. A remote optical detector then monitors this emission.

Gaps Analysis

- Background optical emission noise may limit performance: activation of coolants produces high gamma backgrounds, which leads to background Cherenkov radiation at low reactor power and background scintillation emission is present at low power.

- It is uncertain whether this approach will satisfy the need for an "approach to criticality" monitor.

- The Cherenkov detector must be shielded from all other sources of light.

- Only useful in UV-visible transparent coolants, unless the CO_2-filled detector concept is developed.

- No COTS measurement system currently available.

- The feasibility of the Cherenkov gas detector is uncertain, in terms of sensitivity, dynamic range, and linearly.

- Actual performance and benefits of Cherenkov radiation monitoring must be determined.

Technical Readiness Ranking

The technical readiness for designs based on the Cherenkov radiation neutron/power monitoring concept is **LOW**, because of lack of complete COTS monitoring instruments and the fiber optic radiation-resistance specifications knowledge gaps. While the ranking is **LOW**, all the components needed to develop this monitoring system concept, except the in-vessel gas-filled chamber, are readily available as COTS components.

Proposed Future Research

- Engineering design and development is recommended to examine the feasibility of a fiber-coupled CO_2-filled Cherenkov chamber for in-vessel deployment.

- Further RD&D is recommended to develop methods to minimize optical background signals induced by the activated coolant to maximum the monitoring sensitivity and linearity at low reactor powers.

- Develop COTS components and monitoring instrument integration plan.

- **RD&D of a high temperature fiber-coupled Cherenkov gas detector useful for all AdvSMR concepts.**

- Extensive testing should be conducted in test reactors to determine actual performance.

11.6 References

Al-Masri MS. 1996. "Cerenkov Counting Technique." *Journal of Radioanalytical and Nuclear Chemistry* 207(1):205-213.

Arkani M and M Gharib. 2009. "Reactor Core Power Measurement Using Cherenkov Radiation and Its Application in Tehran Research Reactor." *Annals of Nuclear Energy* 36:896-900.

Atkinson JH and V Perez-Mendez. 1959. "Gas Čerenkov Counters." *Review of Scientific Instruments* 30(10):864-868.

Bliss M, RL Brodzinski, RA Craig, BD Geelhood, MA Knopf, HS Miley, RW Perkins, PL Reeder, DS Sunberg, RA Warner and W N. 1995. "Glass-Fiber-Based Neutron Detectors for High- and Low-Flux Environments." In *Proceedings of SPIE, Photoelectronic Detectors, Cameras, and Systems, Volume 2551*, pp. 108-117. July 13-14, 1995, San Diego, California. The International Society for Optical Engineering, Bellingham, Washington.

Bliss M, DV Jordan, DS Barnett, RL Redding and SK Pearce. 2007. "A MOX Fuel Attribute Monitor." *Nuclear Instruments and Methods in Physics Research A* 579:305-308.

Bliss M and JA Stave. 2012. *Final Report on Actinide Glass Scintillators for Fast Neutron Detection.* PNNL-21976, Pacific Northwest National Laboratory, Richland, Washington.

Brichard B, P Borgermans, AF Fernandez, K Lammens and M Decreton. 2001. "Radiation Effect in Silica Optical Fiber Exposed to Intense Mixed Neutron-Gamma Radiation Field." In *2001 Nuclear and Sapce Radiation Effects Conference (NSREC)*, pp. 2069-2073. July 16-20, 2001, Vancouver, BC, Canada. DOI 10.1109/23.983174. Institute of Electrical and Electronics Engineers Inc., Piscataway, New Jersey.

Catalano E and JB Czirr. 1977. "Development of a New Scintillator Containing Uranium." *Nuclear Instruments and Methods* 143(1):61-62.

Catalano E and EW Wrenn. 1975. "Single-Crystal Growth of MF_2:UF_4:CeF_3 (M=Ca, Sr, Ba) Solid Solutions." *Journal of Crystal Growth* 30:54-60.

Collins GB and VG Reiling. 1938. "Cerenkov Radiation." *Physical Review* 54:499-505.

Derzhiev VI, AG Zhidkov, AV Koval and SI Yakovlenko. 1989. "Kinetic Model of a Penning Ne Laser Utilizing a Beam He-Ne-Ar and Ne-H_2 Plasma." *Soviet Journal of Quantum Electronics* 19(8):1016-1021.

Dragowsky MR, A Hamer, YD Chan, R Deal, ED Earle, W Frau, E Gaudette, A Hallin, C Hearns, J Hewett, G Jonkmans, Y Kajiyama, AB McDonald, BA Moffat, EB Norman, B Sur and N Tagg. 2002. "The ^{16}N Calibration Source for the Sudbury Neutrino Observatory." *Nuclear Instruments and Methods in Physics Research A* 481:284-296.

Frankel S, V Highland, T Sloan, O Van Dyck, W Wales and D Wolfe. 1966. "Large Gas Filled Cerenkov Counter." *Review of Scientific Instruments* 37:15.

GE. 2013. *Power Range Detectors (LPRM)*. General Electric Company (GE). Accessed June 17, 2013. Available at http://www.ge-mcs.com/en/nuclear-reactor-instrumentation/neutron-monitoring-instrumentation/power-range-detectors.html.

Goodings A. 1978. "Experience with High-Temperature Radiation Detectors and Cables for Reactor Instrumentation Systems." In *Nuclear Power Plant Control and Instrumentation, Proceedings of a Symposium*, pp. 225-242 Cannes. International Atomic Energy Agency, Vienna.

Henschel H, O Kohn, S Metzger, M Decreton, P Devos, O Deparis, J Kirchhof and S Grimm. 1997. "Neutron Fluence and Dose Measurements by Optical Fibres." In *Proceedings of SPIE, International Conference Neutrons in Research and Industry, Volume 2867*, pp. 290-295. June 9-15, 1996, Crete, Greece. The International Society for Optical Engineering, Bellingham, Washington.

INL. 2009. *FY 2009 Advanced Test Reactor National Scientific User Facility Users' Guide*. INL/EXT-08-14709, Advanced Test Reactor, Idaho National Laboratory (INL), Idaho Falls, Idaho.

Jelley JV. 1955. "Cerenkov Radiation and Its Applications." *British Journal of Applied Physics* 6(7):227-232.

Kakuta T, K Sakasai, T Shikama, M Narui and T Sagawa. 1998. "Absorption and Fluorescence Phenomena of Optical Fibers under Heavy Neutron Irradiation." *Journal of Nuclear Materials* 285-263:1893-1896.

Kakuta T, K Szuki, H Yamagishi and H Itoh. 2000. "Demonstration of Optical In-Core Monitoring System for Advanced Nuclear Power Reactions." In *Core Monitoring for Commercial Reactors: Improvements in Systems and Methods, Workshop Proceedings*, pp. 95-101. October 4-5, 1999, Stockholm, Sweden. OECD Publishing, Paris, France.

Knoll GF. 2000. *Radiation Detection and Measurement, Third Edition*. John Wiley & Sons, Hoboken, New Jersey.

Lamphere RW. 1960. "Fission Detectors." In *Fast Neutron Physics, Part 1. Techniques*, pp. 449-505 eds: JB Marion and JL Fowler. Interscience, New York.

Lehto WK. 1967. *Measurement of Dynamic Reactor Parameters by Photon Observation*. Ph.D. Thesis, The University of Michigan. Available at http://hdl.handle.net/2027.42/6256

Nakazawa M, M Notani, T Iguchi, T Kakuta, H Yamagishi and M Katagiri. 1994. "An Optical Self-Powered Neutron Detector Using Nuclear Pumping." In *Proceedings of 1994 IEEE Nuclear Science*

Symposium - NSS'94, pp. 176-178, Vol. 1. October 30-November 5, 1994, Norfolk, Virginia. IEEE, New York.

Nelson KA, N Edwards, MJ Harrison, A Kargar, WJ McNeil, RA Rojeski and DS McGregor. 2010. "Investigation of CdZnTe and LiNbO$_3$ as Electro-Optic Neutron Detectors." *Nuclear Instruments and Methods in Physics Research Section A: Accelerators, Spectrometers, Detectors and Associated Equipment* 620(2–3):363-367.

Nelson KA, JA Geuther, JL Neihart, TA Riedel, RA Rojeski, PB Ugorowski and DS McGregor. 2012. "Nuclear Reactor Pulse Tracing Using a CdZnTe Electro-Optic Radiation Detector." *Nuclear Instruments and Methods in Physics Research Section A: Accelerators, Spectrometers, Detectors and Associated Equipment* 680:97-102.

OECD/Nuclear Energy Agency. 2000. "Core Monitoring for Commercial Reactors: Improvements in Systems and Methods." *Core Monitoring for Commercial Reactors: Improvements in Systems and Methods, Workshop Proceedings*, October 4-5, 1999, Stockholm, Sweden. OECD Publishing, Paris, France.

Porges KG, R Gold and WC Corwin. 1970. "Reactor Power Monitor Based on Cherenkov Radiation Detection." *IEEE Transactions on Nuclear Science* 17(1):501-505.

Rippon SE. 1963. "Cherenkov Detectors for the Measurement of Reactor Power." *Nuclear Instruments and Methods* 21(0):192-196.

Sakasai K, T Kakuta, H Yamagishi and M Nakazawa. 1996. "Experiments for Optical Neutron Detection using Nuclear Pumped Laser." *IEEE Transactions on Nuclear Science* 43(3):1549-1553.

Tanabe T, S Tanaka, K Yamagouchi, N Otsuki, T Iida and M Yamawaki. 1994. "Neutron-induced Luminescence of Ceramics." *Journal of Nuclear Materials* 212-215:1050-1055.

Todt Sr. WH. 1996. "Characteristics of Self-Powered Neutron Detectors Used in Power Reactors." In *Specialists' Meeting on In-core Instrumentation and Reactor Core Assessment*. October 14-17, 1996, Mito-shi, Japan. Nuclear Energy Agency. Available at www.oecd-nea.org/science/rsd/ic96/14-2.pdf**.**

Toh K, T Shikama, S Nagata, B Tsuchiya, M Yamauchi and T Nishitani. 2007. "Search for Luminescent Materials under 14 MeV Neutron Irradiation." *Journal of Nuclear Materials* 367-370:1128-1132.

Weiss JD. 2013. "A Proposed Fiber-Optic Neutron Monitor." *Nuclear Instruments and Methods in Physics Research Section A: Accelerators, Spectrometers, Detectors and Associated Equipment* 700:91-98.

Yamane Y, A Uritani, T Misawa, JK-H Karlsson and I Pázsit. 1999. "Measurement of the Thermal and Fast Neutron Flux in a Research Reactor with a Li and Th Loaded Optical Fibre Detector." *Nuclear Instruments and Methods in Physics Research Section A: Accelerators, Spectrometers, Detectors and Associated Equipment* 432(2-3):403-409.

12.0 Proposed Future Research Plan

Employing the use of optical-based measurement and sensing systems in advanced small modular reactors (AdvSMRs) has several key benefits over traditional instruments and sensors used to monitor the state of the reactor process parameters, such temperature, flowrate, pressure, and coolant chemistry. These benefits include standoff noncontact sensing, drift-free monitoring, high bandwith/high-speed data acquisition, and distributed single parameter sensing. However, technical challenges exist in the areas of 1) in-vessel optical acces to protect sensitive equipment, 2) optical materials under extreme conditions, and 3) performance limitations of commercial off-the-shelf (COTS) optical monitoring technologies.

We propose a comprehensive, multi-year research, development, and demonstration (RD&D) plan to advance the concept of in-vessel optical monitoring of AdvSMRs and the technical readiness of COTS optical materials, components, and sensing instrumentation. The plan is organized in three key thrust areas where RD&D is required to advance these goals:

- Thrust Area 1: In-vessel Optical Access Engineering and RD&D

- Thrust Area 2: Optical Materials and Components RD&D

- Thrust Area 3: Optical Monitoring Technology RD&D.

These three thrust areas contain interlinked RD&D, wherein the first two thrust areas define the engineering and materials advancements that are required to enable the optical monitoring technology advancements described in the third thrust area. For each thrust, we summarize the key technical readiness gaps and issues, and propose a research plan to close the gaps. Each thrust area contains a number of tasks that must be achieved to close the key gaps and address the deployment challenges.

12.1 Thrust Area 1: In-vessel Optical Access Engineering and RD&D

Optical access is necessary to enable future in-vessel optical monitoring systems. Furthermore, sensitive optical monitoring components (e.g., electronics, lasers, detectors, and cameras) can be placed outside the reactor vessel in the instrument vault or other locations where temperatures and radiation levels are much lower. Many of the advantages of optical-based sensing methods can be realized by using standpipe viewports and optical-fiber feedthroughs to provide optical access to the in-vessel region. The standpipe viewport concept could be designed as a periscope-type assembly, to inspect normally inaccessible areas within the reactor. Conceptually, a small periscope could be extended down through the downcomer to observe the outlet flow region. A sustained RD&D effort is required to develop engineering solutions that provide optical access into the reactor vessel. This is a high research priority that must be successfully demonstrated early in the program.

Gaps Analysis

Developing optical access into reactor vessels will be a challenging engineering problem to solve because of the high temperatures, extreme temperature variations and differentials, large radiation fluxes, corrosion damage, optical surface contamination issues, high coolant pressures, and vibration, which are all present during normal reactor operations. The technical challenges associated with optical access include physical access in complex nuclear reactor systems, designs that maintain structural integrity, and the materials that support these access concepts.

- Optical access into a nuclear reactor vessel has no prior track record from which to judge past performance and industry acceptance. Optical access engineering designs or hardware prototypes have not been developed for either conventional nuclear reactors or AdvSMR concepts.

- COTS optomechanical components and fail-safe sealing technology, required for future optical access designs, may not be available.

- Vibration and thermal expansion may affect optical alignment of both optical access systems and standoff optical beam paths.

- Coolant contact and corrosion by-products may coat and obscure optical component surfaces.

- Coolant flow may erode optical component surfaces.

- Specific requirements for AdvSMR applications are nascent.

- COTS fiber-optic feedthroughs, designed for extreme environments, have not been developed for AdvSMR applications.

- The feasibility of optical access concepts is dependent on optical component advancements described in Thrust Area 2.

- Few in-vessel periscope designs and prototypes have been developed and evaluated. A literature survey turned up no periscope systems that were tested and demonstrated in a test or conventional reactor.

Proposed Research to Address Technical Readiness Gaps

- **Optical Access Engineering**: In order to demonstrate feasibility of optical access in nuclear reactors, a set of RD&D tasks have been identified to develop engineering solutions that provide robust optical access into the reactor vessel. The successful outcome will result in establishing the basis for optical monitoring of reactor process parameters. Research tasks include:

  - **Task 1**: Develop preliminary engineering designs for in-vessel optical access concepts (standpipe viewport, in-vessel periscope, and fiber-optic feedthrough).

  - **Task 2**: Develop preliminary engineering designs for in-vessel optical alignment and optomechanical mounting.

  - **Task 3**: Develop vibration and thermal expansion compensation concepts that preserve optical alignment of both optical access systems and standoff optical beam paths.

  - **Task 4**: Develop reactor vessel integration and implementation concepts for in-vessel optical access approaches (standpipe viewport, in-vessel periscope, and fiber-optic feedthrough).

  - **Task 5**: Conduct laboratory research to develop and test prototypes in-vessel standpipe viewport and in-vessel periscope. Optimize prototypes as required.

  - **Task 6**: Evaluate COTS and custom fiber-optic feedthrough components. Optimize COTS components as required.

  - **Task 7**: Evaluate and demonstrate prototype optical access concepts in a test loop or test reactor.

12.2 Thrust Area 2: Optical Materials and Components RD&D

Thrust Area 2 outlines key technical readiness gaps currently hindering use of COTS optical materials and components for AdvSMR applications. The RD&D efforts have been organized into two research focuses: fiber-optic components and refractive and reflective optical components and coatings. The discussion below highlights the main tasks and the priority of the research required to demonstrate feasibility of this concept.

12.2.1   Fiber-optic Components

Optical-fiber components form the basic building blocks for optical sensing systems. Optical fiber can provide optical access into the reactor vessel, as well as integrated point and distributed sensing for specific in-vessel locations. Closing the technical readiness gaps listed here will enable many promising optical-fiber-based sensors to be considered for in-vessel AdvSMR monitoring applications. We identified a number of required RD&D efforts to address the established technical readiness gaps in COTS optical fibers and materials.

Gaps Analysis

The temperature and mechanical specifications for most of the optical materials used to construct optical fibers are very promising, but further RD&D will be required to enhance these materials or develop new materials for extended integration into AdvSMR designs. The most significant technology gaps that currently limit COTS optical-fiber deployment in AdvSMRs include:

- COTS optical-fiber coating, shielding, and cabling materials will not survive most in-vessel AdvSMR temperatures. Fluorine-containing plastics are known to fail mechanically in high-neutron environments. COTS high-temperature, metallized optical-fiber coatings have been used successfully in many challenging industrial applications, but they may not survive near-core temperatures and may transmute under intense radiation exposure.

- Most literature regarding the effects of radiation exposure in optical materials is from the 1970–1990 timeframe. Past optical materials exposure studies were mostly focused on long-term, low-level radiation to simulate space environments. This body of literature points to promising materials, but does not provide insight into damage issues under combined high-radiation and high-temperature exposure.

- COTS optical fiber materials may not be chemically compatible with AdvSMR coolants and impurities or have enough mechanical strength for reliable deployment in high-flow AdvSMR coolants.

- COTS photonic crystal fiber (PCF) and silica optical fibers and sapphire light pipes have not been tested under combined high-temperature and high-radiation conditions.

- COTS sapphire optical fibers are not available, only unclad light pipes. COTS fiber can only be grown to 1–4-meter lengths.

- Limited theoretical studies have been conducted to develop useful predictive damage models for optical fibers exposed to high temperature and radiation.

Proposed Research to Address Technical Readiness Gaps

The proposed research tasks to address these technical gaps are separated into four major areas. These are high-temperature fiber-optic components; sapphire, ALON®, and spinel optical fiber; COTS optical-fiber exposure study; and theoretical damage modeling.

- **High-Temperature Fiber-Optic Components**: High-temperature optical-fiber coatings, sheathings, and cabling materials must be developed that protect the optical fiber from mechanical damage and chemical attack. Research tasks include:

  – **Task 1**: Investigate alternate options for high-temperature, corrosion-resistant, and radiation-stable optical-fiber coatings, sheathing, and cabling materials. Collaborate with coating vendors to develop custom coating solutions. Use theoretical modeling results and prior research results to narrow down materials options, and select promising materials for further evaluation.

  – **Task 2**: Develop promising optical-fiber coating, optical-fiber sheathing, and cabling materials. Develop fiber coating process to coating bare COTS optical fiber.

  – **Task 3**: Evaluate optical coatings abrasion resistance, mechanical strength, chemical compatibility, and high-temperature performance. Optimize materials as required.

  – **Task 4**: Downselect promising coating, sheathing, and cabling materials for radiation exposure studies to be conducted in the COTS optical fiber exposure study.

  – **Task 5**: Develop and execute a technology transfer plan to commercial market sector.

- **Sapphire, ALON®, and Spinel Optical Fiber**: High-temperature cladding materials are required to develop useful high-temperature sapphire optical fibers. Research tasks include:

  – **Task 1**: Conduct optical modeling studies to determine optical performance enhancements of clad light pipes compared to bare light pipes. Evaluate the optical performance impact of high-temperature coating application.

  – **Task 2**: Select and develop promising high-temperature cladding materials to evaluate. Develop a fiber-coating process to clad bare COTS optical light pipes.

  – **Task 3**: Evaluate clad sapphire, ALON®, and spinel optical fibers under long-term, high-temperature exposure, as well as high-dose gamma and thermal and fast neutron exposure.

  – **Task 4**: Develop and execute a technology transfer plan to the commercial market sector.

  – **Task 5**: Work with manufacturers to develop feasible approaches for long (>10 m) fiber crystal growth.

- **COTS Optical-Fiber Exposure Study**: Exposure studies are required to determine the robustness of PCF and silica optical fibers and sapphire, ALON®, and spinel light pipes under simulated AdvSMR conditions, such as high temperature, radiation fluence, chemical exposure, and direct coolant immersion. Research tasks include:

  – **Task 1**: Develop plans and preparations for high-temperature and radiation-exposure studies for COTS PCF and silica optical fibers and sapphire, ALON®, and spinel light pipes. Testing will likely require test reactor access.

- **Task 2**: Establish a relationship with U.S. fiber manufacturers and the Russian Academy of Sciences, Fiber Optics Research Center to gain access to high-radiation-resistant FORC pure silica fiber. Develop a future collaboration plan to evaluate and advance this fiber.

- **Task 3**: Develop plans and preparations for corrosion and direct molten coolant immersion studies of promising optical fibers and light pipes.

- **Task 4**: Evaluate COTS optical fiber and light pipes' optical and mechanical performance under long-term, high-temperature and gamma, thermal neutron, and fast neutron exposure.

- **Task 5**: Evaluate COTS optical fiber and light pipes' optical and mechanical performance under long-term molten salt and metal and high-temperature helium gas exposure.

- **Task 6**: Downselect promising COTS optical fiber and light pipes and assemble with high-temperature fiber materials developed in the high-temperature fiber optic components effort list above. Evaluate and demonstrate components in test reactor to determine radiation-resistance performance and expected AdvSMR service life.

- **Theoretical Damage Modeling**: Theoretical modeling studies are required to better understand fundamental damage mechanisms in fiber-optic materials and estimate component lifetime under expected AdvSMR conditions. This includes understanding noncatastrophic effects that shorten useful life, such as plastic deformation under sustained pressure at elevated temperature and slow degradation from extended radiation and chemical exposure. Research tasks include:

  - **Task 1**: Identify available data and modeling tools needed to perform multiscale modeling of optical material degradation.

  - **Task 2**: Perform quantum mechanical calculations to relate radiation-induced defects to optical absorption bands, study defect-dopant interactions, and generate data on defect energetics.

  - **Task 3**: Perform molecular dynamics simulations of radiation damage production, phase stability under damage accumulation, degradation of elastic mechanical properties, crack propagation, dopant diffusion, and interaction of optical material surface with corrosives.

  - **Task 4**: Perform kinetic Monte Carlo simulations and continuum model calculations with parameters from Tasks 2 and 3 as input to study corrosion and plastic deformation at elevated temperature under irradiation.

  - **Task 5**: Compare modeling results to available data from experiments and previous calculations (Task 1) to validate the multiscale modeling. Populate a database with curated data on optical material performance from experiments and modeling. Use the database to estimate useful lifetime under reactor operating conditions and select materials for in-reactor monitoring.

12.2.2 Optical Components and Coatings

Optical materials are used to fabricate optical elements (e.g., windows, mirrors, and lenses), which form the basic building blocks for optical sensing systems. Optical windows are vital elements for the in-vessel optical sensing application, because these components provide the means to gain optical access into the reactor vessel. Some knowledge gaps remain regarding performance and service-life under the extremes of the in-vessel environment. Closing the technical readiness gaps listed here will enable consideration of many promising optical sensing methods for in-vessel AdvSMR monitoring applications.

We identified a number of RD&D efforts that will be required to address the established technical readiness gaps in COTS optical materials.

Gaps Analysis

The temperature and mechanical specifications for most of the optical materials used to construct optical components are very promising, but further RD&D will be required to enhance these materials' extended integration into AdvSMR designs. The most significant technology gaps that limit COTS optical materials and components for use in AdvSMRs include:

- COTS optical materials, components, and coatings may degrade (e.g., chemical reaction, corrosion, and erosion) when exposed to AdvSMR coolants and impurities.

- Vendors do not typically provide radiation-resistance specifications for COTS optical materials, components, and coatings.

- COTS optical materials, windows, mirrors, and coatings have not been tested under combined high-temperature and high-radiation conditions.

- Limited theoretical studies have been conducted to develop useful predictive damage models for optical materials and coatings exposed to high temperature and radiation.

- Large temperature ranges and peak temperatures may induce delamination of optical component coatings (e.g., reflective, anti-reflection, and protection) and substrate layers.

- Most literature regarding the effects of radiation exposure in optical materials is from the 1970–1990 timeframe. Past optical materials exposure studies were mostly focused on long-term, low-level radiation to simulate space environments. This body of literature points to promising materials, but does not provide insight into damage issues under combined high-radiation and high-temperature exposure.

Proposed Research to Address Technical Readiness Gaps

The proposed research tasks to address these technical gaps are separated into three major areas. These are high-temperature optical coatings, COTS optical materials exposure study, and theoretical damage modeling.

- **High-Temperature Optical Coatings**: High-temperature optical coatings (e.g., reflective, anti-reflection, and protection) must be developed. Research tasks include:

  - **Task 1**: Investigate options for high-temperature, corrosion-resistant, and radiation-stable optical coatings. Collaborate with coating vendors to develop custom coating solutions. Use theoretical modeling results and prior research results to narrow down materials options, and select promising materials for further evaluation.

  - **Task 2**: Develop custom vendor and research optical coatings to evaluate.

  - **Task 3**: Evaluate coatings' optical performance, abrasion resistance, chemical compatibility, and high-temperature performance. Optimize materials as required.

  - **Task 4**: Downselect promising coatings for radiation-exposure studies to be conducted in the COTS optical materials exposure study.

- **Task 5**: Develop and execute technology transfer plan to commercial market sector.

- **COTS Optical Materials Exposure Study**: Exposure studies are required to determine the robustness of promising optical materials and components under simulated AdvSMR conditions. Research tasks include:

  - **Task 1**: Develop plans and preparations for high-temperature and radiation-exposure studies for COTS chemical vapor deposition (CVD) diamond, ALON®, spinel, sapphire, and silica windows, and selected metal mirrors and optical coatings. Testing will likely require test reactor access.

  - **Task 2**: Establish collaboration agreements with COTS optical materials and components manufacturers to evaluate and advance the technology.

  - **Task 3**: Develop plans and preparations for corrosion and direct molten coolant immersion studies of promising optical components and coatings.

  - **Task 4**: Evaluate optical and mechanical performance of COTS optical components under long-term, high-temperature exposure, and dose gamma and thermal and fast neutron exposure.

  - **Task 5**: Evaluate optical and mechanical performance of COTS optical components under long-term molten salt and metal and high-temperature helium gas exposure.

  - **Task 6**: Downselect promising COTS optical windows and mirrors, then apply high-temperature optical coatings materials developed in the high-temperature optical coatings task. Evaluate and demonstrate components in test reactor to determine radiation-resistance performance and expected AdvSMR service life.

  - **Task 7**: Develop and execute a technology transfer plan to the commercial market sector.

- **Theoretical Damage Modeling**: Theoretical modeling studies are required to better understand fundamental damage mechanisms in optical materials and coatings and to estimate component lifetime under expected AdvSMR conditions. This includes understanding noncatastrophic effects that shorten useful life, such as plastic deformation under sustained pressure at elevated temperature and slow degradation from extended radiation and chemical exposure. Research tasks include:

  - **Task 1**: Identify available data and modeling tools needed to perform multiscale modeling of optical material degradation.

  - **Task 2**: Perform quantum mechanical calculations to relate radiation-induced defects to optical absorption bands, study defect-dopant interactions, and generate data on defect energetics.

  - **Task 3**: Perform molecular dynamics simulations of radiation-damage production, phase stability under damage accumulation, degradation of elastic mechanical properties, crack propagation, dopant diffusion, and interaction of optical material surface with corrosives.

  - **Task 4**: Perform kinetic Monte Carlo simulations and continuum model calculations with parameters from Tasks 2 and 3 as input to study corrosion and plastic deformation at elevated temperature under irradiation.

  - **Task 5**: Compare modeling results to available data from experiments and previous calculations (Task 1) to validate the multiscale modeling. Populate a database with curated data on optical material performance from experiments and modeling. Use the database to estimate useful lifetime under reactor operating conditions and select materials for in-reactor monitoring.

12.3 Thrust Area 3: Optical Monitoring Technology RD&D

Thrust Area 3 focuses on advancing COTS optical monitoring technologies for imaging, temperature, coolant chemisty, vibration, and power monitoring applications for AdvSMRs. A total of seven optical monitoring technologies are identified that have promising technical maturity, performance, and potential impact for AdvSMR designs. This review highlights the main tasks and research priorities required to demonstrate the feasibility of these concepts.

12.3.1   COTS Laser Absorption Spectroscopy for In-vessel Coolant Monitoring

Coolant and headspace gas monitoring in AdvSMR designs represents a tremendous opportunity where optical-sensing technology could make a major impact to critical reactor operations. Chemical monitoring systems are used to detect corrosion indicators and to maintain coolant corrosion control buffers. These monitoring systems are vital to maintain safe operations and the integrity of the reactor. Standoff COTS laser absorption spectroscopy systems may be feasible for in-vessel coolant monitoring if combined with the viewport discussed in Thrust Area 1.

Gaps Analysis

- Knowledge of reactor integration and implementation requirements and challenges is incomplete. The current COTS systems are mostly benchtop systems, research instruments, or low-resolution portable systems that may not be suitable for the AdvSMR applications. Vendors do not provide radiation-resistance specifications for COTS instruments. Optical alignment is critical and will be affected by reactor thermal cycles and vibrations. The COTS instrument may require significant modifications for this application. AdvSMR integration plan for COTS components and monitoring instrument needed.

- Feasibility and detection limits for optical impurity monitoring in coolants and cover gas must be determined. Pressure broadening of gas-phase absorption measurements may limit performance. The feasibility of spectroscopy measurements directly in transparent coolant must be determined.

- Actual performance, service-lifetime, and benefits of COTS laser absorption spectroscopy systems must be determined by laboratory study and under AdvSMR deployment conditions. Collaborate with vendors to enhance COTS product performance.

Proposed Research to Address Technical Gaps

- **COTS Laser Absorption Spectroscopy**: A high-priority research effort is recommended to determine the approach and effectiveness of laser absorption spectroscopy for in-vessel coolant monitoring. Research tasks include:

  - **Task 1**: Identify absorption spectroscopy details for each chemical compound of interest. Select appropriate laser wavelengths for the spectroscopy measurements. Develop an absorption cell prototype that provides the required measurement path length. Study the impact of high-pressure broadening and determine the detection limits for the chemical compounds of interest. Evaluate absorption measurements through molten salt coolants.

  - **Task 2**: Determine installation requirements, develop implementation plan, modify COTS instruments, and develop required installation hardware. Develop concepts to maintain optical alignment.

– **Task 3**: Evaluate and demonstrate the COTS laser absorption spectroscopy system under laboratory and simulated AdvSMR conditions to determine performance, estimated service-lifetime, and benefit for the AdvSMR application. Collaborate with vendors to enhance COTS product performance.

12.3.2　COTS Backscattering OTDR for In-vessel Temperature Measurement

Temperature is a basic, essential, and widely used measurement parameter for nuclear reactor control and monitoring systems. In-vessel temperature measurements provide plant operators and control systems with real-time data that can be used to monitor and optimize plant control. Standoff COTS backscattering optical time domain reflectometer (OTDR) may be feasible for in-vessel temperature measurements if combined with the fiber-optic feedthrough discussed in Thrust Area 1, and optical-fiber material thermal limitations, as discussed in Thrust Area 2, are resolved.

Gaps Analysis

- Knowledge of reactor integration and implementation requirements and challenges is incomplete. The current COTS backscattering instrumentation, as designed, may not be suitable or suffer performance limitations when deployed in the containment area. The COTS instrument may require significant modifications for this application. Vendors do not provide radiation-resistance specifications for COTS instruments.

- Radioluminescence in the optical fiber may produce optical background noise. The feasibility of direct fiber immersion into molten coolants is uncertain. High temperature combined with high-radiation exposure may affect measurement performance.

- Actual performance, service lifetime, and benefits of COTS backscattering OTDR temperature measurements under AdvSMR deployment conditions must be determined.

- The low-temperature limitations of optical-fiber coatings, sheathings, and cabling materials have been discussed in Thrust Area 2.

Proposed Research to Address Technical Gaps

- **COTS Backscattering OTDR**: Backscattering OTDRs are fiber-based devices that are often implemented in distributed sensor systems, where multiple points on a single fiber can be continuously and simultaneously monitored. Temperature measurement spatial resolution can be less than a centimeter along a fiber, which is more than a 100 m in length. Research tasks include:

  – **Task 1**: Evaluate the COTS backscattering OTDR instruments; determine and implement modifications needed for AdvSMR application.

  – **Task 2**: Determine installation requirements, develop implementation plan, modify COTS instruments, and develop required installation hardware.

– **Task 3**: Evaluate and demonstrate backscattering OTDR under laboratory, simulated AdvSMR conditions, and in a test reactor, to determine performance, estimated service lifetime, and radioluminescence background. Collaborate with vendors to enhance COTS product performance.

12.3.3   Cherenkov Gas Detector for In-vessel Power Monitoring

Neutron flux is measured at several locations around the reactor core as an indirect indicator of reactor power. Neutron flux is currently measured using fission counters, ion chambers, gamma thermometers, and self-powered neutron detectors. AdvSMR have very high coolant temperatures that will challenge these traditional monitoring systems. A fiber-coupled Cherenkov gas detector concept may be feasible for in-vessel power monitoring if combined with the fiber-optic feedthrough discussed in Thrust Area 1.

Gaps Analysis

- Knowledge of reactor integration and implementation requirements and challenges is incomplete. No COTS instruments are available and only limited research studies have been conducted. Feasibility is dependent on successful development of a rugged, high-temperature gas cell and resolution of optical-fiber temperature limitations discussed in Thrust Area 2.

- The feasibility of the Cherenkov gas detector concept is uncertain, in terms of sensitivity, dynamic range, and linearity. Background scintillation noise may reduce performance.

- Actual performance, service lifetime, and benefits of the Cherenkov gas detector concept for power monitoring must be determined by laboratory study and under test reactor conditions.

Proposed Research to Address Technical Gaps

- **COTS LDV**: A high-priority research effort is recommended to determine the approach and effectiveness of LDV for in-vessel vibration monitoring. Research tasks include:

  – **Task 1**: Develop high-temperature Cherenkov gas chamber designs and prototypes. Evaluate performance of high-temperature prototypes. Evaluate optical-fiber feedthrough for the gas chamber. Develop a remote, fiber-coupled Cherenkov radiation detector and processing software.

  – **Task 2**: Determine installation requirements, develop an implementation plan, and develop required installation hardware.

  – **Task 3**: Evaluate and demonstrate the Cherenkov gas detector concept under laboratory conditions, simulated reactor conditions, and in a test reactor to determine performance, estimated service lifetime, and benefit for the AdvSMR application.

12.3.4   COTS Optical Emission Spectroscopy for In-vessel Coolant Monitoring

Coolant and headspace gas monitoring in AdvSMR designs represents a tremendous opportunity where optical-sensing technology could make a major impact to critical reactor operations. Optical emission spectroscopy (i.e., standoff LIBS) may be feasible for in-vessel coolant monitoring if combined with the viewport discussed in Thrust Area 1.

Gaps Analysis

- Knowledge of reactor integration and implementation requirements and challenges is incomplete. The current COTS LIBS systems are mostly benchtop systems or research instruments that may not be suitable for the AdvSMR applications. COTS LIBS instruments may need active cooling for containment vessel deployment. Vendors do not provide radiation-resistance specifications for COTS LIBS instruments. Optical alignment is critical and will be affected by reactor thermal cycles and vibrations. The COTS instrument may require significant modifications for this application. An AdvSMR integration plan for COTS components and monitoring instrument is needed.

- Feasibility and detection limits, solid deposits, and direct coolant impurity monitoring must be determined. Pressure broadening of gas-phase emission measurements may limit performance.

- Actual performance, service-lifetime, and benefits of optical emission spectroscopy measurements must be determined by laboratory study and under AdvSMR deployment conditions.

Proposed Research to Address Technical Gaps

- **COTS Optical Emission Spectroscopy**: A high-priority research effort is recommended to determine the approach and effectiveness of optical emission spectroscopy for in-vessel coolant monitoring. Research tasks include:

  – **Task 1**: Identify emission spectroscopy details for each chemical compound of interest. Study the impact of high-pressure broadening and determine the feasibility of using optical emission spectroscopy to monitor coolants. Determine the detection limits for solid deposits and coolant impurities.

  – **Task 2**: Determine installation requirements, develop an implementation plan, modify COTS LIBS instrumentation, and develop required installation hardware. Develop concepts to maintain optical alignment.

  – **Task 3**: Evaluate and demonstrate the COTS LIBS systems under laboratory and simulated reactor conditions to determine performance, estimated service-lifetime, and benefit for the AdvSMR application. Collaborate with vendors to enhance COTS LIBS product performance.

12.3.5   COTS Cameras for In-vessel Imaging

This RD&D effort will develop in-vessel visualization during full reactor power to enable enhanced reactor safety and control. In-vessel visualization could provide operators access to sophisticated sensing and machine-vision technologies that provide efficient human-machine interface for in-vessel telepresence, telerobotic control, and remote process operations. Standoff COTS radiation-hardened or even disposable cameras may be feasible for this application if combined with the optical viewport, image relay, and periscope concepts presented in Thrust Area 1.

Gaps Analysis

COTS radiation-hardened cameras are a very mature technology that has been developed for inspection and maintenance applications during reactor refueling operations; however, in-vessel use during full-power operation is unlikely.

- Knowledge of reactor integration and implementation challenges is incomplete. An AdvSMR integration plan for COTS camera and supporting optomechanical systems must be developed. Vibration and thermal expansion may affect optical alignment of the standoff camera.

- An optical image relay system, to interface the remote camera with the standpipe viewport or an in-vessel periscope, must be designed and developed.

- COTS imaging processing software tools may require further development to be useful for AdvSMR applications.

- Actual performance, service-lifetime, and benefits of COTS camera imaging measurements must be determined by laboratory study and under AdvSMR deployment conditions (high temperature, for example).

Proposed Research to Address Technical Gaps

- **COTS Cameras**: In-vessel imaging concepts that provide multiplexed monitoring and sensing through optical viewports using COTS radiation-hardened or even disposable camera components are required. Research tasks include:

  – **Task 1**: Develop requirements, preliminary engineering, and optical design for an image relay periscope and the integration concept for standoff COTS cameras for containment vessel deployment.

  – **Task 2**: Develop vibration and thermal expansion compensation concepts that preserve optical alignment of the containment vessel relay periscope to preserve the optical image fidelity of standoff imaging system.

  – **Task 3**: Conduct laboratory research to develop and test the prototype containment vessel image relay periscope, imaging camera system, and optical alignment system. Optimize the prototype as required.

  – **Task 4**: Evaluate the feasibility of low-cost, disposable cameras for AdvSMR applications. Determine integration requirements, service-lifetime, and potential benefit.

  – **Task 5**: Evaluate and develop image-processing software to extract parameter information from camera images and video feeds.

  – **Task 6**: Evaluate and demonstrate a prototype optical imaging system, under laboratory, simulated AdvSMR conditions, and in a test reactor.

12.3.6   COTS Pyrometry for In-vessel Temperature Measurement

Temperature is a basic, essential, and widely used measurement parameter for nuclear reactor control and monitoring systems. In-vessel temperature measurements provide plant operators and control systems with real-time data that can be used to monitor and optimize plant control. Standoff COTS pyrometry may be feasible for in-vessel temperature measurements if combined with the optical viewport presented in Thrust Area 1.

Gaps Analysis

- Knowledge of reactor integration and implementation requirements and challenges is incomplete. The current COTS pyrometer systems, as designed, may not be suitable or suffer performance

limitations when deployed in a containment area. Vendors do not provide radiation-resistance specifications for COTS pyrometers. Vibration and thermal expansion may affect optical alignment of the pyrometry probe beam.

- Transmission through coolants, vapors, particle flow in gas coolants, thermal index gradients, and viewport may degrade pyrometer performance. The hot background-rich AdvSMR in-vessel environment and non-greybody emissivity of stainless steel and metal alloys may also limit performance. The feasibility of pyrometry through transparent liquid coolant is uncertain.

- Actual performance, service-lifetime, and benefits of COTS pyrometry temperature measurements must be determined by laboratory study and under AdvSMR deployment conditions.

Proposed Research to Address Technical Gaps

- **COTS Pyrometry**: Pyrometry is a standoff measurement that provides surface-temperature measurements with low drift. Scanning the probe beam through a reactor viewport could quickly provide temperature profiling of the intermediate heat exchanger (IHX), core, and pump inlet/outlet temperatures. Research tasks include:

  – **Task 1**: Evaluate the COTS pyrometry instruments. Determine and implement the modification needed for AdvSMR application. Determine the performance impact of coolant vapors, particle flow in gas coolants, thermal index gradients, and window viewport heat, vibration, and coolant coatings.

  – **Task 2**: Determine installation requirements, develop an implementation plan, modify COTS instruments, and develop required installation hardware.

  – **Task 3**: Develop and evaluate compensation for coolant vapors, particle flow in gas coolants, thermal index gradients, and window viewport heat, vibration, and coolant coatings. Develop compensation for non-greybody emissivity correction. Develop vibration and thermal expansion compensation concepts. Determine if pyrometry through transparent liquid coolants is feasible.

  – **Task 4**: Evaluate and demonstrate standoff COTS pyrometry under laboratory, simulated AdvSMR conditions, and in a test reactor. Collaborate with vendors to enhance COTS product performance.

12.3.7   COTS Laser Doppler Vibrometry for In-vessel Vibration Monitoring

Vibration monitoring is used in many nuclear reactor applications. Loose-parts monitoring systems and pumps use accelerometers to measure vibration anomalies associated with loose parts in the coolant flow or pending mechanical failure in pumps and other rotating machinery. Vibrometry measurements are important for monitoring in-vessel structures to detect coolant flow-induced vibrations, which is a particularly significant problem in He-cooled reactors. Many conventional sensors to measure in-vessel vibration cannot tolerate the higher AdvSMR coolant temperatures. Laser Doppler vibrometry (LDV) may be feasible for in-vessel vibration monitoring if combined with the viewport discussed in Thrust Area 1.

Gaps Analysis

- Knowledge of reactor integration and implementation requirements and challenges is incomplete. COTS laser vibrometers are primarily used in laboratory settings and may not be suitable for the

AdvSMR applications. Vendors do not provide radiation-resistance specifications for COTS instruments. Optical alignment is critical and will be affected by reactor thermal cycles and vibrations. The impact of intermediate chemical vapor, thermal gradients, and vibrating transparent surfaces to COTS vibration monitoring performance is unclear. The feasibility of measurements through transparent coolants is uncertain. The COTS instrument may require significant modifications for this application.

- Actual performance, service lifetime, and benefits of COTS LDV vibration measurements must be determined by laboratory study and under AdvSMR deployment conditions.

Proposed Research to Address Technical Gaps

- **COTS LDV**: A high-priority research effort is recommended to determine the approach and effectiveness of LDV for in-vessel vibration monitoring. Research tasks include:

  – **Task 1**: Evaluate COTS LDV sensitivity to intermediate chemical vapor, thermal gradients, and vibrating transparent surfaces. Evaluate instrument and software compensation for these potential challenges. Collaborate with vendors to enhance COTS product performance and develop required compensation software. Determine if measurement through molten salt coolants is feasible.

  – **Task 2**: Determine installation requirements, develop an implementation plan, modify COTS instruments as required, and develop required installation hardware. Develop concepts to maintain optical alignment.

  – **Task 3**: Evaluate and demonstrate the COTS LDV system under laboratory and simulated reactor conditions to determine performance, estimated service-lifetime, and benefit for the AdvSMR application.

13.0 Report Summary

This report summarizes a study conducted by the Pacific Northwest National Laboratory (PNNL) to evaluate optical-based instrumentation and control (I&C) concepts for advanced small modular reactor (AdvSMR) applications. These advanced reactor concepts will require innovative thinking in terms of engineering approaches, materials integration, and I&C concepts to realize their eventual viability and deployability. The primary outcomes of this report include:

1. Establishment of preliminary I&C needs, performance requirements, and possible gaps for AdvSMR designs based on best-available published design data.

2. Assessment of commercial off-the-shelf (COTS) optical sensors, components, and materials in terms of their technical readiness to support essential AdvSMR in-vessel I&C systems.

3. Identification of COTS optical sensor and materials technology gaps related to in-vessel monitoring requirements.

4. Development of a future research, development, and demonstration (RD&D) program plan to address these gaps and develop optical-based I&C systems to enhance the viability of future AdvSMR designs.

This report provides an overview of AdvSMR designs, which highlights their uniqueness, principal uses, advantages, and potential shortcomings. The report presents the potential challenge areas for sensing and monitoring instrumentation and opportunities for optical-based techniques. A generalized AdvSMR instrumentation architecture is described for the major control and interface elements, their respective subsystems, and the process monitoring parameters relevant to the reactor I&C requirements. Finally, we present several conceptual approaches to gain optical access into the reactor vessel. Further development of these concepts will be vital to enable eventual deployment of optically based monitoring systems.

The outcomes of an extensive literature and Internet-based survey identified the various optical methods that could be used to measure key reactor parameters, as well as promising optical materials that are used to fabricate optical components (e.g., fiber optics, probes, mirrors, windows, and lenses). The authors documented these optical materials and their key performance specifications (e.g., maximum continuous temperature, radiation resistance, chemical compatibility) in tabular form. We also analyzed the candidate COTS optical materials and components for in-vessel monitoring applications.

Our extensive COTS optical sensor instrumentation survey assessed the commercial market's technical readiness to support the AdvSMR development program. We examined COTS optical sensing technology to measure neutron flux/reactor power, vibration, coolant contaminants, coolant flow, coolant level, pressure, and temperature. We also reviewed the current performance of radiation-hardened cameras. Then we compared I&C and deployment requirements for the AdvSMR application against the COTS optical technology specifications to establish the technology gaps. We established a technology readiness ranking for the optical materials, components, and sensing instrumentation, and then developed a research plan to address the technology gaps and AdvSMR deployment challenges.

We ranked each COTS optical technology based on their estimate of its technical readiness, judged from best-available technology information. The ranking also depended on the location of technology

deployment with respect to the reactor core, because depending on the type of reactor, and location within the reactor vessel, radiation levels will vary significantly.

For COTS optical components located in-vessel or in direct proximity to the vessel, we considered two deployment scenarios:

1. **Near-core**: The first scenario places the optical components near the extremes of the reactor core to facilitate optical access or sensing in this region. Nominal expected conditions include temperatures up to 750°C, gamma at 10^6 Gy/h, and neutron flux at 5×10^{13} n/cm^2 s. Peak instantaneous and off-normal events can far exceed these values and conditions can vary greatly depending on the reactor design.

2. **Near reactor lid (headspace or containment building area)**: The second scenario places optical components near the reactor lid, in the headspace area, or mounted to a standpipe in the containment area to provide optical access into the reactor vessel. In this case, the temperature and radiation conditions are much lower than conditions in the core area. Nominal expected conditions include temperatures that range between 100°C to 400°C, gamma at $<10^4$ Gy/h, and neutron flux at 10^{11} n/cm^2 s or lower.

Based on the requirements of the two scenarios, we established the following ranking criteria for optical materials and optical components:

Three technology readiness tiers have been established to rank COTS optical materials and components against the in-vessel optical component requirements, either for near-core or near reactor lid deployment:

1. **HIGH** – Mature technology, readily suitable to AdvSMR optical access design requirements with modified COTS or semi-custom vendor sensor components, pending exposure studies, some further development, and demonstration studies

2. **MEDIUM** – Evolving technology, some RD&D effort is needed to develop both custom vendor and new R&D optical components, followed by extended exposure and demonstration studies

3. **LOW** – Emerging technology, considerable RD&D is needed to evaluate COTS and develop new optical materials, followed by comprehensive exposure and demonstration studies.

We also considered technical readiness of COTS optical sensing instruments in terms of their ability to meet the AdvSMR I&C requirements. In all ranking levels, a considerable reactor engineering design effort will be required to develop and demonstrate concepts that provide optical access into the reactor vessel. All COTS instruments are either standoff or fiber-based optical sensing systems. We assume that the sensitive sensor control instrumentation is isolated from temperatures above 40°C and radiation exposure is managed using the appropriate shielding. Based on these requirements and assumptions, we established the following ranking criteria for optical sensing instrumentation:

> **Three technology readiness tiers have been established to rank COTS optical sensing systems against the in-vessel AdvSMR monitoring requirements:**
>
> 1. **HIGH** – Mature technology, readily suitable to AdvSMR designs with modified COTS or semi-custom vendor sensor components, pending demonstration studies and some further development
>
> 2. **MEDIUM** – Emerging technology, some RD&D effort is needed to develop both custom vendor and new R&D sensor components, followed by extended performance evaluation
>
> 3. **LOW** – Emerging technology, considerable RD&D is needed to develop new R&D sensor components and test new materials, followed by comprehensive performance evaluation.

Optical access is currently not provided in any commercial nuclear power plant nor featured in any reactor design, although successful implementation was demonstrated in test reactors. Optical access is a vital requirement to enable future in-vessel optical monitoring systems, because few optical monitoring systems will survive in-vessel conditions, even for short-term exposure intervals, during full-power reactor operation. Optical access provides direct and continuous visualization of in-vessel components using external cameras. Point and distributed sensing can be conducted using optical fiber sensor systems. Many optical sensing techniques can be performed remotely using open optical beam path configurations.

We propose several conceptual optical access modes in this report, including in-vessel optical viewports, optical viewports mounted on standpipes, fiber-optic feedthroughs, and optical periscope modules. A sustained RD&D effort is required to develop engineering solutions that provide optical access into the reactor vessel. This will be a challenging engineering problem to solve because of the high temperatures, extreme temperature swings and differentials, large radiation fluxes, corrosion damage and optical surface contamination issues, high pressures (e.g., found in supercritical water reactors [SCWRs], very high-temperature gas reactors [VHTRs], high-temperature gas-cooled reactors [HTGRs], gas-cooled fast reactors [GFRs]), and vibration, all present during AdvSMR operations. Nevertheless, these engineering concepts should be feasible, based on published research and discussions with subject matter experts. Advancing the maturity of these concepts is required early in the program development cycle.

Table 13.1 presents the COTS optical materials and components that ranked **MEDIUM** or higher for at least one of the two deployment scenarios. While many optical materials and components fail to meet the AdvSMR application requirements, we have identified many promising optical materials and components that appear feasible for this application. The maximum working temperature specifications for these optical materials and components are also very promising.

Table 13.1. Summary of COTS Optical Materials and Components

Materials/Components	Near Core Technical Readiness	Near Lid Technical Readiness
CVD Diamond (materials)	MEDIUM	HIGH
ALON (materials)	MEDIUM	HIGH
Spinel (materials)	MEDIUM	HIGH
Sapphire (materials)	MEDIUM	HIGH
Fused Silica (materials)	MEDIUM	HIGH
Single-Crystal Molybdenum (mirror)	HIGH	HIGH
Single-Crystal Tungsten (mirror)	HIGH	HIGH
Single-Crystal Rhodium (mirror)	MEDIUM	MEDIUM
Al, Au metallized mirror	LOW	HIGH
Silica Optical Fiber	LOW	HIGH
Sapphire Optical Light Pipe	LOW	HIGH
Hollow-core Photonic Crystal Fiber	LOW	HIGH

However a key technology gap currently limits in-vessel optical fiber deployment. The maximum working temperature specifications for the coatings, sheathing, and cabling materials used on optical fibers (to improve their abrasion resistance and mechanical strength) is significantly lower than most in-vessel conditions. To advance the technical readiness of this extremely promising and enabling optical component, further RD&D is required to improve the temperature performance of optical-fiber materials. Advancements early in the program development cycle are vital to increase the technology impact for AdvSMR applications.

Knowledge gaps on the combined high-temperature and chronic radiation-exposure effects with respect to in-vessel optical materials lifetime remain. Further RD&D efforts are required to resolve these gaps and establish the actual technical readiness for such a challenging application. Nevertheless, for many optical materials, advancements are expected to come quickly with a focused effort. The impact of this effort will establish a toolbox of optical materials and components that can be used to develop practical, dependable, and robust optical engineering designs for advanced reactors. Advancements are required early in the program development cycle.

Some of the materials and components have **LOW** rankings on the near-core deployment site. We included these when 1) the optical technology could have significant impact to the AdvSMR application, 2) most of the performance specifications were exceptional, and 3) only one significant challenge remained to be solved. Further RD&D efforts are required to quickly resolve these gaps and advance technical readiness for these enabling optical technologies.

Tables 13.2 and 13.3 present the COTS optical sensing systems technical readiness rankings for all rankings **MEDIUM** or higher. Table 13.2 provides the ranking summary of COTS fiber-optical sensing systems. Here we assumed that the sensitive sensor control instrumentation will be isolated from temperatures above 40°C and radiation exposure is managed using the appropriate shielding. Deployment near the biological shield in the containment building may be one option to satisfy this requirement. We envision that the protected optical-fiber sensor instrumentation is linked to a fiber-optic feedthrough, located on the reactor vessel lid, using a conventional optical-fiber cable. A second "sensing" optical fiber, with distributed, embedded sensor elements or a single element at the end of the

fiber, is connected to the in-vessel side of the feedthrough. Both near-core and near-lid sensing applications are considered for this in-vessel sensing application.

Table 13.2. Summary of COTS Fiber-Based Optical Sensor Technology

Optical Sensing Technology	Measurement Parameter	Near Core Technical Readiness	Near Lid Technical Readiness
Semiconductor Bandgap Sensing	Temperature	**LOW**	**MEDIUM**
Backscattering OTDR	Temperature	**LOW**	**HIGH**
Fabry-Pérot Sensing	Temperature, Pressure	**LOW**	**HIGH**
Fiber Bragg Grating Sensing	Temperature, Pressure	**LOW**	**HIGH**
Intensity-Modulated Membrane	Pressure	**LOW**	**HIGH**

Table 13.3 provides the ranking summary of standoff, noncontact optical sensing systems. Here we assume that the sensitive sensor control instrumentation is isolated from temperatures above 40°C and radiation exposure is managed using the appropriate shielding. Deployment near the biological shield in the containment building may be one option to satisfy this requirement. The active or passive standoff optical configuration would gain access into the vessel, through a viewport, to interrogate a region within the reactor vessel. The standoff optical-sensing systems typically can meet the maximum working temperature specifications for the AdvSMR application. Standoff sensing system will require optical components for in-vessel optical viewport, image, or sensing beam relay from the sensor instrumentation to the viewport, and additional optical components within the reactor vessel to guide the optical beam to the intended in-vessel location. The technical readiness rankings for these optical components are given in Table 13.1 and are not factored into the standoff optical sensing systems technical rankings list in Table 13.3.

Table 13.3. Summary of COTS Standoff Optical Sensing Technology

Optical Sensing Technology	Measurement Parameter	Technical Readiness
Absorption-Based Spectroscopy	Chemical Concentration	**MEDIUM**
Tunable Diode Laser Spectroscopy	Chemical Concentration	**MEDIUM**
Emission-Based Spectroscopy	Chemical Concentration	**MEDIUM**
Laser-Induced Breakdown Spectroscopy	Chemical Concentration	**MEDIUM**
Laser Rangefinding	Coolant Level	**MEDIUM**
Laser Doppler Vibrometry	Vibration	**MEDIUM**
Radiation-Hardened/Disposable Cameras	Imaging	**MEDIUM**
Thermographic Cameras	Temperature/Imaging	**MEDIUM**
Pyrometry	Temperature	**MEDIUM**

Fiber and standoff optical sensing systems will require engineering advancements to meet the integration and installation requirements of the AdvSMR application. Further RD&D effort is required to resolve identified technical readiness gaps for each technology and to understand the actual measurement performance under AdvSMR conditions. Advancements towards these ends are required as the optical materials and the optical access engineering efforts begin to demonstrate promising results.

Appendix A

Sodium-Cooled Fast Reactor (SFR)

Appendix A

Sodium-Cooled Fast Reactor (SFR)

The Sodium-Cooled Fast Reactor (SFR) features very high core power densities, high reactor outlet temperatures, low system pressure, and a fast neutron spectrum. An advantage of sodium coolant is its relatively high heat capacity, which provides thermal inertia against overheating during reactor transients and accidents. While the fast neutron spectrum results in large fluences for internal core and reactor vessel components, it also enables fissile and fertile materials (e.g., plutonium, actinides, depleted uranium) to be used considerably more efficiently than thermal spectrum reactors with once-through fuel cycles.

While sodium has the advantage that it does not corrode steel components, it does react chemically with air and water so SFRs must be designed to limit the potential for such reactions. Important safety features of the SFR system include a long thermal response time, a large temperature margin to coolant boiling, a primary system that operates at essentially atmospheric pressure, and an intermediate secondary nonradioactive sodium system between the primary radioactive sodium circuit and the water or gas loop used in the secondary system. The primary coolant system can either be arranged in a pool layout (a common approach, where all primary system components are housed in a single vessel), or in a compact loop layout, favored in Japan. A diagram of a pool type system is included in Figure A.1.
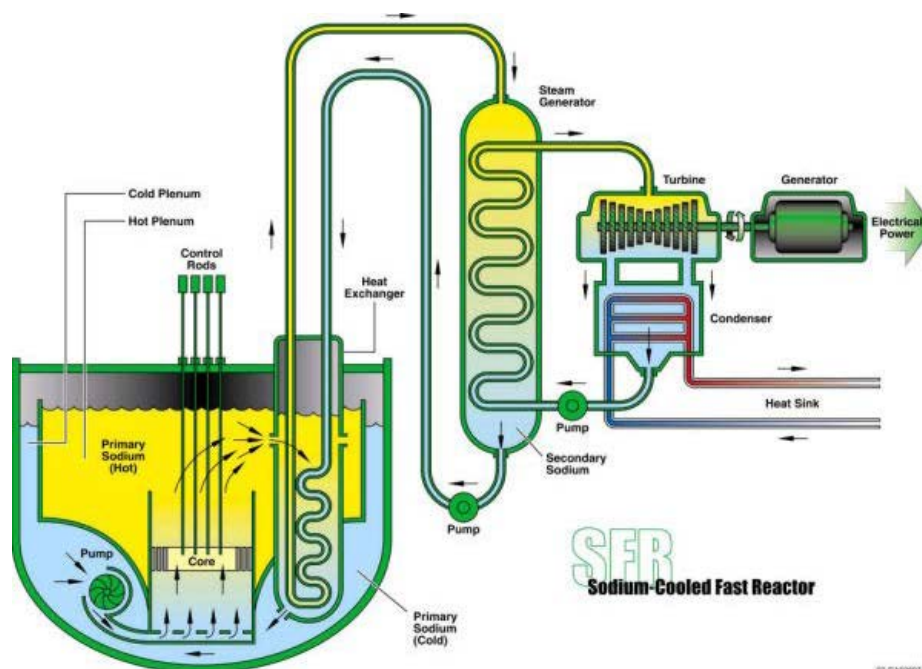
Figure A.1. General Diagram of a Pool-Type SFR Reactor System

Table A.1 provides a listing of several recent SFR concepts along with the associated organization and country of origin and Table A.2 provides an overview of some design parameters. The domestic SFR designs (e.g., PRISM, TWR) utilize a pool-type reactor vessel design containing the reactor core, primary heat exchanger, and electromagnetic (EM) pump(s). The Japanese 4S design utilizes a reactor vessel with a loop design (similar to FFTF [Fast Flux Test Facility]) containing just the reactor core; the primary heat exchanger(s)/pumps are connected by piping to the reactor vessel. An inert cover gas system is used to keep sodium from being exposed to air and/or water and supports the reactor vessel, reactor containment vessel, heat exchangers, and steam generator. In general, all penetrations into the reactor vessel are located at the top of the vessel.

Table A.1. List of Several Recent SFR Concepts and Associated Organization/Country

SFR Concepts	Organization/Country
4S (Super Safe Small Simple)	Toshiba / Japan
PRISM (Power Reactor Innovative Small Modular)	GE Hitachi / USA
ARC-100 (Advanced Reactor Concepts - 100)	Advanced Reactor Concepts LLC / USA
RAPID (Refueling by All Pins, Integral Design)	Central Research Institute of Electric Power / Japan
TWR or TP-1 (Traveling Wave Reactor)	TerraPower / USA

Table A.2. Summary of Design Parameters for Several Recent SFR Concepts

Design Feature	Parameter
Thermal Capacity Range (MWth)	5–840
Gross Electrical Capacity Range (MWe)	0.5–311
Refueling Frequency (years)	2; 10; 20; 40–60
Fuel Cycle	Breed & burn (TWR); once through (4S)

Although there are several SFRs, the general design and operating parameters are similar. The long refueling reactors (4S, TWR) on the order of 20–40+ years will require long-life components with the hope that routine maintenance is limited. The shorter refueling reactors (PRISM) on the order of 1.5+ years require fuel exchange operations that likely will allow some minimal maintenance to be performed. Electromagnetic (EM) pumps are generally used to pump sodium (Na).

The SFR is primarily envisioned for missions in electricity production along with other missions requiring relatively high-temperature process heat, desalination, and bitumen extraction from sand. The SFR design utilizes a series of loop sodium heat exchangers to a steam generator and then steam turbine for electricity and process heat for production of hydrogen. Historically, some of the operational issues with SFRs have included fires as a result of heat exchanger tube leaks, sodium leaks because of structural failures in primary piping, and thermal stratification because of inadequate sodium mixing.

Table A.3. Summary of Typical Operating Parameters for SFRs

Parameter		Typical Values	References
Temperatures (°C)	Core Inlet	355–360	
	Core Outlet	510–550	
	Coolant Max	704 with max ramp rate of 9°C/sec	Minato and Handa (2000) Donoghue et al. (1994)
	Sodium Coolant Boiling	980 @ 0.2 MPa	TAREF (2011)
	Fuel (Max.)	810; ~ 825 (peak bounding)	Minato and Handa (2000) Arie and Grenci (2009) Toshiba (2011) Donoghue et al. (1994)
	Reactor Vessel Wall (Operating)	426	Minato and Handa (2000) Arie and Grenci (2009) Toshiba (2011) Donoghue et al. (1994)
	Reactor Vessel Wall (Max)	705	Minato and Handa (2000) Arie and Grenci (2009) Toshiba (2011) Donoghue et al. (1994)
	Primary Loop (Inlet/Outlet)	338 / 485	Donoghue et al. (1994)
	Secondary Loop (Inlet/Outlet)	282 / 443	Donoghue et al. (1994)
	Steam Generator (water)	285	Donoghue et al. (1994)
Pressures (MPa)	Primary Coolant (normal operations)	Near ambient (enough to circulate sodium) to 0.2	
	Reactor Vessel Design	0.3	Arie and Grenci (2009)
	IHX	0.88	Minato and Handa (2000)
	Water/Steam	6.9–10.5	Minato and Handa (2000) Donoghue et al. (1994)
Flow Rates	Primary Loop (Sodium)	174,128 (l/min)	Donoghue et al. (1994)
	Secondary Loop (Sodium)	156,148 (l/min)	Donoghue et al. (1994)
	At Steam Generator		Donoghue et al. (1994)
	Sodium	8.30×10^6 (kg/h)	
	Water	1.025×10^6 (kg/h)	
	Steam	9.30×10^5 (kg/h)	
Power Density	61–70 (MW/m^3 or kW/l)		
Neutron Flux	Peak Fast Fluence Limit	4.0×10^{23} n/cm^2	Hoffman et al. (2006)
	Reactor Vessel	6.8×10^{12} n/cm^2	Donoghue et al. (1994)

A.1 Historical Operational Issues Noted for LFRs

- Fires have been reported in several foreign SFRs as a result of heat exchanger tube leaks. An example includes the 1995 Na fire at the Monju plant in Japan. This reactor has not operated since.

- Sodium leaks because of structural failures in primary piping and steam generator tubes. Sodium mixing problems that allow temperature gradients in the sodium are a key factor to structural failures.

A.2 Bibliography

A.2.1 Toshiba 4S

Arie K. 2010. "Current Activities on the 4S Reactor Deployment." Presented at *The 4th Annual Asia-Pacific Nuclear Energy Forum on Small and Medium Reactors (SMRs): Benefits and Challenges*, June 18-19, 2010, Berkeley, California. Document Number: AFT-2010-000134 rev.000(1).

IAEA. 2009. *Design Features to Achieve Defence in Depth in Small and Medium Sized Reactors*. IAEA Nuclear Energy Series No. NP-T-2.2, International Atomic Energy Agency, Vienna, Austria.

Toshiba Corporation. 2010. 4S Response to 73 FR 60612, "Policy Statement on the Regulation of Advanced Reactors" and SECY-10-0034, "Potential Policy, Licensing, and Key Technical Issues for Small Modular Nuclear Reactor Designs." AFT-2010-000256rev.000(0), Toshiba Corporation, Tokyo, Japan.

Toshiba. 2012. *Super Safe Small Simple (4S)*. The Ux Consulting Company. Roswell, Georgia. Accessed April 9, 2013. Available at http://www.uxc.com/smr/uxc_SMRDetail.aspx?key=4S.

Toshiba. 2013. *Multipurpose Energy Station 4S*. Toshiba Corporation. Tokyo, Japan. Accessed April 9, 2013. Available at http://www.toshiba.co.jp/nuclearenergy/english/business/4s/introduction.htm, http://www.toshiba.co.jp/nuclearenergy/english/business/4s/features.htm.

Tsuboi Y, K Arie and T Grenci. 2010. "Design Features, Economics and Licensing of the 4S Reactor." In *ANS Annual Meeting*. June 13-17, 2010, San Diego, California. PSN Number: PSN-2010-0577; Document Number: AFT-2010-000133 rev.000(2).

A.2.2 ARC-100

ARC. 2010a. *ARC-100: A Clean, Secure Nuclear Energy Solution for the 21st Century*. WP-ARC100-0610-1, Advanced Reactor Concepts, LLC (ARC), Reston, Virginia.

ARC. 2010b. ARC-100: A Sustainable, Cost-Effective Energy Solution for the 21st Century. Advanced Reactor Concepts, LLC (ARC), Reston, Virginia.

ARC. 2011. Understanding the Japanese Nuclear Accident of March 2011 & Addressing the Underlying Issues Through an Effective Implementation of Generation IV Technology. Advanced Reactor Concepts, LLC (ARC), Reston, Virginia.

ARC. 2013. *Advanced Reactor Concepts - 100 (ARC-100)*. The Ux Consulting Company. Roswell, Georgia. Accessed April 10, 2013. Available at http://www.uxc.com/smr/uxc_SMRDetail.aspx?key=ARC-100.

A.2.3 PRISM

Cahalan J. 2008a. "Sodium Fast Reactor Safety #1." Argonne National Laboratory, Argonne, Illinois. Presented DOE/HQ on June 20, 2007; NRC/White Flint on June 21, 2007; Rev. 1, October, 2008.

Cahalan J. 2008b. "Sodium Fast Reactor Safety #2." Argonne National Laboratory, Argonne, Illinois. Presented at DOE/HQ on October 31, 2007; NRC/White Flint on November 1, 2007; (Rev. 1, October, 2008).

GE. 1987. PRISM: Preliminary Safety Information Document, Volume I: Chapters 1-4. GEFR-00793, Vol. I, General Electric (GE), Advanced Nuclear Technology, San Jose, California. ADAMS Accession No. ML082880369.

GE. 1987. PRISM: Preliminary Safety Information Document, Volume II: Chapters 5-8. GEFR-00793, Vol. II, General Electric (GE), Advance Nuclear Technology, San Jose, California. ADAMS Accession No. ML08280395.

GE. 1987. PRISM: Preliminary Safety Information Document, Volume IV: Chapters 15-17 and Appendices A-E. GEFR-00793, Vol. IV, General Electric (GE), Advance Nuclear Technology, San Jose, California. ADAMS Accession No. ML082880397.

GE. 1987. PRISM: Preliminary Safety Information Document, Volume V: Appendix F. GEFR-00793, Vol. V, General Electric (GE), Advance Nuclear Technology, San Jose, California. ADAMS Accession No. ML082880399.

GE. 1987. PRISM: Preliminary Safety Information Document, Volume III: Chapters 9-14. GEFR-00793, Vol. III, General Electric (GE), Advance Nuclear Technology, San Jose, California. ADAMS Accession No. ML082880396.

GE Hitachi. N/A. "GE Hitachi Advanced Recycling Center: Solving the Spent Nuclear Fuel Dilemma." GE Hitachi Nuclear Energy, Wilmington, North Carolina. http://www.usnuclearenergy.org/PDF_Library/_GE_Hitachi%20_advanced_Recycling_Center_GNEP.pdf.

GE Hitachi. N/A. "GE Hitachi Nuclear Energy PRISM Technical Brief." GE Hitachi Nuclear Energy, Wilmington, North Carolina. http://www.uxc.com/smr/Library/Design%20Specific/PRISM/Other%20Documents/Technical%20Brief.pdf.

GE Hitachi. 2012. *Power Reactor Innovative Small Modular (PRISM)*. The Ux Consulting Company. Roswell, Georgia. Accessed April 10, 2013. Available at http://www.uxc.com/smr/uxc_SMRDetail.aspx?key=PRISM.

General Electric. 1987. "PRISM (Cutaway Diagram)." *Nuclear Engineering International*, Kent, United Kingdom. Published in November 1987 issue. Reed Business Publishing Ltd., Surrey, England.

Hardy RW and GL Stimmell. 1986. *PRISM: Preliminary Safety Information Document, Volume VI: Appendix G: Responses to Issues in Draft SER*. GEFR-00793, Vol. VI, GE Nuclear Energy (GE), Advance Nuclear Technology, San Jose, California. ADAMS Accession No. ML082880400.

A.2.4　RAPID

CRIEPI. 2012. *Refueling by All Pins, Integral Design (RAPID)*. The Ux Consulting Company. Roswell, Georgia. Accessed April 10, 2013. Available at http://www.uxc.com/smr/uxc_SMRDetail.aspx?key=RAPID. Central Research Institute of Electric Power Industry (CRIEPI).

Kambe M. N/A. "RAPID Reactor." *Nuclear Plant Journal*. Responses to questions by Newal Agnihotri, editor of Nuclear Plant Journal. Available at http://nuclearplantjournal.com/uploads/RAPID.pdf.

Kambe M, H Tsunoda, K Nakazima and T Iwamura. 2003. "RAPID-L and RAPID Operator Free Fast Reactor Concepts without Any Control Rods." In *GENES4/ANP 2003*. September 15-19, 2003, Kyota, Japan. Paper #1039.

A.2.5　TWR

Ahlfeld C, T Burke, T Ellis, P Hejzlar, K Weaver, C Whitmer, J Gilleland, M Cohen, B Johnson, S Mazurkiewicz, J McWhirter, A Odedra, N Touran, C Davidson, J Walter, R Petroski, G Zimmerman, T Weaver, P Schweiger and R Russick. 2011. "Conceptual Design of a 500 MWe Traveling Wave Demonstration Reactor Plant." In *Proceedings of ICAPP 2011*, pp. 816-823. May 2-5, 2011, Nice, France. Societe Francaise d'Energie Nucleaire (SFEN). Paper #11199.

Ragheb M. 2011. "Traveling Wave Reactor." http://www.uxc.com/smr/Library/Design%20Specific/TWR/Papers/2011%20-%20TWR.pdf.

A.2.6　INL SMR

Chang YI, P LoPinto, M Konomura, J Cahalan, F Dunn, M Farmer, L Krajtl, A Moisseytsev, Y Momozaki, J Sienicki, Y Park, Y Tang, C Reed, C Tzanos, S Wiedmeyer, W Yang, P Allegre, J Astegiano, F Baque, L Cachon, MS Chenaud, J-L Courouau, PH Dufour, JC Klein, C Latge, C Thevenot, F Varaine, M Ando, Y Chikazawa, M Nagamura, Y Okano, Y Sakamoto, K Sugino, H Yamano, C Grandy and S Kamal. 2005. *Small Modular Fast Reactor Design Description*. ANL-SMFR-1, Argonne National Laboratory, Argonne, Illinois.

A.2.7　Advanced Burner Reactor (ABR)

Chang YI, PJ Finck, C Grandy, J Cahalan, L Deitrich, F Dunn, D Fallin, M Farmer, T Fanning, T Kim, L Krajtl, S Lomperski, A Moisseytsev, Y Momozaki, J Sienicki, Y Park, Y Tang, C Reed, C Tzanos, S Wiedmeyer, W Yang and Y Chikazawa. 2006. *Advanced Burner Test Reactor Preconceptual Design Report*. ANL-ABR-1 (ANL-AFCI-173), Argonne National Laboratory, Argonne, Illinois.

A.2.8   SMFR (ANL)

Chang YI, P LoPinto, M Konomura, J Cahalan, F Dunn, M Farmer, L Krajtl, A Moisseytsev, Y Momozaki, J Sienicki, Y Park, Y Tang, C Reed, C Tzanos, S Wiedmeyer, W Yang, P Allegre, J Astegiano, F Baque, L Cachon, MS Chenaud, J-L Courouau, PH Dufour, JC Klein, C Latge, C Thevenot, F Varaine, M Ando, Y Chikazawa, M Nagamura, Y Okano, Y Sakamoto, K Sugino, H Yamano, C Grandy and S Kamal. 2005. *Small Modular Fast Reactor Design Description*. ANL-SMFR-1, Argonne National Laboratory, Argonne, Illinois.

A.2.9   General

Chang YI, P LoPinto, M Konomura, J Cahalan, F Dunn, M Farmer, L Krajtl, A Moisseytsev, Y Momozaki, J Sienicki, Y Park, Y Tang, C Reed, C Tzanos, S Wiedmeyer, W Yang, P Allegre, J Astegiano, F Baque, L Cachon, MS Chenaud, J-L Courouau, PH Dufour, JC Klein, C Latge, C Thevenot, F Varaine, M Ando, Y Chikazawa, M Nagamura, Y Okano, Y Sakamoto, K Sugino, H Yamano, C Grandy and S Kamal. 2005. *Small Modular Fast Reactor Design Description*. ANL-SMFR-1, Argonne National Laboratory, Argonne, Illinois.

Cheon JS, CB Lee, BO Lee, JP Raison, T Mizuno, F Delage and J Carmack. 2009. "Sodium Fast Reactor Evaluation: Core Materials." *Journal of Nuclear Materials* 392(2):324-330.

Cochran TB, HA Feiveson, G Pshakin, M Ramana, M Schneider, T Suzuki and F von Hippel. 2010. *Fast Breeder Reactor Programs: History and Status*. Research Report 8, The International Panel on Fissile Materials (IPFM), Princeton, New Jersey.

Denman MR, JL LaChance, T Sofu, GF Flanagan, R Wigeland and R Bari. 2012. *Sodium Fast Reactor Safety and Licensing Research Plan - Volume I*. SAND2012-4260, Sandia National Laboratories, Albuquerque, New Mexico.

DOE. 2012. *Gen IV Nuclear Reactor Technical Documents*. U.S. Department of Energy (DOE). Washington, D.C. Accessed October 19, 2012. Available at https://inlportal.inl.gov/portal/server.pt/community/nuclear_energy/277/gen_iv_-_technical_documents_(2)/2604.

European Nuclear Society. 2012. *Transaction Advanced Reactors, European Nuclear Conference (ENC2012)*, December 9-12, 2012, Manchester, United Kingdom. European Nuclear Society, Brussels, Belgium.

Hill RN. 2012. "U.S. Status of Fast Reactor Research and Technology." Argonne National Laboratory, Argonne, Illinois. Presented June 21, 2012.

IAEA. 2002. *Operational and Decommissioning Experience with Fast Reactors: Proceedings of a technical meeting held in Cadarache, France, 11-15 March 2002*. IAEA-TECDOC-1405, International Atomic Energy Agency (IAEA), Vienna, Austria.

IAEA. 2006. *Fast Reactor Database: 2006 Update*. IAEA-TECDOC-1531, International Atomic Energy Agency (IAEA), Vienna, Austria.

IAEA. 2007. *Liquid Metal Cooled Reactors: Experience in Design and Operation*. IAEA-TECDOC-1569, International Atomic Energy Agency (IAEA), Vienna, Austria.

IAEA. 2011. *Working Material: Technical Meeting on Fast Reactors In-service Inspection and Repair: Status and Innovative Solutions*. International Atomic Energy Agency (IAEA), Vienna, Austria. December 19-20, 2011.

IAEA. 2012. *Assessment of Nuclear Energy Systems Based on a Closed Nuclear Fuel Cycle With Fast Reactors: A Report of the International Project on Innovative Nuclear Reactors and Fuel Cycles (INPRO)*. IAEA-TECDOC-1639/Rev.1, International Atomic Energy Agency (IAEA), Vienna, Austria.

IAEA. 2012. *Fast Reactors and Related Fuel Cycles: Challenges and Opportunities (FR09), Proceedings of an International Conference*, December 7-11, 2009, Kyoto, Japan. International Atomic Energy Agency (IAEA), Vienna, Austria.

IAEA. 2012. *Liquid Metal Coolants for Fast Reactors Cooled by Sodium, Lead, and Lead-Bismuth Eutectic*. IAEA Nuclear Energy Series No. NP-T-1.6, International Atomic Energy Agency (IAEA), Vienna, Austria.

IAEA. 2012. *Working Material: Forty-Fifth Meeting of the Technical Working Group on Fast Reactors (TWG-FR)*. IAEA-TM-42720, International Atomic Energy Agency (IAEA), Vienna, Austria. Meeting held at Argonne National Laboratory, Argonne, Illinois, June 20-22, 2012.

IAEA. N/A. "Analyses of and Lessons Learned from the Operational Experience with Fast Reactor Equipment and Systems." International Atomic Energy Agency, Vienna, Austria. Future publication. http://www.iaea.org/NuclearPower/Technology/CRP/index.html.

INL. 2012. *Gas-Cooled Fast Reactor (GFR)*. Idaho National Laboratory (INL). Idaho Falls, Idaho. Accessed April 10, 2013. Available at https://inlportal.inl.gov/portal/server.pt?open=514&objID=2253&parentname=CommunityPage&parentid=13&mode=2&in_hi_userid=291&cached=true.

LaChance JL, J Sackett, R Wigeland, R Bari, R Budnitz, J Cahalen, C Grandy, D Wade, M Corradini, R Denning, GF Flanagan, S Wright, AJ Suo-Anttila, JC Hewson, TJ Olivier, J Phillips, M Farmer, S Miyhara, L Walters, J Lambert, K Natesan, A Wright, A Yacout, S Hayes, P D., F Garner, LJ Ott, MR Denman, DA Powers, B Clement, S Ohno, R Zeyen, R Schmidt, T Sofu, T Wei, J Thomas and JJ Carbajo. 2012. *Sodium Fast Reactor Safety and Licensing Research Plan - Volume II*. SAND2012-4259, Sandia National Laboratories, Albuquerque, New Mexico.

NERAC. 2002. *A Technology Roadmap for Generation IV Nuclear Energy Systems - Ten Nations Preparing Today for Tomorrow's Energy Needs*. GIF-002-00, U.S. DOE Nuclear Energy Research Advisory Committee (NERAC) and the Generation IV International Forum (GIF), Washington, D.C.

OECD Nuclear Energy Agency. 2009. *GIF Symposium*, September 9-10, 2009, Paris, France. http://www.gen-4.org/GIF/About/index.htm.

Rouault JP, P Chellapandi, B Raj, P Dufour, C Latge, L Paret, PL Pinto, GH Rodriguez, G-MF Gautier, G-L, M Pelletier, D Gosset, S Bourganel, G Mignot, F Varaine, B Valentin, P Masoni, P Martin, J-C Queval, D Broc and N Devictor. 2010. "Sodium Fast Reactor Design: Fuels, Neutronics, Thermal-Hydraulics, Structural Mechanics and Safety." In *Handbook of Nuclear Engineering*, pp. 2321-2710. ed: DG Cacuci. Ch. 21. Springer, New York.

Schmidt R, T Sofu, T Wei, J Thomas, R Wigeland, JJ Carbajo, H Ludewig, M Corradini, H Jeong, F Serre, H Ohshima and Y Tobita. 2011. *Sodium Fast Reactor Gaps Analysis of Computer Codes and Models for Accident Analysis and Reactor Safety*. SAND2011-4145, Sandia National Laboratories, Albuquerque, New Mexico.

Vilim RB, YS Park, C Grandy, H Belch, P Dworzanski and J Misterka. 2011. *Simulator Platform for Fast Reactor Operation and Safety Technology Demonstration*. ANL-ARC-208, Argonne National Laboratory, Argonne, Illinois.

Walters L, J Lambert, K Natesan, A Wright, A Yacout, S Hayes, D Porter, F Garner, LJ Ott and MR Denman. 2011. *Sodium Fast Reactor Fuels and Materials: Research Needs*. SAND2011-6546, Sandia National Laboratories, Albuquerque, New Mexico.

WNA. 2012. *Fast Neutron Reactors*. World Nuclear Association (WNA). London. Accessed April 11, 2013. Available at http://www.world-nuclear.org/info/inf98.html (last updated March 15, 2013).

A.3 References

Arie K and T Grenci. 2009. "4S Reactor: Super-Safe, Small and Simple." Toshiba Corporation. AS-2009-000036 Rev.1, PSN-2009-0563. http://www.uxc.com/smr/Library/Design%20Specific/4S/Presentations/2009%20-%204S%20Reactor.pdf.

Donoghue JE, JN Donohew, GR Golub, RM Kenneally, PB Moore, SP Sands, ED Throm and BA Wetzel. 1994. *Preapplication Safety Evaluation Report for the Power Reactor Innovative Small Module (PRISM) Liquid-Metal Reactor. Final Report*. NUREG-1368, U.S. Nuclear Regulatory Commission, Washington, D.C. Available at http://www.osti.gov/energycitations/servlets/purl/10133164-2ZfTJr/native/.

Hoffman EA, WS Yang and RN Hill. 2006. *Preliminary Core Design Studies for the Advanced Burner Reactor over a Wide Range of Conversion Ratios*. ANL-AFCI-177, Argonne National Laboratory, Argonne, Illinois. Available at http://www.osti.gov/energycitations/servlets/purl/973480-o1tvNg/.

Minato A and N Handa. 2000. "Advanced 4S (Super Safe, Small and Simple) LMR." In *Proceedings of an Advisory Group Meeting*, pp. 157-176. July 20-24, 1998, Obninsk, Russian Federation. International Atomic Energy Agency, Vienna, Austria.

TAREF. 2011. *Experimental Facilities for Sodium Fast Reactor Safety Studies*. NEA/CSNI/R(2010)12, Nuclear Enenrgy Agency (NEA), Organisation for Economic Co-operation and Develop (OECD), Task Group on Advanced Reactor Experimental Facilities (TAREF).

Toshiba. 2011. *Status Report 76 - Super-Safe, Small and Simple Reactor (4S)*. International Atomic Energy Agency, Vienna, Austria.

Appendix B

Lead-Cooled Fast Reactor (LFR)

Appendix B

Lead-Cooled Fast Reactor (LFR)

The Lead-Cooled Fast Reactor (LFR) system features the potential for a very high reactor outlet temperature, high power density core, low system pressure, and a fast neutron spectrum. The liquid metal coolant, either lead (Pb) or lead/bismuth eutectic (Pb-Bi) can utilize natural convention for heat removal or can be pumped depending on core power requirements. The LFRs can be configured to use depleted uranium or thorium fuel matrices, and burn actinides from LWR fuel. Fuel is metal or nitride, with full actinide recycle from regional or central reprocessing plants. An illustration of an LFR system is provided in Figure B.1. Several LFR concepts may be suitable to modularization and these concepts are listed in Table B.1 with major design parameters summarized in Table B.2. Table B.3 provides a summary of typical operating parameters for LFR concepts. Some LFR designs for small grids or developing counties, like the Gen4 and SSTAR, utilize a factory-built "battery" or "cassette" design and are optimized for power generation over long periods of time (10–30 years) without refueling. LFR development in Russia has occurred over many decades in submarines utilizing BREST fast reactor technology.

LFR designs provide high-temperature operation, because Pb melts at 327°C and boils at 1737°C. The Pb-Bi coolant melts at 125°C and boils at 1670°C. The primary Pb coolant is a low-pressure coolant that does not boil or flash (in the case of pressure reductions) upon failure of the primary coolant system boundary and can quickly solidify in the case of a leak. Operation at temperatures in excess of 830°C is envisioned with the development of advanced materials that could support thermochemical production of hydrogen. LFR designs allow for relatively high core power density, which translates to a smaller reactor core for a given amount of power. This is important given the weight of the lead coolant and in theory makes the system more cost-effective. Pb and Pb-Bi coolants are inert to air, water, and carbon dioxide eliminating the concerns of vigorous exothermic reactions associated with the use of Na coolant. This also enables the heat exchanger to be located in the primary circuit. High absolute thermal expansion coefficient of these coolants facilitates passive circulation for decay heat removal and provides a large negative temperature coefficient for reactivity feedback. Finally Pb or Pb-Bi coolant shields gamma radiation.

The coolant can be corrosive to fuel cladding and other steel components. Maintaining proper dissolved oxygen concentration in the coolant controls corrosion. Solidification will render the reactor inoperable if the coolant temperature becomes too low. Pb-Bi coolant has a lower melting point than Pb, making de-solidification less challenging. The specific heat per unit volume of Pb-Bi and Pb are similar to Na coolant, but the thermal conductivities are lower by about a factor of four. Pb is the heaviest of all proposed coolants, making it expensive to pump, potentially erosive to pump materials, and a design challenge in terms of requiring seismically robust structures.
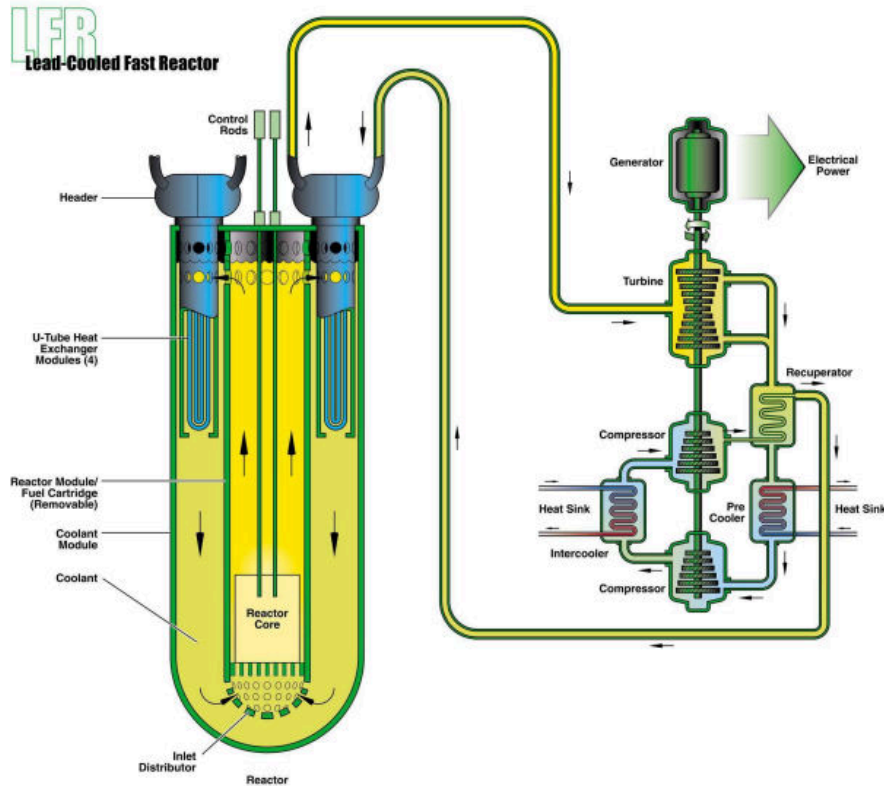
Figure B.1. An Illustration of a LFR Reactor System

Table B.1. List of Several Recent LFR Concepts for Modularization and Associated Organization/ Country

LFR Concepts	Organization/Country
USA Designs	
ENHS (Encapsulated Nuclear Heat Source)	University of California – Berkeley/USA
G4M (Gen4 Module) [formerly HPM (Hyperion Power Module)]	Gen4 Energy Inc. & Los Alamos National Laboratory/USA
SSTAR (Secure, Small Transportable Autonomous Reactor) – included STAR, STAR-H2, STAR-LM	Argonne National Laboratory (ANL)/USA
SUPERSTAR (Sustainable Proliferation-resistance Enhance Refined Secure Transportable Autonomous Reactor)	
Russia Designs	
BREST-OD-300	N.A. Dollezhal Research and Development Institute of Power Engineering (NIKIET)/ Russia
ANGSTREM	
SVBR-100 (Svintsovo Vismutny Bystryl Reactor)	
Other Designs	
LSPR (Long-Life Safe Simple Small Portable Proliferation-Resistant Reactor)	Tokyo Institute of Technology/Japan
PEACER (Proliferation-Resistant Environmentally-Friendly, Accident-Tolerant, Continuous -Energy, and Economical Reactor)	Nuclear Transmutation Energy Research Centre of Korea (NUTRECK)/South Korea

Table B.2. Summary of Design Parameters for Several Recent LFR Concepts

General SMR LFR Design Features	Parameters
Coolant	Lead (Pb) or Lead/Bismuth (Pb-Bi) Note: Lead/Lithium (Li) in one design
Forced or Natural Circulation	Depends on design and power density requirements
Thermal Capacity Range (MWth)	30–700
Gross Electrical Capacity Range (MWe)	6–300
Refueling Frequency (years)	Continuous; 10; 15; 20–30
Fuel Cycle	Closed

Table B.3. Summary of Typical Operating Parameters for LFR Concepts

Parameter		Values	References
Temperature Range (°C)	Core Inlet	290–610	Sienicki et al. (2006)
	Core Outlet	465–*780 (* higher temperature special case for hydrogen production option STAR-H2)	Sienicki et al. (2006)
	Pb/Pb-Bi Coolant Boiling	1740/1670	Sienicki et al. (2006)
	Pb/Pb-Bi Melt	327/125	Sienicki et al. (2006)
	Fuel (Max.)	980 (Hot Spot)/814 (Nominal)	Filin (2003)
	Fuel Rod (Max.)	649 (Hot Spot)/614 (Nominal)	
	Primary Loop (Inlet/Outlet)	405/561	INL (2005)
	Secondary Loop (Inlet/Outlet)	392/541	INL (2005)
Pressure Range (MPa)	Reactor Vessel	~0.1 (1 atm)	
	CO_2 in Turbine Loop Max/Min (SSTAR)	20/7.4	Sienicki et al. (2006)
Flow Rate (kg/s)	Primary Loop (Lead based)	2150–16200	Sienicki et al. (2006)
	Good design practice to limit lead speed to 2 m/s to reduce both pressure loss and erosion of structural material.	2150–16200	Smith (2010)
	CO_2 in Turbine Loop (SSTAR)	245	Sienicki et al. (2006)
Power Density (MW/m^3 or kW/l)	Average	69	Sienicki et al. (2005)
	Peak	119	Sienicki et al. (2005)
Neutron Flux	Peak Fast Fluence	3.7×10^{23} n/cm^2	Sienicki et al. (2006)
	Neutron Flux (Max.)	3.8×10^{15} n/cm^2 - s	Trallero (2011)
	Neutron Flux (Average)	2.35×10^{15} n/cm^2 - s	Trallero (2011)

B.1 Historical Operational Issues Noted for LFRs

- 1968 plugging of core inlet from accumulated slag (lead oxides) caused a partial core meltdown. There was no increase in pressure, primary circuit tightness was not lost, radioactive contamination of air in reactor compartment did not occur. Solution is that concentration of oxygen dissolved in Pb-Bi coolant should be maintained within a certain range, which could be realized automatically (IAEA 2007b).

- 1971 damage of the primary circuit pipelines because of corrosion at the outer side and radioactive coolant leakage (IAEA 2007b).

- 1982 global corrosion damage of steam generator tube bundle caused by poor quality of feed water. (IAEA 2007b).

B.2 Bibliography

B.2.1   STAR Series

Kuznetsov V. N/A. "Design Features to Achieve Defence-in-Depth in Small and Medium Sized Reactors." International Atomic Energy Agency, Vienna, Austria.

Sienicki JJ and BW Spencer. 2002. "Power Optimization in the STAR-LM Modular Natural Convection Reactor System." In *Proceedings of ICONE 10: Tenth International Conference on Nuclear Engineering*, pp. 685-690. April 14-18, 2002, Arlington, Virginia. American Society of Mechanical Engineers, New York.

Sienicki JJ, MA Smith, AV Moisseytsev, WS Yang and DC Wade. 2004. "Small Secure Transportable Autonomous Lead-Cooled Fast Reactor for Deployment at Remote Sites." Presented at *Americas Nuclear Energy Symposium 2004*, October 3-6, 2004, Miami Beach, Florida.

Sienicki JJ, AV Moisseytsev, S Bortot and Q Lu. 2011. "SUPERSTAR: An Improved Natural Circulation, Lead-Cooled, Small Modular Fast Reactor for International Deployment." http://www.uxc.com/smr/Library/Design%20Specific/STAR/Papers/An%20Improved%20Natural%20Circulation,%20Lead-Cooled,%20Small%20Modular%20Fast%20Reactor%20for%20International%20Deployment.pdf.

Smith CF, NW Brown and JA Hassberger. 1999. "The Secure, Transportable, Autonomous Reactor (STAR): A Small Proliferation-Resistant Reactor System for Developing Countries." In *Proliferation-Resistant Power Systems Workshop*. June 2-4, 1999, Livermore, California. UCRL-JC-133319 PREPRINT.

Smith CF, WG Halsey, NW Brown, JJ Sienicki, A Moisseytsev and DC Wade. 2008. "SSTAR: The US Lead-Cooled Fast reactor (LFR)." *Journal of Nuclear Materials* 376(3):255-259.

Wade DC, R Doctor and KL Peddicord. 2002. "STAR-H2: The Secure Transportable Autonomous Reactor for Hydrogen Production and Desalinization." In *Proceedings of ICONE10, 10th International Conference on Nuclear Engineering*, pp. 205-214. April 14-18, 2002, Arlington, Virginia. American Society of Mechanical Engineers, New York.

B.2.2 SVBR-75/10

Antysheva T and S Borovitskiy. 2011. "SVBR-100: New Generation Power Plants for Small and Medium-Sized Power Applications."

Golovin AO, ZV Sivak and MP Leonchuk. 2003. "Analysis of Safety Aspects of the SVBR-75/100 Power Installation as Applied to Regional Nuclear Cogeneration Plant: (Numeric Simulation of Decay Heat Removal Process through the RVACS)." http://www.uxc.com/smr/Library/Design%20Specific/SVBR-100/Papers/2003%20-%20Analysis%20of%20Safety%20Aspects%20of%20the%20SVBR%2075-100%20Power%20Installation%20as%20Applied%20to%20Regional%20Nuclear%20Co-

JSC AKME-Engineering. N/A. "SVBR-100: New Generation Nuclear Power Plants for Small and Medium-Sized Power Applications." Moscow, Russia. http://www.akmeengineering.com/assets/files/SVBR-100%20new%20generation%20power%20plants.pdf.

Kudryavtseva A. 2011. "Russian Experience in SMR Development and Siting." AKME-Engineering, Moscow, Russia. http://www.nrc.gov/public-involve/conference-symposia/ric/past/2011/docs/abstracts/Kudryavtsevaa-h.pdf.

Toshinsky G and V Petrochenko. 2012. "Modular Lead-Bismuth Fast Reactors in Nuclear Power." *Sustainability* 4:2293-2316.

VNIPIET. 2012. *Svintsovo Vismutny Bystryi Reactor - Lead-Bismuth Fast Reactor (SVBR-100).* The Ux Consulting Company. Roswell, Georgia. Accessed April 15, 2013. Available at http://www.uxc.com/smr/uxc_SMRDetail.aspx?key=SVBR-100. OKB Gidropress/Eastern-European Chief Research and Project Institute of Energy Technologies (VNIPIET).

Zrodnikov A, GI Toshinsky, OG Komlev, VS Stepanov, NN Klimov, AV Kudryavtseva, and VV Petrochenko. 2009. "SVBR-100 Module-Type Reactor of the IV Generation for Regional Power Industry." In *International Conference on Fast Reactors and Related Fuel Cycles: Challenges and Opportunities*, p. 30. December 7-11, 2009, Kyoto, Japan. IAEA-CN-176-FR09P1132.

Zrodnikov AV, GI Toshinsky, OG Komlev, KG Melnikov and NN Novikova. 2009. "Fuel Cycle of Reactor SVBR-100." In *Proceedings of Global 2009*. September 6-11, 2009, Paris, France. Paper 9236.

Zrodnikov AV, GI Toshinsky, OG Komlev, UG Dragunov, VS Stepanov, NN Klimov, II Kopytov and VN Krushelnitsky. 2005. "Small Size Modular Fast Reactors in Large Scale Nuclear Power." In *18th International Conference on Structural Mechanics in Reactor Technology (SMiRT 18)*, p. 12. August 7-12, 2005, Beijing, China.

B.2.3 Gen4 Module

Crook P and C Pearson. 2011. "SMR's and The Hyperion Power Module Mini Reactor." Hyperion Power Generation, Denver, Colorado. http://www.lsta.lt/files/events/2011-03-04_LPK_konferencija/2_peter_crook.pdf.

Deal JR. 2010. "The Future Role of Nuclear Power: Advances in Small Scale Nuclear." Hyperion Power Generation, Denver, Colorado.

Gen4 Energy, Inc. 2012. *GEN4Energy Technology*. Gen4 Energy, Inc., Denver, Colorado. Available at http://www.gen4energy.com/technology/.

Gen4 Energy, Inc. (Hyperion Power Generation). 2012. *Gen4 Module (Hyperion Power Module) (G4M (HPM))*. The Ux Consulting Company. Roswell, Georgia. Accessed October 16, 2012. Available at http://www.uxc.com/smr/uxc_SMRDetail.aspx?key=G4M%20(HPM).

Hyperion Power Generation. N/A. A New Paradigm for Power Generation. No. 10-0311.

B.2.4   ANGSTREM

Stepanov VS, SK Legyuenko, OG Grigoriev, BF Gromov, AV Dedul, MP Leonchyk, YG Pashkin, D Pankratov, VV Chekunov and DE Skorikov. 1998. "The ANGSTREM Project: Present Status and Development Activities." In *Advisory Group Meeting on Technology, Design and Safety Aspects of Non-electrical Application of Nuclear Energy*, pp. 157-164. October 20-24, 1997, Obninsk, Russian Federation. International Atomic Energy Agency, Vienna, Austria. IAEA-TECDOC-1056.

B.2.5   BREST-OD-300

Abramov VY, SN Bozin, SV Evropin, BS Rodchenkov, VN Leonov, AI Filin and VG Markov. 2003. "Corrosion and Mechanical Properties of BREST-OD-300 Reactor Structural Materials." In *Proceedings of ICONE11, 11th International Conference on Nuclear Engineering*, p. 4. April 20-23, 2003, Tokyo, Japan. Japanese Society of Mechanical Engineers. ICONE11-36413.

Glazov AG, AV Lopatkin, VV Orlov, PP Poluektov, VI Volk, VF Leontyev and RS Karimov. 2003. "Fuel Cycle of BREST Reactors. Solution of the Radwaste and Nonproliferation Problems." In *International Conference Nuclear Power and Fuel Cycles*. December 1-2, 2003, Moscow-Dimitrovgrad.

IAEA. 2003. *Power Reactors and Sub-critical Blanket Systems with Lead and Lead–Bismuth as Coolant and/or Target Material - Utilization and Transmutation of Actinides and Long Lived Fission Products*. IAEA-TECDOC-1348, International Atomic Energy Agency, Vienna, Austria.

Khalil H, JE Lineberry, JE Cahalan, JL Willit, BW Spencer, SL Hayes, DC Crawford, DC Wade and DJ Hill. 2000. *Preliminary Assessment of the BREST Reactor Design and Fuel Cycle Concept*. ANL-00/22, Argonne National Laboratory, Argonne, Illinois.

NIKIET. 2012. *Bystryi Reactor so Svintsovym Teplonositelem - Fast Reactor with Lead Coolant (BREST-OD-300)*. The Ux Consulting Company. Roswell, Georgia. Accessed April 14, 2013. Available at http://www.uxc.com/smr/uxc_SMRDetail.aspx?key=BREST-OD-300. N.A. Dollezhal Research and Development Institute of Power Engineering (NIKIET).

Orlow VV, VS Smirnov, AI Filin, AV Lopatkin, VG Muratov, VS Khomyakov, AL Kochetkov, IP Matveenko and AM Tsiboulia. 2003. "Experimental and Calculation Investigations of Neutron-Physical Characteristics of BREST-OD-300 Reactor." In *Proceedings of ICONE11, 11th International Conference on Nuclear Engineering*, p. 8. April 20-23, 2003, Tokyo, Japan. Japanese Society of Mechanical Engineers. ICONE11-36406.

Smirnov VP, AI Filin, AG Sila-Novitsky, VN Leonov, AV Zhukov, AD Efanov, AP Sorokin and JA Kuzina. 2003. "Thermohydraulic Research for the Core of the BREST-OD-300 Reactor." In *Proceedings of INCOE11, 11th International Conference on Nuclear Engineering*. April 20-23, 2003, Tokyo, Japan. Japanese Society of Mechanical Engineers. ICONE11-36407.

Trallero AM. 2011. *C-14 Production in Lead-Cooled Reactors*. Master of Science in Technology Thesis, Aalto University, Finland.

Yemelyantseva ZI, VN Leonov, AD Yefanov, YI Orlov, PN Martynov and VA Gulevsky. 2003. "Validation of the Lead Coolant Technology for BREST Reactors." In *Proceedings of ICONE11, 11th International Conference on Nuclear Engineering*. April 20-23, 2003, Tokyo, Japan. Japanese Society of Mechanical Engineers. ICONE11-36408.

B.2.6 ENHS

Brown N, M Carelli, L Conway, M Dzodzo, E Greenspan, Q Hossain, D Saphier, H Shimada, J Sienicki and D Wade. 2001. "The Encapsulated Nuclear Heat Source for Proliferation-Resistant Low-Waste Nuclear Energy." In *International Seminar on Status and Prospects for Small and Medium Sized Reactors*. May 27-31, 2001, Cairo, Egypt. Preprint. UCRL-JC-143186.

Greenspan E. 2007. "Thoughts on Furthering Sustainable Nuclear Power with Low Proliferation Risk." In *Workshop on Nuclear Power Growth: International Cooperation*. May 9, 2007, Washington, D.C.

Greenspan E. 2009. "Improvements in the ENHS Reactor Design and Fuel Cycle." In *LFR Information Exchange Meeting*. September 30–October 1, 2009, Naval Postgraduate School (NPS), Monterey, California.

Hong SG, T Okawa and E Greenspan. 2005. "Molten Salt Cooled ENHS (Encapsulated Nuclear Heat Source)-Like Reactors." In *ARWIF-2005*, p. 33. February 16-18, 2005, Oak-Ridge, Tennessee.

B.2.7 LSPR

IAEA. 2007. "Annex XXV, Lead-Bismuth Eutectics Cooled Long-Life Safe Simple Small Portable Proliferation Resistant Reactor (LSPR)." In *Status of Small Reactor Designs Without On-Site Refueling*, pp. 715-737. International Atomic Energy Agency (IAEA), Vienna, Austria. IAEA-TECDOC-1536.

B.2.8 PEACER

Hwang IS, SH Jeong, BG Park, WS Yang, KY Suh and CH Kim. 2000. "The Concept of Proliferation-Resistant, Environment-Friendly, Accident-Tolerant, Continual and Economical Reactor (PEACER)." *Progress in Nuclear Energy* 37(1-4):217-222.

Kim CS, SH Jeong, IS Lee, KY Suh, CH Kim and IS Hwang. 2003. "Analysis of Heavy Eutectic Loop for Investigation of Operability and Safety." In *International Conference on Global Environment and Advanced Nuclear Power Plants GENES4/ANP2003*. September 15-19, 2003, Kyoto, Japan. Paper 1214.

Lim J-Y and M-H Kim. 2006. "Performance Analysis of a Pb-Bi Cooled Fast Reactor - PEACER-300 in Proliferation Resistance and Transmutation Aspects." In *PHYSOR-2006 - American Nuclear Society's Topical Meeting on Reactor Physics*, p. 8. September 10-14, 2006, Vancouver, BC, Canada. American Nuclear Society. Paper B062.

Nam WC, HW Lee and IS Hwang. 2007. "Fuel Design Study and Optimization for PEACER Development." *Nuclear Engineering and Design* 237(3):316-324.

Park B-G, S-H Jeong and I-S Hwang. 2002. "Partitioning and Transmutation of Spent Nuclear Fuel by PEACER." In *Seventh Information Exchange Meeting on Actinide and Fission Product Partitioning and Transmutation*, pp. 247-256. October 14-16, 2002, Jeju, Republic of Korea. OECD, Nuclear Energy Agency, France.

B.2.9   General

Agostini P, G Grasso, M Tarantino, D Rozzia, L Cinotti, A Alemberti, P Meloni, I Di Piazza, P Gaggini, G Bandini, M Polidori, A Del Nevo, A Ciampichetti, A Gessi and N Forgione. 2012. "ENEA Strategy for Lead Fast Reactor." http://www.nr.titech.ac.jp/~mtakahas/X13/1.10%20(P.%20Agostini).pdf.

Alemberti A. 2012. "ELFR: The European Lead Fast Reactor - Design, Safety Approach and Safety Characteristics." Presented at *Technical Meeting on Impact of Fukushima Event on Current and Future Fast Reactor Designs*, March 19-23, 2012, Dresden, Germany.

Alemberti A. 2012. "The ALFRED Project on Lead-Cooled Fast Reactor." Presented at *ESNII Conference, Advanced Fission Research in Horizon 2020*, June 25, 2012, Brussels, Belgium. European Economic and Social Committee.

Cochran TB, HA Feiveson, G Pshakin, M Ramana, M Schneider, T Suzuki and F von Hippel. 2010. *Fast Breeder Reactor Programs: History and Status*. Research Report 8, The International Panel on Fissile Materials (IPFM), Princeton, New Jersey.

IAEA. 2003. *Power Reactors and Sub-critical Blanket Systems with Lead and Lead–Bismuth as Coolant and/or Target Material - Utilization and Transmutation of Actinides and Long Lived Fission Products*. IAEA-TECDOC-1348, International Atomic Energy Agency, Vienna, Austria.

IAEA. 2006. *Fast Reactor Database: 2006 Update*. IAEA-TECDOC-1531, International Atomic Energy Agency (IAEA), Vienna, Austria.

IAEA. 2012. *Fast Reactors and Related Fuel Cycles: Challenges and Opportunities (FR09), Proceedings of an International Conference*, December 7-11, 2009, Kyoto, Japan. International Atomic Energy Agency (IAEA), Vienna, Austria.

IAEA. 2012. *Liquid Metal Coolants for Fast Reactors Cooled by Sodium, Lead, and Lead-Bismuth Eutectic*. IAEA Nuclear Energy Series No. NP-T-1.6, International Atomic Energy Agency (IAEA), Vienna, Austria.

Li N, JS Zhang, HD Yu and J Jansen. 2006. *Model-Based Analysis of Corrosion Test Results and Extraction of Long-Term Corrosion Rates*. Report G-L0502L01, Idaho National Laboratory, Idaho Falls, Idaho. Gen IV LFR "Lead Coolant Testing" (G-L0502L01) FY06 Final Report (A Level II Milestone Deliverable).

OECD/NEA. 2007. *Handbook on Lead-bismuth Eutectic Alloy and Lead Properties, Materials Compatibility, Thermal-hydraulics and Technologies, 2007 Edition*. Organization for Economic Co-Operation and Development (OECD) Publishing. ISBN 978-92-64-99002-9. NEA No. 6195.

Smith C. 2010. *Lead-Cooled Fast Reactor (LFR) Design: Safety, Neutronics, Thermal Hydraulics, Structural Mechanics, Fuel, Core, and Plant Design*. LLNL-BOOK-424323, Lawrence Livermore National Laboratory, Livermore, California.

Tarantino M, L Cinotti and D Rozzia. 2012. "Lead-Cooled Fast Reactor (LFR) Development Gaps." http://www.iaea.org/NuclearPower/Downloadable/Meetings/2012/2012-02-29-03-02-TM-FR/11a_Tarantino-Cinotti.pdf.

Toshinsky G and V Petrochenko. 2012. "Modular Lead-Bismuth Fast Reactors in Nuclear Power." *Sustainability* 4:2293-2316.

WNA. 2012. *Fast Neutron Reactors*. World Nuclear Association (WNA). London. Accessed April 11, 2013. Available at http://www.world-nuclear.org/info/inf98.html (last updated March 15, 2013).

B.3 References

Filin AI, VV Orlov, VN Leonov, AG Sila-Novitski, VS Smirnov and VS Tsikunov. 2003. "Design Features of BREST Reactors and Experimental Work to Advance the Concept of BREST Reactors." In *Power Reactors and Sub-critical Blanket Systems with Lead and Lead–Bismuth as Coolant and/or Target Material - Utilization and Transmutation of Actinides and Long Lived Fission Products*, pp. 31-40. International Atomic Energy Agency, Vienna, Austria.

IAEA. 2007b. *Liquid Metal Cooled Reactors: Experience in Design and Operation*. IAEA-TECDOC-1569, International Atomic Energy Agency (IAEA), Vienna, Austria.

INL. 2005. "Appendix 4.0, Lead-Cooled Fast Reactor." In *Generation IV Nuclear Energy Systems Ten-Year Program Plan, Fiscal Year 2005*, pp. A4-1 - A4-28. Idaho National Laboratory (INL), Idaho Falls, Idaho.

Sienicki JJ, A Moisseytsev, WS Yang, DC Wade, A Nikiforova, P Hanania, HJ Ryu, KP Kulesza, SJ Kim, WG Halsey, CF Smith, NW Brown, E Greenspan, M de Caro, N Li, P Hosemann, J Zhang and H Yu. 2006. *Status Report on the Small Secure Transportable Autonomous Reactor (SSTAR)/Lead-cooled Fast Reactor (LFR) and Supporting Research and Development*. ANL-GenIV-089, Argonne National Laboratory, Argonne, Illinois. Available at http://www.osti.gov/energycitations/servlets/purl/932940-RHXy5s/.

Sienicki JJ, AV Moisseytsev, PA Pfeiffer, WS Yang, MA Smith, SJ Kim, YD Bodnar, DC Wade and LL Leibowitz. 2005. "SSTAR Lead-Cooled, Small Modular Fast Reactor with Nitride Fuel." Presented at *Workshop on Advanced Reactors with Innovative Fuels ARWIF 2005*, February 16-18, 2005, Oak Ridge, Tennessee.

Smith CM. 2010. *Lead-Cooled Fast Reactor (LFR) Design: Safety, Neutronics, Thermal Hydraulics, Structural Mechanics, Fuel, Core, and Plant Design*. LLNL-BOOK-424323, Lawrence Livermore National Laboratory, Livermore, California.

Trallero AM. 2011. *C-14 Production in Lead-Cooled Reactors*. Master of Science in Technology Thesis, Aalto University, Finland.

Appendix C

Gas-Cooled Reactors

Appendix C

Gas-Cooled Reactors

Gas-cooled reactor (GCR) systems feature either thermal or fast-neutron-spectra. The thermal spectrum reactors are HTGR and VHTR designs and feature the use of TRISO-coated particle fuel dispersed in a graphite matrix and significant use of graphite moderator. The fast spectrum reactors are known as gas-cooled fast reactors (GFRs), which are associated with a closed fuel cycle. The main characteristics common to both types of GCRs include the usage of robust refractory fuel, high operating temperatures, potential direct coupling to He-Brayton energy conversion cycles, and low power density relative to SFRs. The primary coolant boundary in these systems prevents large failures, which would result in air ingress and result in unacceptable chemical reactions within the core causing excessive degradation of the fuel elements or other core components. VHTRs typically have no active safety features and require no operator action to ensure safety. Typical core configurations for VHTRs are based on dispersal of coated-particle fuel into graphite blocks or spherical fuel pebbles. GCRs are primarily envisioned for missions in electricity production and actinide management. Very-high-temperature designs can support hydrogen production as well. Historically, high-temperature gas reactors (HTGRs) have experienced moisture ingress events into the reactor system because of leaking of helium recirculator bearings, which caused significant corrosion issues and unplanned outages (Fort St. Vrain). Newer designs propose to use magnetic bearings.
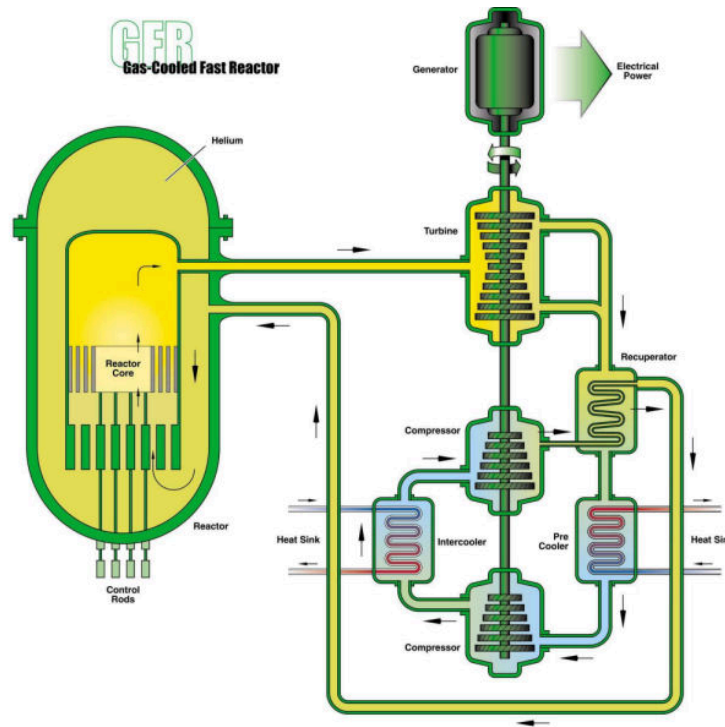
Figure C.1. General Diagram of a GFR Reactor System
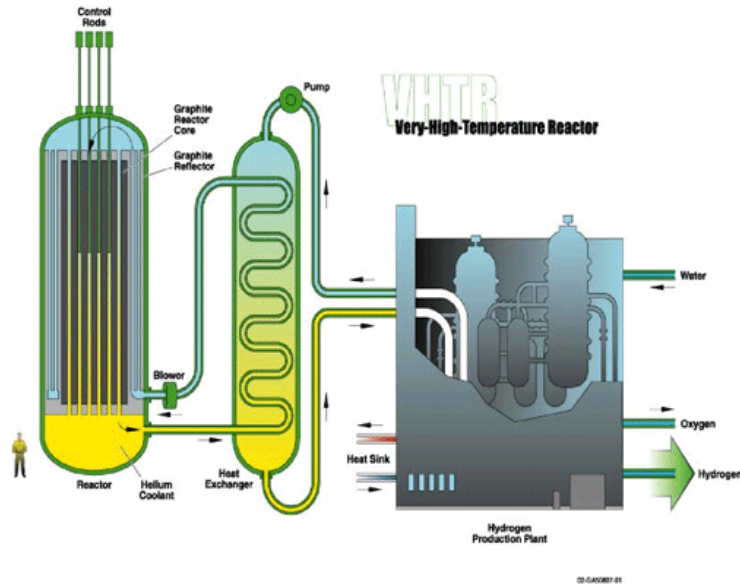
Figure C.2. General Diagram of a VHTR Reactor System

Table C.1. List of Several Recent GCR Concepts and Associated Organization/Country

GCR Concepts	Organization / Country
Fast	
EM2 (Energy Multiplier Module)	General Atomics / USA
Thermal	
GT-MHR (Gas-Turbine Modular Helium Reactor)	General Atomics / USA
RS-MHR (Remote Site - Modular Helium Reactor)	
SC-HTGR (Steam Cycle – High Temperature Gas Reactor) (ANTARES)	AREVA / France
PBMR (Pebble Bed Modular Reactor)	ESKOM & Pty Limited / South Africa
HTR-PM (High Temperature Gas Cooled Reactor – Pebble Bed Module)	Tsinghua University / China

Table C.2. Summary of Design Parameters for Several Recent GCR Concepts

General GCR Design Features	Parameters
Coolant	He (most common); other: N_2, air
Thermal Capacity Range (MWth)	~5–600
Gross Electrical Capacity Range (MWe)	2–285
Refueling Frequency (years)	1.5; 5–10; 30 (continuous for pebble bed)
Fuel Cycle	Once through, breed and burn

Table C.3. Summary of Typical Operating Parameters for GCRs

Parameter	Value		Reference
Temperature Range (°C)	Core Inlet	250–587	
	Core Outlet	530–850	
	For Hydrogen Productions	900–1000	
	Fuel (max.)	1238 (limit 1600)	
Pressure Range (MPa)	5–~9		
He Mass Flow Rate (kg/s)	96–320		General Atomics (2011), IAEA (2007)
Power Density (MW/m^3 or kW/l)	4–6.5		

C.1 Historical Operational Issues Noted for GCRs

- Water-lubricated circulator bearings, which resulted in frequent, water ingress into the reactor system that caused significant corrosion issues and resultant down time (Fort St. Vrain). New designs now use magnetic bearings.

- Lessons Learned: See references (INL 2010; Beck and Pincock 2011).

C.2 Bibliography

C.2.1 EM2

Back C and R Schleicher. 2011. "Configuring EM2 to Meet the Challenges of Economics, Waste Disposition and Non Proliferation Confronting Nuclear Energy in the U.S." In *15th International Conference on Emerging Nuclear Energy Systems (2011 ICENES)*, p. 16. May 16, 2011, San Francisco, California. General Atomics, San Diego, California.

Parmentola J. 2010. "A Potential Technology Solution for Nuclear Waste." Presented at *Blue Ribbon Commission on America's Nuclear Future*, December 8, 2010, San Diego, California. Available at http://www.ga.com/docs/em2/pdf/EM2_presentation.pdf.

General Atomics. 2012. *Energy Multiplier Module: EM2, Transformational Technology Turning Nuclear Waste to Clean Energy*. General Atomics. San Diego, California. Accessed April 18, 2013. Available at http://www.ga.com/docs/em2/pdf/FactSheet_QuickFactsEM2.pdf.

General Atomics. 2012. *Energy Multiplier Module (EM2): Technical Fact Sheet*. General Atomics. San Diego, California. Accessed April 18, 2013. Available at http://www.ga.com/docs/em2/pdf/FactSheet-TechnicalFactSheetEM2.pdf.

C.2.2 GT-MHR

General Atomics. 1996. *Gas Turbine-Modular Helium Reactor (GT-MHR): Conceptual Design Description Report*. Report No. 910720, Rev. 1, General Atomics, San Diego, California. GA Project No. 7658.

C.2.3   RS-MHR

General Atomics. 2001. "Remote Site - Modular Helium Reactor (RS-MHR) Secure Nuclear Power for Remote Locations." General Atomics, San Diego, California.

C.2.4   SC-HTGR/ANTARES

Gauthier J-C, G Brinkmann, B Copsey and M Lecomte. 2004. "ANTARES: The HTR/VHTR Project at Framatome ANP." In *2nd International Topical Meeting on High Temperature Reactor Technology*. September 22-24, 2004, Beijing, China. Paper #A10.

Gauthier J-C, G Brinkmann, B Copsey and M Lecomte. 2006. "ANTARES: The HTR/VHTR Project at Framatome ANP." *Nuclear Engineering and Design* 236(5-6):526-533.

C.2.5   PBMR

Goede P, M van der Walt, L Stassen and F Reitsma. 2009. "PBMR: Product Overview & Source Term Modeling." In *PSI HTR Dust Issues Meeting*, p. 27. November 26-27, 2009, Paul Scherrer Institut, Villigen, Switzerland. Available at http://sacre.web.psi.ch/HTR/Part-Pres/ PBMR%20product%20overview%20and%20source%20term%20modelling.pdf.

Greyling T. N/A. "Pebble Bed Modular Reactor (PBMR) - A Power Generation Leap into the Future." Pebble Bed Modular Reactor (Pty) Ltd, South Africa.

IAEA. 2011. *Status Report 70 - Pebble Bed Modular Reactor (PBMR).* International Atomic Energy Agency (IAEA), Vienna, Austria.

C.2.6   HTR-PM

Dong Y. 2011. "Status of Development and Deployment Scheme of HTR-PM in the People's Republic of China." In *Interregional Workshop on Advanced Nuclear Reactor Technology for Near Term Deployment*, p. 54. July 4-8, 2011, Vienna, Austria. Institute of Nuclear and New Energy Technology (INET), Tsinghua University, Beijing, China.

Sun Y. 2010. "The HTR-PM Reactor and Its Fuel Cycle from Non-proliferation Perspective." In *IAEA Technical Meeting*, p. 12. August 15-18, 2011. Institute of Nuclear and new Energy Technology (INET), Tsinghua University, Beijing, China. Available at http://www.uxc.com/smr/Library/Design%20Specific/ HTR-PM/Presentations/2010%20-%20The%20HTR-PM%20Reactor%20and%20its%20Fuel%20Cycle%20from%20Non-proliferation%20Perspective.pdf.

C.2.7   General

AREVA. 2010. *Pebble Bed Reactor Assessment Executive Summary*. Document No. 12-9155160-000, AREVA NP Inc. 20004-018 (10/18/2010).

Ball SJ, DE Holcomb and MS Cetiner. 2012. *HTGR Measurements and Instrumentation Systems*. ORNL/TM-2012/107, Oak Ridge National Laboratory, Oak Ridge, Tennessee.

Beck JM and LF Pincock. 2011. *High Temperature Gas-Cooled Reactors Lessons Learned Applicable to the Next Generation Nuclear Plant*. INL/EXT-10-19329, Rev. 1, Idaho National Laboratory, Idaho Falls, Idaho.

de Villiers GJ. 2009. *In-core Temperature Measurement for the PBMR Using Fibre-Bragg Gratings*. Masters of Engineering Thesis, University of Stellenbosch, Matieland, South Africa.

INL. 2011. *Summary of Planned Implementation for the HTGR Lessons Learned Applicable to the NGNP*. INL/EXT-11-21545, Idaho National Laboratory (INL), Idaho Falls, Idaho.

INL. 2012. *Gas-Cooled Fast Reactor (GFR)*. Idaho National Laboratory (INL). Idaho Falls, Idaho. Accessed April 10, 2013. Available at https://inlportal.inl.gov/portal/ server.pt?open=514&objID=2253&parentname=CommunityPage&parentid=13&mode=2&in_hi_userid= 291&cached=true.

Moses DL. 2010. *Very High-Temperature Reactor (VHTR) Proliferation Resistance and Physical Protection (PR&PP)*. ORNL/TM-2010/163, Oak Ridge National Laboratory, Oak Ridge, Tennessee.

Suikkanen H. 2008. "Coolant Flow and Heat Transfer in PBMR Core with CFD." In *GEN4FIN: Third Finnish Seminar on Generation IV Nuclear Energy Systems*, p. 27. October 2-3, 2008, Lappeenranta, Finland. Lappeenranta University of Technology, Department of Energy and Environmental Technology.

C.3 References

Andresen PL, Fabry-Pérot Ford, K Gott, RL Jones, PM Scott, T Shoji, RW Staehle and RL Tapping. 2007. *Expert Panel Report on Proactive Materials Degradation Assessment*. NUREG/CR-6923, BNL-NUREG-77111-2006, U.S. Nuclear Regulatory Commission, Washington, D.C.

Beck JM and LF Pincock. 2011. *High Temperature Gas-Cooled Reactors Lessons Learned Applicable to the Next Generation Nuclear Plant*. INL/EXT-10-19329, Rev. 1, Idaho National Laboratory, Idaho Falls, Idaho. Available at http://www.osti.gov/energycitations/servlets/purl/1023461/.

Bond LJ, SR Doctor, JW Griffin, AB Hull and SN Malik. 2011. "Damage Assessment Technologies for Prognostics and Proactive Management of Materials Degradation." *Nuclear Technology* 173(1):46-55.

INL. 2010. *Summary of Planned Implementation for the HTGR Lessons Learned Applicable to the NGNP*. INL/EXT-11-21545, Idaho National Laboratory (INL), Idaho Falls, Idaho.

Appendix D

Molten Salt Cooled Reactors

Appendix D

Molten Salt Cooled Reactors

Molten salt-cooled reactors come in two distinct varieties. Molten salt reactors (MSRs) contain a fluid-fueled core where the molten salt coolant contains dissolved fuel – called "fuel salt" – that allows for refueling without reactor shutdown. Fluoride salt-cooled high-temperature reactors (FHRs) use circulating fluoride salts as a coolant, but the fuel is confined within traditional fuel rods. Although the term "MSR" sounds generic, it is almost always used to refer to this first class of reactors using fuel salt. MSR and FHR designs feature moderate to high power density, high reactor outlet temperatures, and low system pressure. This reactor type can be designed to operate with either a thermal or fast neutron flux (although no fast reactor of this type has ever been operated) and has the unique characteristic that, in theory, very high fuel burnup can be achieved because fuel performance in MSR concepts is not limited to fuel cladding strength and ductility considerations. Modern research and design efforts have focused more on FHR designs (e.g., AHTR, MARS, SmAHTR) using molten salt as the coolant and a more common solid fuel approach. The liquid-fueled MSRs can be used for production of electricity, actinide burning, and the production of hydrogen and fissile fuels.

The molten salt coolant is typically (but not always) a mixture of lithium and beryllium fluoride salts with a boiling point (1400°C) significantly higher than the temperature of the fuel; however, a sodium fluoride salt reactor has recently been evaluated and shown to be feasible. The fuel dissolved in the molten salt coolant can be enriched uranium, thorium, or U-233. The molten fuel salt is circulated through a moderator core, typically unclad graphite, at relatively low pressure where fission occurs. In the MSR core, the highly radioactive fuel salt is heated to a high temperature (700°C or more) and then flows into a primary heat exchanger where heat is transferred to a secondary circuit of clean molten salt coolant before flowing back to the core. The temperature profiles and heat exchange processes are similar in both MSRs and FHRs. As the fuel burns, the waste products are removed from the fuel salt and fresh fuel is added; this can be done at power and therefore plant availability is determined by maintenance schedule and not fuel cycle. This arrangement also enables the breeding of fissile U-233 using the fertile thorium in a fuel cycle. The secondary heat transfer circuit transfers the heat to a high-temperature Brayton cycle that converts the heat to electricity. The Brayton cycle (with or without a steam-bottoming cycle) may use a working gas of either nitrogen or helium. A diagram of an MSR system is provided in Figure D.1. Several MSR concepts with the potential for modularization are provided in Table D.1 with major design parameters summarized in Table D.2. Typical operating parameters for several MSRs are provided in Table D.3.

Key safety features of MSRs with liquid fuel are typically associated with the negative reactivity changes associated with elevated temperatures resulting in coolant/fuel expansion during power excursions and an actively cooled salt plug. During a reactor-overheat condition, the salt plug melts and allows the molten fuel salt mixture to drain into a holding tank configured to disperse the fuel in such a manner that stops the sustaining nuclear chain reaction, thereby shutting down the plant and allowing the mixture to safely cool. As the mixture cools in the tank via passive cooling, it will eventually solidify. In the case of forced flow failure, natural circulation takes over from convective flow. Many of these reactor systems are designed to be "walk away" safe, whereby in the event of complete power loss, with no operator action, the reactor will find a safe state.

FHRs also benefit from passive safety features and negative reactivity coefficients. Since the salts are similar for both designs, reactivity and vapor pressures of the coolants are similar for both FHRs and MSRs.
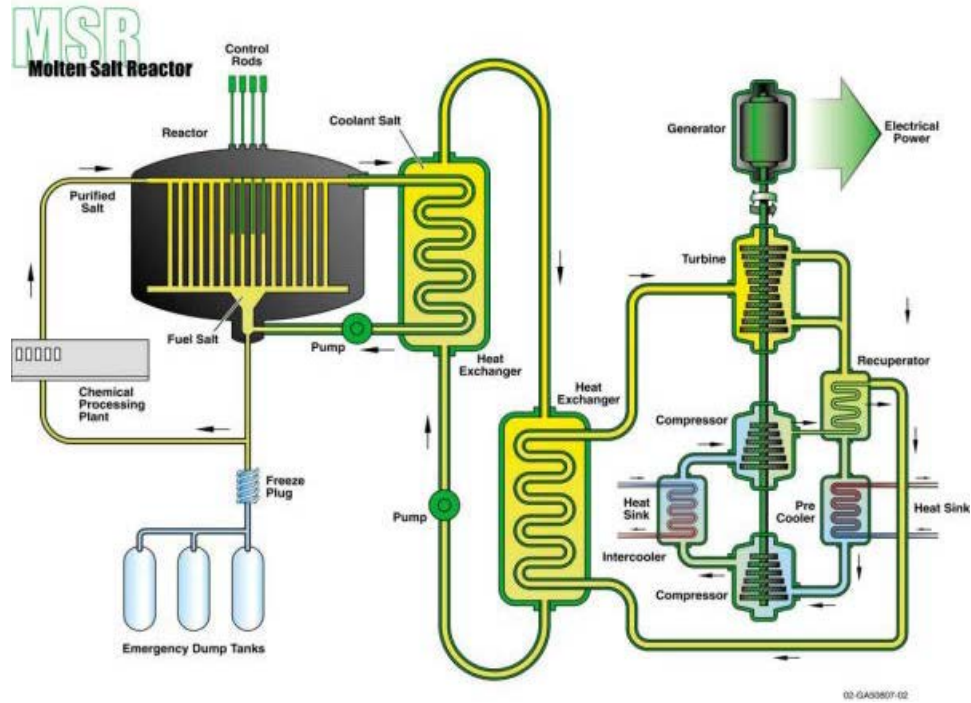
Figure D.1. Depiction of an MSR System

Table D.1. List of Several MSR Concepts and Associated Organization/Country

MSR Concepts	Organization/Country
Fuji MSR (Fuji Molten Salt Reactor)	International Thorium Energy & Molten Salt Technology Inc. Company (IThEMS)/Japan
GEMSTAR (Green Energy Multiplier*Subcritical Technology for Alternative Reactors)[a]	Virginia Tech & Accelerator Driven Neutron Application Corporation (ADNA)/USA
LFTR (Liquid-Fluoride Thorium Reactor)	Flibe Energy/USA
MARS (Microfuel Molten Salt Cooled Reactor of Low Power)[b]	Kurchatov Institute/Russia
SmAHTR (Small Modular Advanced High Temperature Reactor)[b]	ORNL/USA
ThorCon	Martingale, Inc./USA
WAMSR (Waste-Annihilating Molten Salt Reactor)[a]	Transatomic Power/USA
(a) Fast reactor variants.	
(b) Not a fluid-fueled type MSR concept. Uses clean molten salt with solid fuel.	

Table D.2. Summary of Design Parameters for Several Recent SFR Concepts

General SMR MSR Design Features	Parameter	Reference
Coolant	Molten salt	European Nuclear Society (2012)
Thermal Capacity Range (MWth)	16–450	
Gross Electrical Capacity Range (MWe)	6–500+	
Refueling Frequency (years)	For fluid fueled designs – online fueling For solid fueled designs – 5, 15, and 30	
Fuel Cycle	Thorium (thermal to epithermal neutron speed) U-Pu (fast neutron spectrum)	NRC (2012)

Table D.3. Summary of Typical Operating Parameters for MSRs

Parameter	Value		Reference
Temperature Range (°C)	Core Inlet	550–650	
	Core Outlet	700–750 to 800–1000	
	Molten Salt Coolant Freezing	350	
	Molten Salt Coolant Boiling	1300	Alekseev (2010)
	Primary Loop (Inlet/Outlet)	570–650/700–1000	
	Secondary Loop (Inlet/Outlet)	454–600/633–690	
	Graphite Moderator	947 (Max)	Unknown (2004)
Pressure Range (MPa)	Molten Salt Coolant	0.1 (~ 1 atm)–0.5	
Power Density (MW/m^3 or kW/l)	MARS	0.75	
	Fuji MSR & SmAHTR	6.8–9.4	
	ThorCon	25	
Neutron Flux	Fuel Element (MARS)	0.53–2.1 × 10^{21} n/cm^2	Adamovich et al. (2007)
	Reactor Vessel (MARS)	0.33–1.0 × 10^{21} n/cm^2	Adamovich et al. (2007); Yoshioka et al. (2010)
	Graphite in Reactor (Fuji MSR)	3 × 10^{23} n/cm^2	Unknown (2004)

D.1 Historical Operational Issues Noted for LFRs

- Historical issues are minimal because few MSRs have been built and operated. In the 1950s and 1960s, two small prototype thermal spectrum MSRs were built and operated in the United States for a number of years. In the 1970s, Russia has some programs and the United Kingdom was involved in some early work. No fast spectrum MSRs have been built.

D.2 Bibliography

D.2.1 FUJI MSR

Honma Y, Y Shimazu and T Narabayashi. 2008. "Optimization of Flux Distribution in a Molten-Salt Reactor with a 2-region Core for Plutonium Burning." *Progress in Nuclear Energy* 50(2-6):257-261.

IThEMS. 2012. *Fuji Molten Salt Reactor*. The Ux Consulting Company. Roswell, Georgia. Accessed April 17, 2013. Available at http://www.uxc.com/smr/uxc_SMRDetail.aspx?key=Fuji%20MSR. International Thorium Energy & Molten Salt Technology Inc. Company (IThEMS).

Shimazu Y. 2007. "Current Situation of MSR Development in Japan." Hokkaido University, Japan. http://www.uxc.com/smr/Library/Design%20Specific/Fuji%20MSR/Presentations/2007%20-%20Current%20Situation%20of%20MSR%20Development%20in%20Japan.pdf.

Suzuki N and Y Shimazu. 2008. "Reactivity-Initiated-Accident Analysis without Scram of a Molten Salt Reactor." *Journal of Nuclear Science and Technology* 45(6):575-581.

Waris A, IK Agi, Y Yulianti, MA Shafii, I Taufiq and Z Su'ud. 2010. "Comparative Study on 233U and Plutonium Utilization in Molten Salt Reactor." *Indonesian Journal of Physics* 21(3):77-81.

Yoshioka R, K Furukawa, Y Kato and K Mitachi. 2010. "Molten-Salt Reactor FUJI and Related Thorium Cycles." In *Thorium Energy Alliance Spring Conference 2010*. March 29-30, 2010, Mountain View, California. Thorium Energy Alliance, Harvard, Illinois.

D.2.2   GEM*STAR

Bowman C, RB Vogelaar and M Pierson. N/A. "GEM*STAR: Green Energy-Multiplier Subcritical Technology for Alternative Reactors." http://www.uxc.com/smr/Library/Design%20Specific/GEMSTAR/Presentations/GEMSTAR.pdf.

Chang LN. 2009. "GEM*STAR: Transforming the Nuclear Landscape." ADNA Inc. and Virginia Tech. http://www.uxc.com/smr/Library/Design%20Specific/GEMSTAR/Presentations/2009%20-%20GEMSTAR%20Transforming%20the%20Nuclear%20Landscape.pdf.

Virginia Tech and ADNA. 2012. *Green Energy Multiplier*Subcritical Technology for Alternative Reactors (GEMSTAR)*. The Ux Consulting Company. Roswell, Georgia. Accessed April 17, 2013. Available at http://www.uxc.com/smr/uxc_SMRDetail.aspx?key=GEMSTAR. Virginia Tech and Accelerator Driven Neutron Application (ADNA) Corporation.

Vogelaar RB. 2010. "GEM*STAR: Green Energy-Multiplier, Sub-critical, Thermal-spectrum, Accelerator-driven, Recycling reactor." ADNA and GEMSTAR Consortium, University of Virginia Physics Colloquium. November 5, 2010. http://www.uxc.com/smr/Library/Design%20Specific/ GEMSTAR/Presentations/2010%20-%20GEMSTAR.pdf.

Vogelaar RB. 2011. "GEM*STAR: Green Energy-Multiplier Sub-critical, Thermal-spectrum, Accelerator-driven, Recycling Reactor." ADNA & GEMSTAR Consortium. ADS & TU Mumbai, India, December 12, 2011. http://www.uxc.com/smr/Library/Design%20Specific/GEMSTAR/Presentations/ 2011%20-%20GEMSTAR.pdf.

D.2.3   LFTR

Flibe Energy. 2012. *Liquid-Fluoride Thorium Reactor (LFTR)*. The Ux Consulting Company. Roswell, Georgia. Accessed April 17, 2013. Available at http://www.uxc.com/smr/ uxc_SMRDetail.aspx?key=LFTR.

Sorensen K. 2011. "Introduction to Flibe Energy." In *Thorium Energy Conference 2011 (ThEC11)*. October 10-12, 2011, New York.

Sorensen K and K Dorius. 2011. "Introduction to Flibe Energy." In *3rd Thorium Energy Alliance Conference (TEAC3)*, p. 23. May 12, 2011, Washington, D.C.

Hargraves R and R Moir. 2010. "Liquid Fluoride Thorium Reactors - An Old Idea in Nuclear Power Gets Reexamined." *American Scientist* 98(4):304-313.

Sorensen K. 2009. "Lessons for the Liquid-Fluoride Thorium Reactor (from history)." Presented at *Google*, July 20, 2009, Mountain View, California.

D.2.4   MARS

Alekseev P. 2010. "Concept of Small Power Autonomous Molten-Salt Reactor with Micro-Particle Fuel (Reactor MARS)." In *Fluoride Salt-Cooled High-Temperature Reactor Workshop*. September 20-21, 2010, Oak Ridge, Tennessee.

Kurchatov Institute. 2012. *Microfuel Molten Salt Cooled Reactor of Low Power (MARS)*. The Ux Consulting Company. Roswell, Georgia. Accessed April 17, 2013. Available at http://www.uxc.com/smr/uxc_SMRDetail.aspx?key=MARS.

D.2.5   SmAHTR

Greene S. 2010. "FHRs and the Future of Nuclear Energy." In *DOE FHR Workshop*, p. 17. Sept. 20-21, 2010, Oak Ridge, Tennessee. Oak Ridge National Laboratory.

Greene S. 2010. "SmAHTR – the Small Modular Advanced High Temperature Reactor." In *DOE FHR Workshop*. September 20-21, 2010, Oak Ridge, Tennessee. Oak Ridge National Laboratory.

Greene SR, DE Holcomb, JC Gehin, JJ Carbajo, AT Cisneros, WR Corwin, D IIas, DF Wilson, VK Varma, EC Bradley and GL Yoder. 2010. "SMAHTR – A Concept for a Small, Modular Advanced High Temperature Reactor." In *Proceedings of HTR 2010*, p. 9. October 18-20, 2010, Prague, Czech Republic. Paper 205.

Greene SR, JC Gehin, DE Holcomb, JJ Carbajo, D Llas, AT Cisneros, VK Varma, WR Corwin, DF Wilson, GL Yoder and AL Qualls. 2010. *Pre-Conceptual Design of a Fluoride-Salt-Cooled Small Modular Advanced High Temperature Reactor (SmAHTR)*. ORNL/TM-2010/199, Oak Ridge National Laboratory, Oak Ridge, Tennessee.

Ilas D, J Gehin and S Greene. 2010. "Preliminary Nuclear Design Studies for a Small Modular Advanced High Temperature Reactor (SmAHTR)." *Transactions of the American Nuclear Society* 103:607-608.

ORNL. 2012. *Small Modular Advanced High Temperature Reactor (SmATHR)*. The Ux Consulting Company. Roswell, Georgia. Accessed April 17, 2013. Available at http://www.uxc.com/smr/uxc_SMRDetail.aspx?key=SmAHTR. Oak Ridge National Laboratory (ORNL), Oak Ridge, Tennessee.

D.2.6   ThorCon

Devanney J. 2012. *ThorCon Summary Description*. Martingale, Tavernier, Florida. Version 0.60.

Unknown. N/A. "Notes on ThorCon Reactor Preliminary Design Study."

D.2.7   WAMSR/Transatomic

Bullis K. 2013. *Safer Nuclear Power, at Half the Price*. MIT Technology Review. Cambridge, Massachusetts. Accessed April 17, 2013. Available at http://www.technologyreview.com/news/512321/safer-nuclear-power-at-half-the-price/.

D.2.8   General

DOE. 2002. *A Technology Roadmap for Generation IV Nuclear Energy Systems*. GIF-002-00, U.S. Department of Energy (DOE), Washington, D.C.

D.3   References

Adamovich L, S Banerjee, M Bolshunkhin, E Budylov, M Chaki, IV Dulera, P Fomichnko, K Furukawa, B Gabaraev and E Greenspan. 2007. *Status of Small Reactor Designs without On-Site Refueling*. IAEA-TECDOC-1536, International Atomic Energy Agency (IAEA), Vienna, Austria.

Alekseev P. 2010. "Concept of Small Power Autonomous Molten-Salt Reactor with Micro-Particle Fuel (Reactor MARS)." In *Fluoride Salt-Cooled High-Temperature Reactor Workshop*. September 20-21, 2010, Oak Ridge, Tennessee.

European Nuclear Society. 2012. "Transaction Advanced Reactors." *Transaction Advanced Reactors, European Nuclear Conference (ENC2012)*, December 9-12, 2012, Manchester, United Kingdom. European Nuclear Society, Brussels, Belgium.

NRC. 2012. *Report to Congress: Advanced Reactor Licensing*. U.S. Nuclear Regulatory Commission (NRC), Washington, D.C. Available at http://www.nrc.gov/reading-rm/doc-collections/congress-docs/correspondence/2012/frelinghuysen-08-22-2012.pdf.

Unknown. 2004. "Chapter X. MSR-FUJI General Information, Technical Features, and Operating Characteristics." http://www.energyfromthorium.com/pdf/MSR-FUJI.pdf.

Yoshioka R, K Furukawa, Y Kato and K Mitachi. 2010. "Molten-Salt Reactor FUJI and Related Thorium Cycles." In *Thorium Energy Alliance Spring Conference 2010*. March 29-30, 2010, Mountain View, California. Thorium Energy Alliance, Harvard, Illinois.

Appendix E

Supercritical Water Cooled Reactor (SCWR)

Appendix E

Supercritical Water Cooled Reactor (SCWR)

The Supercritical-Water-Cooled Reactor (SCWR) offers moderate core power densities and simplicity in design, by eliminating major components (e.g., pressurizers, primary-to-secondary heat exchangers, steam dryers, and steam generators). The simple design should translate directly into reduced overall plant construction costs. The reactor operates at much higher temperatures and pressures, resulting in higher operating efficiencies (44% compared to 32% as seen in today's LWRs), but requires further development in fuels and materials. This technology is an evolution of existing LWR technology and leverages existing advanced supercritical coal-fired technology and, in theory, can be designed to have high conversion ratios but less than unity (i.e., fissile material produced divided by fissile material loaded in initial core). The energy conversion technology associated with the secondary side of the reactor plant has been fully developed and commercialized by the coal fire industry. Supercritical water technology has been used in coal power plants since the 1960s to increase plant efficiency and reduce emissions, and by the 1990s supercritical water boilers had proven themselves as a reliable and established technology. Currently 85% of the new Western coal power plants are supercritical.

As stated, the SCWR is a high-temperature, high-pressure water-cooled reactor that operates above the thermodynamic critical point of water (374°C, 22.1 MPa or 705°F, 3208 psia). At supercritical pressures, no boiling takes place in the core and the phase transition between liquid and gas is much smoother than the abrupt boiling, which occurs in a commercial boiling water reactor operating at lower pressures. An example of a SCWR system is shown in Figure E.1. These reactors can be designed to operate with either a thermal or fast-neutron spectrum.

Fast spectrum supercritical water reactors have been considered by the Japanese (Yetisir et al. 2012) and have been designed to resolve the undesirable positive void effect seen in previous fast-spectrum designs. The Korean Ministry of Science and Technology (MOST) sponsors research (Danielyan 2003) in supercritical water reactor technology and Europe's High Performance Light Water Reactor program was initiated in 2006 as part of the Gen IV International Forum (GIF) and is focused on assessing "the critical scientific issues and the technical feasibility of a High Performance Light Water Reactor operating under supercritical pressure" (Tulkki 2006).
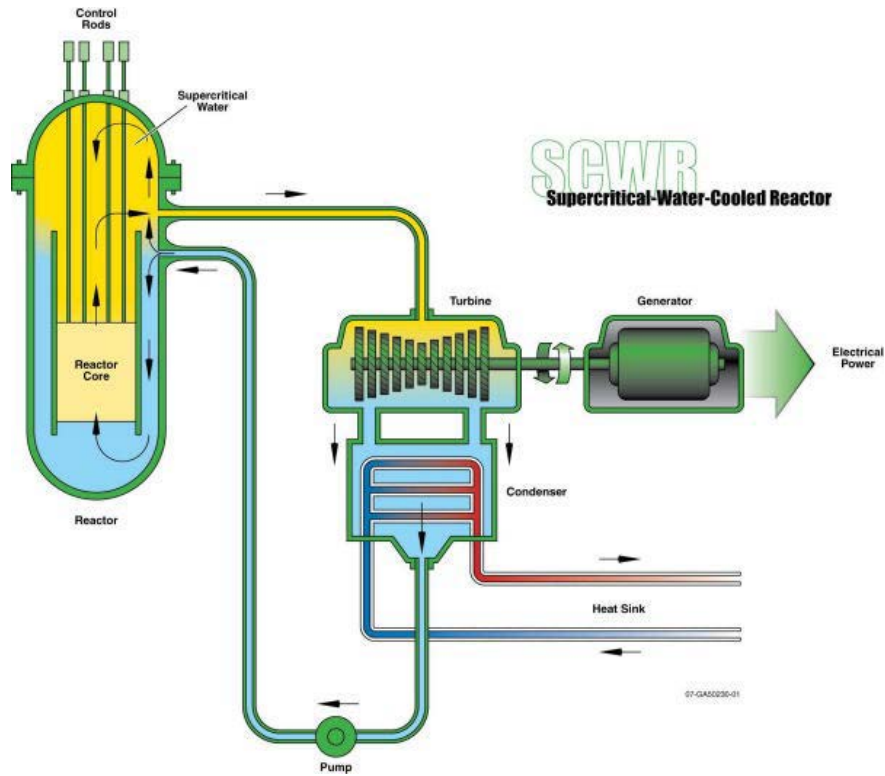
Figure E.1. General Diagram of a SCWR Reactor System

Table E.1. SCWR Concepts for Potential Modularization

Modularized SCWR Reactors	Country
300 MWe SuperSafe© Reactor (SSR)	Canada

Table E.2. Summary of Design Parameters for SCWR Concepts

General SMR SCWR Design Features	Parameters	Reference
Coolant	Water critical	
Thermal Capacity Range (MWth)	400–3800 670 (SSR)	Yetisir et al. (2012)
Gross Electrical Capacity Range (MWe)	175–1700 300 (SSR)	Yetisir et al. (2012)
Refueling Frequency (years)	2–6 yrs	
Fuel Cycle	Thermal, fast, or mixed. Once through, open or closed.	Duffey and Pioro (2005)

Table E.3. Summary of Typical Operating Parameters for SCWRs

Parameter	Value		Reference
Temperature Range (°C)	Core Inlet	350	Duffey and Pioro (2005), Yetisir et al. (2012)
	Core Outlet	625	Duffey and Pioro (2005), Yetisir et al. (2012)
	Coolant Max	625	Yetisir et al. (2012)
	Fuel	1900	
Pressure Range (MPa)	26		Duffey and Pioro (2005)
Flow Rate	1,418 Kg/s Japanese Super LWR concept		
Power Density (MW/m^3 or kW/l)	70 kW/1 (SCWR concept)		Danielyan (2003)
	67–144 MW/m^3		Tulkki (2006)
	300 MW/m^3 (Japan – Super Fast Reactor)		The Energy Library (2009)

E.1 Historical Operational Issues Noted for LFRs

- None specifically found, as there is not much history with SCWR designs.

E.1.1 Bibliography

Abdalla A. 2012. *Sensitivity Analysis of Fuel Centerline Temperatures in SuperCritical Water-cooled Reactors (SCWRs)*. M.S. in Nuclear Engineering Thesis, University of Ontario Institute of Technology, Ontario, Canada. Available at https://ir.library.dc-uoit.ca/bitstream/10155/292/1/Abdalla_Ayman.pdf.

Bae Y-Y, J Jang, H-Y Kim, H-Y Yoon, H-O Kang and K-M Bae. 2007. "Research Activities on a Supercritical Pressure Water Reactor in Korea." *Nuclear Engineering and Technology* 39(4):273-286.

Baindur S. 2008. "Materials Challenges for the Supercritical Water-Cooled Reactor (SCWR)." *Bulletin of the Canadian Nuclear Society* 29(1):32-38.

Buongiorno J and PE MacDonald. 2003. *Supercritical Water Reactor (SCWR) Progress Report for the FY-03 Generation-IV R&D Activities for the Development of the SCWR in the U.S.* INEEL/EXT-03-01210, Idaho National Engineering and Environmental Laboratory, Idaho Falls, Idaho.

DOE. 2002. *A Technology Roadmap for Generation IV Nuclear Energy Systems*. GIF-002-00, U.S. Department of Energy (DOE), Washington, D.C.

Dollezhal NA, IY Emel'yanov, PI Aleshchenkov, AD Zhirnov, GA Zvereva, NG Morgunov, YI Mityaev, GD Knyazeva, KA Kryukov, VN Smolin, LI Lunina, VI Kononov and VA Petrov. 1964. "Development of Power Reactors of BNPP-Type with Nuclear Steam Reheat, (In Russian)." In *3rd International Conference on Peaceful Uses of Nuclear Energy*. August 31–September 9, 1964, Geneva. Report No. 309.

Duffey R, LKH Leung, D Martin, B Sur and M Yetisir. 2011. "A Supercritical Water-Cooled Small Modular Reactor." In *ASME 2011 Small Modular Reactors Symposium*, pp. 243-250. September 28–30, 2011, Washington, D.C.

Garkisch H. 2002. "Design Limits Input for Performance Evaluations." Presented at *SCWR Fuel Rod Design Requirements*.

HPLWR2. 2011. *High Performance Light Water Reactor Phase 2 (HPLWR Phase 2)*. Accessed April 15, 2013. Available at http://www.iket.fzk.de/hplwr/index.html.

INL. 2008. "Supercritical-Water-Cooled Reactor (SCWR)." Idaho National Laboratory (INL), Idaho Falls, Idaho.

Khartabil H. 2009. "SCWR: Overview." In *GIF Symposium*, pp. 143-148. September 9-10, 2009, Paris, France.

Licata JJ and CM Potts. 2011. *Small Modular Nuclear Reactors: LEGO for Adults or the New PC Revolution?* BLUEPHOENIX, New York.

Meyer L. 2012. "Progress and Status of SCWR Systems." Presented at *6th GIF/INPRO Interface Meeting*, March 6-7, 2012, Vienna, Austria.

Miletić M, M Růžičková, R Fukač, I Pioro and E Saltanov. "Supercritical-Water Experimental Setup for Out-of-Pile Operation." In *Proceedings of the 20th International Conference Nuclear Energy for New Europe 2011*, pp. 806.1–806.11. September 12–15, 2011, Bovec, Slovenia.

Mori M, W Maschek and A Rineiski. 2006. "Heterogeneous Cores for Improved Safety Performance: A Case Study: The Supercritical Water Fast Reactor." *Nuclear Engineering and Design* 236(14–16):1573-1579.

Nakatsuka T, Y Oka and S Koshizuka. 2001. "Startup Thermal Considerations for Supercritical-Pressure Light Water-Cooled Reactors." *Nuclear Technology* 134(3):221-230.

NRC. 2012. *Report to Congress: Advanced Reactor Licensing*. U.S. Nuclear Regulatory Commission (NRC), Washington, D.C.

OECD. N/A. *Generation IV Technology : Systems : Supercritical-Water-Cooled Reactor*. Organisation for Economic Cooperation and Development (OECD), Nuclear Energy Agency. Accessed April 15, 2013. Available at http://www.gen-4.org/Technology/systems/scwr.htm.

Oka Y, S Koshizuka, Y Ishikawa and A Yamaji. 2010. *Super Light Water Reactors and Super Fast Reactors: Supercritical-Pressure Light Water Cooled Reactors*. Springer, New York.

Reiss T, G Csom, S Fehér and S Czifrus. 2010. "The Simplified Supercritical Water-Cooled Reactor (SSCWR), a New SCWR Design." *Progress in Nuclear Energy* 52(2):177-189.

Schulenberg T, LKH Leung, D Brady, Y Oka, K Yamada, Y Bae and G Willermoz. 2009. "Supercritical Water-Cooled Reactor (SCWR) Development through GIF Collaboration." In *International Conference on Opportunities and Challenges for Water Cooled Reactors in the 21st Century*. October 27-30, 2009, Vienna, Austria. International Atomic Energy Agency. Paper #IAEA-CN-164-5S06.

Starflinger J. 2010. *High Performance Light Water Reactor Phase 2: HPLWR Phase 2, Public Final Report, Assessment of the HPLWR Concept*. HPLWR-S/T-WP7-11, Karlsruhe Institute of Technology, Germany.

Strati GL, Ed. 2012. "Special Issue on Small Reactors." *AECL Nuclear Review* 1(2).

Wikipedia. 2013. *Supercritical Water Reactor*. Accessed April 14, 2013. Available at http://en.wikipedia.org/wiki/Supercritical_water_reactor (last updated March 23, 2013).

Yetisir M. 2012. "Generation IV Supercritical Water-Cooled Reactor." Presented at Deep River, Canada, 2012 Deep River Science Academy Summer Lecture on July 12, 2012. Available at http://media.cns-snc.ca/uploads/branch_data/branches/ChalkRiver/cns_talks_2012/Yetisir-Jul12.pdf.

E.2 References

Danielyan D. 2003. *Supercritical-Water-Cooled Reactor System - As One of the Most Promising Type of Generation IV Nuclear Reactor Systems*. Available at http://tfy.tkk.fi/aes/AES/courses/crspages/Tfy-56.181_03/Danielyan.pdf.

Duffey R and I Pioro. 2005. "Supercritical Water-Cooled Nuclear Reactors: Review and Status." In *Nuclear Materials and Reactors - Vol. II from Encyclopedia of Life Support Systems (EOLSS)*. Eolss Publishers, Oxford, United Kingdom.

The Energy Library. 2009. *Supercritical-Water-Cooled Reactor (SCWR)*. The Energy Library. Accessed April 14, 2013. Available at http://www.theenergylibrary.com/node/11879.

Tulkki V. 2006. *Supercritical Water Reactors: A Survey on International State of Research in 2006*. M.S. Thesis, Helsinki University of Technology.

Yetisir M, J Pencer, M McDonald, M Gaudet, J Licht and R Duffey. 2012. "The SUPERSAFE Reactor: A Small Modular Pressure Tube SCWR." *AECL Nuclear Review* 1(2):13-18.